H24/3106

MONASH UNIVERSITY
THESIS ACCEPTED IN SATISFACTION OF THE
REQUIREMENTS FOR THE DEGREE OF
DOCTOR OF PHILOSOPHY
ON.....1 February 2002.....
.....[redacted].....
Sec. Research Graduate School Committee

CHARACTERISATION OF NOVEL IMIDAZOLINES WITH K_{ATP} CHANNEL ANTAGONIST ACTIVITY

A thesis submitted to
The Faculty of Medicine,
Monash University
For the degree of
Doctor of Philosophy

KAREN LEANNE ANDREWS B.SC. (HONS)

DEPARTMENT OF PHARMACOLOGY,
MONASH UNIVERSITY,
VICTORIA, 3800,
AUSTRALIA

FEBRUARY, 2001

TABLE OF CONTENTS

Table of Contents.....i
Declaration.....viii
Acknowledgements.....ix
Summary.....xi
Abbreviations.....xiii
Publications.....xv

CHAPTER ONE

General Introduction.....2

1.1 Potassium (K^+) Channels.....2

1.1.1 Classification of K^+ channels.....3

1.1.1.1 Superfamily One: Voltage Sensitive Potassium Channels.....5

1.1.1.2 Superfamily Two: Inwardly Rectifying Potassium Channels.....8

1.2 ATP-Sensitive K^+ Channels.....10

1.2.1 Molecular Structure.....11

1.2.1.1 $K_{IR}6.x$.....13

1.2.1.2 Sulphonylurea receptors (SUR).....14

1.2.1.3 K_{IR}/ SUR Association.....15

1.2.1.3.1 SURx/K_{IR}6.1.....16

1.2.1.3.2 SURx/K_{IR}6.2.....18

1.2.2 Regulation of K_{ATP} channels by ATP and ADP.....19

1.2.2.1 Site of ATP regulation.....20

1.2.2.2 ATP/ADP ratio.....21

1.3 Endogenous regulators of K_{ATP} channels and their physiological function.22

1.3.1 Pancreatic β–cell.....22

1.3.2 Heart.....24

1.3.3 Vasculature.....26

1.3.4 Other tissues.....29

1.4 Exogenous regulators of K_{ATP} channels 30

1.4.1 K_{ATP} channel openers 30

1.4.1.1 Site of action 33

1.4.1.2 How do openers regulate K_{ATP} channels? 34

1.4.2 K_{ATP} channel antagonists 35

1.4.2.1 Sulphonylureas 35

1.4.2.1.1 Characteristics of sulphonylurea binding 39

1.4.2.1.2 Functional properties of sulphonylurea activity 40

1.4.2.1.3 Selectivity of sulphonylureas for K_{ATP} channels 40

1.4.2.2 Other K_{ATP} channel antagonists 41

1.4.2.3 Imidazolines and Imidazolidines 43

1.4.2.3.1 Actions on smooth muscle 43

1.4.2.3.2 Actions on the pancreas 44

1.4.2.3.3 Actions on the heart 46

1.4.2.3.4 Mechanism of antagonism of K_{ATP} channels 48

1.4.2.3.5 Structure-activity relationships 51

1.5 Statement of Aims 54

CHAPTER TWO

Chemical Synthesis of the novel imidazoline analogues 57

2.1 Introduction 57

2.2 Methods 60

2.2.1 Nomenclature 60

2.2.2 Synthesis of Clonidine 62

2.2.3 Alkylations at the central nitrogen of clonidine 64

2.2.4 Alkylations at the imidazoline nitrogen of clonidine 66

2.2.5 Oxygen substitutions in the imidazoline ring 66

2.2.6 Alkylations at both the central and imidazoline nitrogens of clonidine 68

2.2.7 Preparation of HCl salts 68

2.2.8 Confirmation of structure 68

2.2.8.1 Proton Nuclear Magnetic Resonance (^1H NMR) spectroscopy 69

2.2.8.2 Carbon (^{13}C) NMR spectroscopy *70*

2.2.8.3 Thin layer chromatography *71*

2.2.8.4 Electrospray mass spectroscopy *71*

2.3 Results **73**

2.3.1 Alkylations at the central nitrogen 73

2.3.2 Alkylations at the imidazoline nitrogen 75

2.3.3 Oxygen substitutions in the imidazoline ring 75

2.3.4 Alkylations at both the central and imidazoline nitrogens 79

2.4 Discussion **81**

CHAPTER THREE

The levcromakalim and bradycardic actions of the novel imidazoline analogues **84**

3.1 Introduction **84**

3.2 Materials and Methods **85**

3.2.1 Tissue preparation and Mounting procedures 85

3.2.1.1 Porcine isolated right circumflex coronary arteries *85*

3.2.1.2 Rat isolated small mesenteric arteries *86*

3.2.1.2.1 Normalisation procedure 87

3.2.1.3 Rat isolated spontaneously beating right atria *88*

3.2.2 Experimental protocol and Analysis of results 89

3.2.2.1 Levcromakalim antagonism *89*

3.2.2.2 Electrophysiological properties *92*

3.2.2.3 Bradycardic activity *93*

3.2.3.4 Statistics *93*

3.2.3 Drugs 93

3.3 Results **95**

3.3.1 Levcromakalim antagonism by the imidazoline analogues 95

3.3.2 Electrophysiological properties of IMID-4F 105

3.3.3 Bradycardic effects of the imidazoline analogues 105

3.3.4 Levcromakalim antagonism versus bradycardic activity of the imidazoline analogues 113

3.4 Discussion 114

3.4.1 K_{ATP} channel antagonism 114
3.4.2 Electrophysiological activity 117
3.4.3 Bradycardic activity 119
3.4.4 Structure-activity relationship 120
3.4.5 Conclusions 121

CHAPTER FOUR

Vasorelaxant actions of the novel imidazoline analogues 124

4.1 Introduction 124

4.2 Materials and Methods 125

4.2.1 Vascular studies 125
4.2.1.1 Tissue preparation and mounting procedures 125
4.2.1.1.1 Porcine isolated right circumflex arteries 125
4.2.1.1.2 Rat isolated small mesenteric arteries 125
4.2.1.2 Experimental protocol and Analysis of results 125
4.2.1.2.1 Vasorelaxation of the imidazoline analogues in pig isolated coronary arteries 125
4.2.1.2.2 Vasorelaxation of IMID-35MO/O in rat mesenteric arteries 126
4.2.2 Radioligand binding studies 127
4.2.2.1 Membrane preparation 127
4.2.2.1.1 Cerebral cortex membranes 127
4.2.2.2 Experimental protocol 127
4.2.2.2.1 Saturation studies 127
4.2.2.2.2 Competition studies 128
4.2.2.3 Analysis of Results 129
4.2.3 Statistics 130
4.2.4 Drugs 130

4.3 Results **132**

4.3.1 Vasorelaxation by the imidazoline analogues 132

4.3.2 Vasorelaxation of IMID-35MO/O in rat mesenteric arteries 140

4.3.3 Effect of TPP, ODQ and propranolol on the vasorelaxation of IMID-35MO/O 140

4.3.4 [^{3}H]-PN200-110 hot saturation studies 143

4.3.5 [^{3}H]-PN200-110 competition studies 143

4.3.6 Correlation between the imidazoline-induced vasorelaxation and displacement of [^{3}H]-PN200-110 binding 146

4.4 Discussion **148**

CHAPTER FIVE

Characterisation of the novel imidazoline analogues using radioligand binding techniques

5.1 Introduction **154**

5.2 Materials and Methods **156**

5.2.1 Membrane preparations 156

5.2.1.1 Cerebral cortex membranes *156*

5.2.1.2 Bovine smooth muscle cells *156*

5.2.2 Competition studies 157

5.2.2.1 Using cerebral cortex membranes *157*

5.2.2.2 Using bovine smooth muscle cells *159*

5.2.3 Analysis of results 160

5.2.3.1 Statistics *161*

5.2.4 Drugs 161

5.3 Results **163**

5.3.1 Competition studies 163

5.3.1.1 [^{3}H]-Rauwolscine binding *163*

5.3.1.2 [^{3}H]-Prazosin binding *165*

5.3.1.3 [^{3}H]-QNB binding *169*

5.3.1.4 [^{3}H]-Glibenclamide binding *172*

5.3.1.5 [^{3}H]-P1075 ..... *174*

5.4 Discussion **176**

5.4.1 α_1- & α_2-adrenoceptors 176

5.4.2 Muscarinic receptors 179

5.4.3 K_{ATP} channels 180

5.4.4 Conclusions 182

CHAPTER SIX

***In vivo* characterisation of the novel imidazoline analogues in the anaesthetised rat** **185**

6.1 Introduction **185**

6.2 Materials and Methods **186**

6.2.1 Anaesthetised rat preparation 186

6.2.1.1 Blood glucose *188*

6.2.1.2 Insulin Radioimmunoasssay (RIA) *188*

6.2.2 Experimental protocol and Analysis of Results 191

6.2.2.1 Acute effects of the imidazolines on MAP and heart rate *191*

6.2.2.2 Time dependent effects of the imidazolines on MAP, heart rate, blood glucose and insulin *192*

6.2.2.2.1 Four hour study 192

6.2.2.2.2 One hour study 193

6.2.2.3 Statistics *194*

6.2.3 Drugs 194

6.3 Results **195**

6.3.1 Acute effects of the imidazolines on heart rate and MAP 195

6.3.1.2 Effects on MAP *195*

6.3.1.2 Effect on heart rate *199*

6.3.2 Time dependent effects of the imidazolines on MAP and heart rate 199

6.3.2.1 Four hour study *199*

6.3.2.2 One hour study *212*

6.3.3 Time dependent effects of the imidazolines on blood glucose and insulin levels 214

6.3.3.1 Four hour study *214*

6.3.3.2 One hour study *224*

6.4 Discussion **226**

6.4.1 Acute and time dependent changes in MAP and heart rate 226

6.4.3 Time dependent changes in blood glucose and insulin levels 230

6.4.4 Conclusions 234

CHAPTER SEVEN

General Discussion **237**

Appendices **244**

A1.1 Receptor antagonism **244**

A1.1.1 Competitive antagonism 244

A1.1.2 Non-competitive antagonism 245

References **248**

DECLARATION

The material contained in this thesis has not been presented for the award of any other degree or diploma in any other university or institution. The research conducted has been carried out solely by the candidate, and this thesis contains no material previously published or written by another person, except where due reference has been made in the text.

I certify that the writing of this thesis, with the results, interpretation, opinions and suggestions presented are entirely my own work.

KAREN LEANNE ANDREWS
Department of Pharmacology
PO Box 13E
Monash University
Victoria 3800
AUSTRALIA

ACKNOWLEDGEMENTS

To Grant, my supervisor, thanks for giving me the opportunity to complete my PhD, without you, this thesis would have never happened. Thank you for your support, encouragement and help whenever I needed it but most of all, your unique outlook on life.

To my other supervisor Wayne, thanks for all your help, what did you do again?, oh, I remember now. And Bevyn, thank you for making the Monash Pharmacology Department such a pleasure to study in.

A big thank you to Ms Eva Campi from the Department of Chemistry, Monash University for synthesising the compounds studied throughout this thesis and your patience in explaining chemistry and to Mr Ray Spark from the Department of Biochemistry, Monash University, for performing the insulin assays.

To my fellow members of the McPherson lab, Kim thank you for your optimism and enthusiasm for research in general, but most of all the fantastic times we have had outside the lab. Jo, thanks for answering all my questions but more importantly for your baby stories, I am now sure I'm ready if and when the time comes. Barb, thank you for fixing everything I ever asked, legend is the word that best describes you.

To the members of my other laboratory, the Hodgson lab, Lachlan, a person that will do anything for anyone, thanks for your friendship both in and out of the department. Jarrod, the English guru, one of the only people to read this thesis from front to back, thanks for always saying it how it is. Thanks also to Janith, Sharmaine and Tracey.

There are many people from the department (way too many to mention), whom I now call friends that have made my time here a pleasure. Sab, thanks for keeping me company at morning tea and on trips to the union every day and of course, your friendship. Jeremy, my undergraduate buddy, and now Donella, thanks for always being such great friends.

To those with whom I play netball with, Kim, Rob, Laima and Ruth, go Pathos! To those that I tried to play basketball with, Wayne, Jarrod, Randal, Jeremy, Liz, Emma & Guy, it was definitely fun. Tony and Laima, thanks for the water skiing weekends and for making everything in the department run so smoothly. Most of all thank you all for your friendship

My friends outside the department, you know who you are, thanks for your encouragement and understanding especially over the last few months.

To my family, Steve, thanks for always being not only my brother but also my friend. Mum and Dad, thanks for your support and encouragement over all these years and for making sure I got an education, but mostly for giving me everything that you possibly could. Mum, thanks for always making me feel like I was never alone, especially on all those nights, over the many years I have studied, where you stayed up and helped me, this thesis is as much your accomplishment as mine.

Last but definitely not least, to Brett, my husband, my best friend, thank you for all your support over the many years that I have studied and for always understanding, my love always.

SUMMARY

The studies presented in this thesis outline the synthesis and characterisation of a number of novel imidazoline compounds, some of which have potent actions at vascular K_{ATP} channels.

Their potency as K_{ATP} channel antagonists was determined by their ability to antagonise levcromakalim-induced relaxation in pig isolated coronary arteries. It was observed that many of the compounds were as potent as the sulphonylurea compound, glibenclamide. In addition, they did not affect relaxation to sodium nitroprusside, indicating the inhibition was specific for K_{ATP} channels. IMID-4F, was also found to inhibit levcromakalim-induced hyperpolarisation and vasorelaxation in rat isolated mesenteric arteries. These findings suggested that the antagonism of vascular K_{ATP} channels was not tissue or species specific.

Many of the IMID compounds caused bradycardia in the rat isolated spontaneously beating right atria, however, the bradycardic actions of these compounds were some 300 fold less potent than their antagonism of vascular K_{ATP} channels.

It was found that several of IMID compounds induced vasorelaxation in both pig isolated coronary arteries and rat mesenteric arteries precontracted with U46619, acetylcholine, phenylephrine or K^+. The K_{ATP} channel antagonist, TPP, the soluble guanylate cyclase inhibitor, ODQ or the β-adrenoceptor antagonist, propranolol did not affect the vasorelaxation to IMID-35MO/O. However, in radioligand binding studies only the six imidazoline analogues that caused vasorelaxation significantly inhibited binding of [^{3}H]-PN200-110, an L-type calcium channel antagonist to rat cerebral cortex membranes. These results indicated the vasorelaxation was probably due to antagonism of L-type calcium channels in the vasculature.

Additional radioligand binding studies were performed to assess the ability of the IMID compounds to displace binding of the α_1-and α_2-adrenoceptor antagonists, [^{3}H]-prazosin and [^{3}H]-rauwolscine, and the muscarinic antagonist, [^{3}H]-QNB, to rat cerebral cortex membranes. A small number of the imidazoline analogues were found to have activity at muscarinic receptors, while the majority were found to have activity at α_1- and α_2-adrenoceptors. However, as with their calcium channel antagonism, the concentration range in which they were active was 100 fold higher than their K_{ATP} channel antagonism.

In studies carried out to investigate the site of action of the imidazolines it was found that the majority of the imidazoline compounds did not displace binding of [^{3}H]-P1075 or [^{3}H]-glibenclamide to the opener or blocker sites of the K_{ATP} channel, respectively. This indicated they may, in fact, be causing their antagonism at the pore of the K_{ATP} channel, $K_{IR}6.x$.

Assessment of the effects of the imidazoline analogues on cardiovascular parameters including mean arterial pressure (MAP) and heart rate was performed in the anaesthetised rat. Many of the IMID compounds caused a reduction in both MAP and heart rate but only at the higher concentrations tested (3-10 μmol/kg).

The effects of the imidazoline analogues at pancreatic K_{ATP} channels was examined by determining their effects on blood glucose and insulin levels. Several of the IMID compounds actually increased blood glucose and decreased insulin levels. However, this effect is most likely due to their actions at α_2-adrenoceptors, as the α_2-adrenoceptor antagonist, rauwolscine, attenuated these responses.

In the presence of rauwolscine, IMID-4F induced a reduction in blood glucose and an increase in insulin levels similar to that of glibenclamide, indicating that IMID-4F may antagonise pancreatic K_{ATP} channels.

In conclusion, the assessment of novel imidazolines in this thesis, resulted in the identification of several potent K_{ATP} channel antagonists. These compounds appear to inhibit K_{ATP} channels via the channel pore, the K_{IR} subunit and the majority appear to be vascular selective. Although these compounds possessed actions at other receptor sites they were approximately 100 fold more potent at K_{ATP} channels.

ABBREVIATIONS

Abbreviations commonly used in this thesis:

ACh	Acetylcholine
ADP	Adenosine diphosphate
ANOVA	Analysis of Variance
AR	Activity Ratio; = antilog(pK_B - pD_2)
ATP	Adenosine triphosphate
$[ATP]_i$	Intracellular ATP
B_{max}	Density of the binding sites
bpm	Beats per minute
cAMP	cyclic adenosine monophosphate
CR	the concentration ratio of the concentration of an agonist that produces a specified response in the presence and absence of antagonist
DNA	Deoxyribonucleic acid
dpm	Disintergrations per minute
EC_{50}	Molar concentration of an agonist that causes 50 % of the maximal response of that agonist
EtOH	Ethanol
ESI	Electrospray mass spectroscopy
IC_{50}	Molar concentration of an antagonist that reduces specified responses to 50 % of its former value
IPC	Ischaemic preconditioning
I-	Imidazoline receptor
i.p.	Intraperitoneal injection
i.v.	Intravenous injection
K_{ATP}	ATP sensitive potassium channel
K_D	Dissociation constant; molar concentration of an agent (agonist or antagonist) that occupies 50 % of a receptor population
K_{IR}	Inwardly rectifying potassium channel
KPSS	Potassium depolarising solution
LKM	Levcromakalim

MAP	Mean arterial pressure
MeOH	Methanol
NDP	Nucleotide diphosphate
NMR	Nuclear Magnetic Resonance
PKA	Protein Kinase A
PKC	Protein Kinase C
pD_2	$= -\log(EC_{50})$
pK_B	= -log([antagonist concentration (M)] / [Concentration ratio −1]
pK_D	$= -\log (K_D)$
SNP	Sodium nitroprusside
SUR	Sulphonylurea receptor
TLC	Thin layer chromatography

PUBLICATIONS

The work in thesis has resulted in the following publications:

Refereed journal articles:

Bell, K.L., Papanastasiou, M., Campi, E., Jackson, R. & McPherson, G.A. (2001) The K_{ATP} channel and calcium channel antagonism of a novel series of mono- and bis-substituted imidazolines. *Naunyn-Schmeideberg's Archives of Pharmacology,* (in press).

Bell K.L., Favaloro, J.L., Khalil, V., Iskander, M.M. & McPherson, G.A. (2000). The identification of a potent imdazoline based K_{ATP} channel antagonist. *Naunyn-Schmeideberg's Archives of Pharmacology,* **362,** 145-151.

McPherson, G.A., **Bell, K.L.,** Favaloro, J.L., Kubo, M. & Standen, N.B. (1999). Functional and electrophysiological effects of a novel imidazolidine-based K_{ATP} channel blocker, IMID-4F. *British Journal of Pharmacol*ogy, **128,** 1636-1642.

Communications:

Andrews, K.L. & McPherson G.A. (2001). Pharmacological actions of novel di-substituted imidazolines. *Proceedings of the Western Society of Pharmacology (*in press).

Bell, K.L. & McPherson G.A. (2000). Pharmacological actions of novel di-substituted imidazolines. *Proceedings of the Australasian Society of Clinical and Experimental Pharmacology and Toxicology,* **8,** pg 93.

Bell, K.L. & McPherson G.A. (1999). A novel series of imidazolines with calcium channel blocking actions. *Proceedings of the Australasian Society of Clinical and Experimental Pharmacology and Toxicology,* **6,** pg 74.

Bell, K.L. & McPherson, G.A. (1998) The effects of a novel imidazolidine on heart rate, blood pressure and blood glucose in the anaesthetised rat. *Naunyn-Schmeideberg's Archives of Pharmacology.* **358** Suppl 2 pg R634.

Bell, K.L., Favaloro, J.L., Mclean, E. & McPherson, G.A. (1998). Assessment of the imidazolidine-derivative IMID-35MO at vascular K_{ATP} channels. *Proceedings of the Australasian Society of Clinical and Experimental Pharmacology and Toxicology,* **5,** pg 22.

Favaloro, J.L., **Bell, K.L.**, Mclean, E. & McPherson, G.A. (1998). Effect of the imidazolidine-derivative IMID-4F on K_{ATP} activity. *Proceedings of the Australasian Society of Clinical and Experimental Pharmacology and Toxicology,* **5,** pg 22.

Bell, K.L. & McPherson, G.A. (1997). The effects of novel imidazolidines on heart rate, blood pressure and blood glucose in the anaesthetised rat *Proceedings of the Australasian Society of Clinical and Experimental Pharmacology and Toxicology,* **4,** pg 55.

Other publications by the author:

Bell, K.L., Sutherland, S.K. & Hodgson, W.C. (1998). A pharmacological examination of venom from the inland taipan (*Oxyuranus microlepidotus*). *Toxicon,* **36,** 63-74.

Bell, K.L., Kemp, B.K., McPherson, G.A. & Hodgson, W.C. (1999). The smooth muscle relaxant effects of the venom from the inland taipan (*Oxyuranus microlepidotus*). *Toxicon,* **37,** 229-231.

Chapter One

General Introduction

1.1 Potassium (K^+) Channels

Potassium channels are the largest and most diverse family of ion channels and are involved, in some way or another, in the cellular function of most organisms. Indeed, K^+ channels of similar structure have been identified, not only in animals ranging from jellyfish to humans, but also in plants, yeast and bacteria (Jan & Jan, 1997). Within any one organism, the same K^+ channels can often have very diverse functions depending on the cell type. In addition, it is not uncommon to find several types of K^+ channels in any given cell performing completely different roles (Salkoff *et al.*, 1992).

Due to the widespread utilisation of K^+ channels in the regulation of cellular function, a great deal of research has focussed on both the functional properties and on endogenous and exogenous regulators of K^+ channels. Moreover, the possible therapeutic role of targeting K^+ channels, and their endogenous modulators, has resulted in the development of many compounds that can selectively regulate their actions (Grissmer, 1997). Over the last ten years, this research has also been supported by the development of new electrophysiological and molecular biology techniques and consequently, a much better understanding of the structure, function and classification of K^+ channels has been obtained.

The extensive investigations of K^+ channels have relied upon the development of tissue selective, high affinity modulators of K^+ channels, that are important, not only in determining the functional role of the channel, but also its regulation. This thesis involves the design, synthesis and investigation of a number of novel imidazoline compounds which have potent antagonist actions at a specific K^+ channel, the ATP-sensitive K^+ (K_{ATP}) channel. To this end, the following discussion will focus upon the

molecular structure and functional properties of K^+ channels followed by a more in depth discussion of K_{ATP} channels and their regulators.

1.1.1 Classification of K^+ channels

Until recently, K^+ channels were sub-classified based upon their physiochemical properties (eg. conductance) and the factors that regulate their activity. For example, the voltage-sensitive K^+ channels are regulated, as their name suggests, by changes in the membrane potential, Ca^{2+}-sensitive K^+ (K_{Ca}) channels are sensitive to intracellular calcium levels, while the ATP-sensitive K^+ (K_{ATP}) channels are sensitive to intracellular adenosine triphosphate (ATP) levels. The sub-classification of potassium channels based upon their functional properties is shown in Table 1.1 (Watson & Girdlestone, 1999). As is apparent from Table 1.1, the sub-classification of K^+ channels based on their physiochemical properties has resulted in the identification of at least 14 separate subtypes and there are many sub-classifications within these major divisions.

Recent advances in molecular biology have resulted in the cloning and protein sequencing of K^+ channels. These techniques have provided a breakthrough in classification, as it appears that all K^+ channels fundamentally belong to one of two major superfamilies; superfamily one and superfamily two. Superfamily one constitutes the group of K^+ channels which are voltage-sensitive, while superfamily two contains the group which display inwardly rectifying properties (for reviews see Edwards & Weston, 1995; Jan & Jan, 1997).

K^+ Channel Type	Nomenclature	Regulation	Conductance (pS)
Voltage sensitive			
A-channel	K_A	Rapid activation and inactivation	<1-20
Delayed rectifier	K_V	Delayed activation, slow inactivation	<1-20
Rapid delayed rectifier	K_{VR}	Rapid activation	<1-20
Slow delayed rectifier	$K_{V(s)}$	Very slow activation and inactivation	?
Sarcoplasmic reticulum channel	K_{SR}	Strong voltage-sensitivity, low K^+/Na^+ selectivity	180
Ca^{2+}-sensitive			
High conductance Ca^{2+}-activated K^+ channel	BK_{Ca}	Voltage-sensitive	100-250
Intermediate conductance Ca^{2+}-activated K^+ channel	IK_{Ca}	Little or no voltage-sensitivity	18-50
Small conductance Ca^{2+}-activated K^+ channel	SK_{Ca}	Little or no voltage-sensitivity	6-14
Receptor-coupled			
M-current	K_M	Time-dependent & voltage-sensitive, slow activation, non-inactivating	5-18
Atrial muscarinic-activated	K_{ACh}	Voltage-sensitive and inwardly rectifying	7-50
Miscellaneous			
Inward rectifier	K_{IR}	Mg^{2+} and intracellular polyamines	5-30
Cell volume-sensitive	K_{Vol}	Increased cell volume	16-40
Na^+-activated	K_{Na}	Voltage-insensitive	220
ATP-sensitive	K_{ATP}	ATP-inhibited, nucleoside diphosphate-facilitated, inward rectifying, pH-sensitive.	5-90

Table 1.1 A summary of the K^+ channels classified using their electrophysiological properties, their standard nomenclature, the way in which the channel is regulated and conductance (Watson & Girdlestone, 1999).

It has been proposed that, some 700 million years ago, potassium channels belonged to the one family, which was voltage sensitive. These channels consisted of six membrane spanning α-subunits and a pore forming 'P' region that is similar to the voltage-sensitive K^+ channels (superfamily one) observed today (Figure 1.1; Christie, 1995). The fourth membrane spanning subunit was thought to be the voltage sensor for the channel. The inwardly rectifying superfamily (superfamily two) resulted from the deletion of four of the membrane spanning segments including the voltage sensor (see Figure 1.1). This altered the gating of the channel from outward to inwardly rectifying (Christie, 1995). Other ion channels, such as cyclic nucleotide-gated (CNG), Na^+ and Ca^{2+} channels, and receptors such as the purinergic receptor, are also thought to have arisen from the ancestral potassium channel. This information lead to the new method of classification that will now be briefly discussed with particular focus on superfamily two as it contains the K_{ATP} channel.

1.1.1.1 Superfamily One: Voltage Sensitive Potassium Channels

The differing functions of superfamily one, the voltage sensitive K^+ channels, are thought to be the result of events that culminated in different arrangements of subunits and associations with various intracellular β-subunits that conferred novel properties to each channel (Christie, 1995). The K^+ channels in this family include the 'A'-channel (K_A), the large conductance Ca^{2+}-sensitive (BK_{Ca}) channel and the delayed rectifier (K_V) channel. The basic structure of this family is shown in Figure 1.2a. The α-subunit is thought to consist of six transmembrane-spanning segments (S1-S6), of

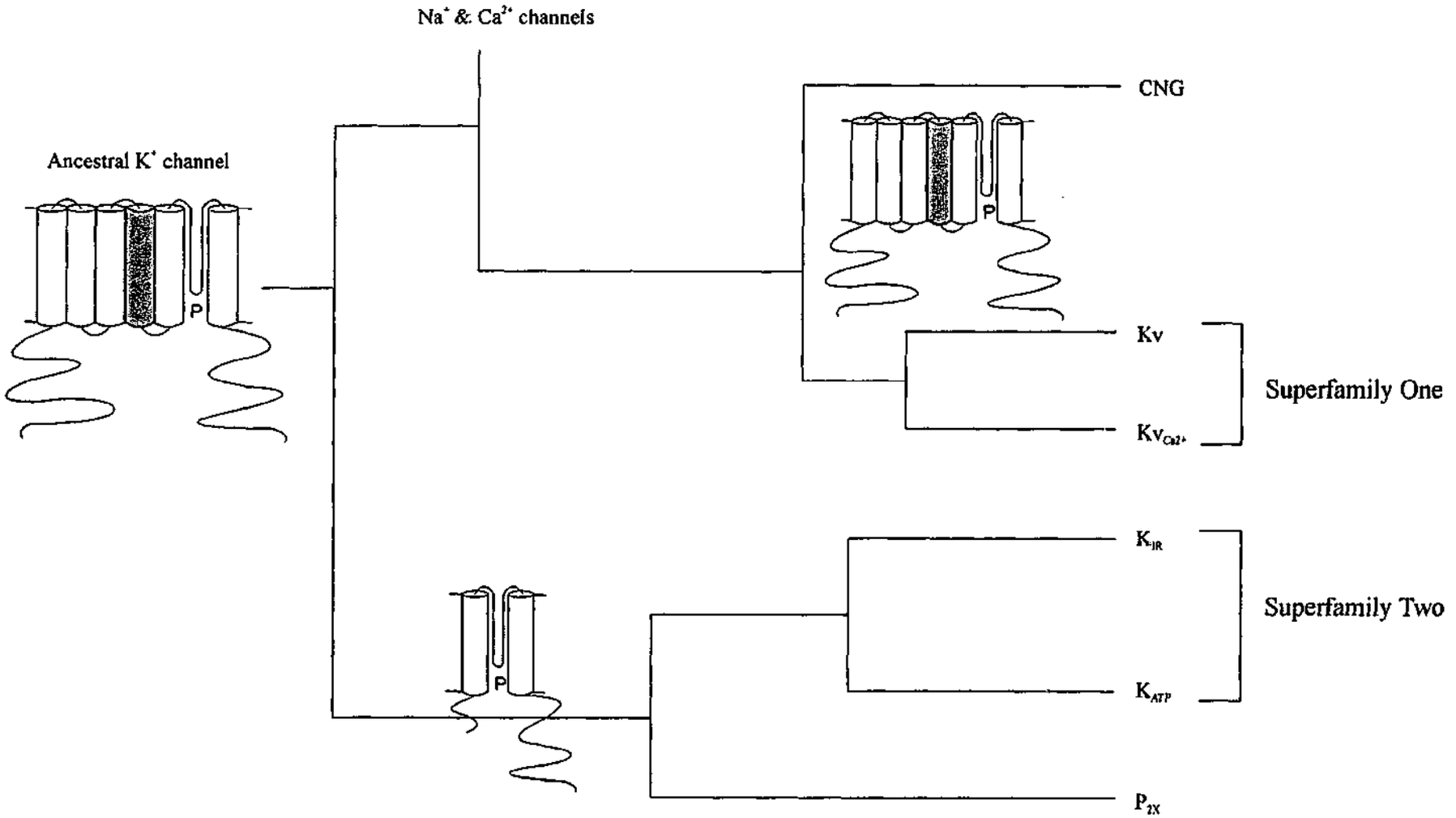

Figure 1.1 An evolutionary schema of K^+ channels and the predicted membrane topology including the voltage sensor and pore forming region (adapted from Christie, 1995).

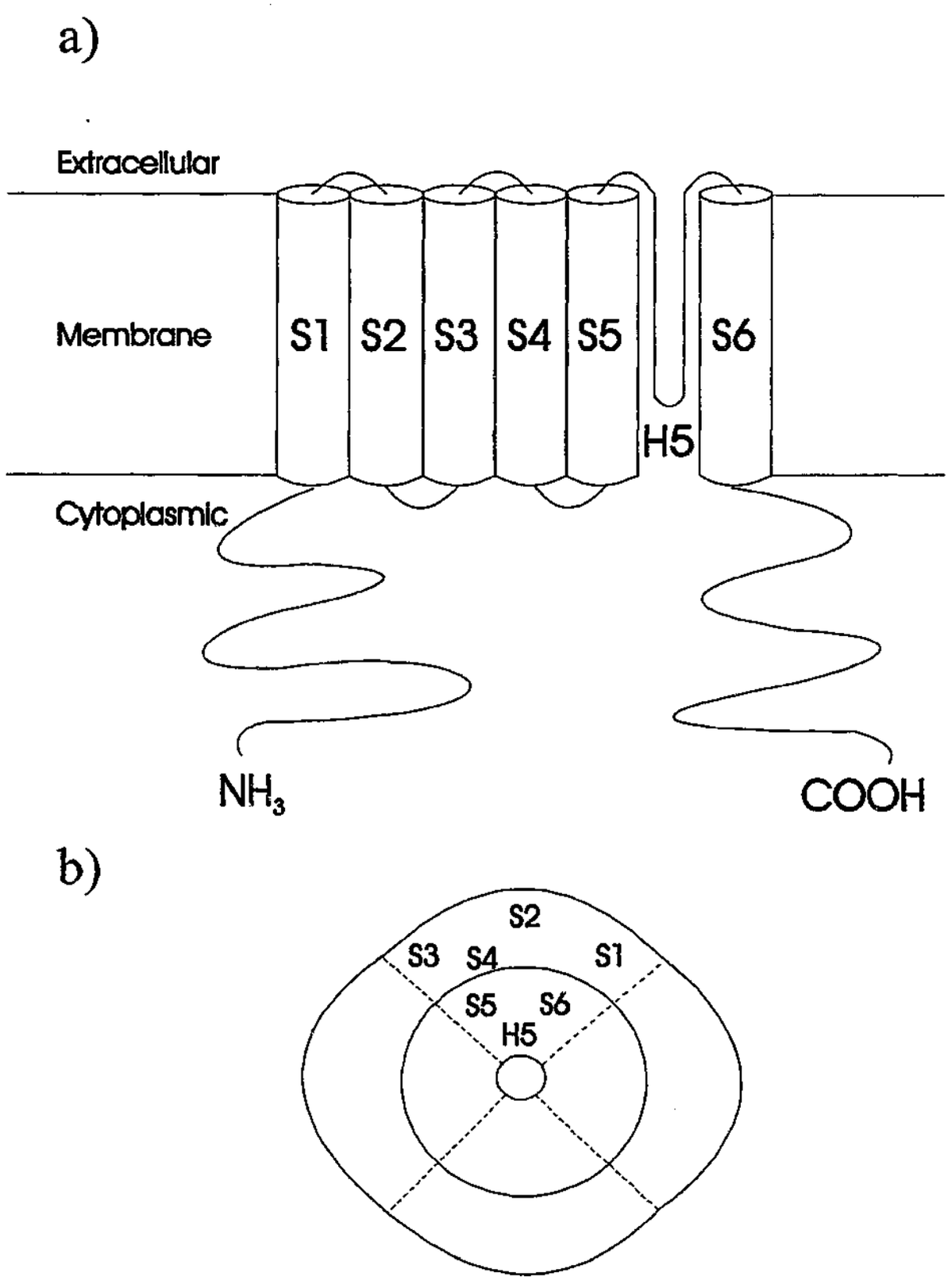

Figure 1.2 Schematic representation of the voltage sensitive potassium channel family illustrating a) the proposed transmembrane topology and b) the proposed stoichiometry (adapted from Garcia *et al.*, 1997; Jan & Jan, 1997).

which S4 has been postulated to act as a voltage sensor (Pongs, 1992; Salkoff *et al.*, 1992), a likely pore forming hairpin loop (H5) and a cytoplasmic N- and C- terminus. Structurally K^+ channels consist of 4 α- subunits at their core position, which make up the channel. Figure 1.2b illustrates the proposed membrane stoichiometry of four α subunits arranged together to form a pore.

1.1.1.2 Superfamily Two: Inwardly Rectifying Potassium Channels

Superfamily two comprises the K_{IR} channels and includes the K_{ATP} channel. Figure 1.3a illustrates the basic structure of the inwardly rectifying potassium channels. Like the voltage sensitive potassium channels, they also contain 4 α-subunits, the same likely pore forming hairpin loop (H5) and cytoplasmic N- and C- terminal domains. However, they have only two membrane-spanning segments, M1 & M2 (Jan & Jan, 1994). The K^+ sensor for these channels may involve the H5 segment since a mutation of the conserved glycine in this segment eliminates the selectivity (Slesinger *et al.*, 1996). The M2 segment is also thought to have a very important role in the K^+ channel conductance as well as regulating the effects of magnesium and polyamines (Stanfield *et al.*, 1994; Wible *et al.*, 1994).

The channels in this family have cDNAs, which are approximately 370-500 amino acids in length with the central 350 amino acids being highly conserved. The amino acids of the carboxy and amino termini are thought to be located on the intracellular side of the membrane where the four subunits converge to form an operating channel (Figure 1.3b). These termini are also highly variable and it is this

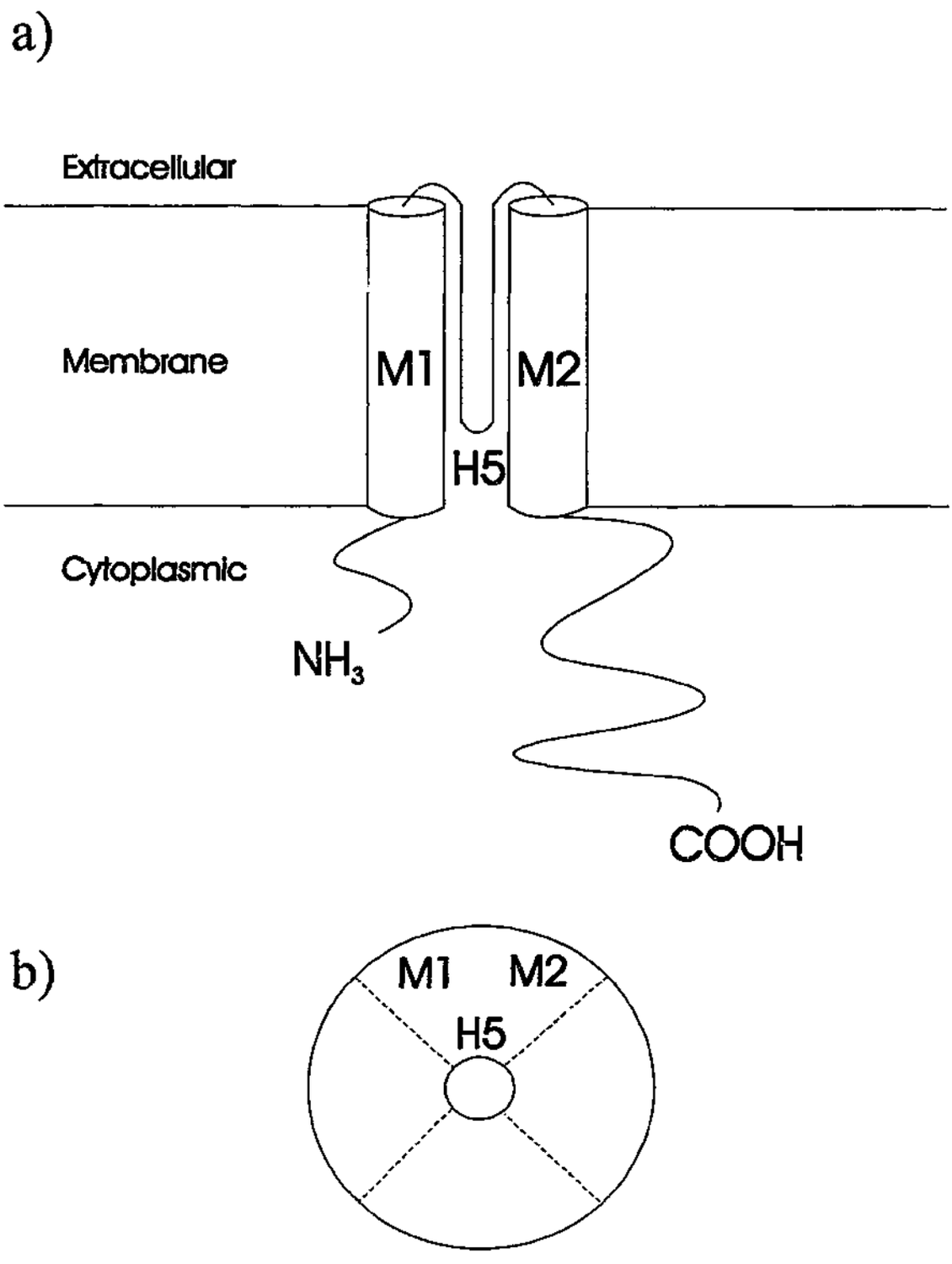

Figure 1.3 Schematic representation of the inward rectifier potassium channel family illustrating a) the proposed transmembrane topology and b) the proposed stoichiometry (adapted from Garcia *et al.*, 1997; Jan & Jan, 1997).

variability which allows the classification of the K_{IR} family into six subfamilies, $K_{IR}1.0$ to $K_{IR}6.0$ (Chandy & Gutman, 1993). Within each subfamily of K_{IR}, there are further subtypes. For example, the $K_{IR}2.0$ subfamily contains subtypes $K_{IR}2.1$, $K_{IR}2.2$ and $K_{IR}2.3$ (Doupnik *et al.*, 1995). Each of the six subfamilies has greater than 70 % sequence homology within them. Between them there is approximately 40 % sequence homology. Although all are inward rectifiers, the degree of inward rectification differs. When the membrane potential is more positive (depolarised), the channel conducts K^+. Strong inward rectifiers conduct less K^+ and therefore, less outward current than weak inward rectifiers. $K_{IR}2.0$, 3.0 and 4.0 are strong inward rectifiers, and $K_{IR}1.0$, 5.0 and 6.0 exhibit only weak inward rectification (for review see Doupnik *et al.*, 1995). The K_{ATP} channel is formed by the association of a $K_{IR}6.x$ channel with a β-subunit, the sulphonylurea receptor (SUR) (Inagaki *et al.*, 1995a). As already mentioned, it is the K_{ATP} channel that is at the centre of the work presented in this thesis and will be discussed in greater detail.

1.2 ATP-Sensitive K^+ Channels

In 1983, Noma identified, in cardiac cells, specific K^+ channels that were inhibited by intracellular ATP at levels greater than 1 mM. Since then, K_{ATP} channels have been identified in a wide variety of tissues throughout the human body, including the pancreatic β-cell (Ashcroft *et al.*, 1984; Cook & Hales, 1984; Rorsman & Trube, 1985), skeletal muscle (Spruce *et al.*, 1985; 1986), the CNS (Ashford *et al.*, 1988), the kidney (Gogelein & Greger, 1987; Parent *et al.*, 1988) and in vascular smooth muscle (Quast & Cook, 1988). In the last 10 years, these channels have also been found in

follicular cells (Honore & Lazdunski, 1991), the mitochondrial inner membrane of rat liver (Inoue *et al.*, 1991) and cardiomyocytes (Paucek *et al.*, 1992).

The functions of K_{ATP} channels are very diverse. For example, in the pancreas, where their role is best understood, K_{ATP} channels regulate insulin secretion (Dunne *et al.*, 1994; see Section 1.3.1). In smooth and cardiac muscle, they may contribute to the resting membrane potential and more importantly, regulate cell function under conditions of metabolic stress (see Section 1.3.3). They are also the target of a number of endogenous regulators (see Section 1.3). Because K_{ATP} channels can be modulated by both endogenous regulators and metabolic stimuli, they have the potential to be important therapeutic targets in a number of pathophysiological conditions in man including hypertension, arrhythmia and diabetes mellitus (for review see Quayle *et al.*, 1997).

1.2.1 Molecular Structure

K_{ATP} channels are characterised by a unique pharmacology, electrophysiology and molecular structure. The K_{ATP} channel is an octomeric (4:4) complex constructed from two distinct subunits (Figure 1.4a). The pore, or channel, is formed from a subunit belonging to the inwardly rectifying K^+ channel family, $K_{IR}6.x$. To form a functional channel, it requires association with a second subunit, the sulphonylurea receptor (SUR), which regulates the channel through an interaction with nucleotides and drugs (Figure 1.4b; Clement *et al.*, 1997; see Section 1.2.1.2).

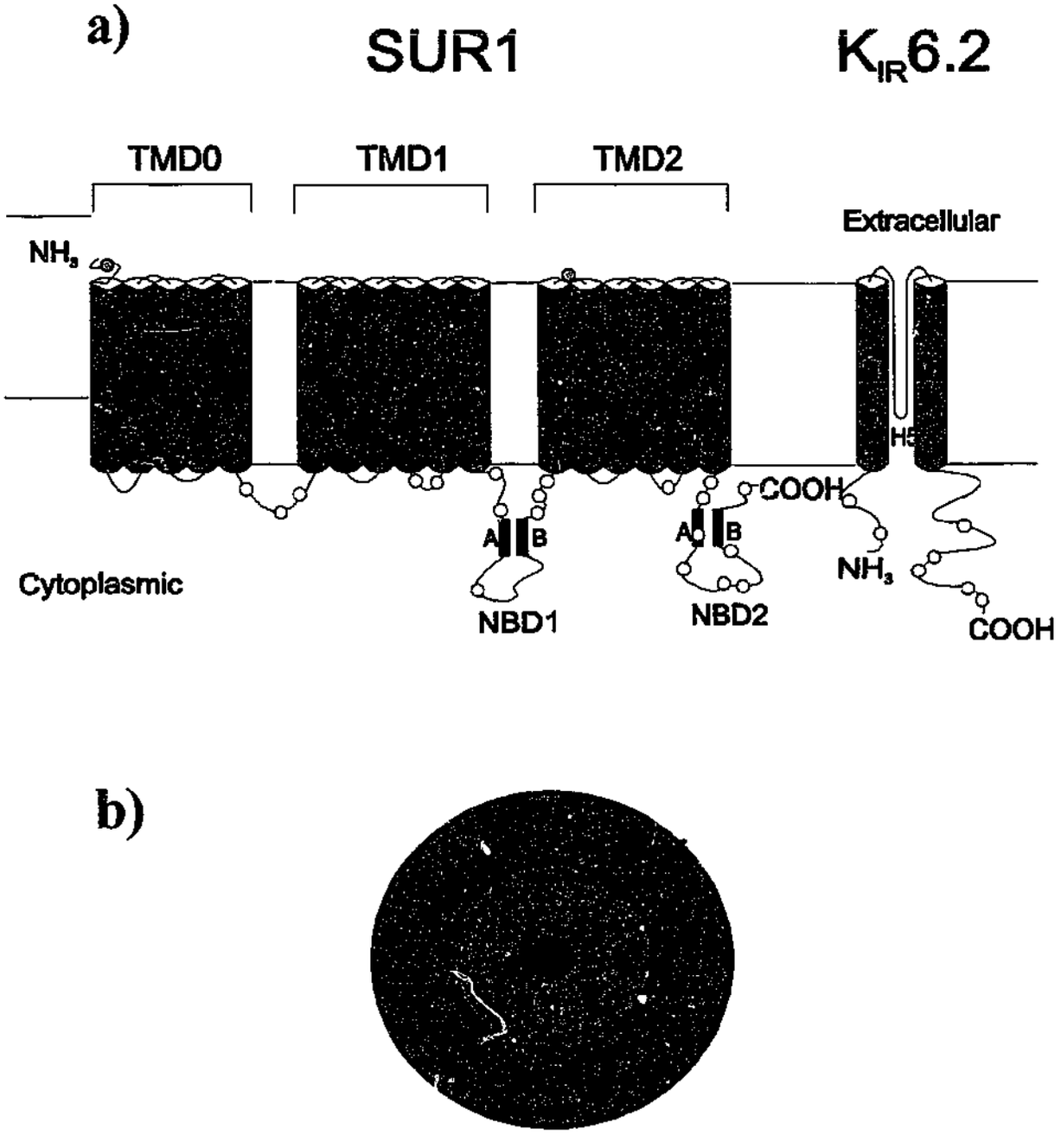

Figure 1.4 Schematic representation of a) the membrane structure of SUR1 and $K_{IR}6.2$ which collectively form a K_{ATP} channel. SUR1 is thought to have 3 transmembrane spanning domains, TMD0, TMD1 and TMD2. Walker A & B motifs are indicated by the boxes (▌); COOH and NH_3 indicate the C and N terminals, respectively. The K_{ATP} channel has several potential protein kinase A- (○) and protein kinase C- (○) dependent phosphorylation sites and 2 proposed N-linked glycosylation sites (◉) (adapted from Seino, 1999). b) The stoichiometry of the K_{ATP} channel with 4 subunits of $K_{IR}6.2$ surrounded by 4 subunits of SUR1 (adapted from Jan & Jan, 1997).

1.2.1.1 $K_{IR}6.x$

Two K_{IR} genes have been identified which form K_{ATP} channels with SURs. The first of the two K_{IR} genes to be identified thus far was cloned by Inagaki and coworkers (1995a) from a rat cDNA library and named $K_{IR}6.1$ or uKATP-1. It showed 43-46 % homology with the $K_{IR}1.0$-5.0 subfamilies and was broadly distributed, although surprisingly it was not found in the pancreas. $K_{IR}6.1$ is a 424 amino acid protein with a K_{IR} structure of 2 putative transmembrane regions (M1 & M2) and a highly conserved H5 region. $K_{IR}6.1$ were thought to function as K_{ATP} channels in their own right since they were inhibited by ATP and activated by diazoxide but not sulphonylureas (Inagaki *et al.*, 1995a) . However, in more recent studies using HEK293 (Ämmälä *et al.*, 1996b) and *Xenopus* oocytes (Gribble *et al.*, 1997b), it was shown that both the $K_{IR}6.1$ and the sulphonylurea receptor (see Section 1.2.1.2) were obligatory to express functional K_{ATP} channels.

Homology screening with $K_{IR}6.1$ resulted in the cloning of an isoform with 71% sequence homology named, $K_{IR}6.2$ or BIR (Inagaki *et al.*, 1995b). $K_{IR}6.2$ is strongly expressed in pancreatic β-cells, heart, skeletal muscle and the CNS. It is a 390 amino acid protein with a K_{IR} structure of two putative transmembrane regions (M1 & M2) and a highly conserved H5 region.

Both $K_{IR}6.1$ and $K_{IR}6.2$ have an asparagine in the M2 position 172, which is an indication of their weak rectification, two possible locations for phosphorylation by adenosine 3',5'-cyclic monophosphate (cAMP)- dependent protein kinase and several possible locations for phosphorylation by protein kinase C (PKC) and protein kinase A (PKA) (Figure 1.4a). It was first thought that they didn't show an apparent sequence for ATP binding (Inagaki *et al.*, 1995a,b; Sakura *et al.*, 1995), yet, new evidence suggests this is not the case and this will be discussed shortly in Section 1.2.2.1.

1.2.1.2 Sulphonylurea receptors (SUR)

The cloning of the β–cell SUR in the pancreas in 1995 by Aguilar-Bryan and coworkers was a significant finding as it demonstrated that SUR (later renamed SUR1) was an integral part of the K_{ATP} channel. It was first thought that the SUR1 would be a typical ion channel protein, however, it has since been shown to be a member of the ATP-binding cassette (ABC) protein superfamily (Aguilar-Bryan *et al.*, 1995). This superfamily of proteins is found in organisms ranging from bacteria through to humans. In man, mutations in this superfamily have resulted in a number of disorders including cystic fibrosis, adrenoleukodystrophy and familial hyperinsulinism (Dean & Allikmets, 1995).

Even though SUR1 itself produced high affinity sulphonylurea binding it did not show channel activity on its own. Therefore, it has been postulated that it requires another subunit to allow ion flow to occur (Aguilar-Bryan *et al.*, 1995). When $K_{IR}6.2$ and SUR1 were co-expressed in mammalian cells (Inagaki *et al.*, 1995b; Sakura *et al.*, 1995) or in *Xenopus* oocytes (Gribble *et al.*, 1997b), functional K_{ATP} channel currents resulted. In addition, the finding that the tissue distribution, single channel conductance, kinetics, rectification properties, K^+ selectivity, inhibition by ATP and the pharmacological properties of the $K_{IR}6.2$/SUR1 complex were identical to those of native K_{ATP} channels, confirmed that the complex was indeed the K_{ATP} channel (Sakura *et al.*, 1995).

SUR1, which has affinity for sulphonylureas in the nanomolar range (Kaubisch *et al.*, 1982), was first thought to consist of 13 transmembrane segments in two groups of nine and four. However, it has recently been proposed by Tusnady and coworkers (1997) that it has 17 transmembrane segments (Figure 1.4a). This model suggests two transmembrane domains (TMD1 & TMD2) with six segments and another domain

(TMD0) with 5 segments ending in the N-terminal. Again, two nucleotide binding domains are proposed (NBF1 & NBF2) of which NBF1 is found between TMD1 and TMD2 and NBF2, in the C terminus. Each NBF has a Walker A and B motif which are believed to be the site of nucleotide regulation (see Section 1.2.2; Seino, 1999). In addition to two possible N-linked glycosylation locations and three-four PKA–dependent phosphorylation sites, there are numerous possible PKC–dependent phosphorylation sites, depending on the animal species (Tusnady *et al.*, 1997).

Another sulphonylurea receptor, SUR2, has also been identified. Two forms have been discovered, SUR2A and SUR2B, which are splice variants of a single gene differing only in their C terminal, the last 42 to 45 amino acids (Chutkow *et al.*, 1996; Inagaki *et al.*, 1996; Isomoto *et al.*, 1996). However, the splice variant, SUR2A, cloned by Chutkow (1996) is different from the SUR2A reported by Inagaki (1996) as it is missing an exon (14). Therefore, two different names have been proposed for the SUR2A cloned by Chutkow (1996), SUR2C by Ashcroft & Gribble (1998) or the more accurate SUR2AΔ14 by Babenko and colleagues (1998). SUR2A has an estimated affinity for sulphonylureas approximately 500 times lower than SUR1 and hence, it is known as the low affinity SUR. The molecular structure of SUR2A is very similar to SUR1, however it has three possible N-linked glycosylation locations and two PKA–dependent phosphorylation sites (Tusnady *et al.*, 1997).

1.2.1.3 K_{IR}/SUR Association

As mentioned briefly in Section 1.2.1, for a K_{ATP} channel to function, a K_{IR} channel and a SUR must combine with one another in a hetero-octameric complex (4:4). Generally speaking, the $K_{IR}6.x$ subunit gives the K_{ATP} channel its potassium selectivity,

inward rectification and unitary conductance and the SUR controls the pharmacology and the channel's receptiveness to nucleotides (see Section 1.2.2). Table 1.2 contains the subunit association proposed thus far. It must be noted that it is not known if all the isoforms of each subunit have been identified yet and that the classifications listed in the table are based only on the pharmacology of the channels.

1.2.1.3.1 SURx/K_{IR}6.1

Reconstitution studies have shown that K_{IR}6.1 can form a functional channel with SUR1 and SUR2A, but not SUR2B (Ämmälä *et al.*, 1996a; Aguilar-Bryan *et al.*, 1998). Although a native channel for SUR1/K_{IR}6.1 is yet to be identified, reconstitution of SUR1 with K_{IR}6.1 results in channels which are activated by metabolic inhibition and by diazoxide. However, the channel rundown is very fast and therefore recordings of channel currents have been difficult to achieve.

The combination of SUR2A/K_{IR}6.1 has not been shown to produce K^+ currents that are regulated metabolically, nor has it been found to be expressed natively (Aguilar-Bryan *et al.*, 1998).

The pairing of SUR2B/K_{IR}6.1 forms a channel with similar pharmacology to cloned K_{ATP} channels but with notable differences. For example, they are activated rather than inhibited by internal ATP and show no spontaneous channel openings (Yamada *et al.*, 1997). SUR2B/K_{IR}6.1 is believed to be the nucleotide diphosphate-dependent K^+ (K_{NDP}) channel first described by Beech and colleagues (1993b) and later by Zhang & Bolton (1995; 1996).

Tissue Type	K_{IR} subunit	SUR subunit	Reference
Pancreatic β-cell	$K_{IR}6.2$	SUR1	Inagaki *et al.*, 1995b; Sakura *et al.*, 1995
Neuronal	$K_{IR}6.2$	SUR1	Gopalakrishnan *et al.*, 1991; 1992
Cardiac	$K_{IR}6.2$	SUR2A	Inagaki *et al.*, 1996
Skeletal	$K_{IR}6.2$	SUR2A	Inagaki *et al.*, 1996
Smooth muscle	$K_{IR}6.2$	SUR2B	Isomoto *et al.*, 1996
	$K_{IR}6.1$	SUR1	Theoretical: not yet identified or reconstituted to date
Vascular smooth muscle (K_{NDP})	$K_{IR}6.1$	SUR2B	Yamada *et al.*, 1997
	$K_{IR}6.1$	SUR2A	Aguilar –Bryan *et al.*, 1998; reconstituted only, not functional

Table 1.2 The proposed subunit association of SURx/K_{IR}6.x and the tissues in which they are found.

1.2.1.3.2 SURx/K_{IR}6.2

The subunits of the pancreatic β-cell K_{ATP} channel have been identified as SUR1 and K_{IR}6.2 (Inagaki *et al.*, 1995b). This complex is sensitive to sulphonylureas at nanomolar concentrations (IC_{50} approximately 1 nM for glibenclamide) and activated by both diazoxide and metabolic inhibition. This channel subtype has also been identified in neuronal tissues (Kaubisch *et al.*, 1982; Gopalakrishnan *et al.*, 1991; 1992). It was first thought that the combination of SUR2A/K_{IR}6.2 would be found in the pancreatic β-cell since the currents and single channel conductance were the same (Inagaki *et al.*, 1996). However, the burst duration and the length of time between bursts were different (Alekseev *et al.*, 1997). In fact, when expressed together, K_{IR}6.2 and SUR2A display all the properties of K_{ATP} channels described in cardiac and skeletal muscle. They are less sensitive to ATP and glibenclamide than the β–cell K_{ATP} channel and they are sensitive to the cardiac K_{ATP} channel openers cromakalim and pinacidil but not diazoxide (Inagaki *et al.*, 1996; Okuyama *et al.*, 1998).

The expression of SUR2B/K_{IR}6.2 together exhibit pharmacology that is similar to K_{ATP} channels found in smooth muscle. Channels with this combination of subunits are activated by diazoxide and inhibited by glibenclamide and tolbutamide, although at significantly lower concentrations than SUR2A/K_{IR}6.2 (Isomoto *et al.*, 1996). Although this evidence is convincing, the tissue distribution of SUR2B and K_{IR}6.2 are not identical. Therefore, it must be questioned whether this combination of subunits is actually the smooth muscle K_{ATP} channel.

1.2.2 Regulation of K_{ATP} channels by ATP and ADP

K_{ATP} channel activity is characterised by bursts of activity in which the channel flickers between open and closed states. The open probability is dependent upon many factors including the binding of Mg^{2+} or polyamines to sites inside the channel (for review see Aguilar-Bryan & Bryan, 1999). ATP inhibits the channel by lengthening the time between opening and also decreasing the length of the burst, whilst magnesium adenosine diphosphate (MgADP) is thought to prolong the open state of the channel. How and where these nucleotides regulate the channel is still the subject of much debate. In the following sections the recent advances in this field will be briefly discussed.

K_{ATP} channels are unique as the majority of ion channels rely on intracellular ATP to sustain their activity since ATP is used as a substrate in phosphorylation of the channel. However, the K_{ATP} channel is distinct from these because non-hydrolysable analogues of ATP are also as effective as ATP (Babenko *et al.*, 1998). ATP and ADP have three major effects in the regulation of K_{ATP} channels; inhibition, stimulation and refreshment.

Inhibition

Intracellular ATP ($[ATP]_i$), with or without Mg^{2+}, is believed to be a major regulator of K_{ATP} channels. There are still conflicting theories, however, as to whether it is the sole regulator. The estimated IC_{50} value of ATP for reconstituted SUR1/K_{IR}6.2 channels and pancreatic β-cell K_{ATP} channels is 10 μM (Inagaki *et al.*, 1995b). Given that the cytosolic $[ATP]_i$ level is thought to be around 1 mM (Schwenke *et al.*, 1981), this amount of ATP would be sufficient to fully inhibit pancreatic β-cell K_{ATP} channels. Pancreatic K_{ATP} channels, however, can spontaneously open, thus ATP does not appear

to be the sole regulator (Cook & Hales, 1984). One of several possible explanations is that only unbound ATP^{4-} can cause inhibition, as the concentration of ATP^{4-} is more near the IC_{50} (Ashcroft & Kakei, 1989).

Stimulation

Generally, ADP and other nucleotide diphosphates (NDPs) stimulate K_{ATP} channels, but unlike the channel inhibition by ATP, Mg^{2+} is essential for this stimulation. When Mg^{2+} is not present, ADP inhibits the channel (Davies *et al.*, 1991; Nichols & Lederer, 1991). However, NDPs have different effects in different tissues. In smooth muscle cells they activate K_{ATP} channels, while in cardiac cells they can antagonise ATP as well as activate the channel (Quayle *et al.*, 1997).

Refreshment

Refreshment is the transformation of the channel from an inactive state, to an active one. When cells are bathed in an ATP-free solution, K_{ATP} channels show a loss of activity. This demonstrates that K_{ATP} channels require a small amount of ATP to be present constantly to prevent a loss of channel activity. Interestingly, the reintroduction of MgATP at millimolar concentrations or hydrolysable analogues of ATP without Mg^{2+} or Mn^{2+} will restore channel activity, whereas non-hydrolysable analogues alone have no effect (Takano & Noma, 1993).

1.2.2.1 Site of ATP regulation

The identity of the site at which ATP acts to inhibit the K_{ATP} channel is now clearer. Originally it was thought that the site for ATP binding was at the level of

SUR1 given SUR1 has two nucleotide binding domains and $K_{IR}6.2$ none (Aguilar-Bryan *et al.*, 1995; Inagaki *et al.*, 1995b). Indeed, high- and low-affinity ATP binding sites were identified on NBF1 and NBF2 respectively, via the finding that MgADP reduced the photolabelling of ATP (Ueda *et al.*, 1997). However, recent work by Tucker and colleagues (1997) has shown that when a truncated form of $K_{IR}6.2$, $K_{IR}6.2\Delta C$, is expressed without SUR1 the channel currents are still blocked by ATP, although with somewhat reduced potency (K_i = 100 μM). Also, several different mutations in $K_{IR}6.2\Delta C$ produced a large decrease in ATP sensitivity (K_i = ~ 4 mM) while leaving its ability to couple to SUR and other channel kinetics unaltered (Tucker *et al.*, 1997). Conversely, mutations in SUR1 did not significantly alter the ability of ATP to inhibit $K_{IR}6.2$/SUR1 channel currents leading to the proposal that SUR1 acts to sensitise $K_{IR}6.2$ to inhibition by ATP (Shyng & Nichols, 1998). Another theory is that SUR and $K_{IR}6.2$ assemble a shared ATP binding site (Babenko *et al.*, 1999). Therefore, it appears that the site for ATP regulation is most probably located on the K_{IR} subunit.

1.2.2.2 ATP/ADP ratio

The ATP/ADP ratio is thought to be important in the control of K_{ATP} channel activity. Several experiments have shown that in the absence of Mg^{2+}, ADP and other nucleotide diphosphates actually inhibited K_{ATP} channel currents. Furthermore, in channels that were inhibited by ATP, MgADP reactivated the channel current (Dunne & Peterson, 1986; Misler *et al.*, 1986). Many studies in pancreatic β-cells also strengthen the theory that ATP and ADP are closely linked (Ghosh *et al.*, 1991; Detimary *et al.*, 1996; Olson *et al.*, 1996). However, as mentioned previously, the study by Gribble and colleagues (1997a) demonstrated that mutations in the Walker A motif produced a K_{ATP}

channel that was still inhibited by ATP but not stimulated by MgADP. This indicated that the two may not be intimately linked, at least at the molecular level. Therefore, the evidence so far suggests that ATP maintains the channel in an operational state and oscillations in ADP are involved in regulation of the channel (Babenko *et al.*, 1998).

1.3 Endogenous regulators of K_{ATP} channels and their physiological function

There are a number of endogenous regulators of K_{ATP} channels within the body. As they vary between tissues the following discussion will focus upon these endogenous regulators in relation to the tissues in which they are active.

1.3.1 Pancreatic β–cell

The K_{ATP} channel is particularly important in the pancreatic β-cell where it regulates insulin secretion (Figure 1.5). In the resting state, the pancreatic β-cell is hyperpolarised, through the opening of K_{ATP} channels, below the threshold for insulin release. When glucose levels within the cell rise, oxidative phosphorylation within the mitochondria increases, leading to an increase in the synthesis of ATP. This elevation in ATP results in K_{ATP} channel inhibition. Subsequently, the cell membrane is depolarised and in turn, calcium channels opened. The resultant influx of Ca^{2+} ions triggers insulin secretion through exocytosis of insulin vesicles (Dunne *et al.*, 1994).

The glucose transporter (GLUT2), present in the β-cell membrane provides enough glucose for it to be used as the predominant fuel for ATP synthesis. Therefore this system provides a very accurate and sensitive regulator of blood sugar levels.

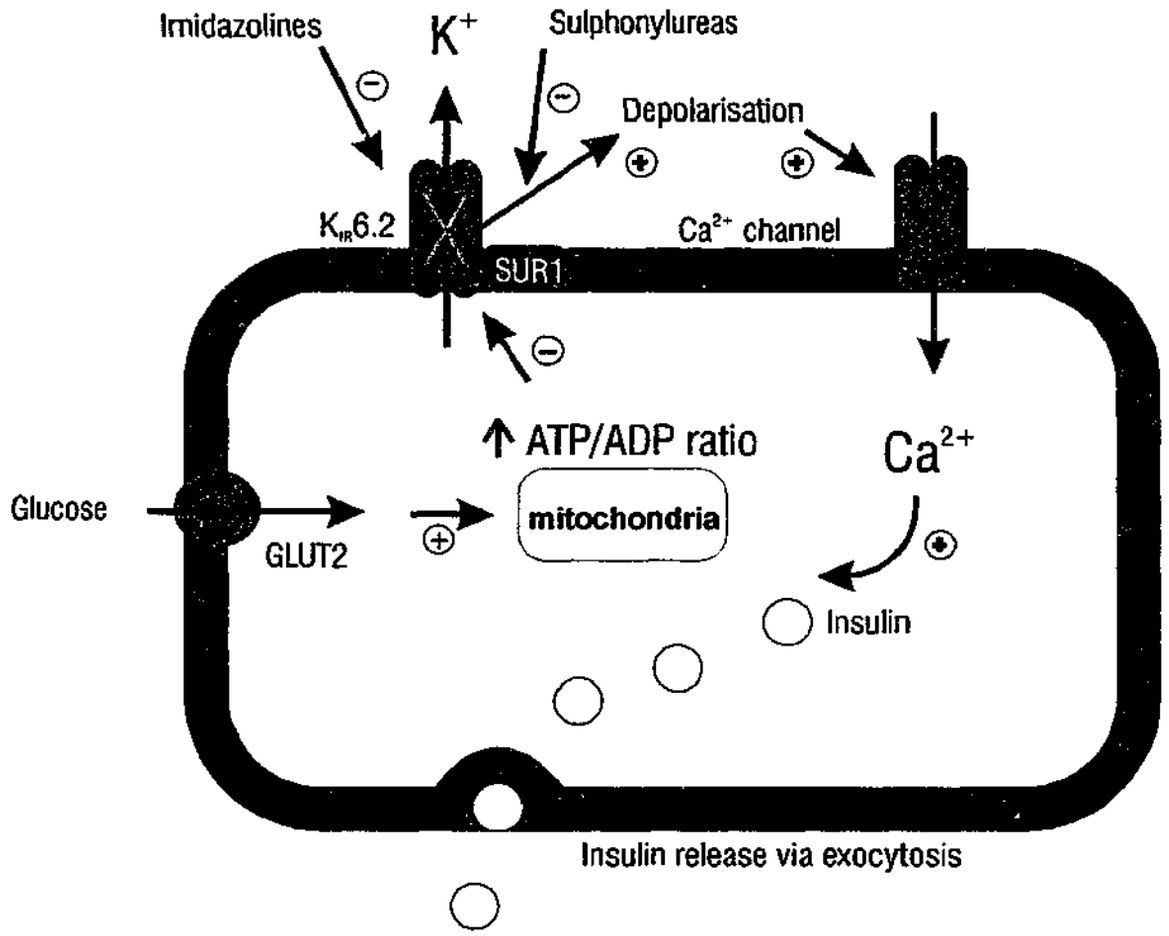

Figure 1.5 Schematic representation of the pancreatic β–cell illustrating the role of the K_{ATP} channel in the regulation of insulin release. An increase in glucose metabolism leads to an increase in oxidative phosphorylation and therefore ATP. The change in the ATP/ADP ratio causes the closure of K_{ATP} channels which in turn depolarises the membrane and opens Ca^{2+} channels. The increase in calcium within the cell induces the release of insulin (adapted from Horie *et al.*, 1997).

Clearly, the K_{ATP} channel presents itself as the primary target for the control of blood sugar when it is impaired by conditions such as diabetes mellitus (Type II). In fact, shortly after the K_{ATP} channel was first identified, work by Sturgess and coworkers (1985) and Trube and coworkers (1986) found that sulphonylureas antagonised pancreatic β-cell K_{ATP} channels. Presently, the principal drug used in the treatment of diabetes mellitus (Type II) is the sulphonylurea, glibenclamide. However, β-cell K_{ATP} channels have now been shown to be sensitive to a wide variety of other agents such as imidazolines (Schulz & Hasselblatt, 1988) and potassium channel openers (Trube *et al.*, 1986; Zünkler *et al.*, 1988) indicating that there may be other treatment options available.

1.3.2 Heart

As mentioned previously, specific K^+ channels that are depressed by intracellular ATP at levels greater than 1 mM, were first identified in cardiac cells by Noma in 1983. In the heart, K_{ATP} channels open when the $[ATP]_i$ falls resulting in hyperpolarisation of the membrane and closure of voltage sensitive calcium channels. This cascade results in attenuation of cardiac myocyte activity (Cason *et al.*, 1995). Nevertheless, this only seems to occur in periods of stress such as hypoxia or ischaemia (Nichols & Lederer, 1991).

Over the last decade there has been much debate on the role K_{ATP} channels in the heart in ischaemic preconditioning (IPC) and, even now, the mechanism is still not fully understood. IPC is a naturally occurring protective mechanism in the heart, which is triggered by a number of brief ischaemic incidents before a more prolonged ischaemic period. Mimicking this protective mechanism would be a great advantage to

patients suffering an infarct (Light, 1999). Several endogenous agents have been shown to induce IPC, namely adenosine, noradrenaline, angiotensin II and endothelin. What actually leads to preconditioning is thought to be the result of signal transduction downstream of adenosine receptor activation where the resultant PKC facilitates opening of K_{ATP} channels (Light *et al.*, 1996; Liu *et al.*, 1996).

The first hypothesis that K_{ATP} channels were involved in IPC came from Gross & Auschampach in 1992, when glibenclamide was found to eliminate preconditioning, and the preconditioning effect was mimicked by a potassium channel opener, aprikalim. Originally it was believed that the opening of surface K_{ATP} channels shortened the action potential duration, thereby reducing calcium influx and conserving energy (Schulz *et al.*, 1994; Terzic *et al.*, 1995). However, subsequent findings have shown that the shortening of the action potential is not actually involved in IPC (Yao & Gross, 1994; Grover *et al.*, 1996). These findings put into question the role of K_{ATP} channels in the sarcolemma and focused investigations onto the mitochondrial K_{ATP} channels. In fact, recent studies have shown that diazoxide, a potassium channel opener, targets mitochondrial but not sarcolemmal K_{ATP} channels and therefore, mitochondrial K_{ATP} channels may be the mediator in IPC (Garlid *et al.*, 1997; Liu *et al.*, 1999). Moreover, Sato and colleagues (1998) found that opening of mitochondrial K_{ATP} channels was hastened by a PKC activator. Therefore, K_{ATP} channels in the mitochondria of cardiac cells are now implicated as a target in myocardial ischaemia and possibly other pathophysiological conditions.

1.3.3 Vasculature

In the vasculature, K_{ATP} channels have a number of different roles depending on the vascular bed. These include metabolic regulation of blood flow, regulation during an ischaemic event such as hypoxia, and in some vascular beds, regulation of membrane potential under normal conditions (for review see Quayle *et al.*, 1997). Apart from their inactivation and activation by ATP and ADP respectively, they are also the target of a number of endogenous vasoactive substances.

In studies using cultured smooth muscle cells many endogenous vasoactive substances have been shown to inhibit K_{ATP} channels in cells, where the K_{ATP} channels currents have been activated by the K_{ATP} channel opener, pinacidil. These include neuropeptide Y (NPY), endothelin, angiotensin II, vasopressin, 5-HT, phenylephrine and histamine (Miyoshi & Nakaya, 1991; Miyoshi *et al.*, 1992; Wakatsuki *et al.*, 1992). In more detailed patch clamping studies using rabbit mesenteric artery it was shown that vasoconstrictors activate phospholipase C, which results in the production of diacylglycerol and the activation of PKC and inhibition of K_{ATP} channel currents (Bonev & Nelson, 1996). It must be noted however, that there have been limited studies in intact vessels to support these findings.

Substances that, at least in part, open K_{ATP} channels and cause membrane hyperpolarisation include calcitonin gene-related peptide (CGRP), adenosine and prostacyclin (Figure 1.6). They achieve this via the G protein, G_s, which causes an increase in cAMP and activation of PKA. The phosphorylation of PKA leads to the opening of K_{ATP} channels. It has been known for some time that when a tissue, such as the coronary artery, is exposed to harmful stimuli, adenosine activates K_{ATP} channels to increase blood flow and possibly decrease the damage to the tissue (Berne, 1980; Daut *et al.*, 1990). Activation of β-adrenoceptors (Randall & McCulloch, 1995) and CGRP

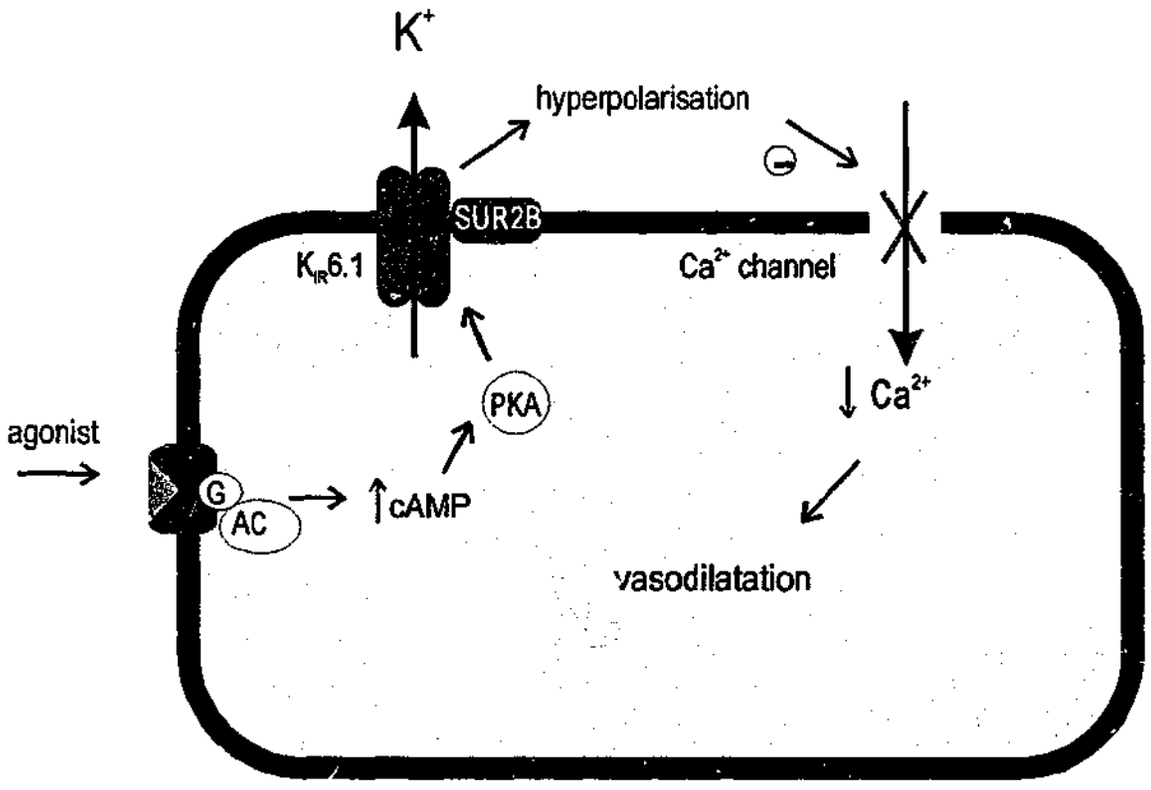

Figure 1.6 Schematic representation of a vascular smooth mucsle cell illustrating the proposed role of the K_{ATP} channel in the regulation of vascular tone by phosphorylation. An agonist (eg. adenosine) stimulates its receptor which activates adenylate cyclase (AC) activity in a G-protein (G) coupled pathway. There is an increase in cAMP and therefore protein kinase A (PKA) phosphorylation which results in the opening of K_{ATP} channel, hyperpolarisation and the inhibition of Ca^{2+} channels and finally, vasodilatation.

(Quayle & Standen, 1994) released from nerve terminals is also known to act in the same way. Endothelial-derived relaxing factors such as NO, EDHF and prostaglandins have all been shown to activate K_{ATP} channels under certain conditions (Garland & McPherson, 1992; Plane & Garland, 1993; Bouchard *et al.*, 1994). However, the hyperpolarisation caused by these factors in different vascular beds is not always glibenclamide sensitive, indicating that they do not activate K_{ATP} channels in all tissues.

There has been much debate on the role of K_{ATP} channels in the control of membrane potential and basal tone. Originally, studies such as that by Quast & Cook (1989) showed that inhibition of K_{ATP} channels by the antagonist, glibenclamide had little effect on resting blood pressure. However, *in vivo* studies assessing the effect of glibenclamide on vascular resistance and arterial diameter, and *in vitro* studies looking at its effects on membrane potential and vascular tone have indicated that this is not the case (Garland & McPherson, 1992; Imamura *et al.*, 1992; Samaha *et al.*, 1992). In fact, there have now been numerous studies in the coronary circulation showing that glibenclamide depolarises the smooth muscle, generally depolarising small arteries more than large arteries (Eckman *et al.*, 1992; Klieber & Daut, 1994).

Hypercapnia, or the increase in arterial carbon dioxide, is known to cause extracellular acidification and subsequently, a change in extracellular pH and vascular dilatation (Wray, 1988). The dilatation has been shown to be the result of hyperpolarisation of the membrane and increased permeability to K^+ (Harder & Madden, 1984). There is now evidence that this involves K_{ATP} channels, as several studies have shown this hypercapnia mediated dilatation to be sensitive to glibenclamide (Faraci *et al.*, 1994; Ishizaka & Kuo, 1996; Kontos & Wei, 1996). In a recent study, both pertussis toxin, an inhibitor of G proteins, and glibenclamide were

found to attenuate acidosis-induced dilatation in pig coronary arteries suggesting an opening of K_{ATP} channels through the activation of G proteins (Ishizaka *et al.*, 1999).

Vascular hypoxia is the fall in oxygen tension in a given blood vessel, resulting in dilatation and increased blood flow. Therefore, a mechanism linking blood flow and metabolic requirement must be present. Daut and coworkers (1990) first suggested that K_{ATP} channels were involved in this process when they showed that the vascular hypoxia response was sensitive to glibenclamide in guinea pig hearts. Adenosine, released in response to hypoxia, has been shown to have a predominant role in the vasodilatation, by acting through K_{ATP} channels (Clayton *et al.*, 1992; Merkel *et al.*, 1992; Marshall *et al.*, 1993). However, adenosine antagonists only partially block, or are ineffective in blocking, the response to adenosine in some tissues (Von Beckerath *et al.*, 1991; Nakhostine & Lamontagne, 1993). One possible explanation is the involvement of the endothelium, which releases other factors such as prostacylin that have been shown to act on K_{ATP} channels during hypoxia (Nakhostine & Lamontagne, 1994). Another is a possible direct action on K_{ATP} channels by metabolic inhibition (Von Beckerath *et al.*, 1991). Hypercapnia, as mentioned above, also plays a role during hypoxia and acts through K_{ATP} channels (Faraci *et al.*, 1994).

1.3.4 Other tissues

Although the role of K_{ATP} channels in the pancreas, heart and vasculature is reasonably well defined, their role in the CNS and skeletal muscle is less well characterised, and it seems that they only come into play under extreme conditions such as hypoxia (Pan *et al.*, 1988; Moser *et al.*, 1995; Reshef *et al.*, 1998).

1.4 Exogenous regulators of K_{ATP} channels

Given the number of endogenous factors that regulate K_{ATP} channel function it is not surprising to find an increasing number of synthetic agents that both open and antagonise, not only K_{ATP} channels, but K^+ channels in general. The subsequent discussion focuses on compounds that do just that in relation to K_{ATP} channels.

1.4.1 K_{ATP} channel openers

K_{ATP} channel openers are an extremely large and chemically diverse group of agents, which were initially characterised by their ability to open smooth muscle K^+ channels and cause relaxation *in vitro*. There is no common structure for K_{ATP} channel openers and therefore classification is difficult. However, five main classes have been identified including the benzopyrans (eg levcromakalim), the thioformamides (eg aprikalim), the pyrimidines (eg minoxidil sulphate), the benzothiadiazines (eg diazoxide) and the cyanoguanidines (eg pinacidil) (Edwards & Weston, 1995). The structures of these compounds are illustrated in Figure 1.7.

The first synthetic compound found to cause relaxation of vascular tissue by increasing K^+ conductance and hyperpolarising the membrane was nicorandil (Figure 1.7). It was found, however, that the relaxation to nicorandil was not entirely abolished by high K^+ (Furukawa *et al.*, 1981; Itoh *et al.*, 1981). It is now known that nicorandil can open both K^+ channels and act as a nitrovasodilator due to the presence of a nitrate group in its structure. The real interest in K^+ channel openers was initiated by the work of Hamilton and colleagues (1985; 1986) when they characterised the activity of the compound, cromakalim, which was found to selectively open K_{ATP} channels. It was found that the actions of cromakalim, and many other K^+ channel openers

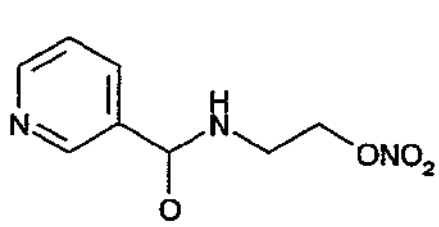

Nicorandil

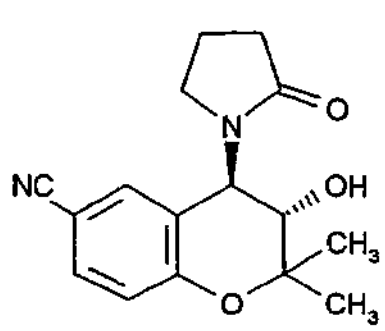

Levcromakalim

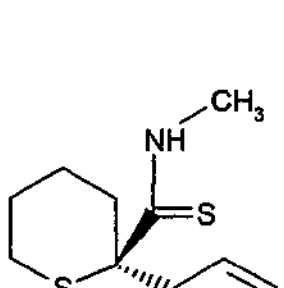

Aprikalim

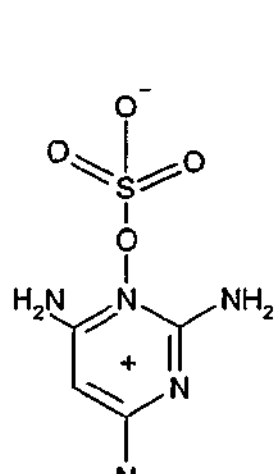

Minoxidil sulphate

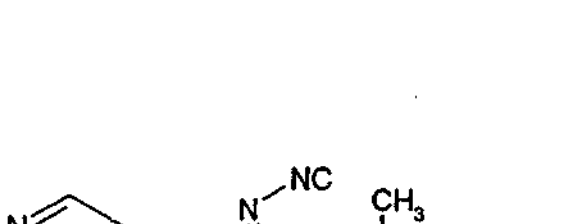

Pinacidil

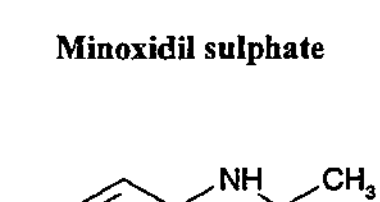

Diazoxide

Figure 1.7 Chemical structures of some K^+ channel openers.

subsequently synthesised, could be inhibited by the sulphonylurea, glibenclamide, and other selective K_{ATP} channel antagonists (Buckingham *et al.*, 1989; Quast & Cook, 1989; Winquist *et al.*, 1989). Several additional criterion were also used to establish whether or not these compounds acted through K_{ATP} channels including $^{86}Rb^+$ and $^{42}K^+$ studies showing K^+ efflux from cells (Edwards *et al.*, 1991; Longmore *et al.*, 1991) and patch clamping experiments, using single smooth muscle cells, showing activation of K_{ATP} channel currents (Noack *et al.*, 1992).

The actions of K_{ATP} channel openers are not limited to vascular K_{ATP} channels. They also have an effect in other tissues containing K_{ATP} channels such as the pancreatic β-cell, cardiac muscle, skeletal muscle and neurones (Escande *et al.*, 1988; Zünkler *et al.*, 1988; Weik & Nemucke, 1990). However, they are generally less potent in activating K_{ATP} channels in these tissues than in vascular smooth muscle. One exception to this is diazoxide, which activates pancreatic K_{ATP} channels with equal potency (Schwanstecher *et al.*, 1992; Quayle *et al.*, 1995).

In vascular smooth muscle, the ability of K_{ATP} channel openers to cause relaxation also differs between animal species and vascular beds. For instance, the EC_{50} for levcromakalim (the negative isomer of cromakalim) varies from 12 nM in the guinea pig portal vein (Quast, 1987) to 440 nM in the rat basilar artery (Ksoll *et al.*, 1991). Moreover, in the cerebral circulation of the rat, levcromakalim has differing actions since it hyperpolarises the basilar artery, but not the anterior cerebellar or middle cerebral arteries (McPherson & Stork, 1992). This is also similar in small and large peripheral arteries in the rat, where levcromakalim is more potent in the former than the latter (Nagao *et al.*, 1992). There are several possible explanations for all these differences, including changes in the tissue distribution of K_{ATP} channels or differences in subtypes of K_{ATP} channels present (Quayle *et al.*, 1997).

1.4.1.1 Site of action

The recent cloning of the sulphonylurea receptors, SUR1, SUR2A and SUR2B by Inagaki and coworkers (1995b; 1996) identified the SURs as an integral part of the K_{ATP} channel. In addition, it was found that they appear to have a site for the regulation of the K_{ATP} channel openers. Evidence for this includes the discovery that the K_{ATP} channel currents expressed by SUR1/K_{IR}6.2 are activated by diazoxide, SUR2A/K_{IR}6.2 by cromakalim and pinacidil but not diazoxide, and SUR2B/K_{IR}6.2 by diazoxide and pinacidil (Inagaki *et al.*, 1995b; Inagaki *et al.*, 1996; Isomoto *et al.*, 1996).

Radioligand binding studies using the pinacidil analogue [^{3}H]-P1075 have also been carried out to look at the relationship between K_{ATP} channel blockers such as glibenclamide and K_{ATP} channel openers (Bray & Quast, 1992; Quast, 1993). They found that, in rat aorta, [^{3}H]-P1075 met all the requirements of a K^+ channel opener as it caused glibenclamide-sensitive relaxation and $^{86}Rb^+$ efflux and hence, the labelled receptor was of functional relevance. Nevertheless, binding of openers took place at a concentration that was much lower than was needed for channel opening and sulphonylurea binding took place at a much higher concentration than was needed to block the channel. This lead Quast and coworkers (1993) to postulate that there is a complex model involved, perhaps involving 2 binding sites which are coupled by negative cooperativity. Subsequent studies used [^{3}H]-glibenclamide labelled high and low affinity binding sites. The high affinity site was identified as the sulphonylurea receptor since it was inhibited by K_{ATP} channel openers and abolished by prolonged hypoxia and metabolic inhibition (Löffler & Quast, 1997). This study provided further evidence that the site at which K_{ATP} channel openers and inhibitors bind is found on the SUR and that they are negatively allosterically coupled. In fact, in a recent study by Schwanstecher and coworkers (1998), utilising molecular pharmacology techniques, it

was found that mutations in the NBFs of the SUR receptors resulted in abolished or weakened binding of [^{3}H]-P1075. This indicates that opener binding requires a conformational change induced by ATP hydrolysis in both NBFs.

1.4.1.2 How do openers regulate K_{ATP} channels?

The mechanism by which the K_{ATP} channel openers actually activate K_{ATP} channels is not yet fully understood. However, there are several theories based on different experimental evidence. The predominant theory is that openers decrease the sensitivity of the channel to ATP. For instance, diazoxide can activate channels which have been inhibited by ATP, yet, when no $[ATP]_i$ is present they are ineffective (Trube *et al.*, 1986; Sturgess *et al.*, 1988). Openers also cause a shift to the right in the concentration-response curve for ATP inhibition with no effect on the slope or maximum, indicating that openers and ATP are antagonists of each other (Thuringer & Escande, 1989). However, when there are high levels of ATP present, openers cannot reverse the inhibition, which suggests two separate sites for openers and ATP binding, with the ATP affinity regulated by the opener binding site (Fan *et al.*, 1990).

Although this theory seems to be possible for many tissues, in studies using the rabbit portal vein, increasing $[ATP]_i$ did not antagonise the effects of levcromakalim indicating that in some tissues other factors may be important (Zhang & Bolton, 1996). It has been proposed that MgNDPs may be required for K_{ATP} channels to continue to be operational in some tissues (Clapp, 1995). In cardiac tissue, nicorandil did not activate K_{ATP} channels in the presence of MgATP but did so in the presence of MgNDPs (Shen *et al.*, 1991). Similar findings were made for diazoxide in pancreatic β-cells in which activation of K_{ATP} channels was independent of MgATP (Larrson *et al.*, 1993). From

this work it was hypothesised that MgADP binds to a stimulatory site which neither nonhydrolysable ADP, or ADP without Mg can bind and that MgADP is required for diazoxide to act.

In summary, the current theory is that openers decrease the sensitivity of the K_{ATP} channel for ATP and that MgNDPs may be required in some tissues to enhance the activation by openers.

1.4.2 K_{ATP} channel antagonists

K_{ATP} channel antagonists are agents that restrict the movement of K^+ ions through K_{ATP} channels or inhibit channel opening. They have been very important in studying and identifying K_{ATP} channels in many different tissues. As discussed previously, the most well known inhibitor of K_{ATP} channels is the sulphonylurea, glibenclamide. However, there are additional compounds that can antagonise K_{ATP} channels. These include other sulphonylureas such as tolbutamide, imidazolines such as phentolamine and alinidine, quaternary ions such as tetraphenylphosphonium (TPP) and the structurally unrelated compounds, 5-hydroxydecanoic acid and U-37883. Table 1.3 provides a brief summary of these inhibitors and the concentrations at which they are active and Figure 1.8 shows some of their structures. Appendix A contains a brief discussion on receptor antagonism, which may aid in the ensuing discussion of K_{ATP} channel antagonists.

1.4.2.1 Sulphonylureas

Initially, it was through studies with sulphonylureas that SUR was first thought to be part of the K_{ATP} channel. Tolbutamide, a first generation sulphonylurea, was

Compound	Conc.	Tissue	References
Sulphonylureas:			
Glibenclamide	20-200 nM	vsm	(Challinor & McPherson, 1993; Beech *et al.*, 1993a; 1993b)
	0.3-10 nM	β-cells	(Schmid-Antomarchi *et al.*, 1987; Sturgess *et al.*, 1988; Panten *et al.*, 1989)
	20-100 nM	cardiac	(Fosset *et al.*, 1988; Findlay, 1992)
Tolbutamide	3-7μM	β-cells	(Trube *et al.*, 1986; Jonas *et al.*, 1992)
Imidazol(id)ines:			
Phentolamine	1-20 μM	vsm	(McPherson & Angus., 1989)
	1-20 μM	β-cells	(Plant & Henquin, 1990; Dunne, 1991; Jonas *et al.*, 1992)
	1-20 μM	cardiac	(Wilde *et al.*, 1994; Lee *et al.*, 1995)
Alinidine	10 μM	vsm	(Challinor & McPherson, 1993)
Clonidine	10 μM	cardiac	(Lee *et al.*, 1995)
	11 μM	β-cells	(Jonas *et al.*, 1992)
Cibenzoline	1-5 μM	β-cells	(Jonas *et al.*, 1992; Ishida-Takahashi *et al.*, 1996)
Quaternary ions:			
TPP	0.1-0.3 μM	vsm	(McPherson & Piekarska, 1994)
Miscellaneous:			
U-37883	1 μM	vsm	(Ohmberger *et al.*, 1993)
5-hydroxydecanoic acid	23 μM	β-cells	(Hayashi *et al.*, 1993)
	0.2 μM	cardiac	(Notsu *et al.*, 1992)

Table 1.3 A brief summary of K_{ATP} channel antagonists, the concentration range over which they are active as K_{ATP} channel antagonists and the tissues (vsm = vascular smooth muscle, β-cells = pancreas, cardiac = heart) in which the studies were carried out.

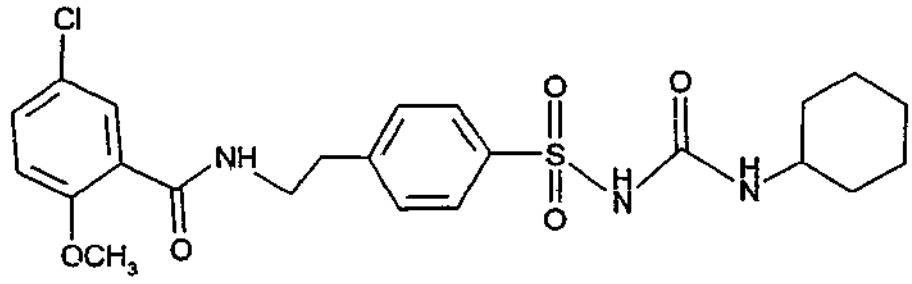

Glibenclamide

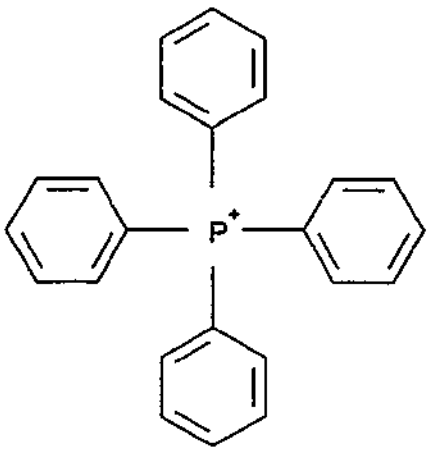

Tetraphenylphosphonium

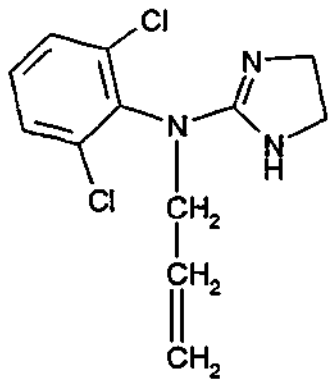

Alinidine

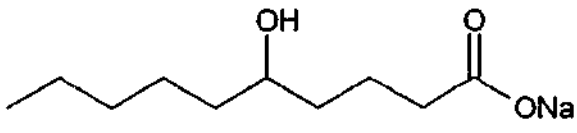

5-Hydroxydeconoate

Figure 1.8 Chemical structures of molecules able to either inhibit channel opening or the flow of K^+ ions through K_{ATP} channels.

found to inhibit single channel K_{ATP} currents from pancreatic β-cells. In whole cell recordings, K_{ATP} channel currents were blocked by tolbutamide with a K_i of 7 μM and a Hill coefficient near 1. This indicated that 1 molecule per receptor is required for inhibition (Trube *et al.*, 1986). However, tolbutamide was more than 1000 fold less potent than glibenclamide, a second generation sulphonylurea, that has an estimated K_i for inhibition of K_{ATP} channel currents of 4 nM (Sturgess *et al.*, 1985; Zünkler *et al.*, 1988). Furthermore, in binding studies, a specific SUR was found by the identification of a high affinity binding site that displayed binding that was reversible, could be saturated and was displaced by other sulphonylureas (Geisen *et al.*, 1985; Schmid-Antomarchi *et al.*, 1987; Gaines *et al.*, 1988; Niki *et al.*, 1989). It was also found that the binding affinity was similar to the K_i *in vivo*. This evidence implied that binding to this receptor resulted in a functional effect and this effect was mediated through K_{ATP} channels. Ultimately it was confirmed that SUR was, in fact, an integral part of the K_{ATP} channel (Inagaki *et al.*, 1995a).

Sulphonylureas have been shown to inhibit K_{ATP} channels not only in the pancreas but also in smooth and cardiac muscle, albeit at higher concentrations (Ashcroft & Ashcroft, 1992). For example, in vascular smooth muscle, glibenclamide inhibits whole cell currents with estimated K_i values of 20 nM to 3 μM (Noack *et al.*, 1992; Beech *et al.*, 1993a; 1993b; Quayle *et al.*, 1995). Furthermore, in smooth muscle, glibenclamide has been shown to inhibit whole cell currents which have been activated by a number of mechanisms including K_{ATP} channel openers (Ibbotson *et al.*, 1993; Beech *et al.*, 1993b; Criddle *et al.*, 1994), vasodilators such as adenosine (Dart & Standen, 1993), ATP depletion (Silberberg & van Breeman, 1992) and hypoxia (Clayton *et al.*, 1992).

In the heart, certain sulphonylureas are more potent than they are in smooth muscle. For instance, glibenclamide inhibits cardiac K_{ATP} currents with a K_i of 7 nM (Findlay, 1992). In contrast, tolbutamide inhibits both cardiac and smooth muscle K_{ATP} channel currents at a similar potency of around 350 μM (Belles *et al.*, 1987).

1.4.2.1.1 Characteristics of sulphonylurea binding

Considering the role of sulphonylureas in tissues other than the pancreas, it is not surprising that it has now been shown that the use of sulphonylureas in the treatment of diabetes may lead to increased cardiovascular mortality in some instances (Leibowitz & Cerasi, 1996). Indeed, specific binding sites for sulphonylureas have been identified not only in the pancreas (Kaubisch *et al.*, 1982), but in the cerebral cortex (Kaubisch *et al.*, 1982; Lupo & Bataille, 1987), the heart (Fosset *et al.*, 1988; French *et al.*, 1990), smooth muscle (Gopalakrishnan *et al.*, 1991; Zini *et al.*, 1991), adipocytes (Martz *et al.*, 1989) and in the liver (Inoue *et al.*, 1995). Also, high and low affinity binding sites for sulphonylureas have been identified in most of these tissues (Geisen *et al.*, 1985; Niki *et al.*, 1989; Gopalakrishnan *et al.*, 1991; Zini *et al.*, 1991; Nelson *et al.*, 1992; Hicks *et al.*, 1994).

In the pancreas, the K_D for glibenclamide binding to the high affinity site is similar to the EC_{50} for functional glibenclamide inhibition in the pancreas, both being in the nanomolar range (Ashcroft & Ashcroft, 1990). However, in certain tissues, for example smooth muscle, the K_D for the high affinity binding site for glibenclamide (0.4 nM), determined through radioligand binding studies, is much less than the concentration required to see a functional effect (7 μM; Challinor-Rogers *et al.*, 1994). This concentration is more like the K_D for the low affinity binding site (83 nM; Zini *et*

al., 1991). On the other hand, in studies conducted in our laboratory, using sulphonylurea analogues, it was found that there was no significant correlation between K_{ATP} channel antagonism in the vasculature and binding to the low affinity site (Challinor-Rogers *et al.*, 1995). As a result, the role of the low affinity binding site is yet to be determined, but it does seem to be more important in some tissues such as smooth muscle (Quayle *et al.*, 1997).

1.4.2.1.2 Functional properties of sulphonylurea activity

Many studies have found that sulphonylureas show all the characteristics of competitive antagonism in vascular smooth muscle in inhibiting cromakalim-induced relaxation, exhibiting a pA_2 of around 7 (Eltze, 1989; Edwards *et al.*, 1991; Challinor & McPherson, 1993). This was determined by the finding that sulphonylureas shift the concentration-effect curve to the right without affecting the maximum or slope of the response to cromakalim (see Appendix A). This would also indicate, when following a traditional pharmacological approach, that the site of action would be the same for glibenclamide and cromakalim (Challinor & McPherson, 1993). However, as already discussed in Section 1.4.1.1, a study by Bray & Quast (1992) found that the interaction between glibenclamide and P1075 was allosteric, suggesting that the two act at different sites on the SUR, which are negatively coupled.

1.4.2.1.3 Selectivity of sulphonylureas for K_{ATP} channels

A widespread practice in assessing the possibility of a novel drug acting as an agonist at K_{ATP} channels is the use of channel specific antagonists in isolated tissue experiments. To obtain an accurate result, the K_{ATP} channel antagonist, usually

glibenclamide, needs to be selective for $K_{A^{TP}}$ channels. Recently, there has been evidence that this is not the case as it has been found that SURs can couple to other K^+ channels, such as $K_{IR}1.0$, and that this coupling results in sensitivity to sulphonylureas (Ämmälä *et al.*, 1996a). Other K^+ channels have also been shown to be inhibited by sulphonylureas, including the calcium-activated K^+ channel (Gelband *et al.*, 1993), the voltage-activated K^+ channel (Crepel *et al.*, 1993) and the sodium-activated K^+ channel (Seutin *et al.*, 1996). Moreover, glibenclamide has been found to antagonise the thromboxane A_2 mimetic, U46619 in both dog and pig coronary artery (Cocks *et al.*, 1990; McPherson *et al.*, 1997). It is yet to be determined if these additional actions of sulphonylureas result from interactions with other classes of SURs or are mediated via different mechanisms.

In summary, sulphonylureas are important tools for investigating K_{ATP} channels. However, their lack of selectivity highlights the need to investigate the actions of other K_{ATP} channel antagonists such as the quaternary ions, 5-hydroxydecanoic acid, U-37883, imidazolines and imidazolidines.

1.4.2.2 Other K_{ATP} channel antagonists

Historically, quaternary ions have been used predominantly to measure the polarity of membrane potential. This is because their lipophilic nature allows a passive equilibrium with the electrical potential across the cell membrane (Haydon & Hladky, 1972). However, studies performed over the last decade have found that quaternary ions are also potent inhibitors of K_{ATP} channels. Davies and colleagues (1989) and Quast and Webster (1989) both used $^{86}Rb^+$ efflux techniques to identify tetraethylammonium (TEA) as an inhibiter of K_{ATP} channels from both inside and

outside the cell membrane albeit at a high concentration of 3 mM. These findings were the foundation of many studies which followed including experiments by our laboratory, which identified two quaternary ions, tetraphenylphosphonium and tetraphenylarsonium, as potent antagonists of levcromakalim-induced relaxation of pig isolated coronary artery with a potency similar to glibenclamide (McPherson & Piekarska, 1994). Interestingly, it was found that another quaternary ion, tetraphenylboron could reverse this blockade. It has been postulated that this is a result of the negative charge of tetraphenylboron, which allows it to combine with other positively charged quaternary ions to form a chemically inactive compound. The same study by McPherson & Piekarska (1994) also found that the antagonism displayed by the quaternary ions was non-competitive.

The site of action of quaternary ions is still under debate. However, work with TEA, for example, has led to the hypothesis that they "plug" the ion pore to prevent movement through the channel (Heginbotham & McKinnon, 1992). Although potent K_{ATP} channel inhibitors, quaternary ions have also been shown to alter ATP synthesis and cellular growth by concentrating in the mitochondria (Saito *et al.*, 1992) and affecting the Na^+/K^+-ATPase (Klodos & Plesner, 1992).

Other inhibitors include compounds such as U-37883 and 5-hydroxydecanoic acid. U-37883 is a synthetic agent that was found to block vascular K_{ATP} channels with an estimated K_i of 1 μM. It also seems to be vascular selective as it does not stimulate insulin secretion or inhibit K_{ATP} currents in the pancreas (Ohrnberger *et al.*, 1993). 5-hydroxydecanoic acid is believed to inhibit ventricular arrhythmias in guinea-pig ventricular myocytes also by inhibiting K_{ATP} channels (K_i 0.2 μM; Notsu *et al.*, 1992).

Unfortunately, like sulphonylureas the majority of these blockers are relatively non-selective. Therefore, in pursuit of a more selective K_{ATP} channel antagonist, studies in our laboratory have focused upon imidazol(id)ines.

1.4.2.3 Imidazolines and Imidazolidines

Imidazolines, such as phentolamine, and imidazolidines, such as alinidine and other structurally related compounds, have been known for some time to antagonise K_{ATP} channels.

1.4.2.3.1 Actions on smooth muscle

Our laboratory was the first to demonstrate that imidazol(id)ines inhibit K_{ATP} channels in vascular smooth muscle. Phentolamine, alinidine, and structurally related analogues, all at 30 μM, blocked cromakalim in both functional and electrophysiological studies (McPherson & Angus, 1989). Phentolamine, a well known α-adrenoceptor antagonist, was selective for cromakalim since other α-adrenoceptor antagonists, prazosin, rauwolscine and phenoxybenzamine, at sufficient concentrations, failed to antagonise cromakalim. In addition, this study also showed that clonidine, the compound from which the imidazoline compounds studied in this thesis are derived, is ineffective in blocking cromakalim. In a subsequent study, phentolamine and alinidine were used as valuable tools, along with glibenclamide, in characterising K_{ATP} channels in vascular smooth muscle, non-vascular smooth muscle and cardiac muscle (McPherson & Angus, 1990).

In another study, phentolamine and alinidine (1-30 μM) were shown to cause concentration-dependent depolarisation in endothelium-denuded rat small mesenteric

arteries (McPherson & Angus, 1991). Subsequent experiments by Okumura and coworkers (1992) showed that imidazolines such as phentolamine and antolazine attenuated the relaxation to the K_{ATP} channel opener, nicorandil, in vascular smooth muscle.

Imidazolines have also been shown to antagonise K_{ATP} channels present in non-vascular smooth muscle after studies found that phentolamine and glibenclamide inhibited cromakalim induced relaxation and pinacidil-induced relaxation in guinea-pig isolated trachealis muscle (Murray *et al.*, 1989; Bang & Nielson-Kudsk, 1992).

1.4.2.3.2 Actions on the pancreas

In the pancreatic β-cell it is well known that phentolamine reverses the inhibition of insulin release caused by diazoxide (Burr *et al.*, 1971), whereas other α-adrenoceptor antagonists, such as yohimbine, do not (Henequin *et al.*, 1982). Moreover, a study by Schultz & Hasselblatt (1989) demonstrated that other imidazoline compounds related to phentolamine, such as tolazoline and antazoline, also acted in the same way as phentolamine. Using diazoxide, an agent recently found to open K_{ATP} channels (Trube *et al.*, 1986; Dunne *et al.*, 1987), Plant and Henquin (1990) investigated the possibility that phentolamine was acting through K_{ATP} channels. Using patch clamping techniques, they showed that phentolamine (20 μM), inhibited $^{86}Rb^{+}$ efflux caused by diazoxide (100 μM) in pancreatic islet cells in the presence of 6 mM glucose. Also, single K_{ATP} channel currents were inhibited in a concentration-dependent manner by phentolamine (20-100 μM). They concluded that phentolamine inhibited K_{ATP} channels in pancreatic β-cells in a manner similar to glibenclamide. This study was followed by many others showing that imidazolines blocked K_{ATP} channels in

pancreatic β-cells (Chan *et al.*, 1991; Dunne, 1991; Jonas *et al.*, 1992). Therefore, from these studies and those described in smooth muscle, it is now known that imidazolines are another chemical group of antagonists, in addition to sulphonylureas, that inhibit K_{ATP} channels.

Given all this evidence, it was surprising that following a study by Chan and colleagues (1993) where the imidazoline, efaroxan, was shown to be stereoselective and down-regulated in the presence of agonists, it was hypothesised that an 'imidazoline receptor', and not K_{ATP} channels, may be responsible for its effects in the pancreas. This may have been possible, as binding sites for imidazolines had been identified in the pancreas (Michel & Insel, 1989; Michel & Ernsberger, 1992). Imidazoline receptors are divided into two subtypes, I_1- and I_2-receptors (Ernsberger *et al.*, 1992b). I_2-receptors had already been described in the pancreas (Lancombe *et al.*, 1993) and in insulinoma cells (Remaury & Paris, 1992). Nevertheless, the pharmacology of the I_1- and I_2-sites was not consistent with the pharmacology of the imidazoline responses so it was proposed that they might be acting through a third, yet unidentified, I-receptor site. A study utilising [^{3}H]-RX812002, an imidazoline that can also stimulate insulin release, identified both high and low affinity binding sites. Efaroxan displaced the [^{3}H]-RX812002 binding to the low affinity site in concentration-dependent manner, indicating that the low affinity site may, in fact, represent a new receptor (Chan *et al.*, 1994).

However, this evidence was controversial and inconclusive. Indeed, a study by Olmos and colleagues (1994) using rat insulinoma cells confirmed that imidazolines were not acting at I_1- or I_2-receptors. I_1-receptors were shown not to be present and the imidazolines cirazoline and idazoxan (100 μM), both known to have potent actions at I_2- receptors, caused the release of insulin, yet were not blocked by the I_2 antagonist,

clorgyline (10 μM). They did however, reverse the inhibition of insulin release by diazoxide (250 μM), indicating that they were acting at a novel binding site related to the K_{ATP} channel and not at an imidazoline receptor. In support of this theory, imidazolines showed stereoselectivity in blocking α_2-adreonceptors but not K_{ATP} channels, in contrast to findings with respect to efaroxan (Chan *et al.*, 1993). This also suggested that imidazoline receptors were not involved.

1.4.2.3.3 Actions on the heart

Phentolamine has been used extensively to characterise the role of α-adrenoceptors in the heart under both normal and pathophysiological conditions such as ischaemia. It has been shown to be a potent anti-arrhythmic in *in vivo* cat studies (Sheridan *et al.*, 1980), as well as in *in vitro* studies using guinea-pig hearts (Penny, 1984; Penny *et al.*, 1985; Gwilt *et al.*, 1992) and rat hearts (Thandoroyen *et al.*, 1983). It has been shown to inhibit the shortening of the cardiac action potential under both ischaemic (Penny *et al.*, 1985) and hypoxic conditions (Tweedie *et al.*, 1992). These effects were always thought to be a result of blockade of α-adrenoceptors. However, with the findings that phentolamine blocked K_{ATP} channels in the pancreas and vascular and non-vascular smooth muscle, as already discussed in Sections 1.4.2.3.1 & 2, it was proposed that the anti-arrhythmic effects of phentolamine may be mediated by cardiac K_{ATP} channels. In a study by Wilde and coworkers (1994) using rabbit ventricular cells, phentolamine (5 μM) applied to the intracellular side of the membrane reduced K_{ATP} channel activity almost completely as the open probability decreased by 94%. Shortly afterwards, Lee and coworkers (1995), using guinea-pig ventricular cells, found that this effect was not seen with other α-adrenoceptors antagonists, but was apparent for other

imidazoline analogues such as idazoxan. However, it remains to be determined if antagonism of cardiac K_{ATP} channels accounts for the anti-arrhythmic effects of phentolamine.

Alinidine, as already mentioned previously, has been shown to block K_{ATP} channels in vascular and non-vascular smooth muscle. In addition, it has been shown first *in vitro* (Kobinger *et al.*, 1979; Lillie & Kobinger, 1983a) and then *in vivo* (Siegl *et al.*, 1984; Hageman *et al.*, 1985) to slow heart rate. Studies in our laboratory compared the cromakalim antagonism and bradycardic actions of a number of novel series of alinidine analogues to determine if the bradycardia of alinidine was related to an affect at K_{ATP} channels (Challinor-Rogers *et al.*, 1994). It was found that there was no statistically significant correlation between the two and hence, alinidine did not cause bradycardia through an action at cardiac K_{ATP} channels. In fact, the mechanism of action of alinidine in regards to its bradycardic effects is yet to be determined. Moreover, alinidine has been shown to possess anti-ischaemic (Kobinger *et al.*, 1979) and antiarrhythmic (Harron *et al.*, 1985; Reichhalter *et al.*, 1988) actions which were originally attributed to the bradycardic effects. However, in later studies this anti-ischaemic protective effect was still observed using paced hearts (Hanet *et al.*, 1989; Streller & Walland, 1990). In a study examining the antiarrhythmic and anti-ischaemic activities of novel alinidine analogues it was concluded that the antiarrhythmic effects were solely due to either the bradycardia or blockade of K_{ATP} channels since an equipotent concentration of glibenclamide was less effective as an antiarrhythmic agent (Challinor-Rogers *et al.*, 1997). Also, it is unlikely that K_{ATP} channel blockade is involved in the anti-ischaemic actions, which is in accordance with other studies that found that glibenclamide either worsens ischaemia (Kamigaki *et al.*, 1994) or has no effect (Iwamoto *et al.*, 1993; Warltier *et al.*, 1993).

1.4.2.3.4 Mechanism of antagonism of K_{ATP} channels

It is well recognised that imidazolines antagonise K_{ATP} channels, yet the mechanism via which they do so appears to differ from that of glibenclamide. Thus, a study by Brown and coworkers (1993) found that imidazolines were unable to displace [^{3}H]-glibenclamide binding to β-cell membranes implying that they were acting at a site other than the one for glibenclamide. Furthermore, a study by Challinor & McPherson (1993) also suggested that alinidine and phentolamine did not act at the same site as glibenclamide. Imidazol(id)ines exhibit the characteristics of a non-competitive antagonist in vascular smooth muscle when antagonising K_{ATP} channel openers. This can be seen as a slight rightward shift of the concentration-effect curve to cromakalim, a flattening of the slope, and on occasion, a reduced maximum response. As this is clearly different from the competitive antagonism displayed by the sulphonylureas, it was thought that the mechanism by which the imidazol(id)ines antagonised the K_{ATP} channel openers differed. To clarify these findings the concentration-ratio method for combined antagonists described by Paton & Rang (1965) was used. The Paton and Rang concentration-ratio method postulates that if two antagonists are acting at the same site, the concentration-ratio will be equal to each antagonist's concentration ratio added together. Conversely, if two antagonists are acting at different sites the concentration ratio will be equal to each antagonists concentration ratio multiplied. The concentration-ratios for glibenclamide and phentolamine were multiplicative, indicating that they act at different sites to antagonise cromakalim. Conversely, the two sulphonylureas, glibenclamide and glipizide and the two imidazol(id)ines, phentolamine and alinidine, both had concentration-ratios which were additive, thus indicating that they act at the same site (Challinor & McPherson, 1993).

More conclusive evidence of the site of action of imidazolines came from a recent study by Proks and Ashcroft (1997) utilising *Xenopus* oocytes that provided a C-terminally truncated form of $K_{IR}6.2$ which had either the last 26 ($K_{IR}6.2\Delta C26$) or last 36 ($K_{IR}6.2\Delta 36$) amino acids deleted. The 2 truncated forms of $K_{IR}6.2$ have previously been shown to possess K_{ATP} currents in the absence of SUR1 (Gribble *et al.*, 1997a). They found that phentolamine (100 μM), when applied to the intracellular solution, inhibited K_{ATP} currents by 97 % in a voltage independent manner and furthermore, similar results were obtained for both $K_{IR}6.2\Delta C26$ and $K_{IR}6.2\Delta C36$ currents. This suggested that the site where phentolamine inhibits the K_{ATP} channel resides on $K_{IR}6.2$. These results were also duplicated in HEK293 cells transfected with cDNA encoding to $K_{IR}6.2\Delta C36$, indicating that it is indeed $K_{IR}6.2$ that phentolamine is inhibiting and not an endogenous protein in *Xenopus* oocytes (Tucker *et al.*, 1997). The actual site on $K_{IR}6.2$ where phentolamine acts also seems to differ from the site where ATP binds because the mutation in the latter has been shown to decrease ATP sensitivity without affecting phentolamine sensitivity. These findings may also explain the similar potency of phentolamine for pancreatic and cardiac K_{ATP} channels.

In support of this finding, work by Mukai and coworkers (1998) discovered that the antiarrhythmic, cibenzoline, inhibited K_{ATP} channels by binding to $K_{IR}6.2$. Using COS7 cells expressing the C-terminal truncated $K_{IR}6.2\Delta C26$ with and without SUR1, they found that glibenclamide inhibited $K_{IR}6.2\Delta C26$ together with SUR1 but not $K_{IR}6.2\Delta C26$ alone, whereas cibenzoline inhibited both. Figure 1.9 illustrates the proposed site of action of imidazolines on the K_{ATP} channel, the K_{IR} subunit and not SUR. Considering this evidence, it is not surprising that imidazol(id)ines display non-competitive antagonism (see Appendix A). This can be seen in our studies, where

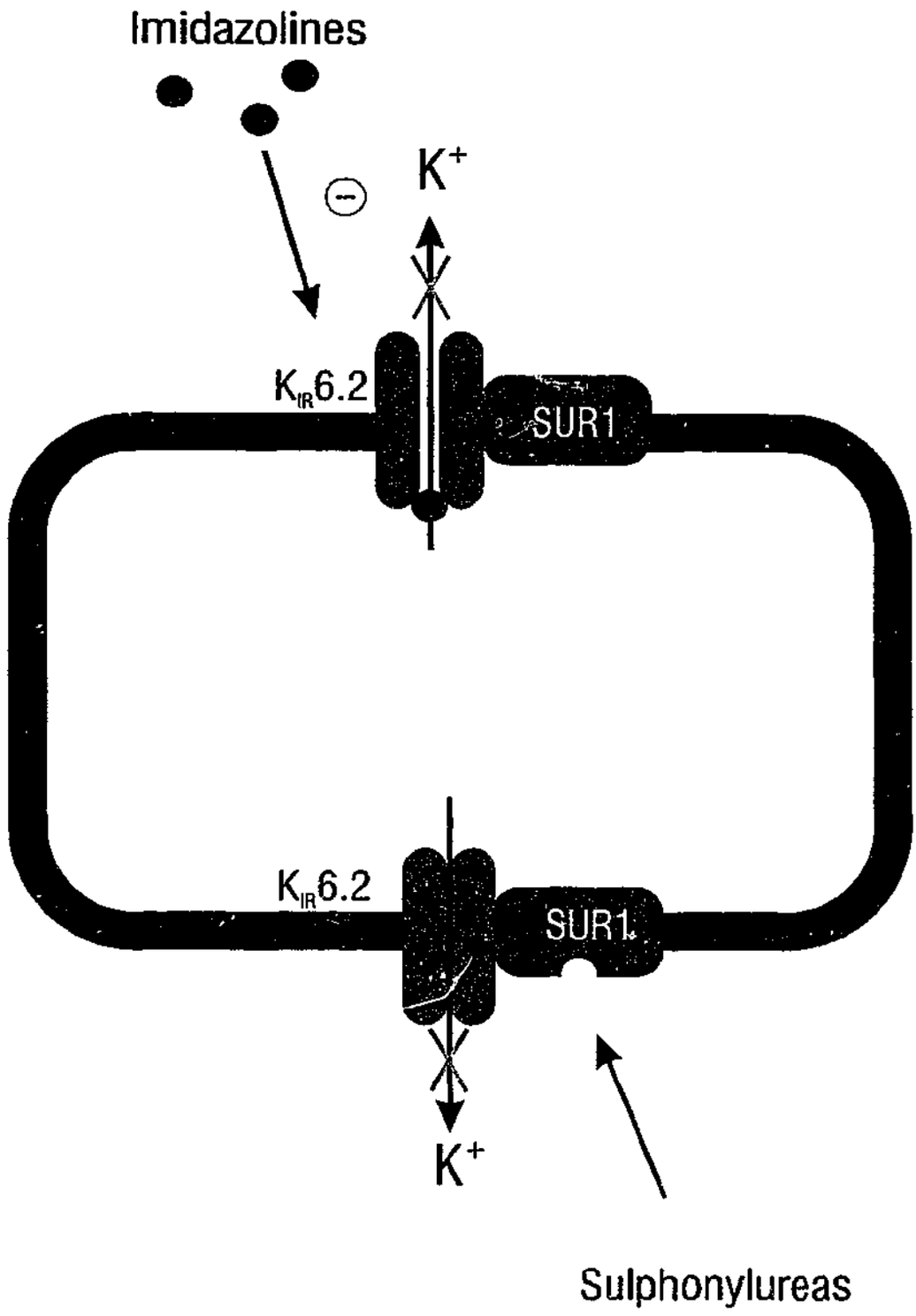

Figure 1.9 Proposed site of action of imidazolines and sulphonlureas at the K_{ATP} channel in the pancreatic β-cell. Imidazolines act by blocking the K_{ATP} channel pore, the $K_{IR}6.2$ subunit (Proks & Ashcroft, 1997) while the sulphonylureas act at the sulphonylurea receptor (SUR) to close $K_{IR}6.2$ (Aguilar-Bryan *et al.*, 1995).

phentolamine caused a suppression of the maximum and no significant shift of the concentration-response curve for cromakalim in many different vascular beds (McPherson & Angus, 1989). The same can be seen for alinidine and many other imidazolines (Challinor-Rogers *et al.*, 1994).

1.4.2.3.5 Structure-activity relationships

With many different imidazolines and imidazolidines of different potencies, the question that must be answered is, what structure makes an imidazoline or imidazolidine a good K_{ATP} channel antagonist? Figure 1.10 illustrates the different structures of a number of common imidazoline and imidazolidines. There have been limited studies investigating structure-activity in relation to K_{ATP} channels. However, a study by our laboratory has looked to answer this question (Challinor-Rogers *et al.*, 1994).

The study assessed the cromakalim antagonism in rat isolated aorta and the bradycardic activity in rat isolated atria of a number of alinidine analogues. It was the first study to investigate structure activity relationships for imidazolidines at K_{ATP} channels. The alinidine analogues, named the TH series, were found to be the most potent imidazolidine based K_{ATP} channel antagonists to date. The TH series assessed modifications on the carbon side chain attached to the central nitrogen of alinidine. The structures of some of the derivatives used in the study can be seen in Figure 1.11. The most potent compounds, TH91:22 and TH91:21, both of which had pK_B values of around 6.2, had increased carbon side chain lengths. Those with similar carbon chain lengths to alinidine, such as TH92:4, did not posses improved K_{ATP} channel antagonism having a pK_B of around 5.5, which was not significantly different to alinidine (5.5).

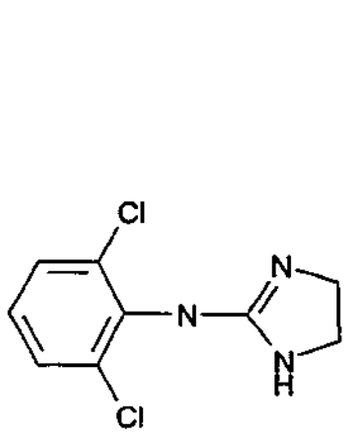

Clonidine

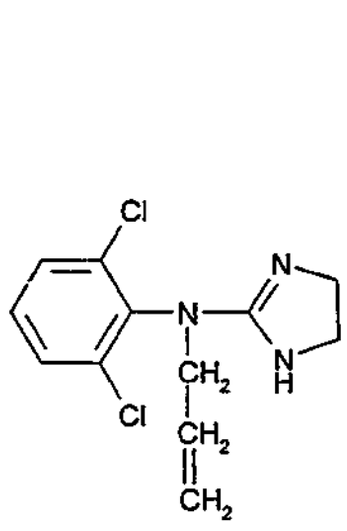

Alinidine

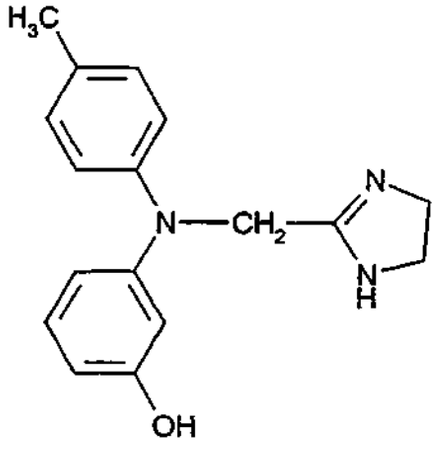

Phentolamine

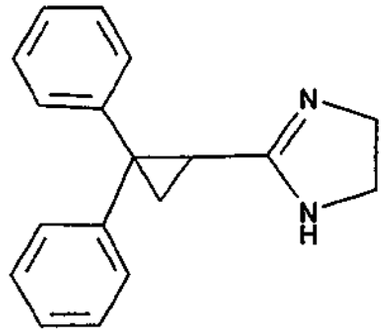

Cibenzoline

Figure 1.10 Chemical structure of the imidazolidines, clonidine and alinidine and the imidazolines, phentolamine and cibenzoline.

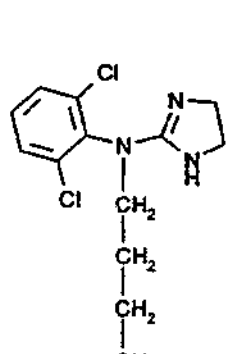

TH91:22

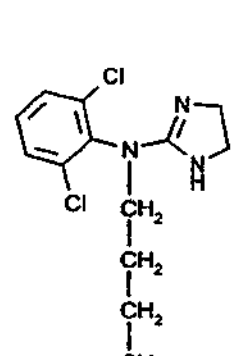

TH91:21

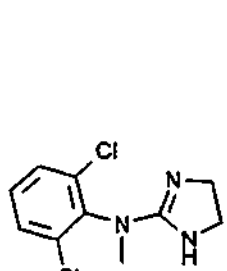

TH:92:4

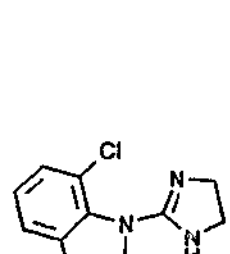

Alindine

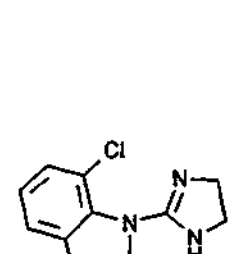

TH:92:17

Figure 1.11 Structure of some of the TH series of compounds. Alinidine is included as a comparison.

Furthermore, the derivative with a hydroxy group attached to the carbon side chain, TH:92:17, actually displayed significantly decreased K_{ATP} channel potency with a pK_B of around 4.4.

Also, a study by Sakuta & Okamoto (1994), utilised *Xenopus* oocytes to assess the K_{ATP} channel antagonism of a number of imidazoline and imidazolidine derivatives. Their findings suggested that at least one aromatic ring is essential to block K_{ATP} channels and the blocking ability of these compounds is associated with alkylation of the benzene ring and the presence of a tertiary amine structure.

From our study and the study by Sakuta & Okamoto (1994) it was apparent that the structural differences of imidazol(id)ines could alter the potency of K_{ATP} channel antagonism. To date, however, the structural alterations made to imidazol(id)ines still rendered the compounds 10-30 times less potent than glibenclamide. Therefore, in this thesis we wished to expand our previous work examining the importance of side chain substitutions and incorporate the finding that aromatic rings increased K_{ATP} channel antagonism (Sakuta & Okamoto, 1994), with the aim of generating more potent imidazolines. To this end, this thesis involved the design, synthesis and investigation of a novel series of imidazoline analogues with various aromatic ring side chain substitutions.

1.5 Statement of Aims

Widespread research on the functional properties of K^+ channels and their endogenous and exogenous regulators has taken place over the last twenty years. It has become apparent that K^+ channels play an important role in the regulation of numerous cellular functions, many of which can be regulated by selective modulators.

Therefore, the development of these modulators can be very important in the treatment of many different disease states.

Agonists and antagonists of the K_{ATP} channel are useful in the treatment of conditions such as hypertension, diabetes mellitus (Type II) and cardiac dysfunction. The sulphonylureas and anti-arrhythmic drugs are the predominant classes of K_{ATP} channel antagonists used in the treatment of these states. However, they are not as selective as first thought. Imidazol(id)ines have also been shown to be potent K_{ATP} channel antagonists, yet, they too have also been shown to have non-specific effects. Nevertheless, differences in structure of imidazolidines have been shown, by previous work in our laboratory, to be capable of altering the potency of K_{ATP} channel antagonism.

Therefore, the aim of the work described in this thesis was to design, synthesise and characterise the functional and electrophysiological properties of a novel series of imidazolines and to examine their ability to antagonise K_{ATP} channels. Additional aims were to investigate their selectivity and to identify their site of action.

Chapter Two

Chemical Synthesis of the Novel Imidazoline Analogues

2.1 Introduction

This chapter focuses on the synthesis of the novel imidazoline analogues examined in this thesis. The compounds were designed in conjunction with Dr Magdy Iskander from the Victorian Pharmacy College and synthesised by Ms Eva Campi from the Department of Chemistry, Monash University.

In total, 14 clonidine analogues were synthesised for this study. The structures of the analogues synthesised can be seen in Figure 2.1. All the compounds were named with the laboratory code IMID, followed by their unique number and letter code. The 'parent' compound, IMID-1M, was a clonidine analogue with a benzyl group substitution at the central nitrogen. From this compound, several groups of compounds were derived.

The first group were methoxy-benzyl derivatives, whereby a methoxy group was incorporated at the centrally substituted benzyl ring either at the number 4 position (IMID-4MO) or at the 3 and 5 positions (IMID-35MO). Other related compounds include the compound with a methoxy-benzyl substitution at the nitrogen of the imidazoline ring rather than the central nitrogen (IMID-35MO/IN), or an oxygen molecule substitution for a nitrogen in the imidazoline ring (IMID-35MO/O) to give an oxazoline ring.

The second group of compounds were fluoro-benzyl derivatives, where a fluorine was substituted at the number 2 and 6 positions (IMID-26F), or the number 4 position (IMID-4F), of the centrally substituted benzene ring. Other related compounds include the compound with a fluoro-benzyl substitution at the nitrogen of the imidazoline ring (IMID-4F/IN) or an oxygen molecule substitution for a nitrogen of the imidazoline ring (IMID-4F/O) to give an oxazoline ring.

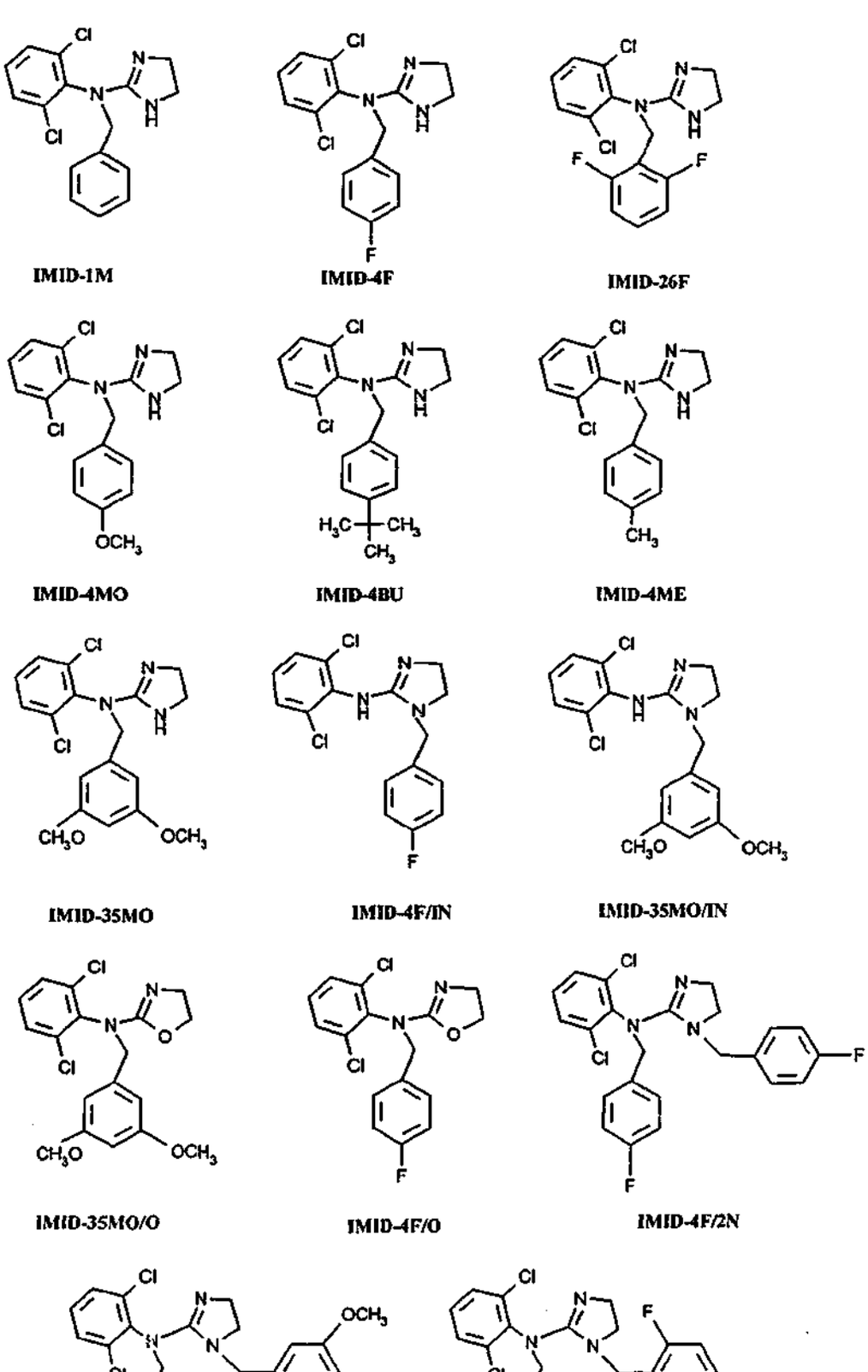

Figure 2.1 Structures of the IMID compounds synthesised and investigated in this thesis.

All the above compounds were mono-substituted compounds in that they only had one substitution at either the central or imidazoline nitrogen. The third group of compounds were related to the above two groups in that they had a methoxy-benzyl or fluoro-benzyl substituents. They were termed the "bis" compounds since the substitution was at both the central nitrogen and imidazoline nitrogen. Two fluoro-benzyl compounds (IMID-26F/2N & IMID-4F/2N) and one methoxy-benzyl (IMID-35MO/2N) were synthesised.

The final group were mono-substituted compounds with either a methyl-benzyl or *t*-butyl-benzyl substitution at the number 4 position of the centrally substituted benzene ring giving compounds IMID-4ME and IMID-4BU, respectively.

This chapter focuses upon the synthesis and the methods used to confirm the structure of the imidazoline analogues studied throughout this thesis.

2.2 Methods

2.2.1 Nomenclature

Clonidine has been shown to exist in two different forms or tautomers, an imino tautomer and two equivalent amino tautomers, with the imino tautomer considered to be the most common (Figure 2.2a; Stähle & Pook, 1971). If the imidazoline ring of a compound has a double bond within it, the compound is known as an imidazoline, while a compound with no double bond in the imidazoline ring is known as an imidazolidine. As the imino tautomer of clonidine is the more prevalent, clonidine is commonly known as an imino imidazolidine rather than an amino imidazoline. However, in this thesis all the analogues are illustrated in the amino form, either with a hydrogen or a R group on the central or imidazoline nitrogen.

The scientific naming of the analogues is based on the precedent already set in the literature, rather than the more accurate IUPAC (International Union of Pure and Applied Chemistry) names. For example, the compound with the laboratory code IMID-4F, based on the literature method of naming, is named, 2-[*N*-(2,6-dichlorophenyl)-*N*-(4-fluorobenzyl)amino]-2-imidazoline. Compounds with a benzyl substituent are named as such rather than the more correct phenylmethyl. The 2-imidazoline refers to the double bond in the imidazoline ring, the 2 because the imidazoline is numbered so the nitrogens have the lowest number (Figure 2.2b). Also, the IUPAC nomenclature for the imidazoline ring would be 4,5-dihydro-1*H*-imidazole but again, in keeping with the literature, these will be known as imidazolines.

In addition, the IMID compounds IMID-35MO/O and IMID-4F/O are not imidazolines but rather oxazolines due to the oxygen substitution in the imidazoline

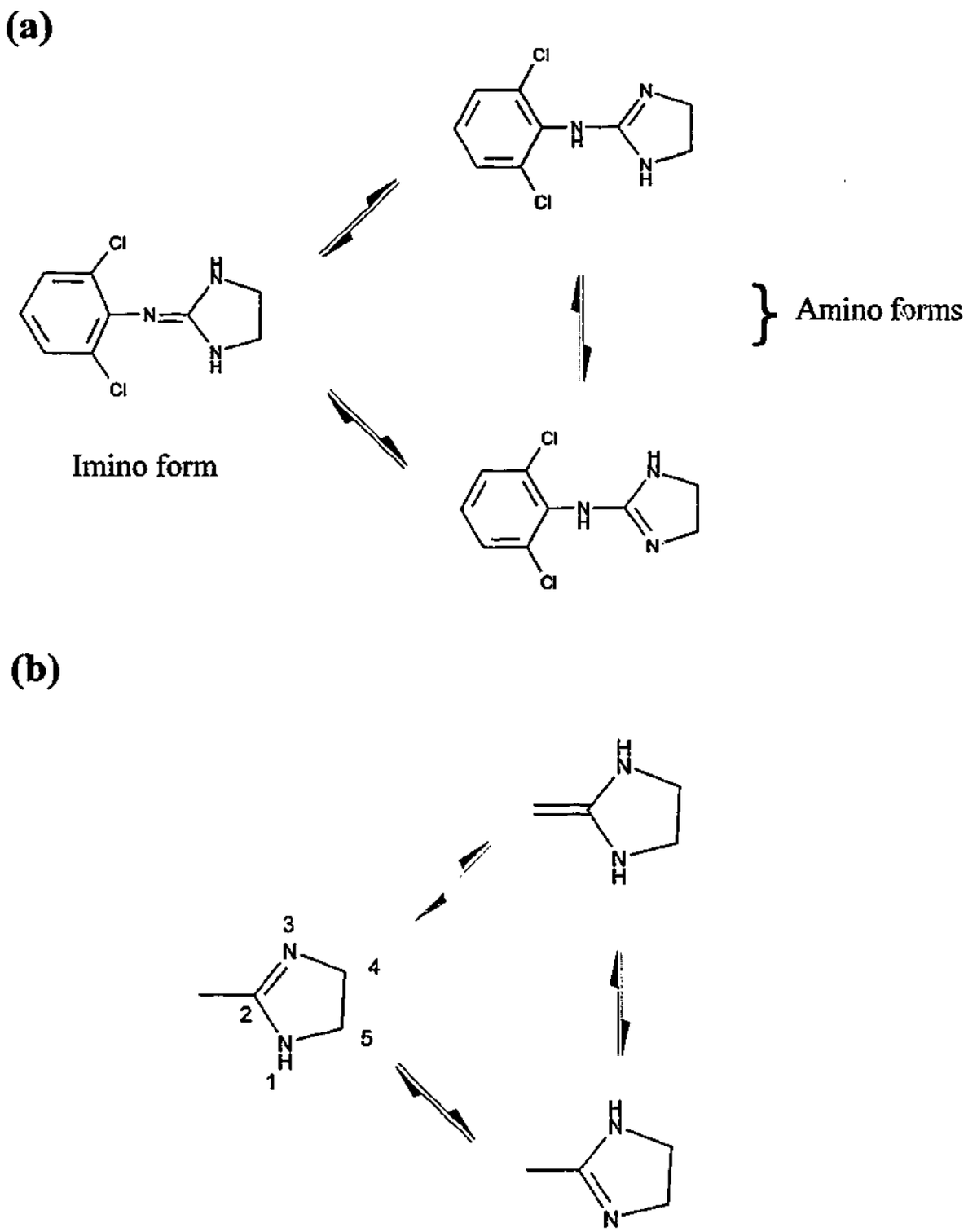

Figure 2.2 (a) Structures of the two different tautomers of clonidine, the imino tautomer and the two equivalent amino tautomers. (b) Tautomers of the imidazoline ring including a ring numbered so that the nitrogens have the lowest numbers.

ring. However, for the purpose of this thesis all of the IMID compounds will now be referred to as imidazolines.

Although some of the compounds are referred to by both their scientific name and their laboratory code in this chapter, throughout the remainder of this thesis the analogues will be referred to using only their laboratory codes as already listed in Figure 2.1.

2.2.2 Synthesis of Clonidine

As stated previously, all the IMID compounds in this study were synthesised by substituting clonidine. To this end, clonidine was synthesised from starting materials using the method of Rouot and colleagues (1976) which is illustrated in Scheme 2.1. Firstly, 2,6-dichloroaniline was used as a starting material to form 2,6-dichlorophenylformamide, the anhydride from the reaction with formic acid and acetic anhydride. This reaction was repeated several times and the initial product recrystallised to give a yield of between 51-81 %, a percentage which compared well with the value reported in the literature of 80 % (Hay, 1994). The next step involved the conversion of 2,6-dichlorophenylformamide to 2,6-dichlorophenylisocyanide dichloride using chlorination with thionyl chloride and sulphuryl chloride. The product (isocyanide dichloride) was purified by distillation to give a relatively high yield of 78-88 %. Finally, the imidazoline ring was added by reacting the isocyanide dichloride with ethylenediamine in the presence of triethylamine. A yield of approximately 35-36 % was obtained.

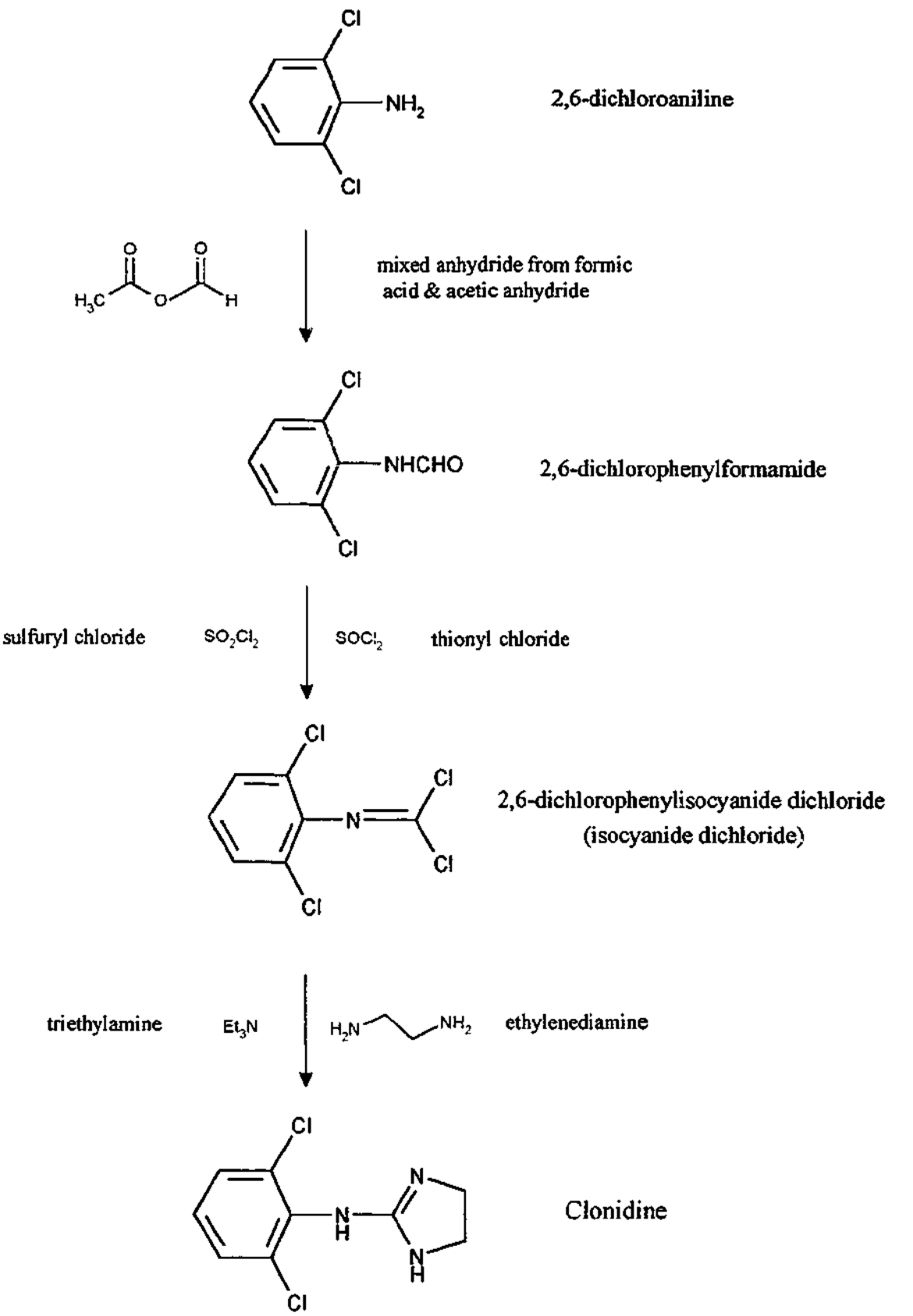

Scheme 2.1 Schematic diagram illustrating the three steps in the synthesis of clonidine.

2.2.3 Alkylations at the central nitrogen of clonidine

To synthesise the mono-substituted compounds, clonidine was alkylated at the central nitrogen with a benzyl group with or without substituents. This involved reacting one and a half equivalents of the benzyl chloride to one equivalent of clonidine in methanol or acetonitrile in the presence of a weak base (Na_2CO_3) (Scheme 2.2 eg. IMID-4F). The central nitrogen atom has been reported to be more basic than the imidazoline nitrogens and therefore more susceptible to substitution (Stähle & Pook, 1971). The imidazoline nitrogens are found in various tautomeric forms, stabilising the imidazoline ring and therefore making the nitrogens less susceptible to substitutions (Figure 2.2b). The mixture was stirred at reflux overnight, filtered to remove inorganic salts and the solvent removed under vacuum and evaporated to dryness. Some compounds were purified by crystallisation, which involved dissolving the products in hot ether and methanol and a trace dichloromethane to prevent stickiness and then cooling in an ice bath. In theory, pure crystals form and precipitate and the impurities remain in solution. However, this method was not used for the majority of compounds as the optimal method was found to be flash column chromatography, which produced much higher yields and allowed easier separation of products.

Flash chromatography involves making a silica slurry with dichloromethane and methanol in a ratio of 9:1. The compound was dissolved in a small amount of the same solvent and absorbed onto the column. Solvent was then passed down the column and fractions collected. The different compounds pass through the column at different rates with the least polar compounds collected first and the most polar last. In this case, the bis-substituted compound was collected first. After the bis was collected the solvent was changed to methanol and then methanol with 5 % ammonium hydroxide. The products were then recrystallised to produce the pure analogues. This procedure

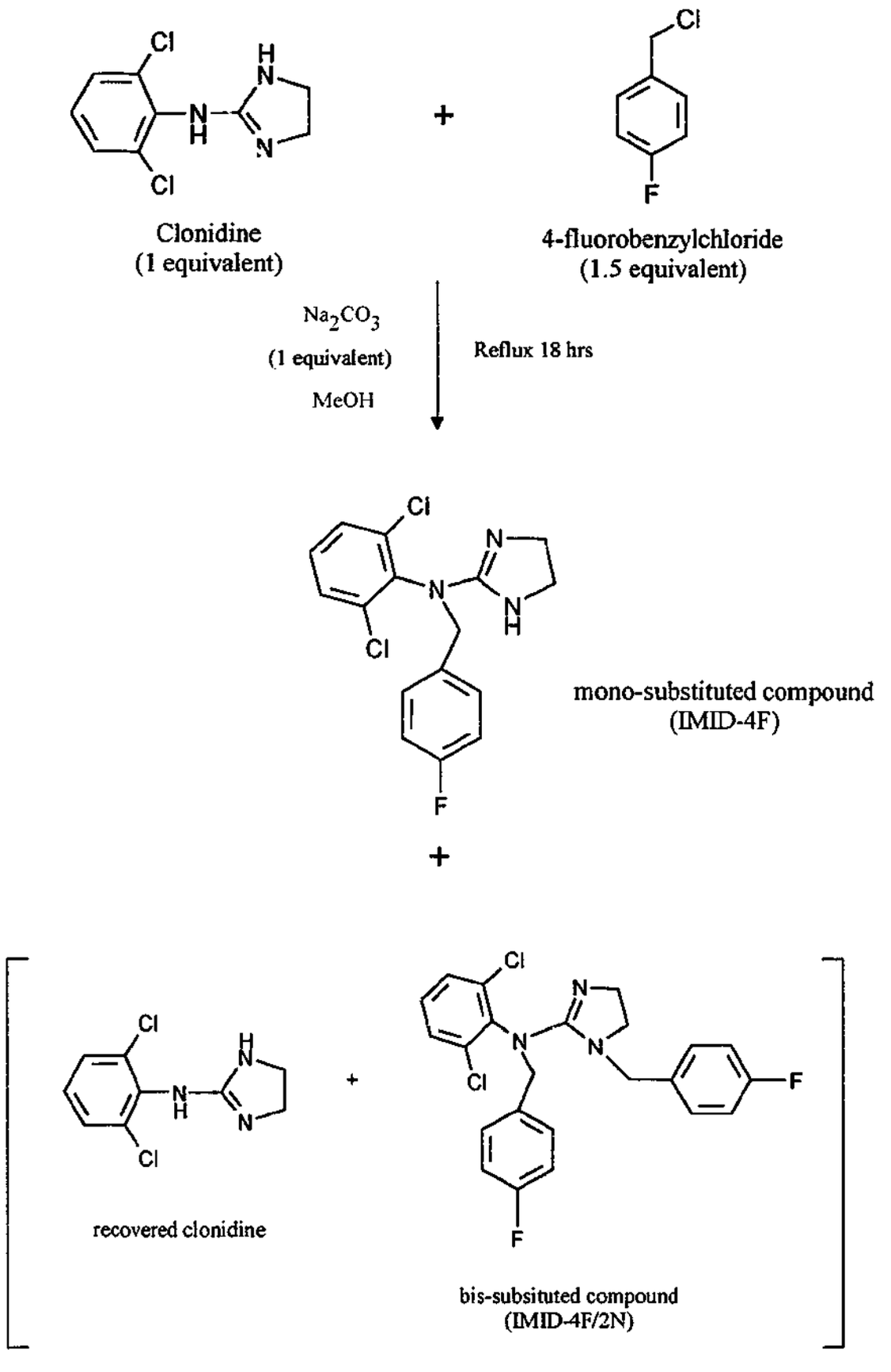

Scheme 2.2 Schematic diagram of the alkylation at the central nitrogen to synthesise 2-[*N*-(2,6-dichlorophenyl)-*N*-(4-fluorobenzyl)amino]-2-imidazoline (IMID-4F) and the side products of recovered clonidine and the bis-substituted compound (IMID-4F/2N).

resulted in the synthesis of IMID-1M, IMID-26F, IMID-4F, IMID-4ME, IMID-4BU, IMID-4MO and IMID-35MO.

2.2.4 Alkylations at the imidazoline nitrogen of clonidine

Alkylation at the imidazoline nitrogen involved the use of either a mono- 4-fluorobenzyl chloride or a 3,5-dimethoxybenzyl substituted ethylene diamine in the final step of the procedure used for the synthesis of clonidine (Scheme 2.1). This modification resulted in the production of IMID-4F/IN or IMID-35MO/IN, respectively. Scheme 2.3 illustrates the synthesis of IMID-4F/IN. A large excess (approximately 10 fold) of ethylene diamine was reacted with 4-fluorobenzyl chloride at 90 °C for 4 hrs. This produced the mono substituted ethylene diamine product, *N*-(4-fluorobenzyl)ethylene diamine, which in the presence of triethylamine was reacted with 2,6-dichlorophenylisocyanide dichloride to produce IMID-4F/IN.

2.2.5 Oxygen substitutions in the imidazoline ring

The synthesis of the oxygen substituted IMID compounds, IMID-4F/O and IMID-35MO/O was very similar to the synthesis of IMID-4F and IMID-35MO. 2-Aminoethanol was reacted (instead of ethylenediamine), in the presence of triethylamine with 2,6-dichlorophenylisocyanide dichloride to produce 2-[*N*-(2,6-dichlorophenyl)amino]-1,3-oxazoline. This compound, with an oxygen substitution in the imidazoline ring incorporated instead a 1,3-oxazole ring. The compounds were then alkylated at the central nitrogen and purified as described in Section 2.2.3.

(a)

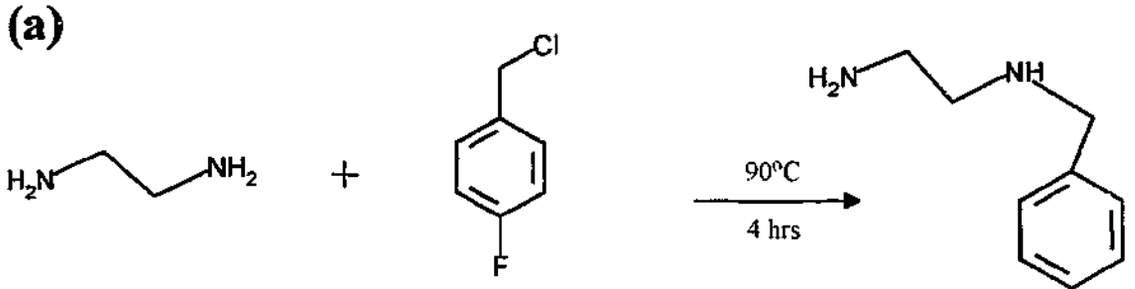

ethylene diamine (10 equivalents)

4-fluorobenzylchloride (1 equivalent)

N-(4-flurobenzyl)ethylene diamine

(b)

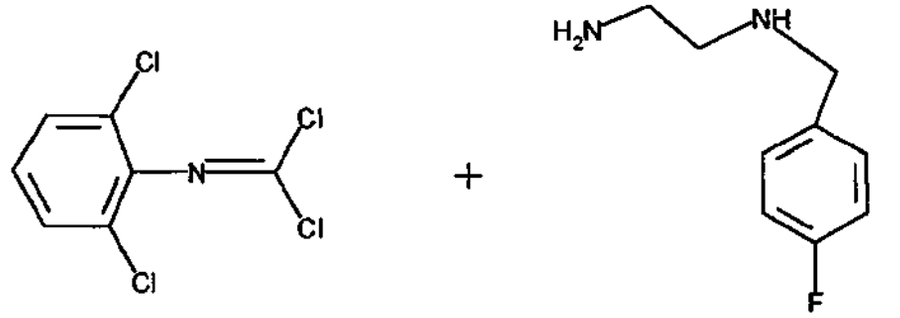

2,6-dichlorophenylisocyanide dichloride

N-(4-flurobenzyl)ethylene diamine

Et_3N triethylamine

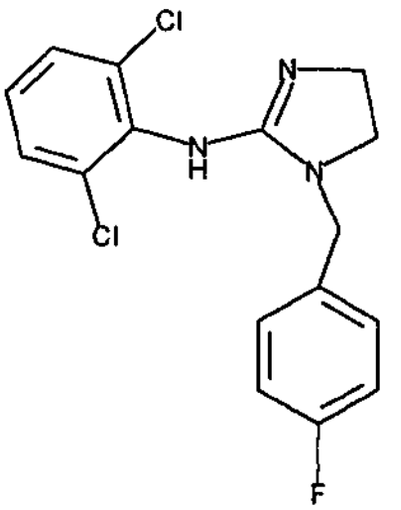

IMID-4F/IN

Scheme 2.3 Schematic diagram of (a) synthesis of *N*-(4-fluorobenzyl)ethylene diamine and (b) the alkylation at the imidazoline nitrogen to synthesise 2-[*N*-(2,6-dichlorophenyl)-amino]-1-(4-flurobenzyl)-2-imidazoline (IMID-4F/IN).

2.2.6 Alkylations at both the central and imidazoline nitrogens of clonidine

The procedure for alkylations at both the central and imidazoline nitrogen to synthesise the bis-substituted compounds was similar to the procedure for the mono-substituted compounds. However, three or four equivalents of the benzyl chloride were used to obtain alkylations on both the central and imidazoline nitrogens. Also, ethanol or acetonitrile was used as the solvent rather than methanol to increase the reaction temperature and therefore make the further alkylation possible. Again, flash chromatography, followed by recrystallation, was used to purify the analogues. This procedure resulted in the synthesis of IMID-35MO/2N, IMID-26F/2N and IMID-4F/2N.

2.2.7 Preparation of HCl salts

In order to increase the solubility of the compounds and therefore allow them to be assessed at high concentrations, the IMID compounds were all converted to HCl salts. This was achieved by generating hydrochloride gas from the dropwise addition of concentrated sulphuric acid to solid ammonium chloride and bubbling it through solutions of the IMID compounds in ether or ether/methanol, followed by recrystallisation.

2.2.8 Confirmation of structure

A number of different techniques were used to characterise and confirm the structure of the compounds synthesised.

2.2.8.1 Proton Nuclear Magnetic Resonance (^{1}H NMR) spectroscopy

As each hydrogen atom has different atoms surrounding it, in any given compound, hydrogens can have different environments. ^{1}H NMR is used to provide a 'chemical map' by creating a spectrum of peaks for each compound, all corresponding to different hydrogen environments. Most nuclei spin about an axis and because they are positively charged they can interact with an externally applied magnetic field. Both the ^{1}H and the ^{13}C nucleus have nuclear spins which are equal to one half as they have a spherical charge distribution. To measure these spins, a radio frequency is used to irradiate the nuclei, which results in energy absorption and a transformation to a higher energy state. The nuclei are now termed to be in resonance with the applied radiation. Different nuclei require different radio frequencies and therefore, ^{1}H and ^{13}C spectra are not recorded at the same time. The position of the absorptions is reflected on a NMR chart which is recorded using an arbitrary scale of frequency (delta (δ) scale) rather than magnetic units. An internal standard is always included as a zero point.

Taking all this information into account we can therefore use the NMR to calculate the location of all the different hydrogen atoms. This is done by looking at the chemical shift (exact position on chart), the integrated intensity (corresponding to the number of hydrogen atoms) and the splitting patterns for each proton. Hydrogen atoms can have their signal split by other hydrogen atoms that are close by. For example a single hydrogen atom on a neighbouring carbon would split the signal into a doublet, two hydrogens, a triplet and so on (McMurray, 1988).

^{1}H NMR spectroscopy were obtained for all reactants and products. All spectra were recorded at 300 MHz with a Varian Mercury or Bruker AM-300 spectrometer or at 400 MHz with a Bruker DRX-400 spectrometer. Generally, the spectra were measured in deuterchloroform ($CDCl_3$) or dimethyl sulphoxide (DMSO) solutions with

tetramethylsilane (TMS) as the internal standard (δ 0.00 ppm) unless otherwise specified. Each resonance was assigned according to the following convention: chemical shift measured in parts per million (ppm) downfield from TMS, multiplicity, number of protons, observed coupling constant (*J* Hz) and assignment. Multiplicities were denoted a s (singlet), d (doublet), t (triplet), q (quartet) or m (multiplet) and prefixed b (broad) where appropriate.

2.2.8.2 Carbon (^{13}C) NMR spectroscopy

Similarly, ^{13}C NMR spectra will show different shifts that reflect the chemical environment of the different carbon atoms. The signals are generally obtained as single lines, decoupled from accompanying protons. However, for some compounds, coupling of ^{13}C to ^{19}F was observed.

Carbon NMR spectra were obtained for all reactants and products. The spectra were recorded on a Mercury Varian 300 spectrometer operating at 75 MHz or a Bruker DRX-400 spectrometer at 100 MHz and were measured in deuterchloroform solutions as the solvent and internal standard (δ 77.04 ppm) unless otherwise specified. Each resonance was assigned according to the following convention: chemical shift (ppm) and assignment. Assignments were determined from J-modulated Spin Echo experiments for X-nuclei coupled to ^{1}H in order to determine the number of attached protons. When the ratio of compounds was determined by ^{13}C NMR, use was made of the relative signal peak heights of comparable carbons.

Assignment of previously unassigned proton and carbon spectra was based on the results of 2-dimensional NMR experiments. Correlation Spectroscopy (COSY) was used to correlate the chemical shifts of ^{1}H nuclei, which were J-coupled to one another.

The experiments were conducted on a Bruker DRX-400 spectrometer and used the standard COSY 45 pulse program. Heteronuclear Multiple Quantum Correlation (HMQC) or inverse chemical shift experiments were used to determine the corresponding ^{13}C nuclei to which ^{1}H nuclei were bonded. These were conducted on a Bruker DRX-400 spectrometer using the standard HMQC pulse program. Heteronuclear Multiple Bond Correlation (HMBC) is a modified HMQC experiment and was used to determine long range ^{1}H-^{13}C connectivity.

2.2.8.3 Thin layer chromatography

Thin layer chromatography (TLC) is a useful tool in the qualitative assessment of different components present in a reaction product. It involves observing how far each component will travel up a silica-coated slide. The separated compounds can be observed on the silica strip under UV light. The R_f value, a ratio of the distance travelled by the compound as a proportion of the distance travelled by the solvent, is then calculated for each component.

TLC was performed on Polygram Sil G/UV_{254} or Polygram Alox N/UV_{254} plastic plates coated with 0.25 mm of silica or 0.2 mm of alumina with the fluorescent indicator, UV_{254}. Components were revealed by fluorescent quenching under 254 nm ultraviolet irradiation or by exposure to iodine vapour where necessary.

2.2.8.4 Electrospray mass spectroscopy

Electrospray mass spectroscopy (ESI) was used to characterise each compound and its isotopes and show their molecular weights. This is done by measuring the masses of the fragments produced when a stream of high-energy electrons separates

molecules. The positively charged fragments are then deflected in relation to their mass-to-charge ratio (*m/z* value) and recorded in peaks (McMurray, 1988).

ESI was carried out on a Micromass Platform II API QMS Electrospray Mass Spectrometer with cone voltage at 25 V, using methanol as the mobile phase. Analyses were conducted in either positive or negative mode. ESI accurate mass measurements were obtained at high resolution with a Bruker BioApex 4.7T ultrahigh resolution FT-ICR mass spectrometer and were reported within ± 5 ppm.

An advantage of this procedure is that it allows the predicted ESI to be calculated, based upon the theoretical structure, which can then be compared to the actual ESI generated.

2.3 Results

In the following sections representative ^{1}H and ^{13}C NMRs of several of the compounds (IMID-4F, IMID-4F/IN, IMID-4F/O & IMID-4F/2N) synthesised for the studies throughout this thesis are presented. In addition, a typical ESI pattern for IMID-4F is also included. It should be noted that these are representative examples only and all of the compounds were processed in a manner similar to those described below.

2.3.1 Alkylations at the central nitrogen

NMR clearly shows monosubstitution at the central nitrogen since the 4 protons in the imidazoline ring are equivalent (due to resonance forms) and appear as a broad singlet. For example the ^{1}H NMR of IMID-4F in $CDCl_3$ has a broad peak at δ 3.65 integrating for 4H for the 4 imidazoline protons in the $CDCl_3$ spectrum, with the benzyl CH_2 as a singlet at δ 5.1 integrating for 2H (Figure 2.3a). The peaks at around 7 are indicative of hydrogens in an aromatic environment, in this case those around the benzene ring. The ^{13}C NMR spectrum of IMID-4F in $CDCl_3$ shows the benzyl CH_2 at δ 51.7 but the imidazoline CH_2 molecules are broad and not clear. A spectrum run with some added DMSO clearly shows both CH_2 types, the benzyl CH_2 at δ 53.2 and the imidazoline CH_2 at δ 45.0 (Figure 2.3b). The ^{13}C NMR also shows doubling of some signals in the aromatic region, for example at δ 114, which is due to coupling of the carbons with ^{19}F which also has a spin of a half.

The correct isotope pattern was observed in the spectra of the halogenated compounds when ESI was performed. For example, when the predicted ESI for the

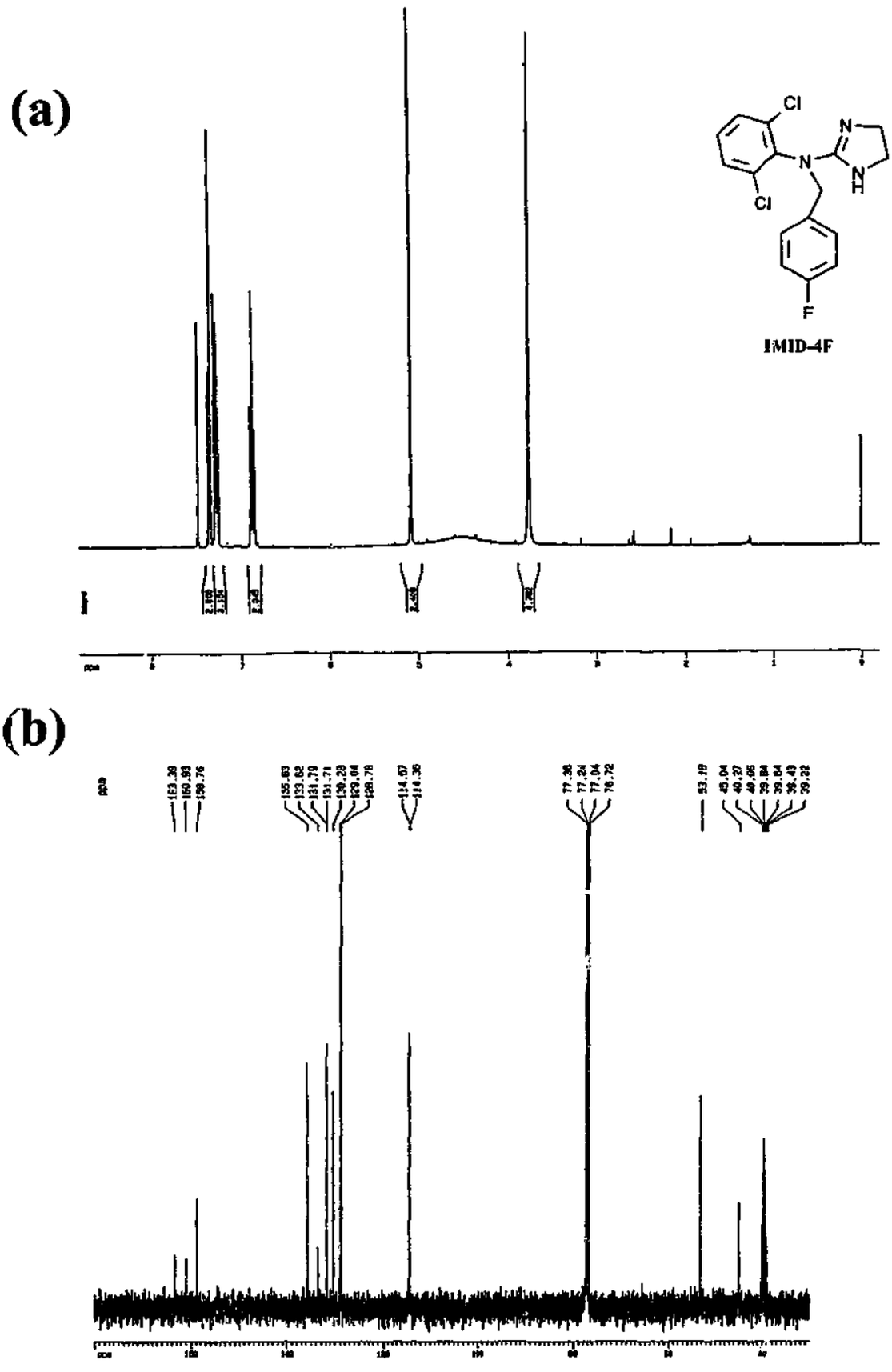

Figure 2.3 (a) A representative ^{1}H NMR spectrum for IMID-4F. The different peaks relate to distinct hydrogen environments. Monosubstitution is evident by the broad singlet at δ 3.65 for the 4 equivalent hydrogens in the imidazoline ring. (b) A representative ^{13}C NMR spectrum for IMID-4F. Each peak relates to a distinct carbon environment. The differing CH_2 molecules of the benzyl and imidazoline rings are evident at δ 53.2 and δ 45.0, respectively. ^{13}C-^{19}F coupling is apparent in the aromatic region, for example, the doublet at δ 114.

molecular ion for IMID-4F was generated and compared with the actual isotope pattern, no substantial difference was observed (Figure 2.4).

2.3.2 Alkylations at the imidazoline nitrogen

The NMRs for compounds such as IMID-4F show equivalent hydrogen and carbon environments for the imidazoline atoms. As IMID-35MO/IN and IMID-4F/IN have alkylations at the imidazoline nitrogen, the carbon and hydrogen atoms of the imidazoline ring are not equivalent. As a result, the ^{1}H NMR for IMID-4F/IN shows a multiplet at δ 3.3 for the imidazoline CH_2 molecules and HMQC experiments show the CH_2's are not equivalent (Figure 2.5a). The ^{13}C NMR for IMID-4F/IN clearly shows the non-equivalence of the imidazoline CH_2's as there are 3 CH_2 signals, δ 40.1, 45.6 and 47.7 (Figure 2.5b). Again doubling of some signals in the aromatic region, for example at δ 115, can be seen, which is due to coupling of the carbons with ^{19}F.

2.3.3 Oxygen substitutions in the imidazoline ring

The two compounds IMID-4F/O and IMID-35MO/O, had oxygen substitutions in the imidazoline ring, resulting in compounds that are oxazolines rather than imidazolines. The ^{1}H NMR spectrum for IMID-4F/O illustrates the non-equivalence of the hydrogens, which results in 2 clear triplets at δ 3.9 and 4.3. The difference is due to the different environments of the hydrogens, one next to the nitrogen and the other next to the oxygen of the oxazoline ring (Figure 2.6a). Again, the ^{13}C NMR spectrum for IMID-4F/O shows the non-equivalence of the imidazoline CH_2 molecules resulting in 3

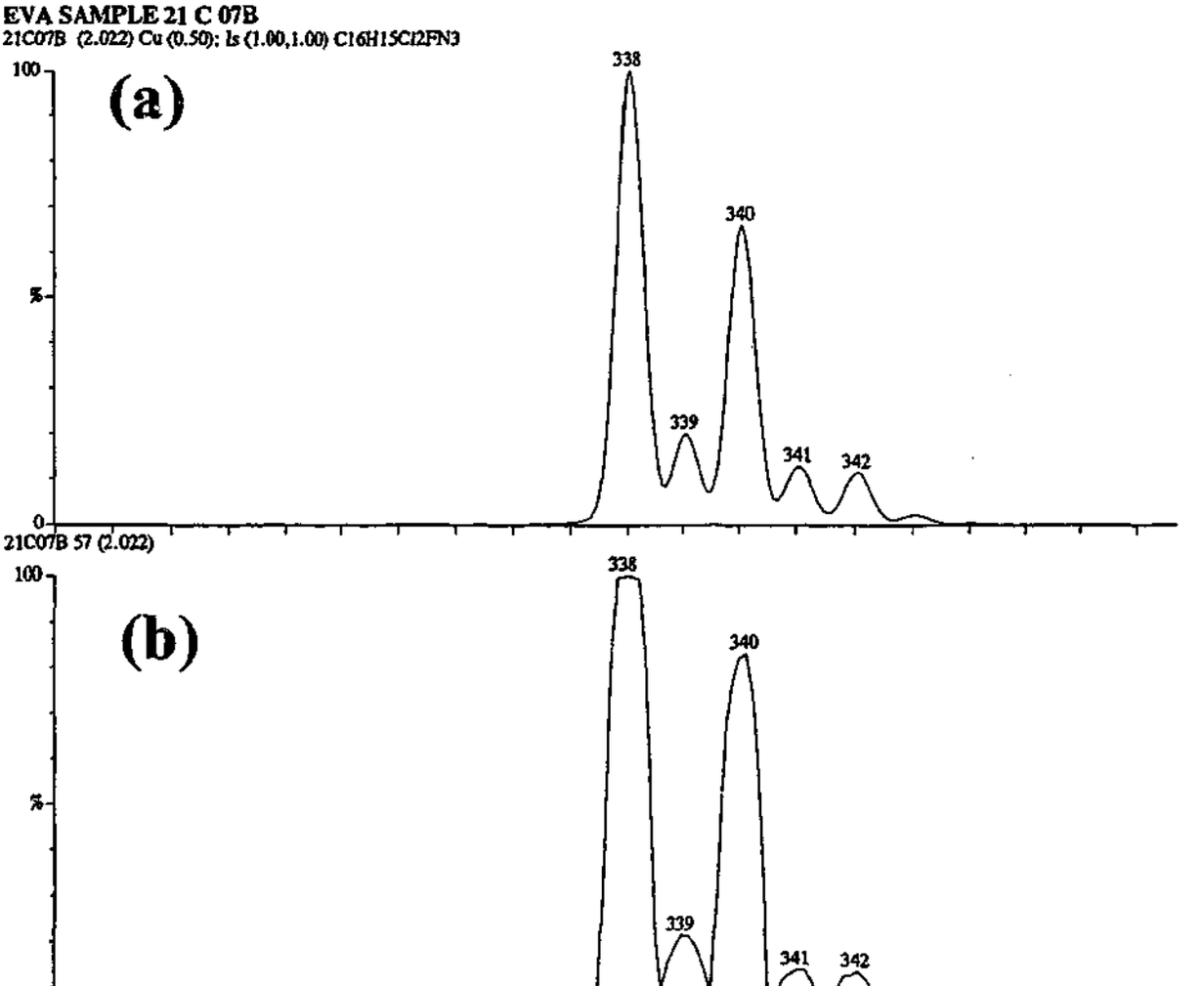

Figure 2.4 (a) Predicted isotope model for molecular ion of IMID-4F and (b) the actual isotope pattern for IMID-4F using electrospray mass spectroscopy confirming the presence of 2 Cl atoms in the molecular makeup of the compound.

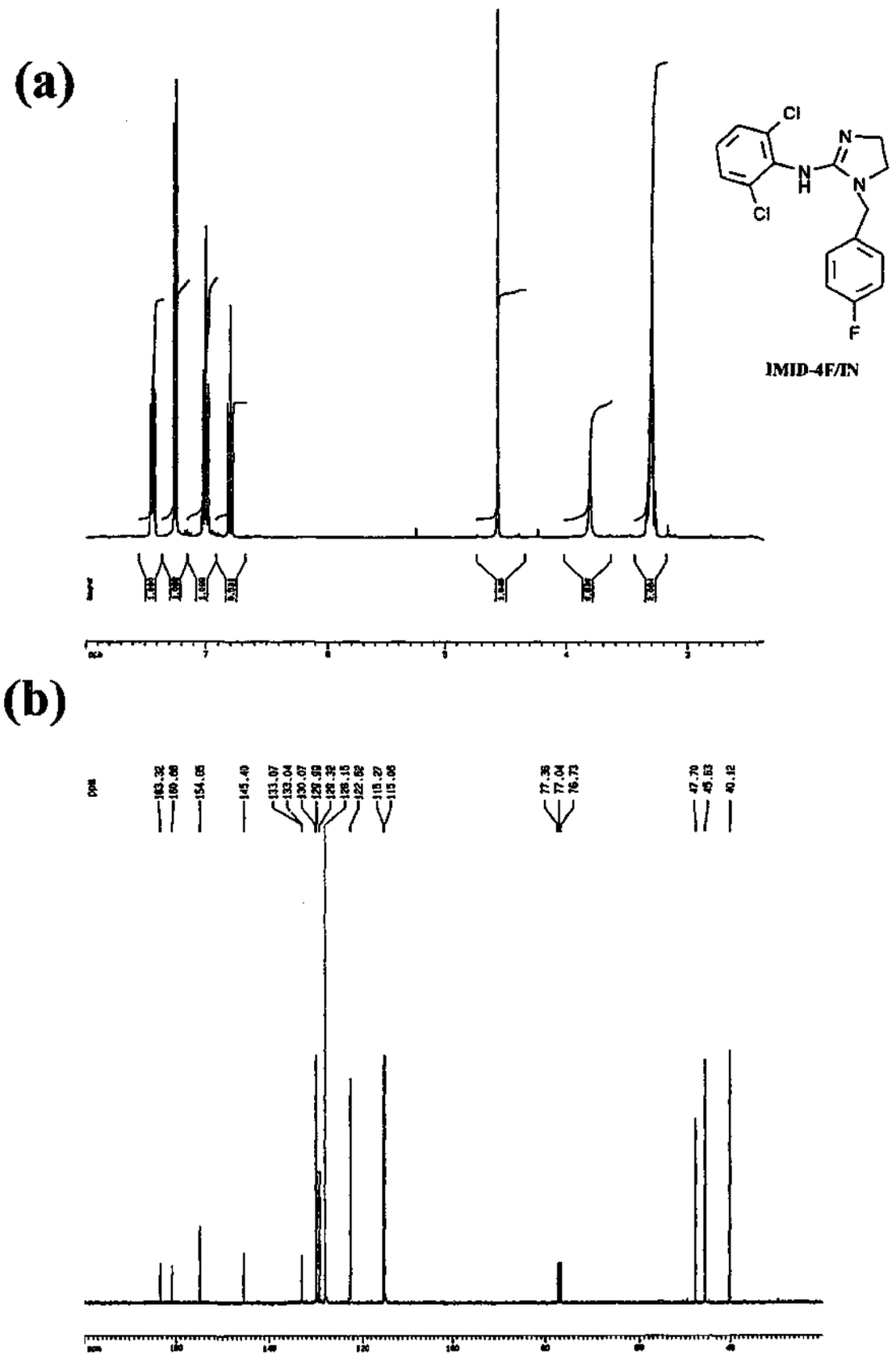

Figure 2.5 (a) A representative ^{1}H NMR spectrum for IMID-4F/IN. The different peaks relate to distinct hydrogen environments. A multiplet at δ 3.3 represents the imidazoline CH_2 molecules (b) A representative ^{13}C NMR spectrum for IMID-4F/IN. Each peak relates to a distinct carbon environment. The non-equivalence of the imidazoline CH_2 molecules is apparent as there are 3 CH_2 signals at δ 40.1, 45.6 and 47.7. Again, a doublet at δ 115 represents ^{13}C-^{19}F coupling in the aromatic region.

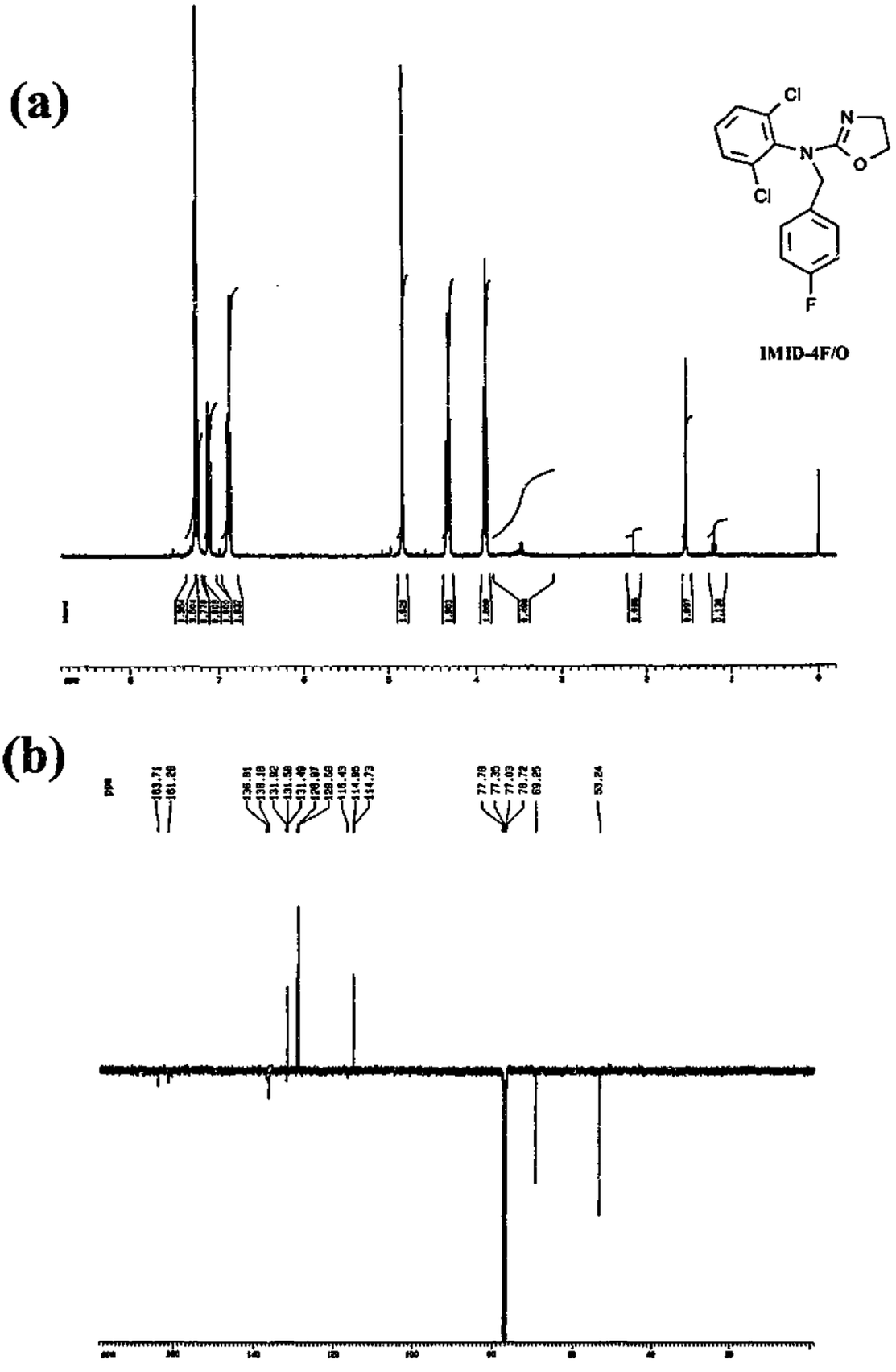

Figure 2.6 (a) A representative ^{1}H NMR spectrum for IMID-4F/O. The different peaks relate to distinct hydrogen environments. The non-equivalence of the hydrogens in the oxazoline ring is evident by the 2 triplets at δ 3.9 and 4.3. (b) A representative ^{13}C NMR spectrum for IMID-4F/O. Each peak relates to a distinct carbon environment. Note the shift at δ 77.35 for the CH_2 next to the O in the oxazoline ring and peaks at δ 53.25 and 69.24 for the remaining CH_2 molecules.

peaks at δ 53.24, 69.25 and 77.35 since they are either next to the oxygen or the nitrogen (Figure 2.6b).

2.3.4 Alkylations at both the central and imidazoline nitrogens

Alkylations of this type resulted in the synthesis of the bis compounds, IMID-35MO/2N, IMID-26F/2N and IMID-4F/2N, which had substitutions at both the central and imidazoline nitrogens. The ^{1}H NMR spectrum for IMID-4F/2N clearly showed 2 triplets for the non-equivalent imidazoline CH_2 molecules at δ 3.34 and δ 3.76 and 2 singlets for the 2 benzyl CH_2 molecules at δ 3.9 and δ 4.9 (Figure 2.7a). The IMID-4F/2N ^{13}C NMR spectrum shows 4 CH_2 peaks at δ 51.3–53.5. There were also 2 doublets at δ 114, illustrating the coupling of ^{13}C-^{19}F for both benzyl groups (Figure 2.7b).

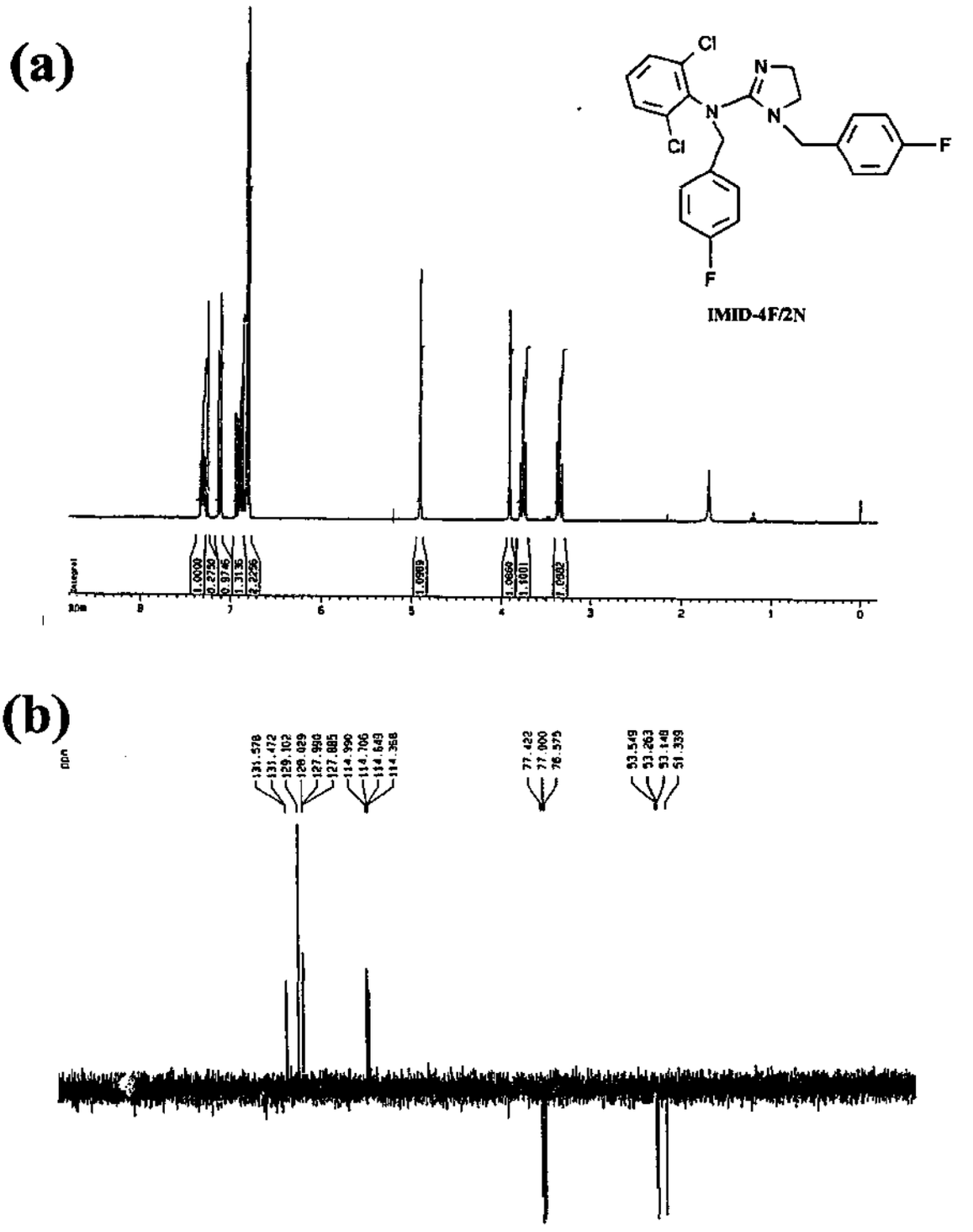

Figure 2.7 (a) A representative ^{1}H NMR spectrum for IMID-4F/2N. The different peaks relate to distinct hydrogen environments. The non-equivalent imidazoline CH_2 molecules are seen as triplets at δ 3.34 and 3.76 and the benzyl CH_2 molecules as 2 singlets at δ 3.9 and 4.9 (b) A representative ^{13}C NMR spectrum for IMID-4F/2N. Each peak relates to a distinct carbon environment. The 4 CH_2 peaks can be seen at δ 51.3-53.5 and evidence of the coupling of ^{13}C-^{19}F of both benzyl groups is seen by the 2 doublets at δ 114.

2.4 Discussion

In this chapter the methods for the synthesis of the novel imidazoline analogues studied throughout this thesis were described. Of the imidazoline analogues already studied by our laboratory the TH series of alinidine analogues have been shown to be more potent than alinidine as K_{ATP} channel antagonists (Challinor-Rogers *et al.*, 1994). Although this was an improvement, the pK_B for the most potent TH compound (TH91:22) was around 6, 10 fold less potent than glibenclamide, which has a pK_B of around 7. Therefore, the need for a group of imidazolines with a pK_B similar to that of glibenclamide was highly desirable.

For this thesis, most of the imidazolines we have synthesised have benzyl groups attached to the central nitrogen with or without substituents attached to the phenyl ring. These modifications were aimed at altering the steric, electronic and lipophilic nature of the compounds in order to increase their potency as K_{ATP} channel antagonists. The 'parent' compound, which had no substituents, is IMID-1M. Several substituents were also added and they included fluoro, methoxy, *t*-butyl and methyl groups. Different positions on the phenyl ring were also examined, the number 4 or para position, the 3 and 5 or meta positions and the 2 and 6 or ortho positions. These modifications resulted in the IMID compounds IMID-4F, IMID-26F, IMID-4MO, IMID-35MO, IMID-4BU and IMID-4ME.

The imidazoline ring has long been thought to possess much of the undesirable, α-adrenoceptor and muscarinic receptor activity of imidazolines (Kobinger & Pichler, 1980; Ogiwara *et al.*, 1987). It was thought that altering the imidazoline ring might either increase or maintain potency as a K_{ATP} channel antagonist while reducing the α-adrenoceptor and muscarinic receptor activity. To this end, an oxygen was substituted

in the imidazoline ring to result in the compounds IMID-4F/O and IMID-35MO/O.

It was also of interest to observe the effect of attaching a benzyl group containing substituents to one of the imidazoline nitrogens, rather than the central nitrogen. This substitution resulted in IMID-4F/IN and IMID-35MO/IN. In addition, compounds with substitutions on both the central and imidazoline nitrogens were made to produce the compounds IMID-26F/2N, IMID-4F/2N and IMID-35MO/2N.

All of these compounds were synthesised in the hope of discovering a potent K_{ATP} channel antagonist with minimal α-adrenoceptor, muscarinic and bradycardic effects.

Chapter Three

The Levcromakalim Antagonist and Bradycardic Actions of the Novel Imidazoline Analogues

3.1 Introduction

As discussed earlier, previous work by our laboratory (Challinor-Rogers *et al.*, 1994) and others have identified two prominent actions for imidazoline based drugs; an ability to antagonise K_{ATP} channels and an ability to lower heart rate through an unrelated action on the sinoatrial node of the heart.

The present study was aimed at testing the new group of novel imidazoline analogues for K_{ATP} channel antagonism. In the present Chapter, the details of experiments performed to determine the potency of these imidazoline analogues as levcromakalim antagonists using the pig isolated coronary artery are presented. In addition, we wanted to determine the underlying electrophysiological effects of selected IMID compounds as well as the interaction of these compounds with the K_{ATP} channel opener, levcromakalim. To this end, electrophysiological studies were performed using rat isolated mesenteric artery to assess the ability of IMID-4F to antagonise levcromakalim-induced hyperpolarisation. Finally, the bradycardic actions of the analogues were assessed using the rat isolated spontaneously beating right atria.

3.2 Materials and Methods

3.2.1 Tissue preparation and Mounting procedures

3.2.1.1 Porcine isolated right circumflex coronary arteries

The porcine isolated right circumflex coronary artery was used to assess the ability of the imidazoline analogues to antagonise vascular K_{ATP} channels. This was achieved by determining their ability to antagonise vasorelaxation to levcromakalim. Porcine hearts were obtained from freshly killed pigs at an abattoir. The right circumflex artery was rapidly removed and placed in ice-cold Krebs solution (composition in mM: NaCl 119, KCl 4.7, $MgSO_4.7H_2O$ 1.17, KH_2PO_4 1.18, $CaCl_2$ 2.5, $NaHCO_3$ 25, and glucose 11). The artery was then pinned out in a silicone coated glass petri dish, cleared of all connective tissue and fat, and cut into 4 mm long segments. Each ring was suspended on two stainless steel wire hooks, 400 μm in diameter, in 25 ml jacketed glass organ baths containing Krebs solution gassed with 5 % CO_2 in O_2. The lower hook was fixed to a support leg attached to a micrometer, while the upper wire hook was suspended from a Grass FT03C force transducer. Isometric force was recorded via an online data acquisition system (CVMS Version 2.0, World Precision Instruments, USA) and displayed on a 6 channel Panasonic printer (Model KX-P3200 Forms Printer). The temperature was maintained at 37°C by a Julabo P water heater and circulator (Julabo Labortech, Seelbach, West Germany). Vessels were left to equilibrate under zero force for 30 min before an initial force of 5 g was applied (Kilpatrick & Cocks, 1994). After another 30 min, the force was re-adjusted to 5 g and the tissues were left for a further 30 min.

3.2.1.2 Rat isolated small mesenteric arteries.

Rat isolated small mesenteric arteries were utilised to assess the direct effects of IMID-4F on membrane potential and the ability of this compound to antagonise hyperpolarisation responses to levcromakalim. Wistar Kyoto (WKY) rats were rendered unconscious by a brief exposure (30 sec.) to 20 % O_2/80 % CO_2 and then exsanguinated. The mesentery was rapidly removed and placed in ice-cold Krebs solution. A segment of rat small mesenteric artery, 2 mm in length, corresponding to a third or fourth order branch from the superior mesenteric artery, was mounted in a small vessel myograph (J.P. Trading, Aarhus, Denmark) to measure isometric force. The myograph was filled with Krebs solution, gassed with 5 % CO_2 in O_2. A 40 μm wire was threaded through the lumen of the vessel segment. The vessel was then placed between the jaws of the myograph where the wire was attached to one of the jaws. A second wire was threaded through the lumen of the vessel and the jaws moved together to trap both wires. The second wire was then attached to the second jaw. The first wire was attached to an isometric force transducer, while the second was attached to a stationary support driven by a micrometer.

Responses were recorded on an online data acquisition system (CVMS Version 2.0, World Precision Instruments, USA) and displayed on a dual-channel flat bed recorder (W+W Scientific Instruments, model 320). Vessels were allowed to equilibrate under zero force for 30 minutes and the temperature was warmed to 37 °C. After the equilibration period the vessels underwent the normalisation procedure described below.

3.2.1.2.1 Normalisation procedure

Each vessel was normalised using a procedure based on the Mulvany & Halpern (1977) method for determining the optimal passive tone in small diameter arteries as follows in short. Passive tension is placed on the vessel by moving the jaws apart and therefore increasing the external circumference. Since the vessel wall is flat between the wires, the internal circumference can be determined using the formula:

$$C = (\pi + 2)d + 2w \qquad \text{Equation 3.1}$$

where d = wire diameter (ie. 40 μm) and

w = distance between the inner edges of the wires.

As the value of C can be calculated it is then possible to determine the effective internal diameter (D) using the following formula:

$$D = C/\pi \qquad \text{Equation 3.2}$$

The tension (T) is related to the force (F) generated by the vessel by the following formula:

$$T = F/l \qquad \text{Equation 3.3}$$

where l = vessel length (typically 2 mm)

The normalisation procedure involves stepwise increases in the internal circumference and readings of the force developed at 60 sec. intervals. The effective transmural pressure (P) is then calculated using the following formula:

$$P = 2\ T/\pi\ D$$

P is an estimation of the pressure that would be required for that diameter and tension to occur if the vessels were *in situ*.

This is carried out until the pressure reaches approximately 100 mmHg (approximately 5 mN/mm for a 300 μm vessel; (McPherson, 1992b). An exponential

curve is then fitted to the data and the vessel diameter set by the myograph at approximately 90 % of the diameter for 100 mmHg. This passive tension has previously been shown to be the optimal tension for the development of maximal active tension in arteries (Mulvany *et al.*, 1977; McPherson, 1992a). The vessel diameters are expressed in the text as the diameter at a transumural pressure of 100 mmHg (D_{100}).

3.2.1.3 Rat isolated spontaneously beating right atria

Rat isolated spontaneously beating right atria were used to assess the bradycardic activity of the imidazoline analogues. Male Sprague-Dawley rats (200-400 g) were anaesthetised with a short (30 second) exposure to 20 % O_2/ 80 % CO_2 and exsanguinated. The heart was rapidly removed and placed in warmed, oxygenated Krebs solution and the right atria was dissected free. The atria was then placed vertically on stainless steel S-shaped hooks and suspended in Krebs solution in a jacketed 25 ml organ bath maintained at 37 °C. The atria were washed with Krebs solution and left to equilibrate for approximately 30 minutes until the resting atrial rate was stable. Basal tension was maintained at approximately 0.5 g throughout the experiments. Chronotropic responses were recorded (as 5 second averages) with an online data acquisition system (CVMS Version 2.0, World Precision Instruments, USA) and displayed on a 6 channel Panasonic printer (Model KX-P3200 Forms Printer).

3.2.2 Experimental protocol and Analysis of results

3.2.2.1 Levcromakalim antagonism

After the equilibration, a potassium depolarising solution (KPSS; composition in mM: KCl 123, $MgSO_4.7H_2O$ 1.17, KH_2PO_4 1.18, $CaCl_2$ 2.5, $NaHCO_3$ 25, and glucose 11) was added to constrict the rings. This response was used to determine the maximum constrictor response of the tissue. After a plateau to KPSS was reached, the vessels were washed twice with Krebs solution and left until the response returned to the initial baseline, before commencing the experiment.

After this period each coronary ring was constricted to approximately 50 % of the KPSS value with the thromboxane-mimetic U46619 (3-30 nM). Several of the imidazoline compounds clearly caused vasorelaxation of the passive tension applied to the vessels. In addition preliminary data also showed that some compounds affected the vasoconstrictor response to U46619. However, as we wished to assess the imidazoline analogue potency as K_{ATP} channel antagonists it was important that all the rings were precontracted equally. Therefore, in these cases, the amount of U46619 used to contract the vessel was increased until the level of precontraction was at the 50% KPSS level. The imidazoline compound-induced relaxation will be discussed in greater detail in Chapter 4. When responses to U46619 plateaued, cumulative concentration-response curves to levcromakalim (0.1-30 μM) (or in some cases sodium nitroprusside; 1 nM-30 μM), were constructed (0.5 log increments). Concentrations of levcromakalim were added when the response to the previous concentration had reached a plateau. Only one concentration-response curve was obtained with any one coronary artery ring. A single concentration of the imidazoline compound (IMID series) tested was added 20 min prior to submaximally constricting the tissue with U46619. Preliminary experiments

indicated that this incubation period was sufficient for equilibrium antagonism to be produced (data not shown). In some cases levcromakalim did not cause full tissue relaxation, hence sodium nitroprusside (10 μM) was added at the end of each curve to obtain maximal vessel relaxation. For a detailed summary of the protocol used refer to Figure 3.1.

The contraction to U46619 (3-30 nM) was taken as 100 % response and the relaxation produced by different concentrations of levcromakalim or SNP was expressed as a percentage of this response. It was observed that, at high concentrations, most of the imidazoline analogues shifted the levcromakalim concentration-response curve in a non-parallel fashion. The slope of the curve was reduced and the maximum response to levcromakalim appeared to be depressed. This suggested that the type of antagonism displayed by the compounds was non-competitive, preventing us from the use of Schild analysis (Jenkinson, 1991) as a means of determining the potency of the active ions. Instead, an 'apparent pK_B' was estimated, based on a single concentration of antagonist.

The following equation was used:

Apparent pK_B = -Log([Antagonist Concentration (M)] / [Concentration ratio -1])

Equation 3.4

Therefore, the percentages obtained were represented graphically and the pD_2 (- log EC_{50}) values calculated as the concentration of relaxant required to cause 50 % of the maximal relaxant response. pD_2 values were only calculated for each concentration of antagonist where the relaxation was near 100 %. The single concentration of the antagonist used to calculate the apparent pK_B was selected on the basis that it produced

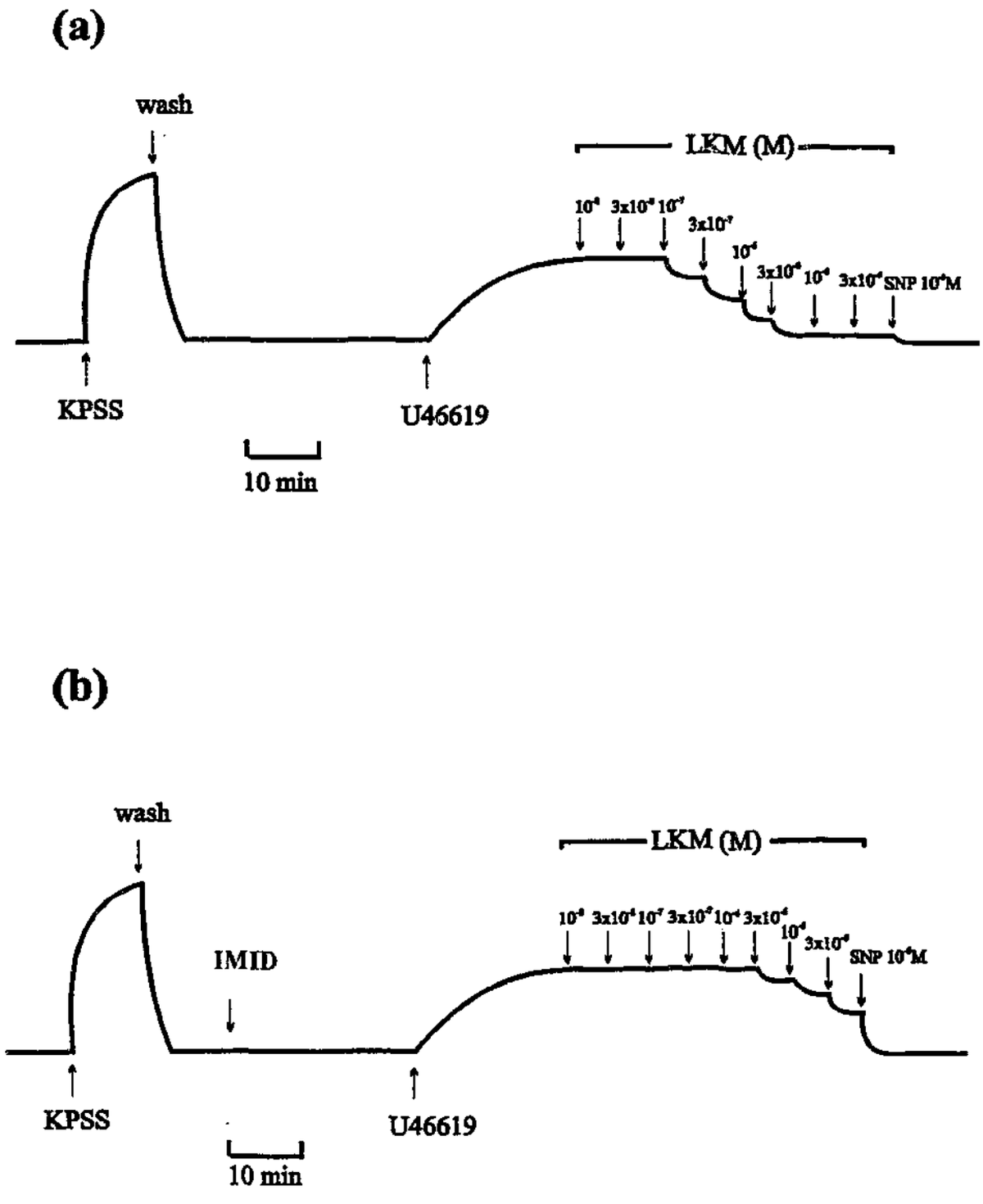

Figure 3.1 Experimental protocol for testing the IMID compounds for levcromakalim (LKM) antagonism in pig isolated right circumflex coronary artery. After equilibration rings were constricted with a potassium depolarising solution (KPSS), washed and then after an incubation period of 20 minutes precontracted with U46619 (1-30 nM) either, (a) in the absence, or (b) in the presence of an IMID compound. A concentration-response curve to levcromakalim was then obtained and sodium nitroprusside (SNP) added at the end of each curve to produce full tissue relaxation.

a parallel-like shift in the levcromakalim concentration-response curve without overtly affecting the maximal levcromakalim response.

3.2.2.2 Electrophysiological properties

After normalisation of the rat small mesenteric artery, the vessel was left for a further 30 minutes. An aluminosilicate glass electrode (1.0 mm blanks, World Precision Instruments Inc., USA) filled with 0.2 M KCl (tip resistance approximately 80-100 MΩ) was used to impale a single smooth muscle cell. A Burleigh Inchworm motor, driven by a 6000 series controller (Burleigh, USA) positioned the microelectrode. The microelectrode was advanced using 1 μm steps until a stable impalement was achieved. The bath (15 ml volume) containing the vessel was part of a 25 ml recirculating system that contained a jacketed organ bath, where the Krebs solution was warmed and oxygenated, and drugs could be added. This design allowed cumulative steady-state concentration-response curves to levcromakalim in the presence and absence of IMID-4F to be constructed. After impalement the intracellular membrane potential of a single smooth muscle cell from the rat isolated small mesenteric artery was monitored using the CVMS Version 2.0, data acquisition system (World Precision Instruments, USA). A cumulative concentration-response curve to levcromakalim (0.1–10 μM) alone, was constructed and the tissue was then washed. A cumulative concentration-response curve to IMID-4F (1–10 μM) was carried out, and without washing, another concentration-response curve to levcromakalim was determined in the presence of IMID-4F (10 μM). Concentrations of the either levcromakalim or IMID-4F were added when the response to the previous concentration had reached a plateau.

3.2.2.3 Bradycardic activity

Cumulative concentration-response curves (0.5 log increments) were constructed for each imidazoline analogue (0.1-30 μM) in the rat isolated spontaneously beating right atria. Further concentrations of the compounds were added when the response to the previous concentration had reached a plateau.

Bradycardic responses were expressed as a percentage of the resting atrial rate measured in beats per minute (bpm) with 100 % referring to initial resting atrial rate. The percentages obtained were then represented graphically and where a maximum was reached the pD_2 (-log EC_{50}) for each individual experiment calculated. In cases where the bradycardic response did not reach a lower plateau the pD_2 could not be calculated, therefore, only estimates are given.

3.2.3.4 Statistics

Results in the text are given as mean ± S.E.M. Statistical tests used are stated in the text. In general, Students *t*-tests and unpaired *t*-tests were used to compare values/groups of two, while Analysis of Variance (ANOVA) was used to test more than two values/groups that were dependent and the Bonferroni *t*-test for all pairwise multiple comparisons was used for post-hoc analysis. Groups were considered significantly different from each other if $P<0.05$, unless otherwise stated. All statistical calculations were performed using SigmaStat (Jandel Scientific, USA).

3.2.3 Drugs

Drugs used and their sources were: acetylcholine (Sigma Chemical Co., U.S.A.); alinidine (Boehringer Ingelheim); IMID compounds (Eva Campi, Department of

Chemistry, Monash University; Figure 2.1); levcromakalim (SmithKline Beecham, UK); sodium nitroprusside (SNP; Sigma Chemical Co., U.S.A.) and U46619 (The Upjohn Co., Kalamazoo, USA). Alinidine, levcromakalim and the imidazoline analogues were made up in 100% methanol (MeOH) as stock solutions of 10 mM. The first additional dilution for the imidazoline analogues was made in 40 % MeOH and all further dilutions were made in Krebs. Acetylcholine, sodium nitroprusside and U46619 were dissolved in distilled water and diluted in Krebs.

3.3 Results

3.3.1 Levcromakalim antagonism by the imidazoline analogues

The ability of several imidazoline analogues to antagonise the vasorelaxant responses of the K_{ATP} channel opener, levcromakalim, was assessed in isolated segments of pig coronary artery precontracted with U46619 (3–30 nM).

In each experiment the contractions to U46619 were matched to approximately 50 % of the KPSS contraction whether in the absence or in the presence of increasing concentrations of the imidazoline analogues (ie. IMID-1M; Fig 3.2b). Several of the imidazoline analogues (IMID-35MO/IN, IMID-35MO/O, IMID-4F/O, IMID-4F/2N, IMID-26F/2N & IMID-35MO/2N) significantly affected the vasoconstriction to U46619. However, as the aim of this series of experiments was to assess their ability as K_{ATP} channel antagonists, in these cases, additional U46619 was used to achieve the same level of tone (50% KPSS) in each blood vessel. The vasodilator effects of these compounds are further characterised and discussed in Chapter 4.

Addition of levcromakalim resulted in a concentration-dependent relaxation of U46619 precontracted pig isolated coronary arteries with a pD_2 of 6.65 ± 0.04 (n=75; control curves, Figures 3.2-3.8). In instances when levcromakalim did not cause full relaxation, SNP (10 μM) was added to induce full tissue relaxation. The majority of the imidazoline analogues antagonised levcromakalim-induced vasodilatation (Figures 3.2-3.8). The nature of this antagonism was characterised by a shift to the right in the concentration-response curves to levcromakalim, followed at higher concentrations by a flattening of the curve and a reduction in maximum vasodilatation. As a result a Schild

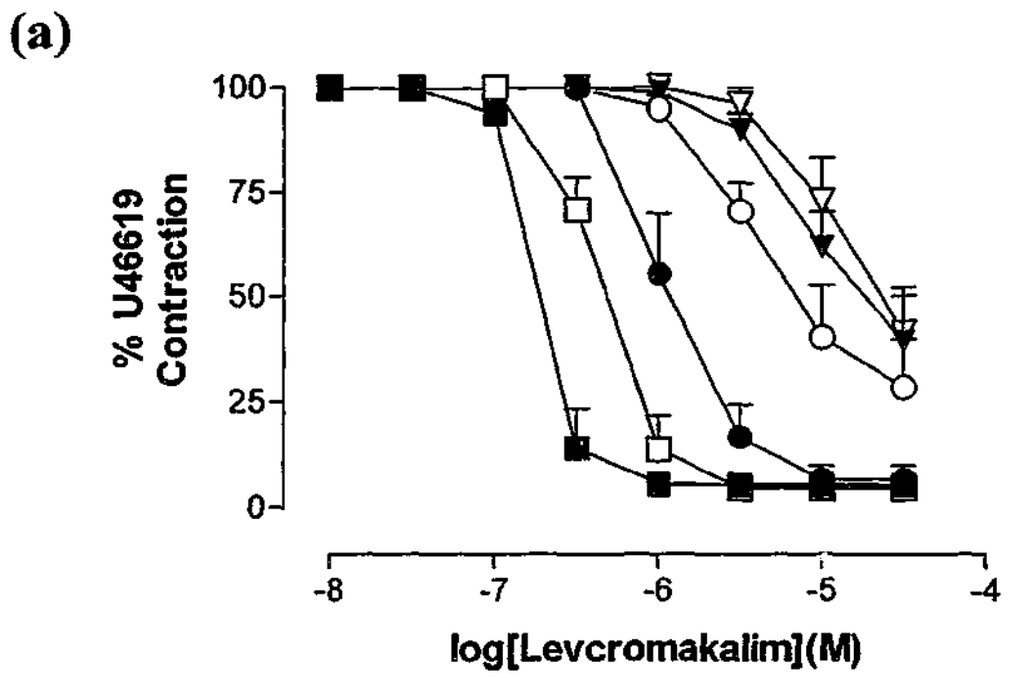

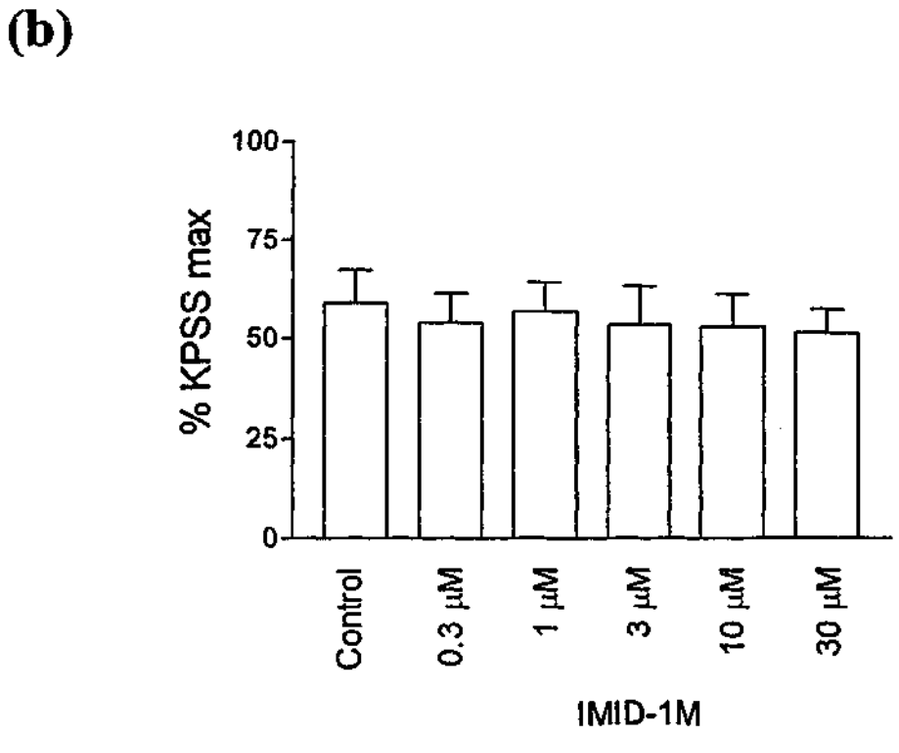

Figure 3.2 (a) Mean levcromakalim concentration-response curves in the pig isolated right circumflex coronary artery in the absence (■) and presence of increasing concentrations of IMID-1M, 0.3 (□), 1 (●), 3 (○), 10 (▼) and 30 (▽) μM. (b) Initial tone as a percentage of KPSS in the absence (control) and presence of increasing concentrations of IMID-1M. Error bars are ± S.E.M. and if not visible are contained within the symbol (n=5-7).

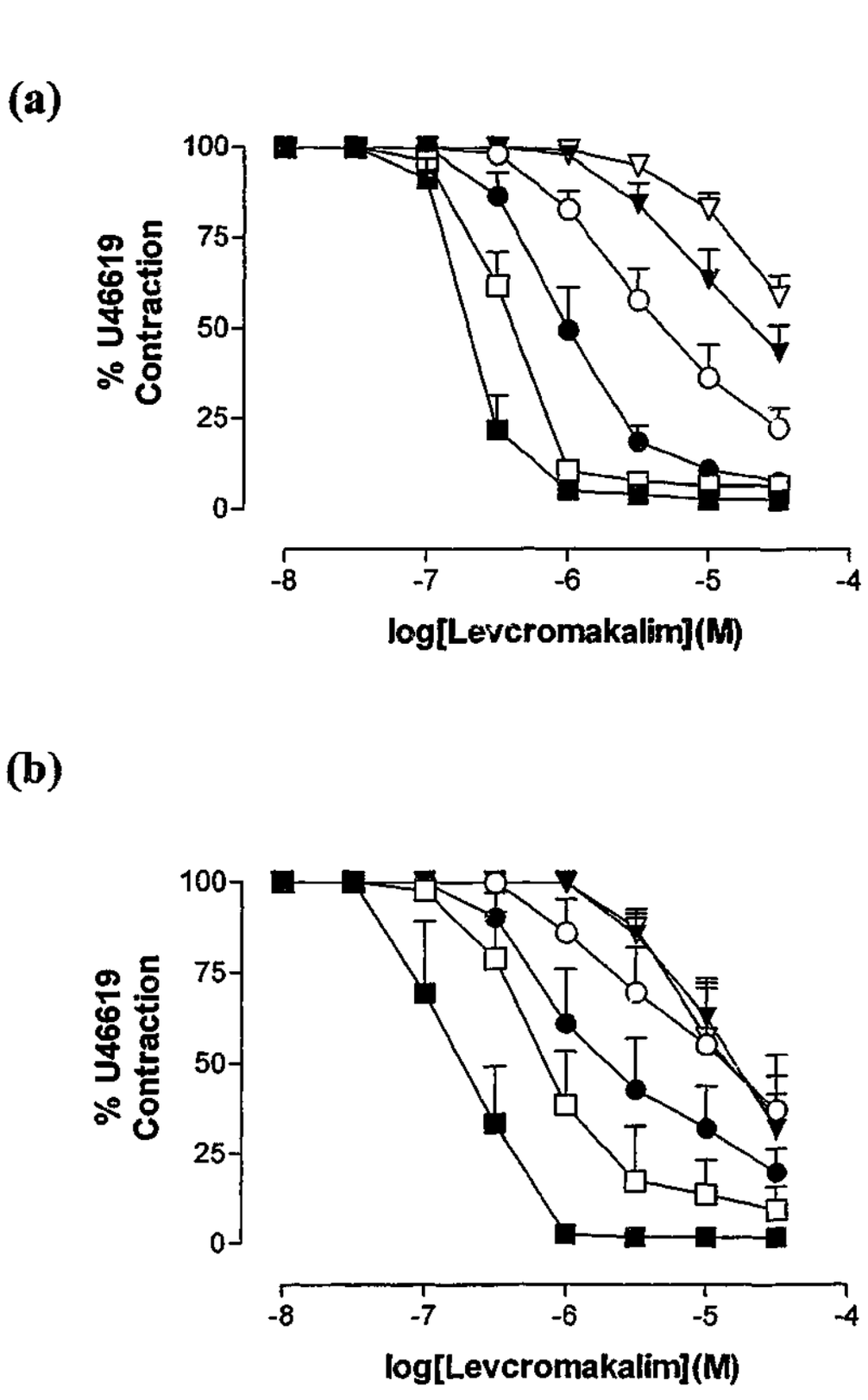

Figure 3.3 Mean levcromakalim concentration-response curves in the pig isolated right circumflex coronary artery in the absence (■) and presence of increasing concentrations of (a) IMID-4F and (b) IMID-26F. The concentrations used were 0.3 (□), 1 (●), 3 (○), 10 (▼) and 30 (▽) μM. Error bars are ± S.E.M. and if not visible are contained within the symbol (n=5-8).

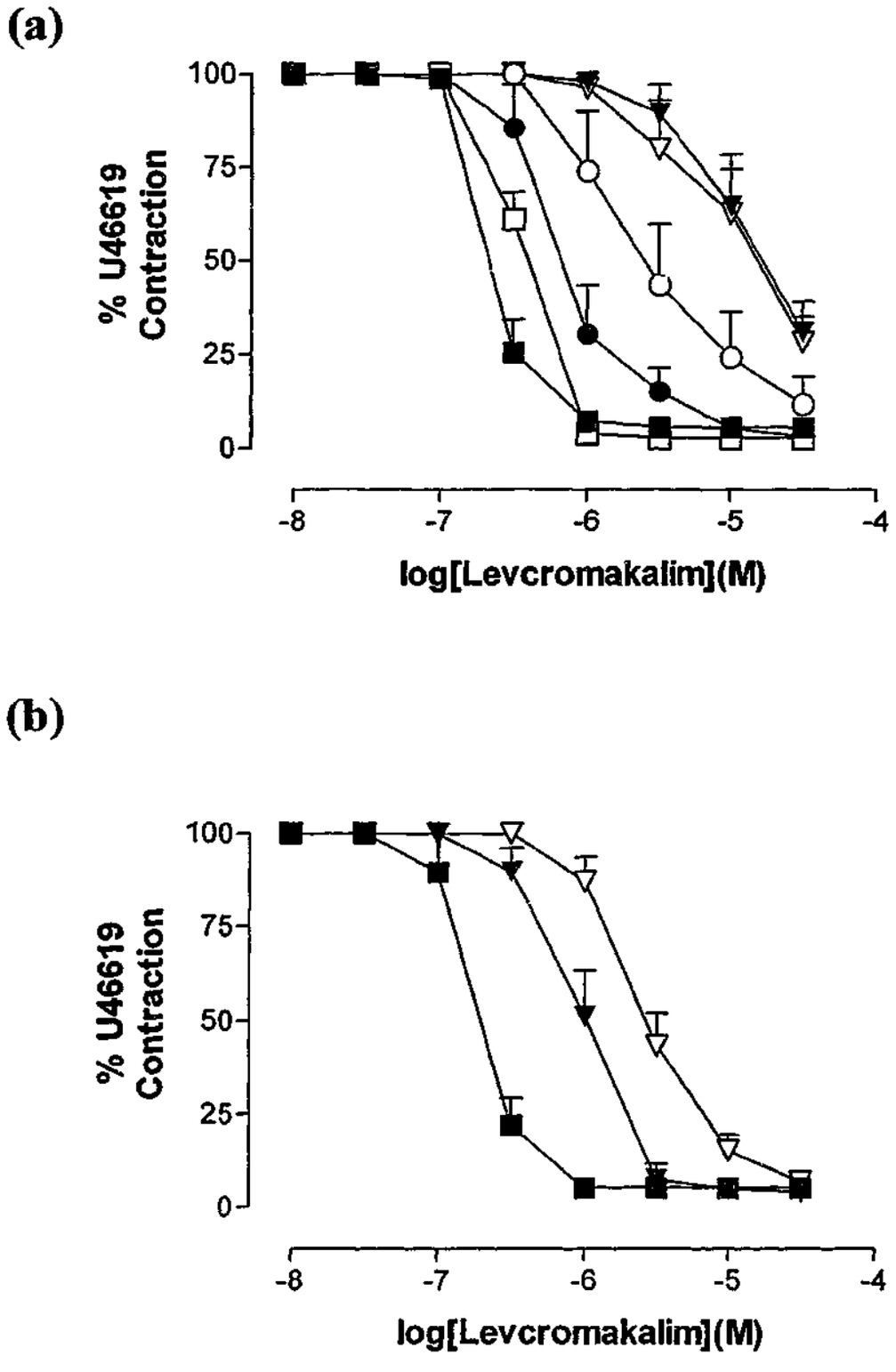

Figure 3.4 Mean levcromakalim concentration-response curves in the pig isolated right circumflex coronary artery in the absence (■) and presence of increasing concentrations of (a) IMID-4ME and (b) IMID-4MO. The concentrations used were 0.3 (□), 1 (●), 3 (○), 10 (▼) and 30 (▽) μM. Error bars are ± S.E.M. and if not visible are contained within the symbol (*n*=5-10).

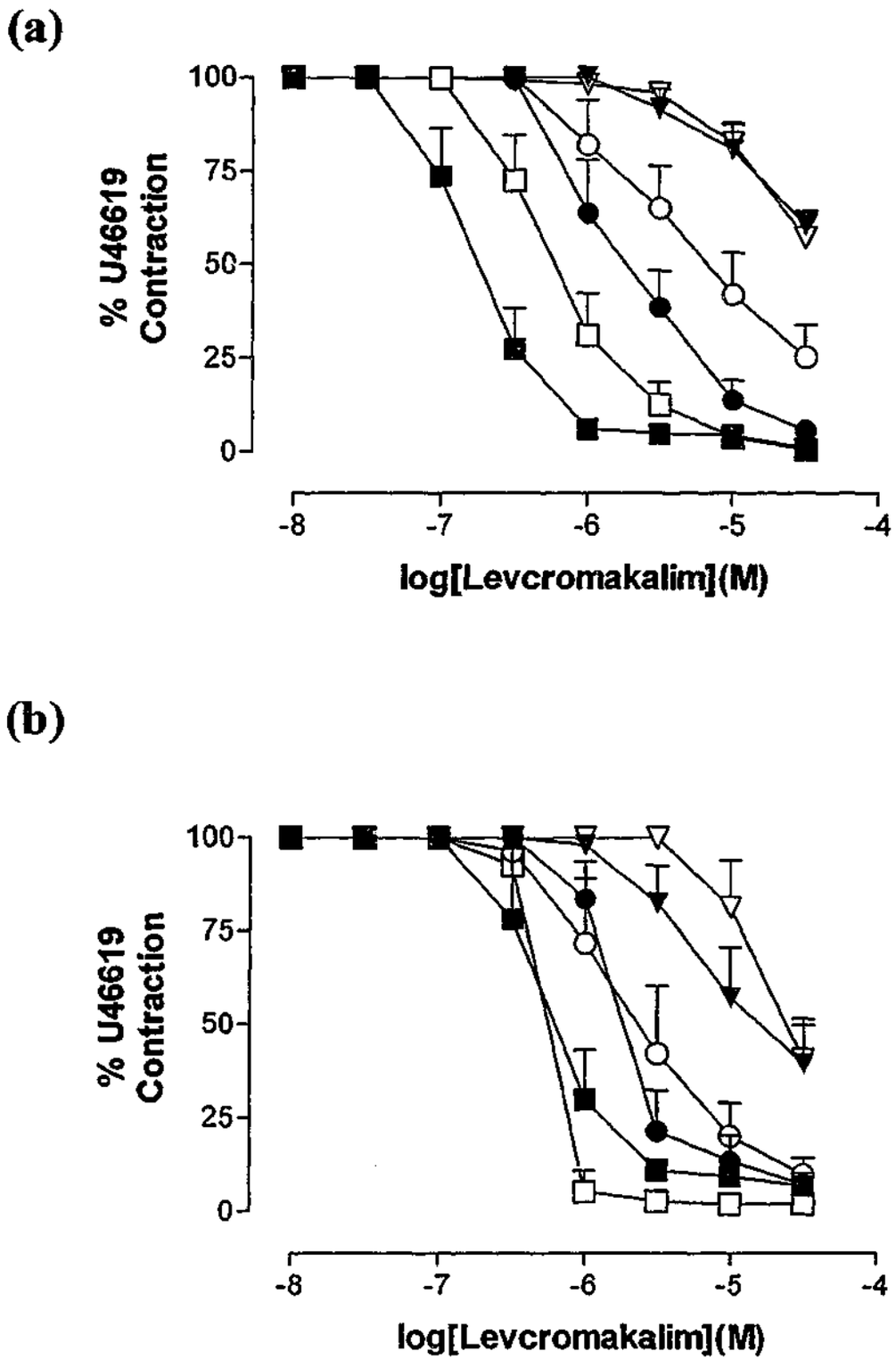

Figure 3.5 Mean levcromakalim concentration-response curves in the pig isolated right circumflex coronary artery in the absence (■) and presence of increasing concentrations of (a) IMID-35MO and (b) IMID-35MO/IN. The concentrations used were 0.1 (□), 0.3 (●), 3 (○), 10 (▼) and 30 (▽) μM. Error bars are ± S.E.M. and if not visible are contained within the symbol (n=5-8).

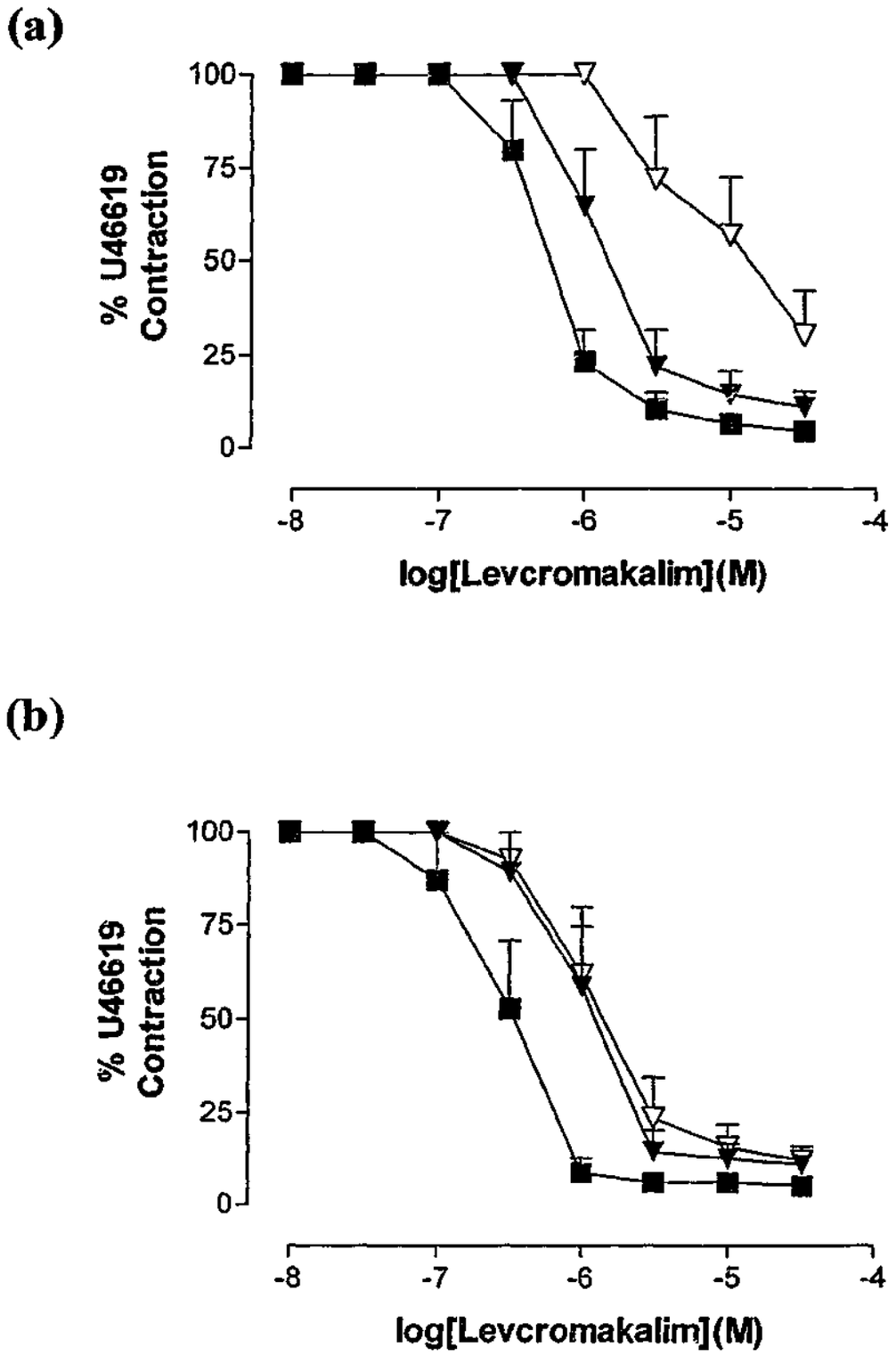

Figure 3.6 Mean levcromakalim concentration-response curves in the pig isolated right circumflex coronary artery in the absence (■) and presence of increasing concentrations of (a) IMID-4F/O and (b) IMID-35MO/O. The concentrations used were 10 (▼) and 30 (▽) μM. Error bars are ± S.E.M. and if not visible are contained within the symbol (n=5-6).

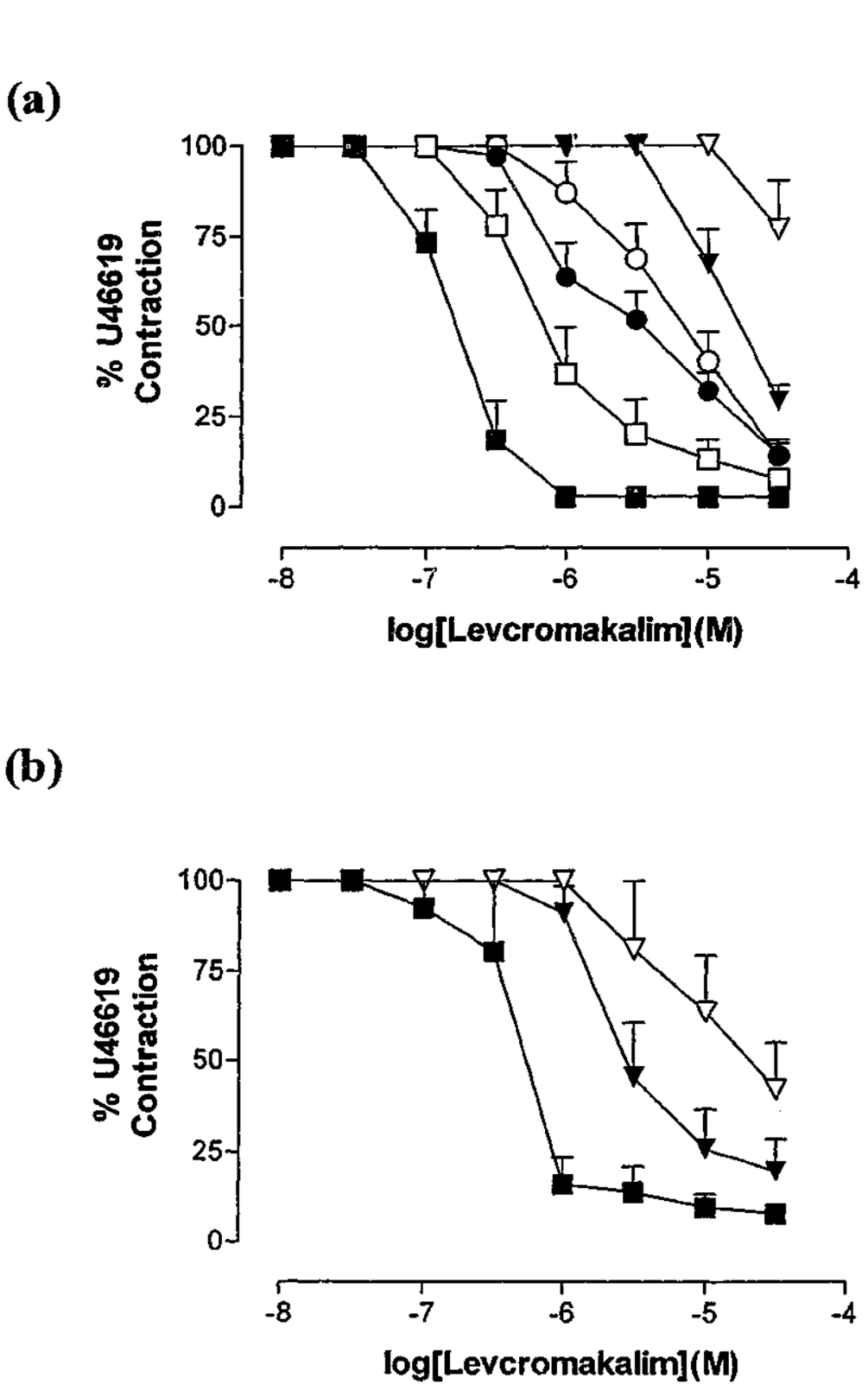

Figure 3.7 Mean levcromakalim concentration-response curves in the pig isolated right circumflex coronary artery in the absence (■) and presence of increasing concentrations of (a) IMID-4F/2N and (b) IMID-4F/IN. The concentrations used were 0.1 (□), 0.3 (●), 3 (○), 10 (▼) and 30 (▽) μM. Error bars are ± S.E.M. and if not visible are contained within the symbol (*n*=5-6).

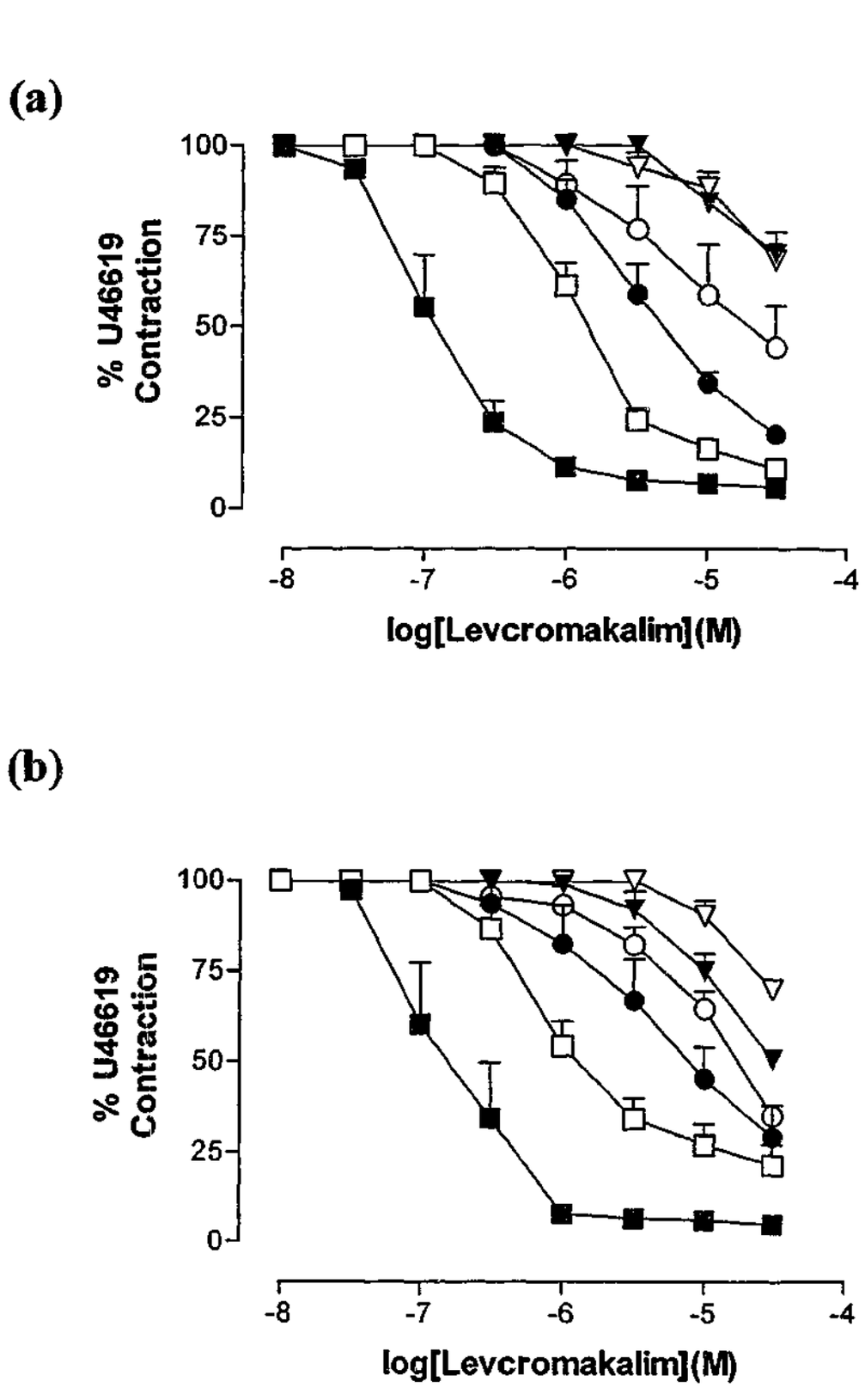

Figure 3.8 Mean levcromakalim concentration-response curves in the pig isolated right circumflex coronary artery in the absence (■) and presence of increasing concentrations of (a) IMID-35MO/2N and (b) IMID-26F/2N. The concentrations used were 0.1 (□), 0.3 (●), 3 (○), 10 (▼) and 30 (▽) μM. Error bars are ± S.E.M. and if not visible are contained within the symbol (*n*=5-8).

analysis could not be performed and an 'apparent pK_B' value was determined instead using equation 3.4 (see Section 3.2.2.1). The concentration of the imidazoline analogue that was used to calculate its pK_B was the highest concentration of analogue that allowed full vasodilatation to levcromakalim. Table 3.1 summarises the pK_B values determined for each analogue.

From this analysis a group of compounds were identified that displayed high potency as levcromakalim antagonists with pK_B values of approximately 7. These included IMID-4F/2N (pK_B = 7.40), IMID-35MO/2N (7.40), IMID-26F/2N (7.26), IMID-35MO (7.02), IMID-26F (6.97), IMID-4F (6.93) and IMID-1M (6.85), which were all significantly more potent than the remaining 7 compounds (n= 5-8, P<0.05, ANOVA, Figures 3.2, 3.3, 3.5, 3.7 & 3.8). Of the remaining compounds, IMID-4ME (pK_B = 6.45) was the next in order of potency, followed by IMID-35MO/IN (6.16), IMID-4F/IN (5.62), IMID-4MO (5.52), IMID-35MO/O (5.51) and IMID-4F/O (5.25) (Figures 3.4, 3.5, 3.6b, 3.7 & 3.8b). The final analogue, IMID-4BU was inactive as an antagonist of levcromakalim-induced relaxation (control levcromakalim pD_2 = 6.58 ± 0.02; plus IMID-4BU (30 μM) pD_2 = 6.45 ± 0.06; n=5, P>0.05; Students t-test, data not shown).

In similar experiments the antagonist potency of IMID-1M (30 μM) and IMID-35MO (30μM) was determined using sodium nitroprusside (1 nM - 30 μM), a compound that causes vasodilatation via cGMP and therefore, through a different mechanism than the opening of K_{ATP} channels. There was no significant shift in the pD_2 value when concentration-effect curves to sodium nitroprusside were obtained in the absence or the presence of IMID-1M (Figure 3.9a; control pD_2 = 7.23 ± 0.1; plus

Compound	K_{ATP} channel antagonism		Bradycardic effect	
	pK_B	μM^a	pD_2	AR^b
IMID-1M	6.85 ± 0.10*	1	>4.5	>224
IMID-26F	6.97 ± 0.17*	0.3	≥4.5	≥295
IMID-4F	6.93 ± 0.08*	3	>4.5	>269
IMID-4ME	6.45 ± 0.16	3	>4.5	>89
IMID-4MO	5.52 ± 0.06	30	>4.5	>10
IMID-35MO	7.02 ± 0.16*	3	≥4.5	≥331
IMID-35MO/IN	6.16 ± 0.15	3	≥4.5	≥46
IMID-4F/IN	5.62 ± 0.12	10	≥4.5	≥13
IMID-35MO/O	5.51 ± 0.09	10	✞	-
IMID-4F/O	5.25 ± 0.17	30	>4.5	>6
IMID-35MO/2N	7.40 ± 0.19*	0.3	5.18 ± 0.22	166
IMID-4F/2N	7.40 ± 0.22*	1	5.15 ± 0.12	178
IMID-26F/2N	7.26 ± 0.15*	0.3	5.26 ± 0.13	100
IMID-4BU	INACTIVE	30	>4.5	-
Alinidine	5.49 ± 0.01ψ	10	>4.5	>10

a Concentration of compound used in pK_B calculation for K_{ATP} channel antagonism.
b Activity Ratio = antilog(pK_B - pD_2) ie. ratio of K_{ATP} channel antagonism to bradycardic activity.
* Compounds significantly more potent than other derivatives ($P<0.05$; ANOVA with Bonferroni *t*-test)
ψ Calculated in a previous study in our laboratory (Challinor-Rogers *et al.*, 1994)
✞ Caused 12.1 ± 2.0 % reduction in atrial rate at 30 μM.
- not calculated.

Table 3.1 Summary of 'apparent' pK_B values obtained for the imidazolines assessed for their ability to antagonise levcromakalim-induced relaxation of pig isolated coronary arteries precontracted with U46619 and their pD_2 values calculated for causing bradycardia in rat spontaneously beating right atria (pig coronary artery n=5-8, atria n=4).

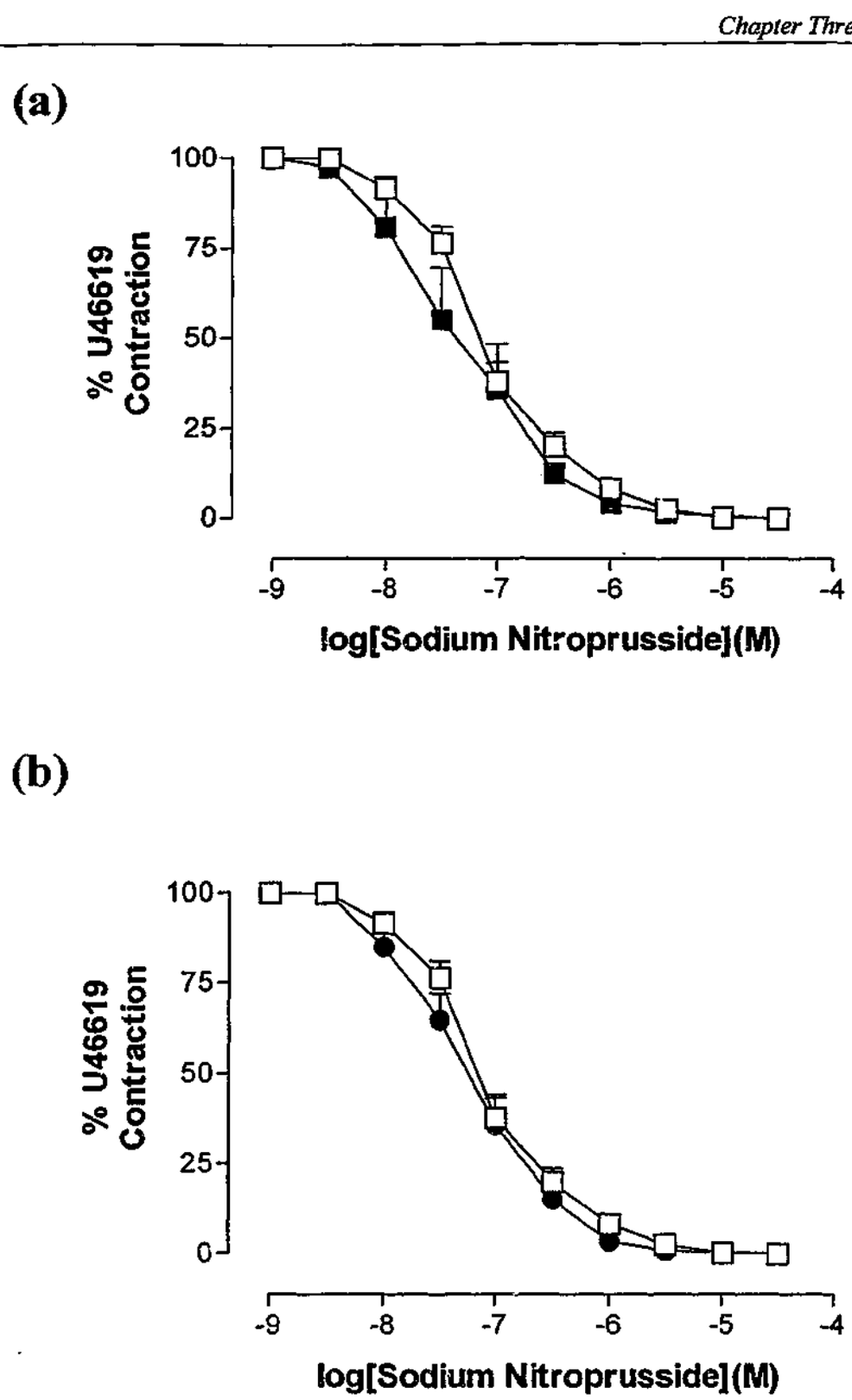

Figure 3.9 Mean sodium nitroprusside concentration-response curves obtained in the pig isolated coronary artery in the absence (□) and in the presence of (a) IMID-1M (■) or (b) IMID-35MO (●). Error bars are ± S.E.M. and if not visible are contained within the symbol (n=4, P>0.05; students t-test).

IMID-1M $pD_2 = 7.42 \pm 0.3$; $n=4$, $P>0.05$, Students *t*-test) or IMID-35MO (Figure 3.9b; control $pD_2 = 7.02 \pm 0.1$; plus IMID-35MO (30 μM) $pD_2 = 7.27 \pm 0.1$; $n=4$, $P>0.05$; Students *t*-test).

3.3.2 Electrophysiological properties of IMID-4F

Single smooth muscle cells of the rat isolated small mesenteric artery (D_{100} = 320 ± 22 μm, $n=3$) had a resting membrane potential of –62 ± 4 mV ($n=3$ cells, 3 separate vessels). The addition of IMID-4F (0.1–10 μM) caused a concentration-dependent depolarisation from a resting membrane potential of -60 ± 1 mV to –53 ± 2 mV ($n=3$ cells, 3 separate vessels; $P<0.05$; one way RM ANOVA); a depolarisation of approximately 7 mV (Figures 3.10 & 3.11). Levcromakalim (0.1–10 μM) alone caused a concentration-dependent membrane hyperpolarisation from –62 ± 4 mV to -74 ± 4 mV ($n=3$ cells, 3 separate vessels; $P<0.05$; one way RM ANOVA); a hyperpolarisation of approximately 12 mV. This hyperpolarisation to levcromakalim (10 μM) was totally abolished in the presence of IMID-4F (10 μM; $n=3$, $P<0.05$; two way repeated measures ANOVA; Figures 3.10 & 3.11).

3.3.3 Bradycardic effects of the imidazoline analogues

In this series of experiments the ability of the imidazoline analogues to cause bradycardia was assessed in the rat isolated spontaneously beating right atria preparation. Concentration-response curves were determined for all the analogues. An original trace and the mean concentration-response curve for IMID-26F is shown in Figure 3.12a and Figure 3.12b, respectively. The mean initial atrial rate before the

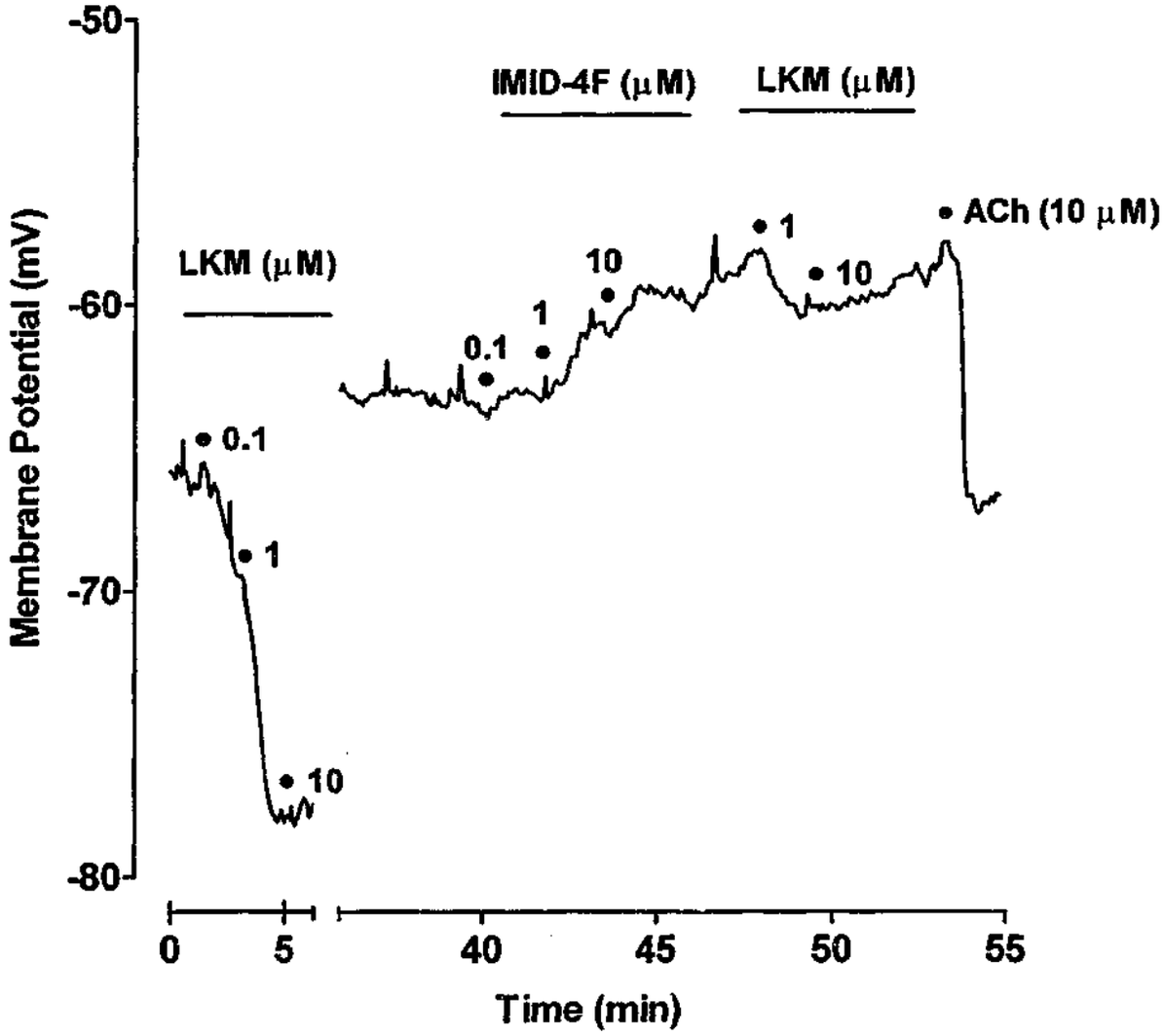

Figure 3.10 An original trace illustrating the electrophysiological effects of IMID-4F on membrane potential in the rat isolated small mesenteric artery. Illustrated is the effect of levcromakalim (LKM; 0.1-10 μM) alone, followed by IMID-4F (0.1-10 μM) alone and then levcromakalim (LKM; 1-10 μM) in the presence of IMID-4F (10 μM). Acetylcholine (ACh; 10 μM), an agent which causes hyperpolarisation of the membrane via a method other than K_{ATP} channel opening was still able to cause membrane hyperpolarisation.

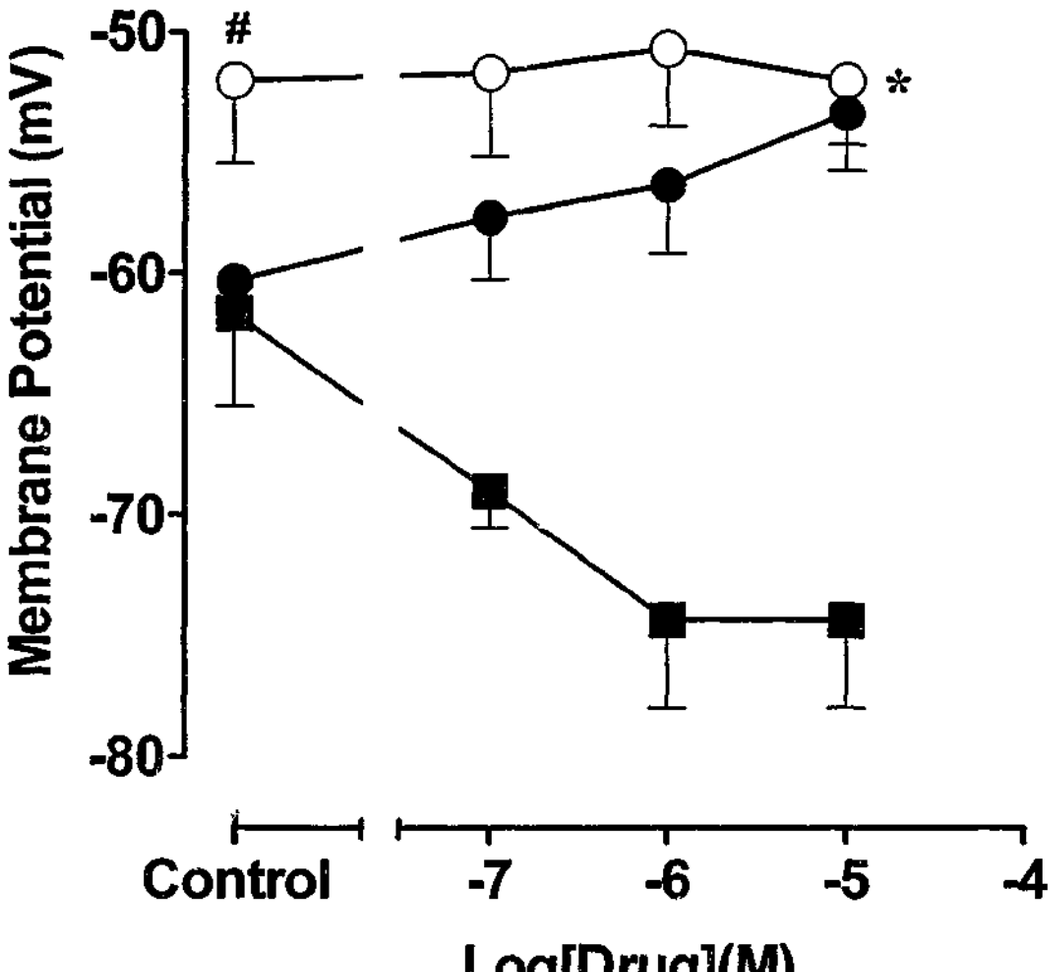

Figure 3.11 Mean electrophysiological concentration-response curves obtained in the rat isolated mesenteric artery to levcromakalim alone (■), IMID-4F alone (●) and levcromakalim in the presence of IMID-4F (○). Error bars are ± S.E.M. and if not visible are contained within the symbol. * indicates a significant difference in the membrane potential of levcromakalim in the presence of IMID-4F (n=3, P<0.05; two way repeated measures ANOVA). # indicates a significant difference in the resting membrane potential in the presence of IMID-4F (10 μM; n=3, P<0.05; students t-test).

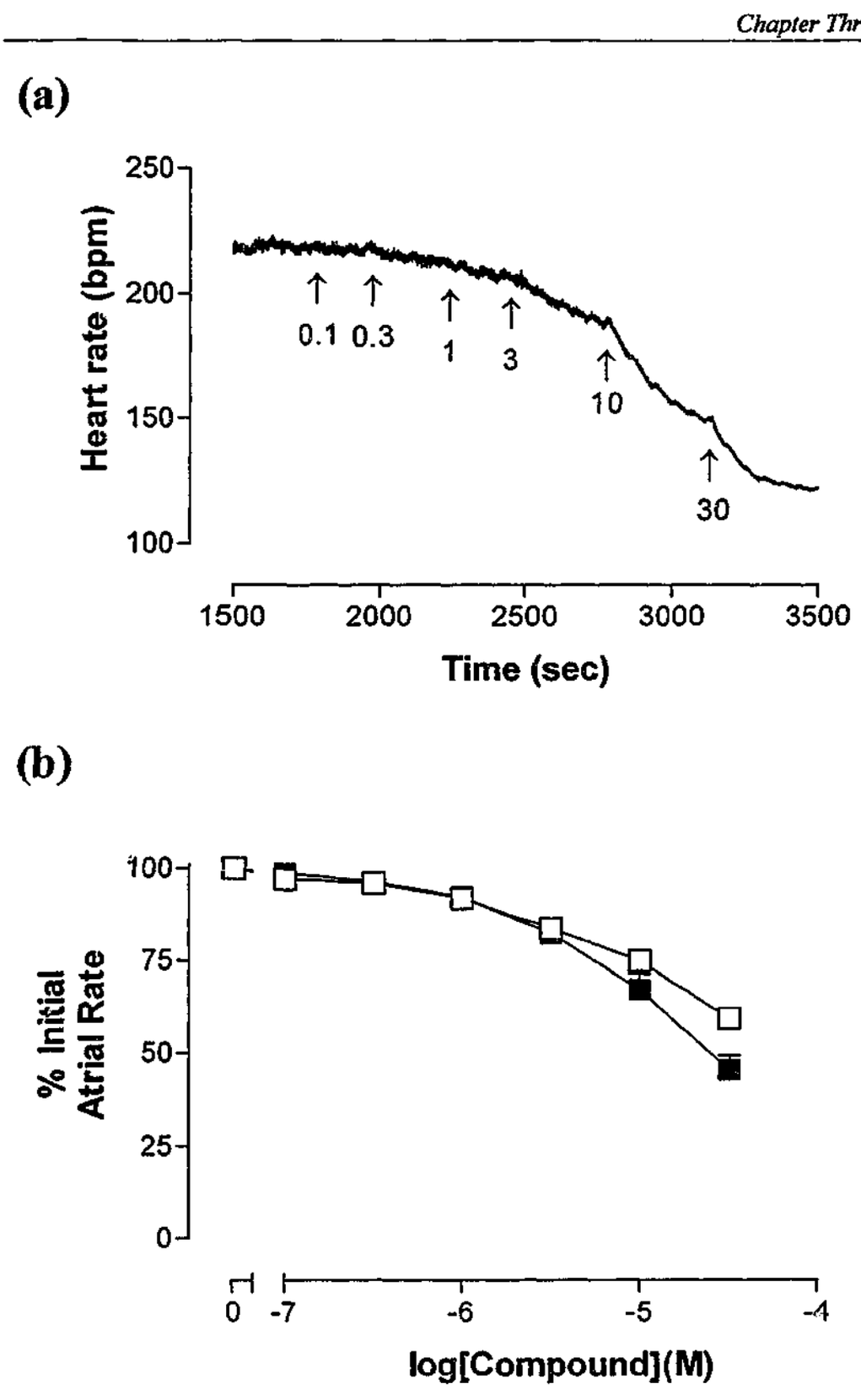

Figure 3.12 Bradycardic response to IMID-26F (■; 0.3-30 μM) in the rat isolated spontaneously beating right atria illustrated as (a) an original trace and (b) mean concentration-response curve (n=4). The bradycardic response to alinidine (□) is also included as a comparison (n=4). Error bars are ± S.E.M. and if not visible are contained within the symbol.

addition of IMID-26F was 253 ± 24 bpm and after the highest concentration tested, 30 μM, 122 ± 5 bpm. Table 3.1 lists the pD_2 values or estimated pD_2 values obtained for all the imidazoline analogues tested. The majority of the compounds investigated did not possess marked bradycardic activity with estimated EC_{50} values that are greater than or equal to 30 μM. The imidazoline analogue, IMID-35MO/O that has an oxygen substitution in the imidazoline ring was the only analogue that did not cause a significant concentration-dependent reduction in heart rate (Table 3.1; n=4, P>0.05; one way ANOVA).

The most potent compounds were the bis-substituted compounds, IMID-4F/2N, IMID-26F/2N and IMID-35MO/2N, which caused a concentration-dependent decrease in heart rate (Figure 3.13; n=4-6; P<0.05; one way ANOVA with Bonferroni t-test). At the highest concentration tested (30 μM) they caused total abolition of spontaneous beating of the rat isolated right atria. The calculated pD_2 values were IMID-26F/2N (5.26), IMID-35MO/2N (5.18) and IMID-4F/2N (5.15). The bradycardic actions of all the imidazoline analogues tested at 30 μM is illustrated in Figure 3.14. The vehicle is included in Figure 3.13 illustrating its lack of effect and alinidine is included on both figures as a comparison. IMID-4F/2N, IMID-26F/2N and IMID-35MO/2N together with IMID-26F caused a significant reduction in atrial rate when compared to alinidine at the same concentration (30 μM) (Figure 3.14; n=4, P<0.05, ANOVA with Bonferroni t-test).

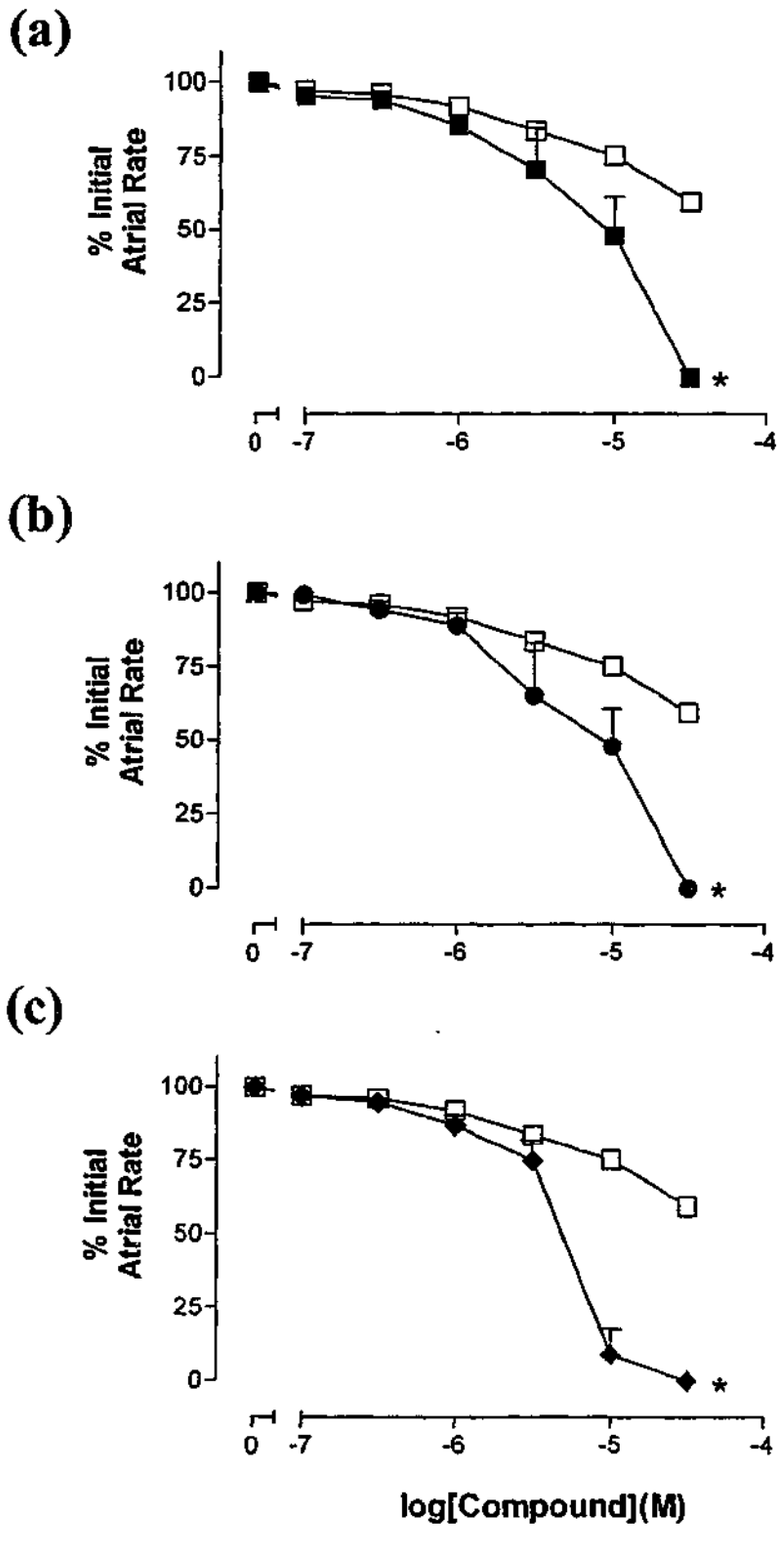

Figure 3.13 Mean concentration-response curves illustrating the bradycardic response to (a) IMID-4F/2N (■), (b) IMID-35MO/2N (●) and (c) IMID-26F/2N (◆) in the rat isolated spontaneously beating right atria. The bradycardic response to alinidine (□) is also included as a comparison. Error bars are ± S.E.M. and if not visible are contained within the symbol. * indicates a significant difference from alinidine (n=4-6; P<0.05; two way RM ANOVA).

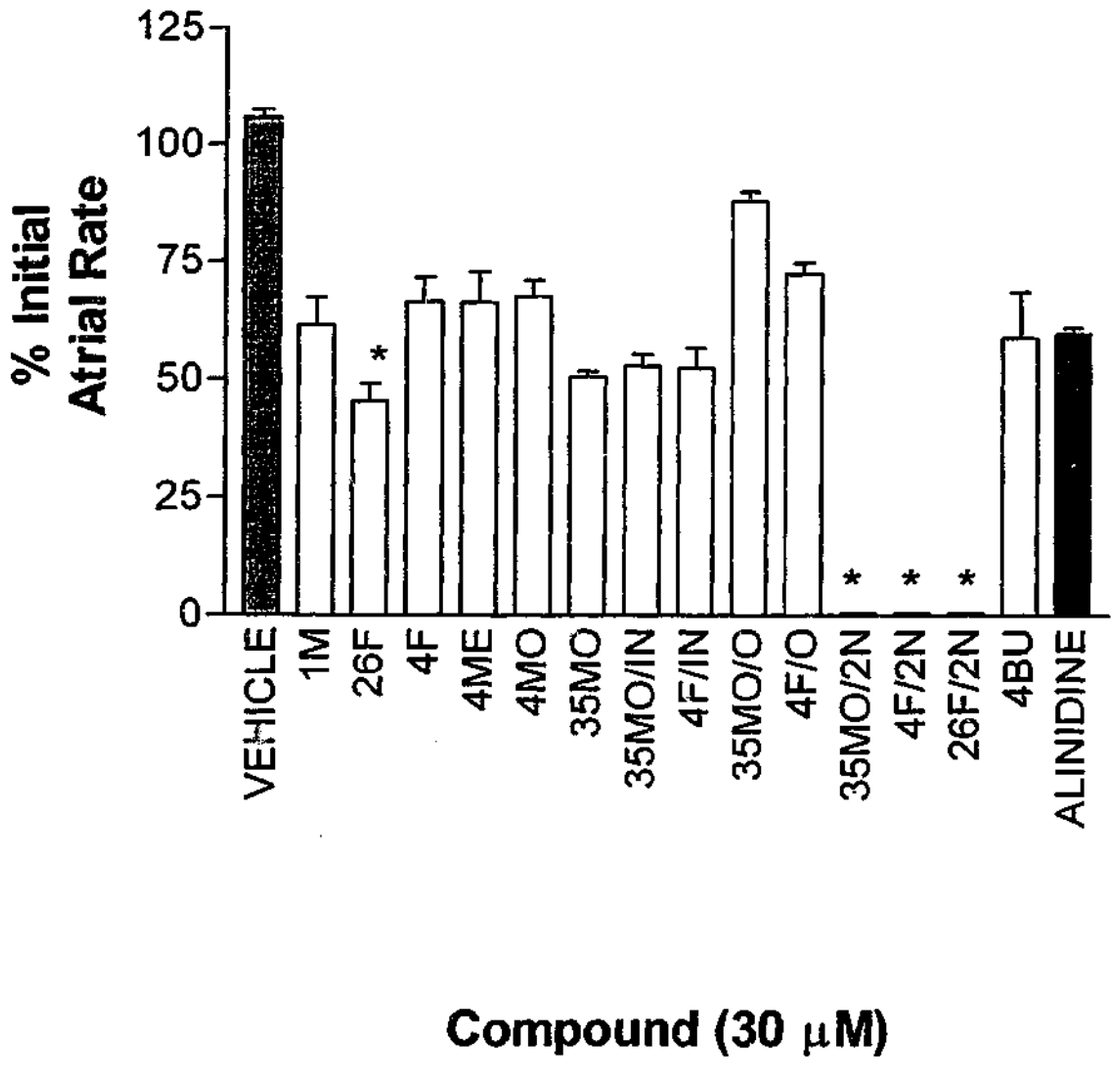

Figure 3.14 Histogram plot illustrating the mean maximum bradycardic effect of the IMID compounds at 30 μM in rat isolated spontaneously beating right atria. Results are expressed as a percentage of the initial atrial rate. Error bars are mean ± S.E.M. and if not visible are contained within the symbol. * indicates a significant difference from alinidine (n=4-6, P<0.05; one way ANOVA)

3.3.4 Levcromakalim antagonism versus bradycardic activity of the imidazoline analogues

The relatively high potency of these compounds to antagonise the vasorelaxant actions of levcromakalim together with their poor ability to cause bradycardia, indicate that these compounds are highly selective for vascular K_{ATP} channels. Table 3.1 shows that the mono-substituted compounds, IMID-1M, IMID-26F, IMID-4F and IMID-35MO are the most selective agents with calculated activity ratios of 224, 295, 269 and 331, respectively. Other compounds that also showed a high degree of selectivity include the bis-substituted compounds IMID-35MO/2N (166), IMID-4F/2N (178) and IMID-26F/2N (100).

3.4 Discussion

3.4.1 K_{ATP} channel antagonism

The main finding from the present study is that some, but not all n-benzyl derivatives of clonidine are potent antagonists of the K_{ATP} channel opening effects of levcromakalim on vascular smooth muscle. Studies in our laboratory were the first to show that imidazolines (eg. alinidine & phentolamine) were antagonists of the vascular smooth muscle relaxant actions of cromakalim (McPherson & Angus, 1989; 1990). Using techniques identical to those used in the present studies, the 'apparent' pK_B for alinidine in rat thoracic aorta was calculated to be approximately 5.5 (Challinor-Rogers *et al.*, 1994). Replacing the n-allyl substituent of alinidine with an n-benzyl derivative (unsubstituted or substituted), generated compounds (IMID-1M, IMID-26F, IMID-4F & IMID-35MO) that had 'apparent' pK_B values of approximately 7; some 30 fold more potent than alinidine itself. In addition, the bis substituted compounds (IMID-4F/2N, IMID26F/2N & IMID-35MO/2N), those which had identical substitutions on both the central nitrogen and the imidazoline ring nitrogen of clonidine, had calculated 'apparent' pK_B values of approximately 7.4; some 100 fold more potent than alinidine.

In addition, the antagonism of levcromakalim vasorelaxant responses was also specific for levcromakalim since both IMID-1M (30 μM) and IMID-35MO (30 μM), failed to affect the vasorelaxant responses to sodium nitroprusside, a nitro-vasorelaxant compound that acts via cGMP. This is consistent with previous findings which showed that imidazoline based compounds specifically inhibited vasorelaxant responses to K_{ATP} channel openers (McPherson & Angus, 1989).

A number of chemically diverse compounds are known to antagonise the K_{ATP} channel opening effects of levcromakalim. Most notable of these are the sulphonylureas typified by glibenclamide. Previous studies have shown that glibenclamide behaves as a classical competitive antagonist of levcromakalim mediated vasorelaxant responses in a number of vascular preparations, with a pA_2/pK_B of approximately 7 and slope value near unity (Eltze, 1989; Edwards *et al.*, 1991). Thus, when using sulphonylurea based compounds the levcromakalim concentration-response curve is shifted to the right in a parallel manner with no obvious effect on the maximum response.

The K_{ATP} channel is an octameric complex of two subunits: a pore forming K^+ channel subunit, $K_{IR}6.x$, and a regulatory subunit, the sulphonylurea receptor (SUR) (Sakura *et al.*, 1995; Inagaki *et al.*, 1996). Binding studies have shown that the site of the K_{ATP} channel where sulphonylureas and potassium channel openers act is found on the SUR and that they are negatively allosterically coupled (Bray & Quast, 1992; Quast et al., 1993b; Löffler & Quast, 1997).

Another potent group of levcromakalim antagonists that have been identified are the lipophilic quaternary ions such as tetraphenylphosphonium ($pK_B = 7.2$; McPherson & Piekarska, 1994; Piekarska & McPherson, 1997). While displaying the same potency as glibenclamide, tetraphenylphosphonium (and related compounds) show a markedly different type of antagonism as that displayed by the sulphonylureas. They cause a non-parallel shift of the levcromakalim concentration-response curve to the right and, at higher concentrations, suppress the maximum vasorelaxant response that levcromakalim can elicit. At this time it is uncertain where lipophilic quaternary ions interact with the K_{ATP} channel. However, previous studies with other quaternary ions have suggested that they interact with the pore of the K_{ATP} channel, now known as the K_{IR} subunit, to

inhibit K^+ efflux from the cell and that this may be related to their positive charge (McPherson & Piekarska, 1994).

The potency and nature of the antagonism displayed by the imidazolines characterised in this Chapter are similar to that displayed by the lipophilic quaternary ions. Thus, the imidazolines cause a non-competitive antagonism of the K_{ATP} channel opening effects of levcromakalim. Since imidazolines can be positively charged at physiological pH (McPherson & Piekarska, 1994) it is possible that these compounds may effect K_{ATP} channel opening through a mechanism similar to that of the lipophilic quaternary ions. Indeed, this possibility is supported by the recent finding that the imidazoline, phentolamine, inhibited pancreatic K_{ATP} channels by directly interacting with the K_{IR} component of the K_{ATP} channel (Proks & Ashcroft, 1997).

In this study, the vasoconstrictor used was U46619 (3-30 nM). Recent studies have shown that glibenclamide can antagonise the effects of U46619 in some species by directly acting at the thromboxane A_2 receptor (Cocks *et al.*, 1990; Kemp & McPherson, 1998). With this in mind there was a possibility that the imidazoline analogues may affect the responses to U46619. Indeed, a small subgroup of the imidazoline analogues did affect the responses to U46619. However, as this Chapter dealt with the K_{ATP} channel antagonism of the compounds, more U46619 was added in these cases to match the level of tone before the antagonism of levcromakalim was assessed. Further characterisation and discussion of the effects of this subgroup on U46619 contractions can be found in Chapter 4. Nevertheless, the majority of the imidazoline analogues did not affect U46619 contractions and due to their similar potency to glibenclamide they may be considered as an alternative to the use of glibenclamide under experimental conditions utilising vascular preparations.

3.4.2 Electrophysiological activity

Previous studies by our laboratory utilising the rat small mesenteric artery have shown that K_{ATP} channel antagonists (ie. alinidine & glibenclamide) and the quaternary ion, tetraphenylphosphonium cause a concentration-dependent depolarisation of smooth muscle cells (McPherson & Angus, 1991; Zhang *et al.*, 1998). It has been suggested earlier that, in this tissue, K_{ATP} channels are spontaneously open and hold the membrane potential approximately 10 mV more negative than would otherwise be expected (McPherson & Angus, 1991). Consistent with this idea, IMID-4F, at concentrations expected to antagonise K_{ATP} channels (1-10 μM), also caused a small concentration-dependent depolarisation of this magnitude.

As well as antagonising the spontaneously opened K_{ATP} channels present in this tissue, we also confirmed that IMID-4F (10 μM) completely antagonised the hyperpolarising responses to levcromakalim observed in the rat small mesenteric artery. This study also provides evidence that the imidazoline analogues or IMID-4F in this case, are active as levcromakalim antagonists in another vascular bed and in another species.

In addition to the electrophysiological data presented in this Chapter, recent patch clamping studies in our laboratory (McPherson *et al.*, 1999) measured the ability of IMID-4F to reverse levcromakalim-induced current in rat mesenteric myocyte cells (Figure 3.15). In cells that were held at a potential of –60 mV, in the presence of 140 mM K^+, the basal inward current (-25 ± 10 pA) was increased by levcromakalim (10 μM; -124 ± 50 pA). This increase was inhibited by IMID-4F (0.3 - 3 μM) in a concentration-dependent manner. The pIC_{50} for IMID-4F against the K_{ATP} current was 6.22 ± 0.01.

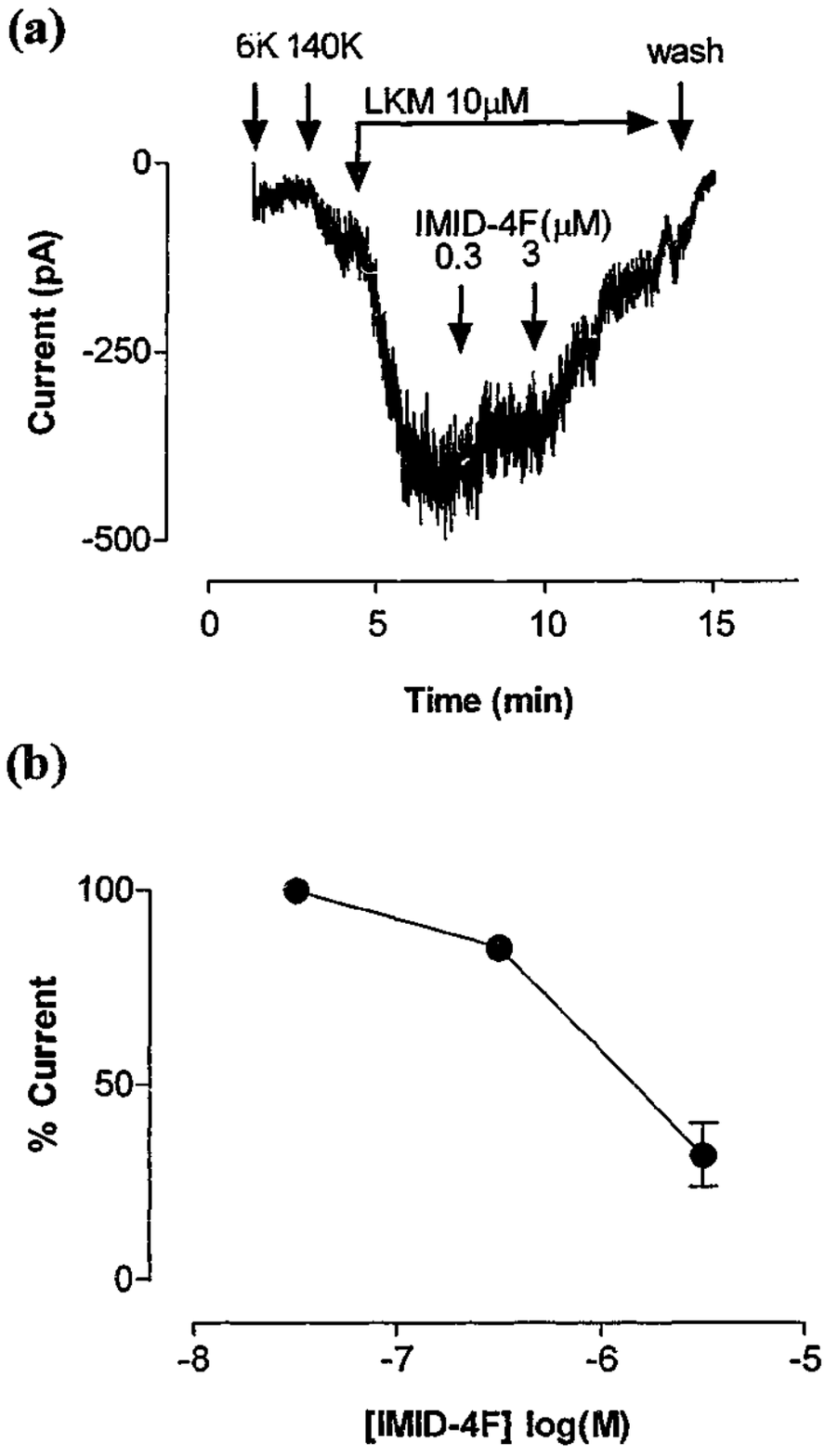

Figure 3.15 (a) Representative trace obtained in a single rat mesenteric myocyte cell showing the production of K_{ATP} channel K^+ current with levcromakalim (LKM; 10 μM), then reversal of this current with increasing concentrations of IMID-4F (0.3-3 μM). (b) Mean concentration-response curve in a single rat mesenteric myocyte cell to IMID-4F (0.3-3 μM). Error bars are ± S.E.M. and if not visible are contained within the symbol (n=3).

3.4.3 Bradycardic activity

As well as antagonising K_{ATP} channels in vascular and non-vascular smooth muscle (McPherson & Angus, 1989; see Section 1.4.2.3.1), alinidine has been shown in *in vitro* and *in vivo* studies to slow heart rate (Kobinger, *et al.,* 1979; Lillie & Kobinger, 1983a,b; Siegl, *et al.*, 1984; Hageman, *et al.*, 1985). Previous studies in our laboratory using the TH series of compounds, compared the cromakalim antagonism and bradycardic actions to determine if the bradycardia of alinidine was related to an effect at K_{ATP} channels (Challinor-Rogers *et al.*, 1994; see Section 1.4.2.3.3). It was found that there was no statistically significant correlation between the two, which suggested that the TH series of alinidine analogues did not cause bradycardia through an action at cardiac K_{ATP} channels. There are a number of different theories as to how alinidine brings about its actions upon the heart. One theory suggests alinidine has a direct action upon the sinoatrial node to slow diastolic depolarisation and systolic repolarisation (Tritthart *et al.*, 1981; Millar & Vaughan Williams, 1981a; Millar *et al.*, 1983; Bouman *et al.*, 1984; Kawada *et al.*, 1984; Satoh & Hashimoto, 1986). It has been suggested that alinidine causes this effect by partially blocking I_f or I_h currents (Bouman *et al.*, 1984; Dennis & Vaughan Williams, 1986). Another theory has suggested that alinidine restricts the flow of current through anion selective channels (Millar & Vaughan Williams 1981a,b; Lillie & Kobinger, 1983a,b). In any case, the mechanism by which alinidine, and most likely the IMID series of compounds studied in this thesis, causes bradycardia remains unclear.

The majority of the IMID analogues used in this study were found to be very poor bradycardic agents with estimated EC_{50} values greater than or equal to 30 μM. These are similar to that of alinidine. The most interesting finding during this study was that the bis substituted compounds (IMID-4F/2N, IMID-26F/2N & IMID-35MO/2N)

caused the cessation of the rat isolated spontaneously beating right atrial preparation at the highest concentration tested (30 μM). As will become evident in Chapter 4 we found that these same compounds also have calcium channel antagonist actions that may contribute to this effect.

3.4.4 Structure-activity relationship

It has been known for some time that the substituent on the central nitrogen of alinidine is important in determining K_{ATP} channel potency. Thus while the parent compound, clonidine (which lacks the n-allyl substitution), is not active as a levcromakalim antagonist (McPherson & Angus, 1989) many substituted compounds including alinidine, the TH series and the IMID series all display varying activity. From this study it was apparent that the substitution of a benzene ring on the extra-cyclic nitrogen causes a substantial increase in potency as a K_{ATP} channel antagonist (IMID-1M; pK_B=6.85). However, substitutions onto the benzene ring either had little effect on the potency (IMID-4F (6.93), IMID-26F (6.97) & IMID-35MO (7.02)) or actually decreased the potency (IMID-4MO (5.52), IMID-4ME (6.45) & IMID-4BU (inactive)) of these compounds as levcromakalim antagonists. Identical benzyl substitutions on the imidazoline nitrogen of clonidine rather than the central nitrogen generated the compounds IMID-4F/IN (5.62) and IMID-35MO/IN (6.16). Again these substitutions actually decreased their potency as K_{ATP} channel antagonists. The substitution of an oxygen molecule for one of the imidazoline nitrogens in the latter two compounds, IMID-4F/IN and IMID-35MO/IN, resulted in IMID-4F/O (5.25) and IMID-35MO/O (5.51). This further decreased the ability of these compounds to inhibit levcromakalim-induced vasorelaxation.

In contrast to these results, we found that the substitution of 2 benzyl groups (one on the bridging nitrogen and one on the imidazole nitrogen) giving rise to IMID-4F/2N (7.44), IMID-26F/2N (7.26) and IMID-35MO/2N (7.44), produced compounds that were of similar potency to the parent compound IMID-1M in their K_{ATP} channel antagonism. However, as already noted, these compounds were significantly more potent in their maximum bradycardic effect than the majority of the compounds tested.

To determine the selectivity of the compounds as vascular K_{ATP} channel antagonists versus bradycardic activity, an activity ratio was calculated. This was calculated from each compounds' pK_B obtained in the pig isolated coronary artery compared with estimated pD_2 for inducing bradycardia. From this it was found that IMID-1M, IMID-4F, IMID-26F and IMID-35MO were the most selective agents with activity ratios of 224, 295, 269 and 331, respectively. Following these were IMID-4F/2N, IMID-35MO/2N and IMID-26F/2N, which had calculated activity ratios between 100-180. Therefore, based on the relatively high potency of these compounds for antagonising the vasorelaxant actions of levcromakalim and their poor ability to cause bradycardia, many of the compounds were found to be highly vascular selective.

3.4.5 Conclusions

The results of the present study have identified a novel group of potent imidazoline-based vascular K_{ATP} channel antagonists after experiments performed using the pig isolated coronary artery. Several of the imidazoline analogues, IMID-4F/2N, IMID-26F/2N, IMID-35MO/2N, IMID-1M, IMID-4F, IMID-26F and IMID-35MO are as potent as the sulphonylurea glibenclamide and the lipophilic quaternary ion

tetraphenylphosphonium, which have similar pK_B values of around 7 in vascular smooth muscle.

In addition, the levcromakalim antagonism demonstrated by the analogues was specific since vasodilatation to sodium nitroprusside was not affected in the presence of IMID-1M and IMID-35MO. It was also demonstrated that IMID-4F blocked the hyperpolarisation to levcromakalim in rat isolated mesenteric artery, a different vascular bed and species to the first series of experiments in the pig isolated coronary artery. Finally, the bradycardic actions of these compounds were found to be very weak, suggesting that the imidazoline analogues characterised in this Chapter were highly vascular selective.

4.1 Introduction

During studies designed to characterise the K_{ATP} channel antagonist actions of the IMID compounds (Chapter 3) it was discovered that several of them (ie IMID-35MO/IN, IMID-35MO/O, IMID-4F/O, IMID-26F/2N, IMID-35MO/2N & IMID-4F/2N), at high concentrations (10–30 μM), appeared to affect contractions to the thromboxane A_2 mimetic, U46619 and caused the relaxation of the passive tension of pig isolated coronary artery rings. The aim of the work described in the present Chapter was to determine the mechanism/s underlying this phenomenon.

To achieve this, studies were performed in pig coronary arteries and rat small mesenteric arteries using a variety of different vasoconstrictors, U46619, ACh, K^+ and phenylephrine and a number of selective antagonists. Tetraphenylphosphonium (TPP; 3μM), a quaternary ion, which has been previously shown to antagonise vascular K_{ATP} channels (Piekarska & McPherson, 1997) was used to assess the possibility that the compounds also opened K_{ATP} channels. ODQ (10 μM), the soluble guanylate cyclase inhibitor, was utilised to examine the possibility that the IMID compounds were acting through guanylate cyclase activation. Propranolol (1 μM) was used to assess the possibility of actions at β-adrenoceptors. Finally, radioligand-binding studies were performed to assess the ability of the IMID compounds to displace binding of the calcium channel antagonist [^{3}H]-PN200-110 to rat cerebral cortex membranes.

4.2 Materials and Methods

4.2.1 Vascular studies

4.2.1.1 Tissue preparation and mounting procedures

4.2.1.1.1 Porcine isolated right circumflex arteries

The porcine isolated right circumflex artery was used to assess the ability of the imidazoline analogues to cause vasorelaxation. Segments of pig endothelium denuded coronary artery were prepared and mounted as previously described in Section 3.2.1.1.

4.2.1.1.2 Rat isolated small mesenteric arteries

Rat isolated small mesenteric arteries were used to assess the ability of IMID-35MO/O to cause vasorelaxation in a vascular preparation other than the pig isolated coronary artery. Segments of rat mesenteric artery were prepared and mounted in a small vessel myograph as previously described in Section 3.2.1.2 and normalised as described in Section 3.2.1.2.1.

4.2.1.2 Experimental protocol and Analysis of results

4.2.1.2.1 Vasorelaxation of the imidazoline analogues in pig isolated coronary arteries

Following equilibration, the maximum constrictor response was determined with the addition of KPSS as described in Section 3.2.2.1. The tissues were submaximally constricted with U46619 (3–10 nM) and cumulative concentration-response curves to

all the IMID compounds (0.3–30 μM) or nifedipine (0.01-3 μM) were constructed. Further concentrations of the IMID compounds were added when the response to the previous concentration had reached a plateau and only one concentration-response curve was obtained with each coronary artery ring. Subsequently, experiments were carried out to assess the ability of the imidazoline derivatives and nifedipine to relax contractions to ACh (10-30 nM) and K^+ (30 mM). In most cases, the IMID compounds did not cause full tissue relaxation, hence, sodium nitroprusside (10 μM) was added at the end of each curve to obtain maximal vessel relaxation. In some instances, ODQ (10 μM), propranolol (1 μM) or TPP (3 μM) were used in an attempt to inhibit the imidazoline-induced relaxation. They were added 20 minutes prior to submaximally constricting the tissue with U46619 (3-10 nM).

The initial contractions to either U46619, ACh, or K^+ were taken as 100 % response and the contraction or relaxation produced by different concentrations of the IMID compounds expressed as a percentage of this response. The percentages were then represented graphically and the pD_2 ($-\log EC_{50}$) values calculated as described in Section 3.2.2.1.

4.2.1.2.2 Vasorelaxation of IMID-35MO/O in rat mesenteric arteries

After normalisation the vessel was left to equilibrate for a further 30 minutes. The maximal tissue contraction was determined by the addition of KPSS (Section 3.2.2.1). The segments were constricted to approximately 50 % of the tissue maximum with either phenylephrine (PE; 1–10 μM) or K^+ (40–60 mM). Concentration response curves to IMID-35MO/O (0.1–30 μM) were constructed.

The results and analysis were performed in an identical fashion to those described above in Section 4.2.1.2.1

4.2.2 Radioligand binding studies

4.2.2.1 Membrane preparation

4.2.2.1.1 Cerebral cortex membranes

Male Sprague-Dawley rats (250-350 g) were rendered unconscious by a brief exposure to 20 % O_2/80 % CO_2 and then exsanguinated. The cerebral cortex was dissected free and placed in phosphate buffer (composition in mM: NaH_2PO_4 2.79 and Na_2HPO_4 7.19; pH = 7.4) and maintained at 4 °C. Membranes were prepared by homogenisation of the cerebral cortex in 20 vol (w/v) of ice-cold phosphate buffer. The homogenate was centrifuged (35,000 g for 15 min at 4 °C), the supernatant discarded, the resultant pellet washed and the above procedure repeated. The final membrane suspension was prepared by suspending the pellet in 50 vol (w/v) phosphate buffer. Each ml of homogenate therefore contained 20 mg wet weight of original tissue mass.

4.2.2.2 Experimental protocol

4.2.2.2.1 Saturation studies

Initially, saturation studies were performed to determine the apparent dissociation constant (K_D) and the density of the binding sites (B_{max}) values for [^{3}H]-PN200-110. Hot saturation studies were performed, in triplicate, by combining 100 µl of increasing concentrations of [^{3}H]-PN200-110 (final concentrations; 0.02–5 nM) with

and without 10 µl of nifedipine (final concentration; 0.1 µM), which was used to define non-specific binding. The binding reaction was initiated by the addition of 500 µl of cerebral cortex membrane preparation. The tubes, with a total volume of 1 ml in a phosphate buffer, were lightly vortexed and incubated for 1 hour at room temperature. As [^{3}H]-PN200-110 is light sensitive, incubations were also performed in reduced light and under foil to minimise exposure and therefore, degradation of the ligand. The incubation was terminated by adding 5 ml of ice-cold phosphate buffer. The bound and free ligand was then separated by filtration under vacuum over glass microfibre filters (Whatman GF/B) using a Brandell Harvester. The filters were washed twice with 5 ml phosphate buffer and counted for ^{3}H in 2.5 ml scintillant (EcoLite, ICN Biomedicals, USA) using a Minaxi Tri-Carb 4000 series β-counter (United Technologies Packard). The disintergrations per minute (dpm) were counted for 5 minutes.

4.2.2.2.2 Competition studies

Drug displacement experiments were carried out, in duplicate, by initiating a binding reaction by incubating the 500 µl of membrane preparation with tubes already containing 100 µl of [^{3}H]-PN200-110 (final concentration; 1 nM) and 10 µl of either the cold displacing drug, used to define non-specific binding (nifedipine; final concentration; 0.1 µM), or an IMID compound. The tubes, with a total volume of 1 ml in phosphate buffer, were lightly vortexed and incubated. After an incubation time of 1 hour at room temperature the incubation was terminated by adding 5 ml of ice-cold phosphate buffer. The experiments were then carried out in an identical manner to that of the hot saturation studies described above (Section 4.2.2.2.1).

Initial displacement experiments were completed using a single high concentration (10 μM) for all the IMID analogues. If considerable displacement was observed, full drug-displacement studies were performed using a range of concentrations of the IMID compounds (10 nM–100 μM).

4.2.2.3 Analysis of Results

Weighted non-linear curve fitting is now accepted as the most accurate method of analysing radioligand binding experiments. It eliminates many potential sources of error as no transformation of the data is required and the exact models can be used (McPherson, 1985). RADLIG (McPherson, 1995), a computer program, which uses a weighted non-linear curve fitting method involving the Marquardt-Levenberg modifications of the Gauss-Newton technique (Rodbard, 1984) was used to analyse the results from both the hot saturation and competition studies. Initially, a model is first specified and initial estimates are generated. These are then iteratively refined until there is the least amount of deviation of predicted line from the experimental data (ie. the lowest weighted sum of squares). This process results in the calculation of the apparent dissociation constant (K_D), expressed as the pK_D (-log K_D) in the competition studies and the density of the binding sites (B_{max}). Together with the final estimates, an approximation of the standard error is provided to give an indication of the reliability of the calculations. In this thesis, error values were considered acceptable if they were below 10 % and those over this value were excluded.

In all the binding experiments throughout this thesis the results were expressed as % of total binding or % bound. Both the vehicle and drug used to define non-specific binding were also included on the figures as a comparison.

4.2.3 Statistics

Results in the text are given as mean ± S.E.M. Statistical methods used were carried out as stated in the text. One way Analysis of Variance (ANOVA) was used to test more than two values that were dependent. If statistical significance was observed a Bonferroni *t*-test was used post ANOVA for pairwise multiple comparisons and for multiple comparisons to a control group. Groups were considered significantly different from each other if $P<0.05$, unless otherwise stated. All statistical calculations were performed using SigmaStat (Jandel Scientific, U.S.A.).

4.2.4 Drugs

The radioligand and its source was: [^{3}H]-PN200-110 (specific activity: 85 Ci/mmol; Amersham, U.K.). [^{3}H]-PN200-110 was made up in phosphate buffer as a stock solution of 50 nM and all further dilutions were also made in phosphate buffer.

Drugs used and their sources were: Acetylcholine (ACh; Sigma Chemical Co., U.S.A.); IMID compounds (Eva Campi, Department of Chemistry, Monash University; Figure 2.1); nifedipine (Sigma Chemical Co., U.S.A.); phenylephrine (PE; Sigma Chemical Co., U.S.A.); sodium nitroprusside (SNP; Sigma Chemical Co., U.S.A.); U46619 (The Upjohn Co., USA). The imidazoline analogues were made up in 100% methanol (MeOH) as stock solutions of 10 mM for the *in vitro* experiments. For the radioligand-binding experiments the imidazoline analogues and nifedipine were made up in 100% ethanol (EtOH) as stock solutions of 10 mM and 1 mM. The first additional dilution for the imidazoline analogues was made in 40 % EtOH and all further dilutions were made in distilled water. Nifedipine was dissolved and diluted in distilled water.

Acetylcholine, phenylephrine, sodium nitroprusside and U46619 were dissolved in distilled water and diluted in Krebs solution.

4.3 Results

4.3.1 Vasorelaxation by the imidazoline analogues

In this series of experiments the ability of the imidazoline analogues to cause vasorelaxation in isolated segments of pig coronary artery precontracted with U46619 (3–10 nM), ACh (0.1–0.3 μM) or K^+ (30 mM) was assessed. As with previous experiments with this tissue, the contractions to each vasoconstrictor were matched to approximately 50 % of the KPSS contraction (Figures 4.2b, 4.3b, 4.4b & 4.5b). Concentration-response curves were constructed for all the imidazoline analogues in arterial segments precontracted with U46619. Six analogues were found to cause concentration-dependent vasorelaxation (IMID-35MO/IN, IMID-35MO/O, IMID-4F/O, IMID-26F/2N, IMID-35MO/2N & IMID-4F/2N) that was significantly different to the vehicle, methanol (Figure 4.1 & 4.2a; n=4-8; P<0.05; one way ANOVA with Bonferroni t-test).

The remaining seven imidazoline analogues, IMID-4ME, IMID-4MO, IMID-4F/O, IMID-1M, IMID-35MO, IMID-4F/IN and IMID-26F did not cause vasorelaxation that was significantly different from the vehicle (Figure 4.3; n=4; P>0.05; one way ANOVA). In contrast, IMID-4F/IN and IMID-1M both caused a small concentration-dependent contraction, additional to that of U46619, which was significantly different to the vehicle (n=4; P<0.05; one way ANOVA with Bonferroni t-test). pD_2 values were calculated for all the analogues that caused relaxation and they are summarised in Table 4.1. They were IMID-4F/O (pD_2 = 5.3), IMID-35MO/O (5.3), IMID-35MO/2N (4.8), IMID-4F/2N (4.7), IMID-35MO/IN (4.7) and IMID-26F/2N (4.6). Both IMID-4F/O and IMID-35MO/O were significantly different from

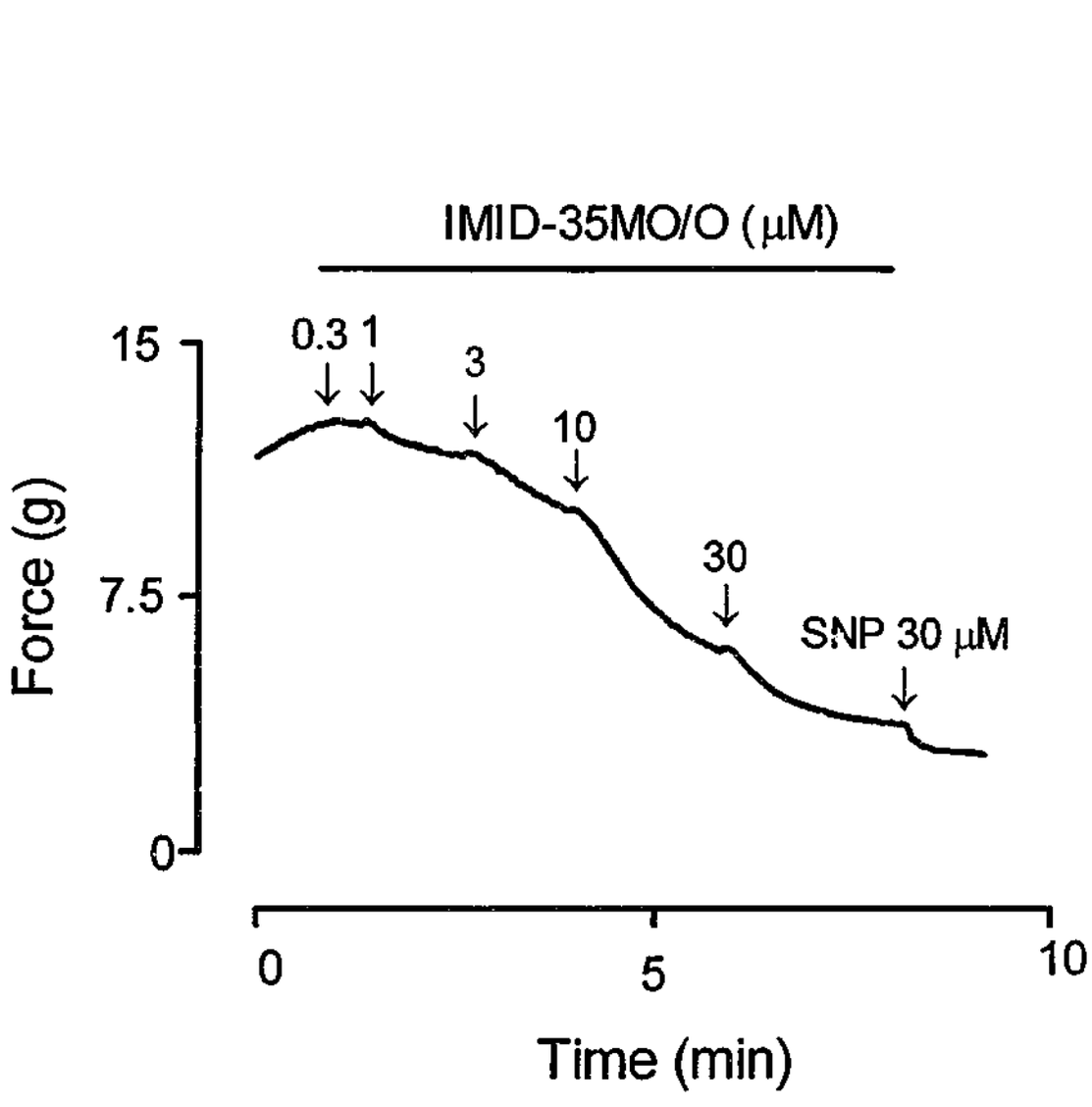

Figure 4.1 Original trace of the concentration-dependent relaxation of IMID-35MO/O (0.3–30 μM) in a segment of pig isolated coronary artery precontracted with U46619 (3 nM).

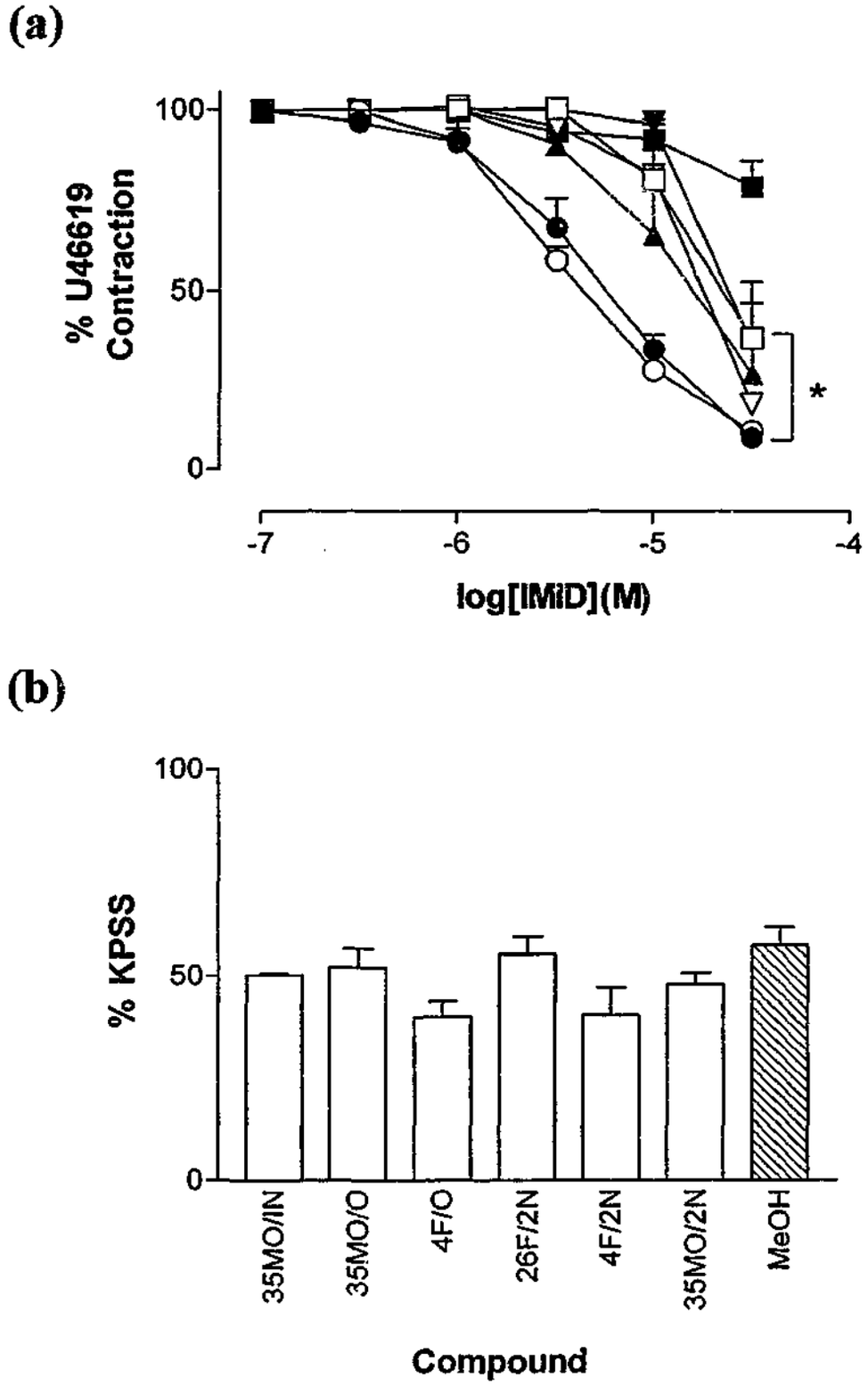

Figure 4.2 Mean concentration-response curves in pig isolated right circumflex arteries precontracted with U46619 (3–10 nM) for IMID-35MO/IN (□), -35MO/O (●), -4F/O (○), -26F/2N (▼), -4F/2N (▽), -35MO/2N (▲) and the methanol vehicle (■). Error bars are ± S.E.M. and if not visible are contained within the symbol. * indicates all compounds were significantly different from the vehicle at the highest concentration (30 μM; n=4; P<0.05; one way ANOVA with Bonferroni t-test). (b) Initial tone generated by U46619 (3-10 nM) as a percentage of KPSS (n=4).

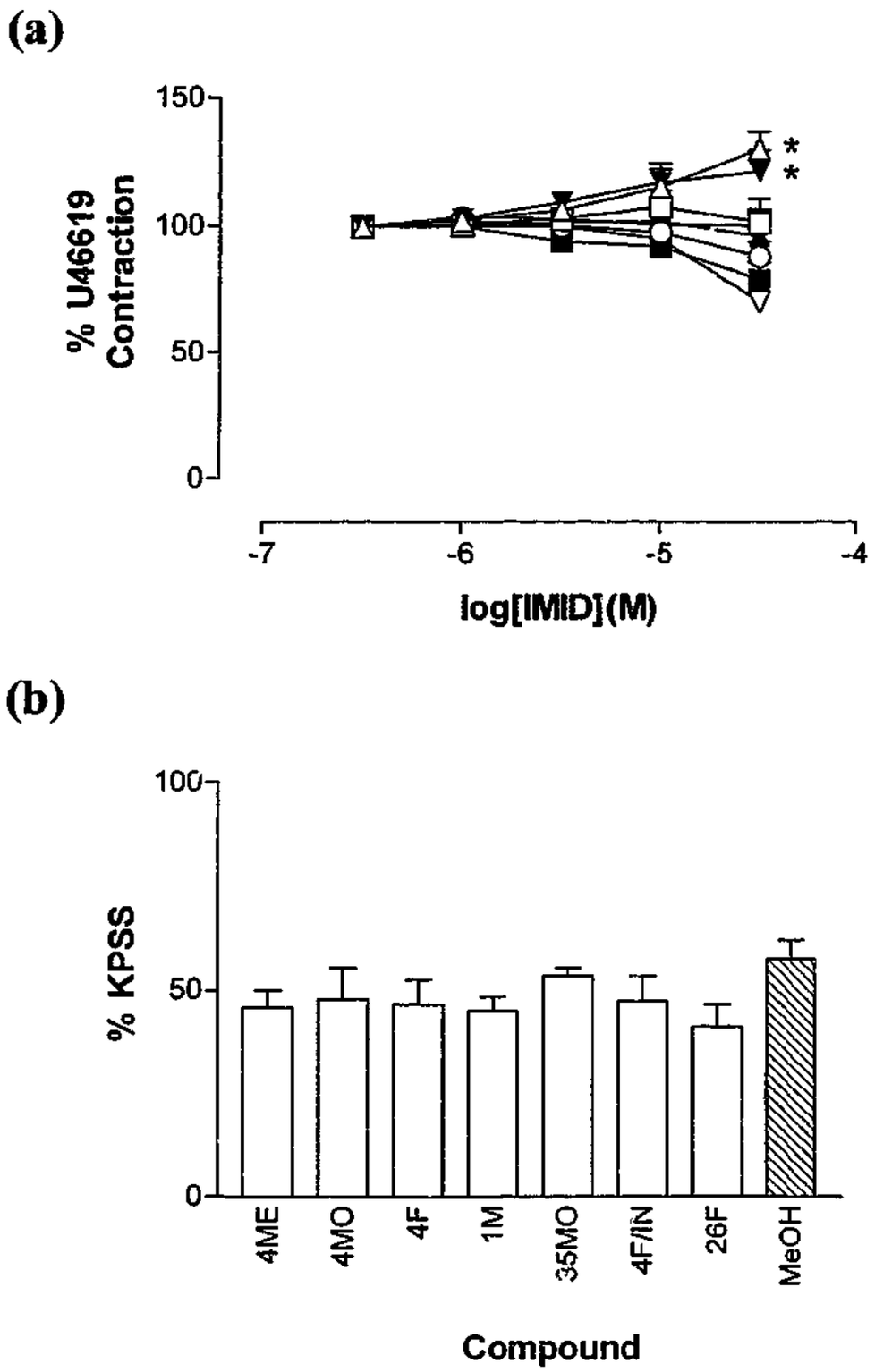

Figure 4.3 (a) Mean concentration-response curves in pig isolated right circumflex arteries precontracted with U46619 (3-10 nM) for IMID-4ME (□), -4MO (●), -4F (○), -1M (▼), -35MO (▽), -4F/IN (△), -26F (◆) and the methanol vehicle (■). Error bars are ± S.E.M. and if not visible are contained within the symbol. * indicates a significant difference from the vehicle at the highest concentration (30 μM; n=4; P<0.05; one way ANOVA with Bonferroni t-test). (b) Initial tone generated by U46619 (3-10 nM) as a percentage of KPSS (n=4).

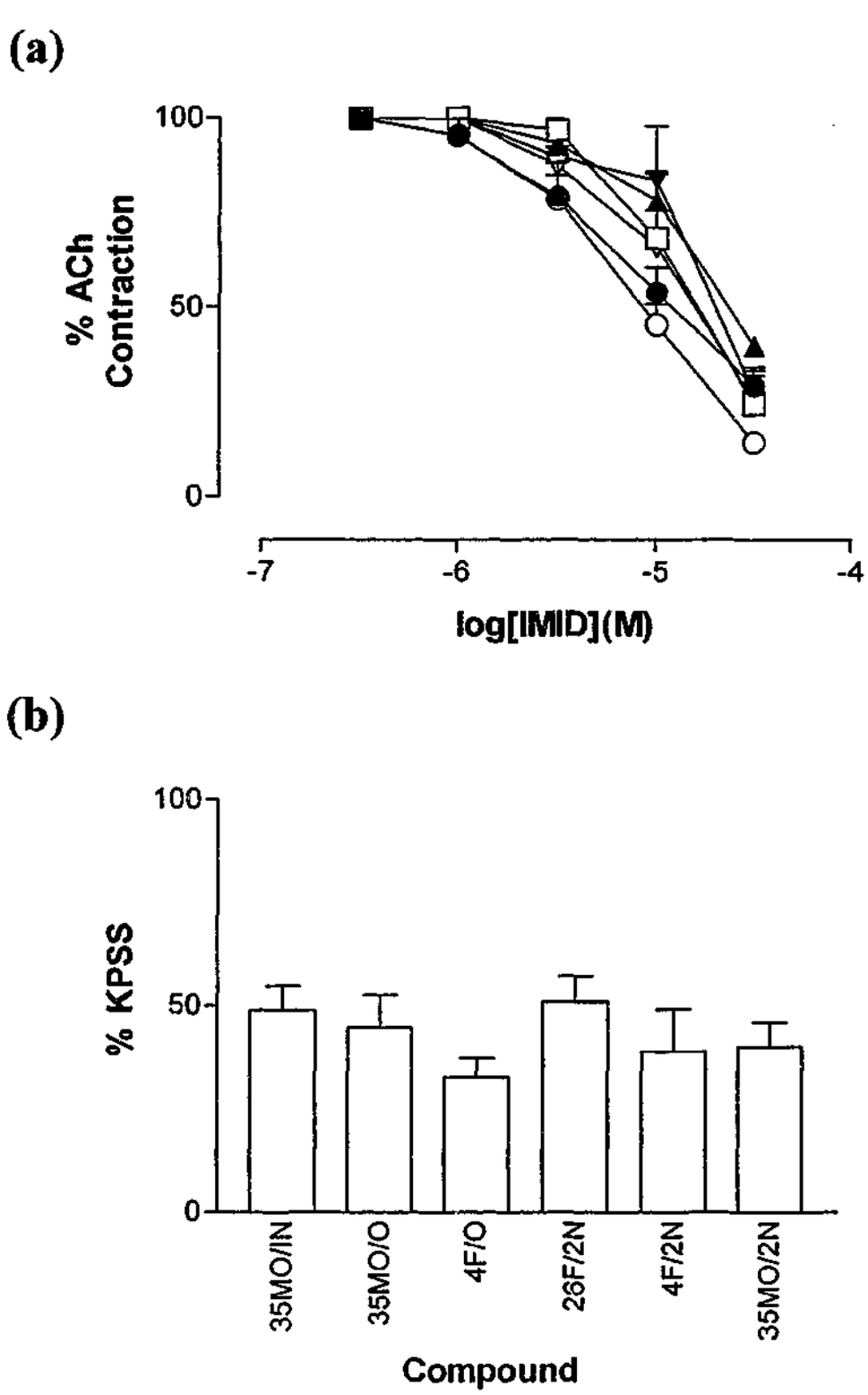

Figure 4.4 Mean concentration-response curves in pig isolated right circumflex arteries precontracted with ACh (0.1 - 0.3 μM) for IMID-35MO/IN (□), -35MO/O (●), -4F/O (○), -26F/2N (▼), - 4F/2N (▽), -35MO/2N (▲). Error bars are ± S.E.M. and if not visible are contained within the symbol (n=4). (b) Initial tone generated by ACh (0.1 - 0.3 μM) as a percentage of KPSS (n=4).

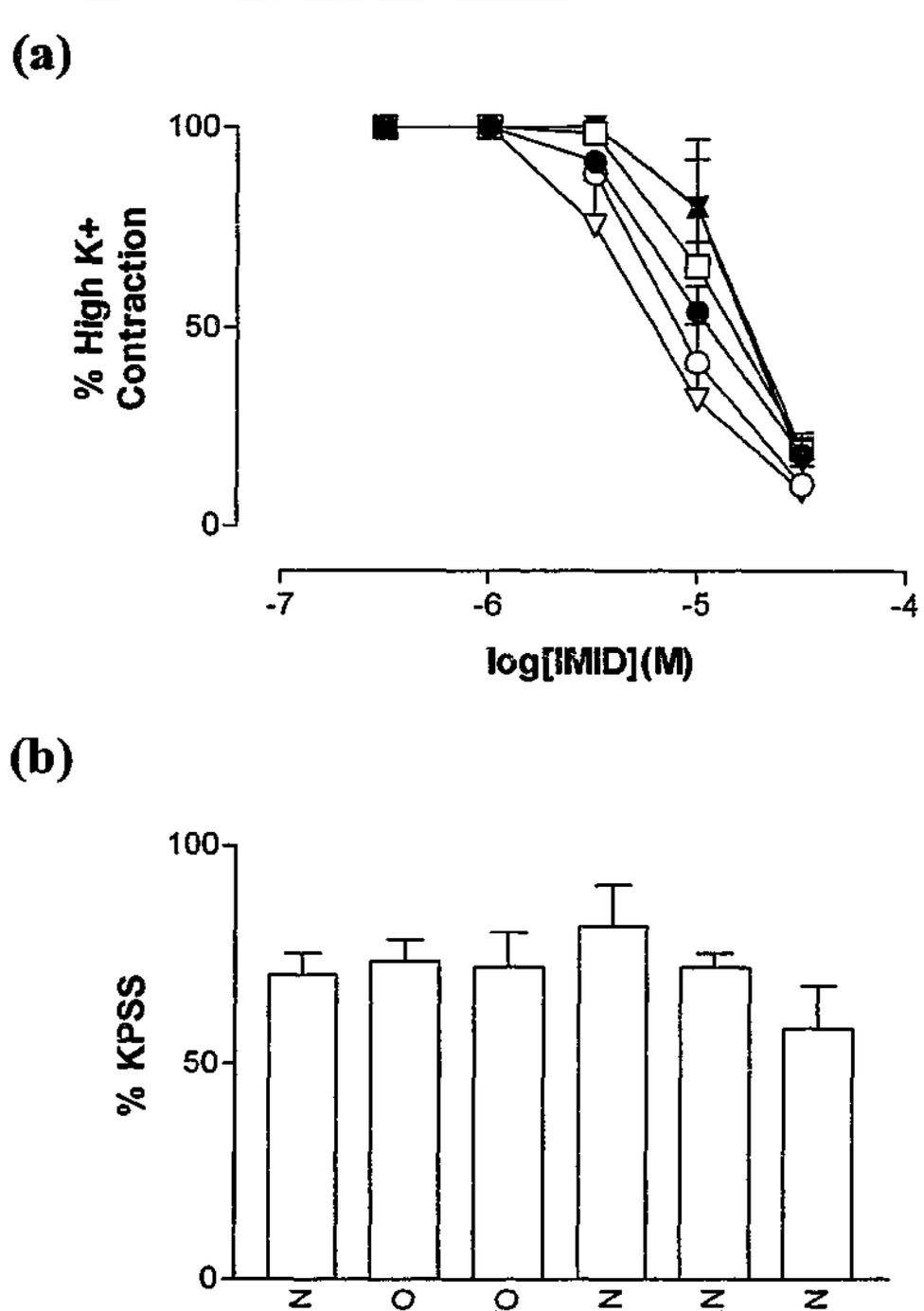

Figure 4.5 Mean concentration-response curves in pig isolated right circumflex arteries precontracted with K^+ (30 mM) for IMID-35MO/IN (□), -35MO/O (●), -4F/O (○), -26F/2N (▼), - 4F/2N (▽), -35MO/2N (▲). Error bars are ± S.E.M. and if not visible are contained within the symbol (n=4). (b) Initial tone generated by K^+ (30 mM) as a percentage of KPSS (n=4).

Experiment type	*In vitro* (pD_2)			Binding
Compound	Constrictor			(pK_D)
	U46619	ACh	K^+	
IMID-35MO/IN	$4.7 \pm 0.1^{\#}$	4.8 ± 0.1	4.8 ± 0.1	4.7 ± 0.1
IMID-35MO/O	5.3 ± 0.1*	4.9 ± 0.1	4.9 ± 0.1	5.5 ± 0.5
IMID-4F/O	5.3 ± 0.1*	5.1 ± 0.1	5.1 ± 0.1*	5.2 ± 0.2
IMID-26F/2N	$4.6 \pm 0.1^{\#}$	4.7 ± 0.2	$4.8 \pm 0.1^{\#}$	5.1 ± 0.1
IMID-4F/2N	4.7 ± 0.1	4.8 ± 0.1	5.2 ± 0.1	5.5 ± 0.1
IMID-35MO/2N	4.8 ± 0.2	4.6 ± 0.1	4.9 ± 0.1	4.7 ± 0.1
Nifedipine	$6.8 \pm 0.1^{\Psi}$	$6.8 \pm 0.1^{\Psi}$	$7.1 \pm 0.1^{\Psi}$	$8.6 \pm 0.1^{\Psi}$

Table 4.1 Summary of pD_2 values for the imidazolines that induced vasorelaxation of pig isolated coronary arteries precontracted with either U46619, ACh or K^+ and the calculated pK_D values for displacing binding of [^{3}H]-PN200-110 to rat cerebral cortex membranes (pig coronary artery n=4-8, radioligand binding n=4-5).
* indicates compounds significantly more potent than compounds denoted with # (P<0.05; one way ANOVA with Bonferroni t-test) precontracted with the same constrictor or at displacing binding.
$^{\Psi}$ indicates significantly more potent than all compounds (P<0.05; one way ANOVA with Bonferroni t-test) precontracted with the same constrictor or at displacing binding.

IMID-35MO/IN and IMID-26F/2N (n=4-8; P<0.05; one way ANOVA with Bonferroni t-test).

To assess if the vasorelaxation of the six imidazoline analogues was vasoconstrictor specific, experiments using both ACh (0.1–0.3 μM) and K^+ (30 mM) as the vasoconstrictors were carried out in an identical manner to the experiments using U46619 described above. The same six IMID compounds that caused relaxation of arteries constricted with U46619, also caused concentration-dependent relaxation in pig coronary arteries constricted with ACh (Figure 4.4a) and K^+ (Figure 4.5a) over the same concentration range. Again, pD_2 values were calculated and are summarised in Table 4.1. The pD_2 values were similar to those obtained with U46619 as the preconstrictor. In fact, the pD_2 values calculated for the vasorelaxation to each IMID compound for the three vasoconstrictors were not significantly different from each other (n=4-8; P>0.05; one way ANOVA).

When ACh was used to constrict the tissues, none of the pD_2 values for the IMID compounds (4.6–5.1) were significantly different from one another (n=4-7; P>0.05; one way ANOVA). When the tissues were precontracted with K^+, only the pD_2 values calculated for IMID-4F/2N (5.2) and IMID-26F/2N (4.8) were significantly different from each other (n=4-5; P<0.05; one way ANOVA with Bonferroni t-test). Nifedipine (0.01- 3 μM), which also relaxed contractions to all three constrictors, was significantly more potent as a vasodilator than all the IMID compounds (Table 4.1; n=4-5; P<0.05; one way ANOVA with Bonferroni t-test).

4.3.2 Vasorelaxation of IMID-35MO/O in rat mesenteric arteries

To discover if the relaxation induced by the IMID compounds was specific to pig coronary arteries, another vascular tissue, rat isolated small mesenteric arteries were used in this series of experiments. Different vasoconstrictors, PE (1–10 μM) and K^+ (40–60 mM) were used to confirm the results in Section 4.3.1, ie that the relaxation of the IMID compounds was not vasoconstrictor specific. IMID-35MO/O (0.3–30 μM), caused concentration-dependent vasorelaxation of rat mesenteric arteries that was significantly different from the methanol vehicle (Figure 4.6; n=4-5; P<0.05; Students t-test). The vasoconstrictors, PE or K^+ did not effect the vasorelaxation to IMID-35MO/O (PE $pD_2 = 5.0 \pm 0.1$; K^+ $pD_2 = 5.1 \pm 0.0$; n=4-5; P>0.05; Students t-test).

4.3.3 Effect of TPP, ODQ and propranolol on the vasorelaxation of IMID-35MO/O

In an endeavour to discover the mechanism of action of the IMID compounds' vasorelaxation, several antagonists/inhibitors were used to try to attenuate the vasorelaxation to IMID-35MO/O. Again, pig isolated coronary arteries precontracted with U46619 (3–10 nM) were used in this series of experiments.

There was no significant shift in the pD_2 values when the concentration-response curves to IMID-35MO/O (0.3–30 μM) were obtained in the absence or the presence of TPP (3 μM), a K_{ATP} channel antagonist, ODQ (10 μM), a soluble guanylate cyclase inhibitor or propranolol (1 μM), a β-adrenoceptor antagonist (Figure 4.7; control $pD_2 = 5.2 \pm 0.0$; plus TPP $pD_2 = 5.1 \pm 0.1$; plus ODQ $pD_2 = 5.1 \pm 0.0$; plus propranolol $pD_2 = 5.4 \pm 0.1$; n=4 – 13; P>0.05; one way ANOVA).

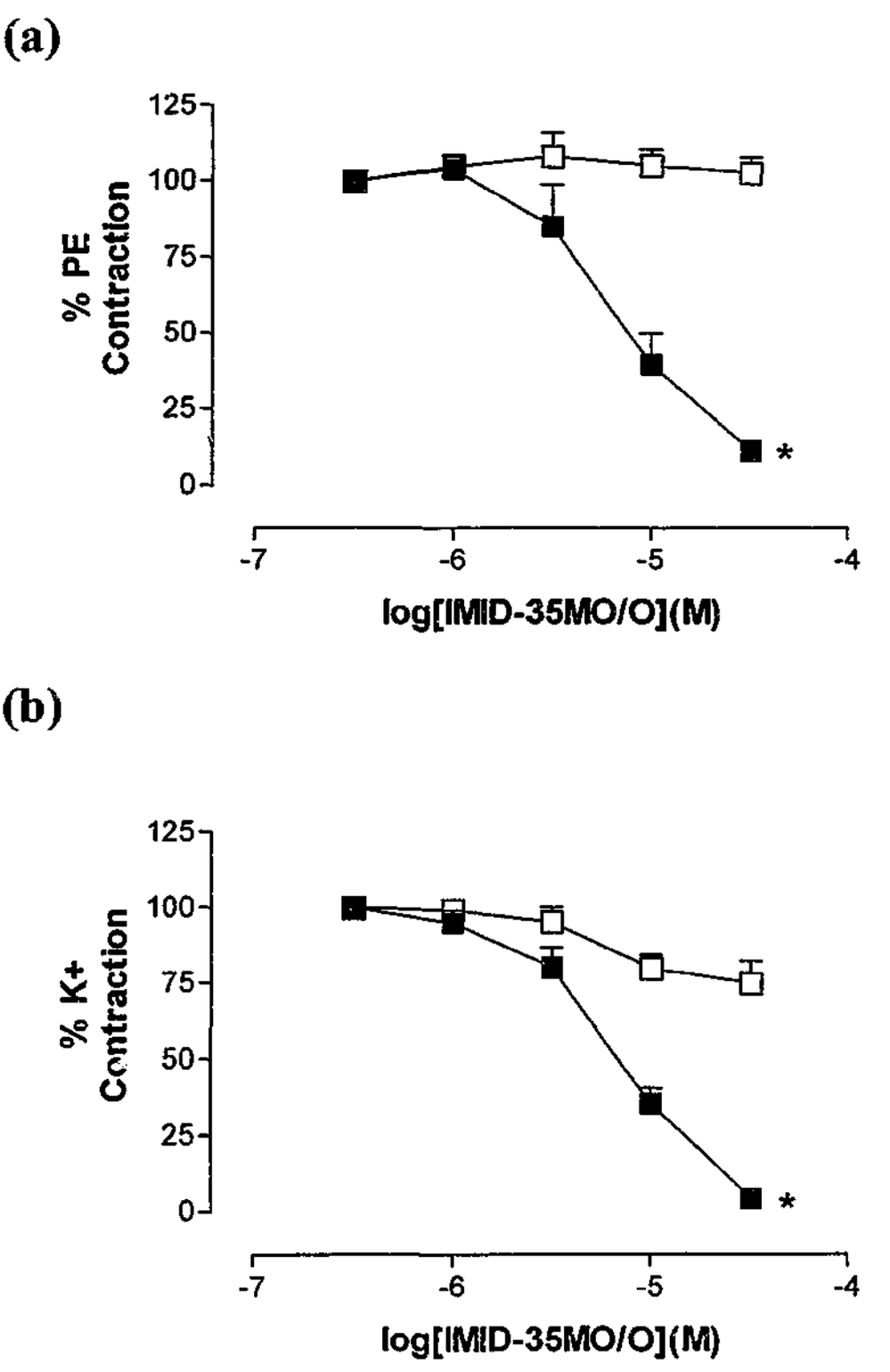

Figure 4.6 Mean concentration-response curves in rat isolated small mesenteric arteries precontracted with either (a) phenylephrine (PE; 1–10 μM) or (b) K^+ (40–60 mM) for IMID-35MO/O (■) and the methanol vehicle (□). Error bars are ± S.E.M. and if not visible are contained within the symbol. * indicates a significant difference from the vehicle at the highest concentration (30 μM; n=4-5; P<0.05; one way ANOVA with Bonferroni t-test).

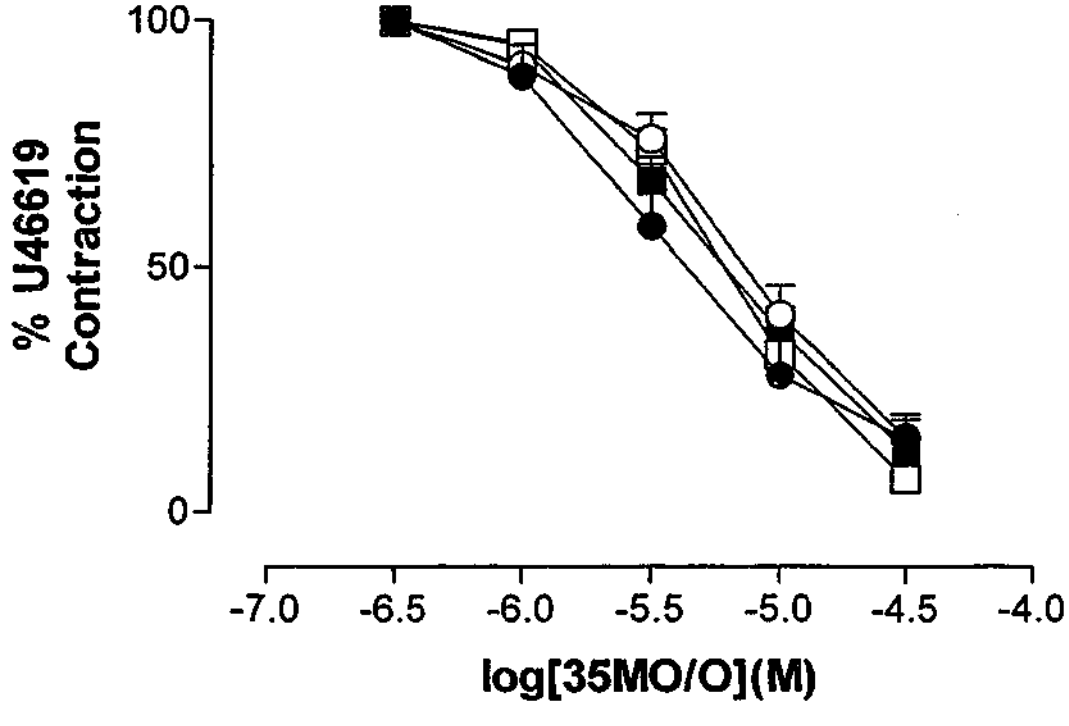

Figure 4.7 Mean concentration-response curves in pig isolated right circumflex arteries precontracted with U46619 (3–10 nM) for IMID-35MO/O in the absence of treatment (■), or in the presence of TPP (3 μM; ○), ODQ (10 μM; □) or propranolol (1 μM; ●) (n=4 – 13; P>0.05; one way ANOVA). Error bars are ± S.E.M. and if not visible are contained within the symbol.

4.3.4 [^{3}H]-PN200-110 hot saturation studies

Saturation studies were performed to determine the apparent dissociation constant (pK_D) and the density of the binding sites (B_{max}) values for [^{3}H]-PN200-110. Figure 4.8 shows a typical example of the equilibrium saturation binding of [^{3}H]-PN200-110 to rat cerebral cortex membranes and the Scatchard analysis, both generated using RADLIG. Non-specific binding increased linearly with the concentration of the labelled ligand. The pK_D was 9.7 ± 0.0 and the B_{max} 6.1 ± 0.3 fmol/kg/protein (n=3).

4.3.5 [^{3}H]-PN200-110 competition studies

The ability of the IMID compounds to displace binding of [^{3}H]-PN200-110 to rat cerebral cortex membranes was investigated to characterise their activity at L-type calcium channels. Figure 4.9 illustrates the findings from this study where several of the IMID compounds (10 μM) significantly displaced binding (n=5-8; P<0.05; one way ANOVA with Bonferroni t-test). The IMID compounds that caused significant displacement represented as percentage of total binding of [^{3}H]-PN200-110 were IMID-4F/2N (52 ± 4 %), IMID-4F/O (68 ± 7 %), IMID-35MO/O (73 ± 6 %), IMID-26F/2N (79 ± 6 %), IMID-35MO/2N (87 ± 2 %) and IMID-35MO/IN (90 ± 2 %). However, the majority of the compounds, IMID-4F/IN (100 ± 5 %), IMID-26F (113 ± 5 %), IMID-4ME (118 ± 5 %), IMID-4F (122 ± 5 %) and IMID-1M (122 ± 5 %) did not significantly displace binding of [^{3}H]-PN200-110 when compared to the vehicle (100 % ethanol, 110 ± 4 %; n=5-8; P>0.05; one way ANOVA). Nifedipine (0.1 μM) was used to define non-specific binding and was found to significantly displace binding to 20 ± 2 % of total binding (n=5-8; P<0.05; one way ANOVA).

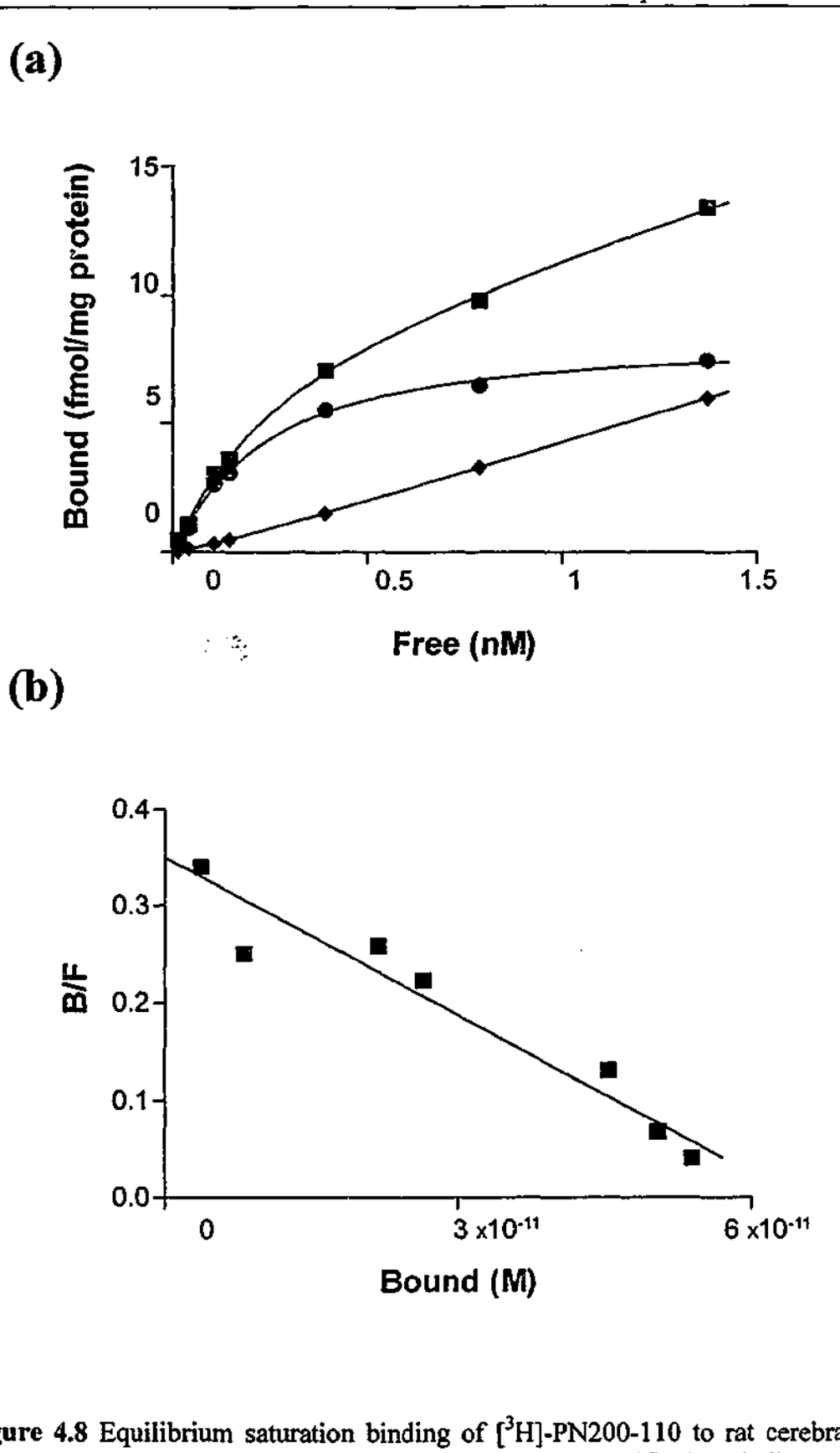

Figure 4.8 Equilibrium saturation binding of [^{3}H]-PN200-110 to rat cerebral cortex membranes. (a) Total (■), specific (●) and non-specific (◆) binding are shown as a function of the free label concentration (F). Points are means of triplicate measurements from one typical experiment. Non-specific binding was determined in the presence of nifedipine (1 μM). The pK_D and B_{max} values obtained from this fitted curve were 9.7 and 6.5 fmol/mg/protein, respectively. (b) Scatchard transformation of the saturation binding in (a).

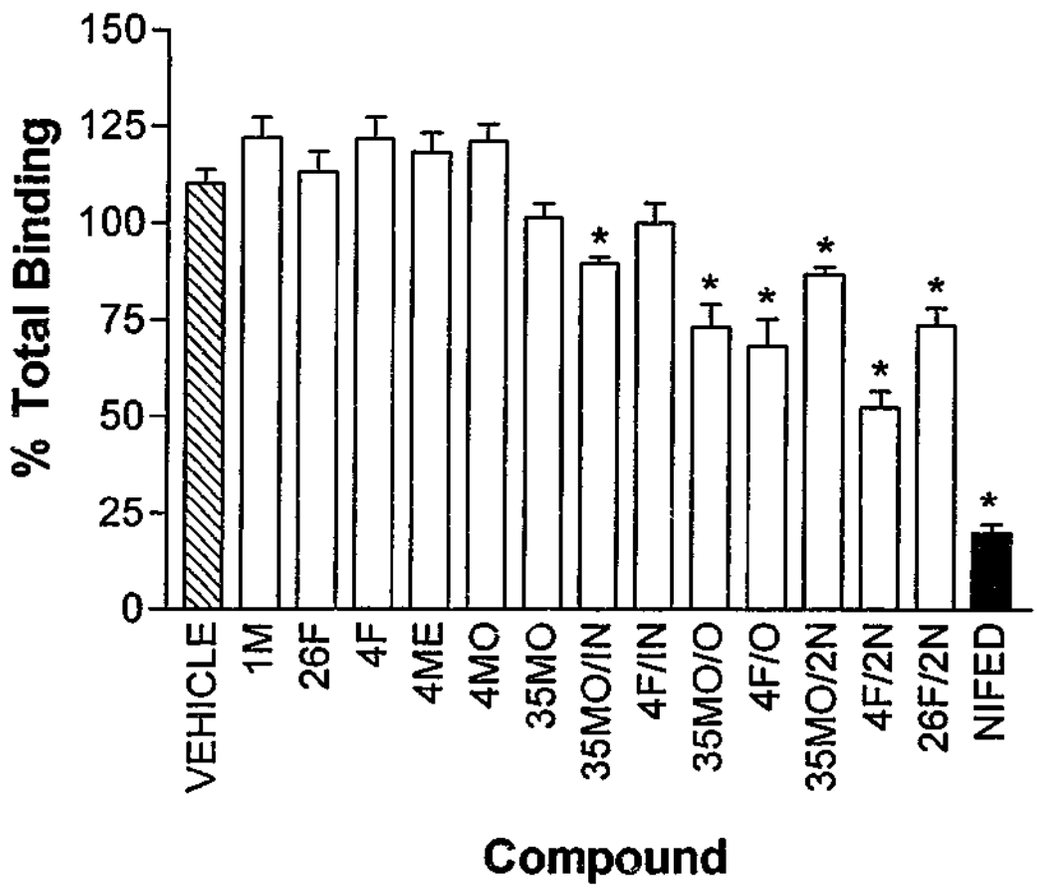

Figure 4.9 Histogram plot illustrating the total binding of [^{3}H]-PN200-110 in the absence of treatment (vehicle) or in the presence of the IMID compounds (10 μM) or nifedipine (0.1 μM). Results are expressed as a % of total binding. Error bars are ± S.E.M. and if not visible are contained within the symbol. * indicates a significant displacement by a treatment when compared to vehicle (n=5-8; P<0.05; one-way ANOVA with Bonferroni t-test).

For those compounds that displaced binding at 10 μM, more extensive investigations were carried out. Full concentration-displacement curves were constructed for each IMID compound (10 nM–100 μM). The pK_D values were calculated using RADLIG for each IMID analogue and they can be seen in Table 4.1. Of the IMID compounds (pK_Ds 4.7–5.5) that displaced binding, none were significantly different from one another (n=4; P>0.05; one way ANOVA). However, all were significantly different from nifedipine (8.6 ± 0.1; n=4; P<0.05; one way ANOVA with Bonferroni t-test). Figure 4.10 illustrates full concentration-displacement curves for IMID-4F/2N (10 nM–100 μM) and nifedipine (0.01 nM–1 μM). IMID-4F/2N is significantly less potent than nifedipine (n=4; P<0.05; Students t-test).

4.3.6 Correlation between the imidazoline-induced vasorelaxation and displacement of [^{3}H]-PN200-110 binding

Every IMID compound that caused vasorelaxation also displaced binding of [^{3}H]-PN200-110, over a similar range in potency. As the compounds had equal potency as vasorelaxants and at displacing [^{3}H]-PN200-110 binding, a correlation analysis was not performed. Conversely, those IMID compounds that did not cause vasorelaxation did not displace [^{3}H]-PN200-110 binding.

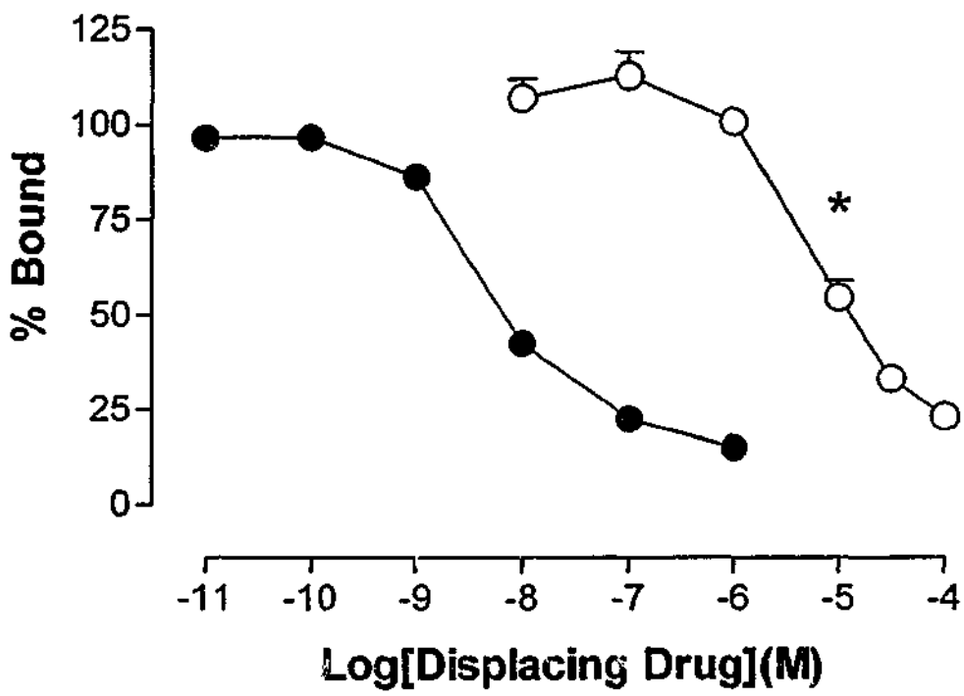

Figure 4.10 Mean displacement curve for [^{3}H]-PN200-110 in the presence of increasing concentrations of nifedipine (●) or IMID-4F/2N (○). Results are expressed as % bound. Error bars are ± S.E.M. and if not visible are contained within the symbol. * indicates a significant difference between treatments (n=4; P<0.05; Students t-test).

4.4 Discussion

As described in Chapter 3, it was found that several of the imidazoline analogues, IMID-35MO/IN, IMID-35MO/O, IMID-4F/O, IMID-26F/2N, IMID-35MO/2N & IMID-4F/2N, were able to antagonise U46619 contractions in pig isolated coronary arteries. The present study was carried out to investigate this vasorelaxant property. The findings indicate that the relaxation observed in the *in vitro* experiments, using isolated segments of artery, may in fact be due to antagonism of L-type calcium channels.

Initially, the vasorelaxation phenomenon was investigated using segments of pig coronary artery that were constricted with U46619. In studies specifically designed to assess the vasorelaxant potency, six imidazoline analogues relaxed contractions to U46619 in a concentration-dependent manner. The remaining seven IMID compounds either had no vasorelaxation effect on contractions to U46619 (IMID-4F, IMID-4ME, IMID-4MO, IMID-35MO & IMID-26F) or caused small additional concentration-dependent increases in tension (IMID-1M and IMID-4F/IN). The six imidazoline analogues that induced vasorelaxation were then investigated further.

The vasorelaxation responses were not vasoconstrictor specific. The concentration-dependent vasorelaxation to the six imidazoline analogues were similar and independent of which vasoconstrictor (ie U46619, ACh & K^+) was used. This finding suggested the imidazolines were not specifically affecting thromboxane A_2 receptors. In addition, the vasorelaxation was not tissue specific as the pD_2 values for IMID-35MO/O were similar to those obtained in pig coronary arteries in rat isolated mesenteric arteries constricted with either phenylephrine or K^+.

All the experiments in this Chapter were performed in pig endothelium-denuded coronary arteries, indicating that the vasorelaxation was not endothelium-dependent.

Therefore, several mechanisms by which the imidazolines may be inducing relaxation were investigated. It is well known that imidazolines have actions at vascular K_{ATP} channels (eg McPherson & Angus, 1989; Chapter 3). The prospect that the imidazolines were opening rather than antagonising K_{ATP} channels was investigated. However, two lines of evidence suggest this is not the case, (i), K^+ did not affect the vasorelaxant response to the imidazolines and (ii), the K_{ATP} channel inhibitor, tetraphenylphosphonium (TPP; Piekarska & McPherson, 1997) did not affect the relaxation to IMID-35MO/O.

Another possibility was that the imidazoline derivatives were acting in a similar way to nitric oxide to induce relaxation. The haem group present within nitric oxide binds to soluble guanylate cyclase activating the enzyme (Schmidt *et al.*, 1993). The active enzyme than catalyses the generation of cGMP, which results in activation of protein kinase G (PKG) and phosphorylation of the target proteins and vasodilatation. However, the soluble guanylate cyclase inhibitor, ODQ had no effect on the relaxation to IMID-35MO/O indicating that the imidazolines were not activating guanylate cyclase.

Numerous imidazolines have been shown to have actions at β-adrenoceptors (eg Hamada *et al.*, 1985) and decreases in vascular tone are thought to be mediated by β_2-adrenoceptors (Wilffert *et al.*, 1982). Therefore, the possibility that IMID-35MO/O was activating β-adrenoceptors was investigated by using the β-adrenoceptor antagonist, propranolol. Propranolol did not significantly inhibit the relaxation to IMID-35MO/O, indicating that the imidazolines in this study possessed no such actions at β-adrenoceptors.

Calcium channel antagonists such as nifedipine cause vasorelaxation similar to the relaxation observed in this study by the imidazolines. In accordance with this, in

radioligand binding studies utilising the dihydropyridine analogue [^{3}H]-PN200-110, which binds to L-type calcium channels, in rat cerebral cortex membranes only the six imidazoline analogues that caused vasorelaxation significantly inhibited binding of [^{3}H]-PN200-110. The remaining seven IMID compounds did not affect binding of [^{3}H]-PN200-110. The pK_D values obtained from full concentration-displacement curves, carried out for those imidazoline derivatives that displaced binding, were some 100 fold less potent than nifedipine. In addition, the pK_D values (displacement) and the pD_2 values (vasorelaxation) are comparable for both the imidazolines and nifedipine. Together, these studies provide evidence that the six imidazoline analogues produce vasorelaxation via an action at L-type calcium channels.

These finding are in line with several recent studies that examined the actions of several other imidazolines at calcium channels. While investigating the actions of isothiocyanatobenzyl imidazoline (IBI) in rat isolated aorta, Slavica and colleagues (1994) found the slow onset sustained contractions did not involve actions at α-adrenoceptors or imidazoline receptors but involved voltage-dependent calcium channels. Another study by the same group, which investigated these contractions further, found that IBI and derivatives bind to L-type calcium channels and interact allosterically with the dihydropyridine binding site (Lei *et al.*, 1998). They also found that the isothiocyanato (NSC) group attached to the phenyl ring was an essential requirement for these actions. IBI also produces a slow developing contraction in other smooth muscle preparations, including the guinea-pig stomach, that are also attributed to an action at voltage-dependent calcium channels (Jing *et al.*, 1999). In RINm5F insulin producing cells an imidazoline derivative, calmidazolium, inhibited the influx of calcium through voltage-dependent calcium channels that may involve it either binding

directly to calcium channels, or binding to Ca^{2+}-calmodulin dependent protein kinases (Kindmark *et al.*, 1994).

Although IBI is thought to open calcium channels, calidazolium is thought to inhibit them. Therefore, the prospect that the IMID compounds that caused vasorelaxation did so via an action at calcium channels was investigated. The dihydropyridine, nifedipine, an L-type calcium channel antagonist, caused vasorelaxation of contractions to U46619, ACh and K^+ in the pig isolated coronary arteries. However, although the responses were similar to those of the imidazoline analogues, nifedipine was approximately 100 fold more potent.

From this study, it appears that the IMID compounds with altered imidazoline rings exhibit actions at calcium channels. The six imidazoline analogues which are thought to have calcium channel actions either have oxygen substitutions in the imidazoline ring (IMID-35MO/O & IMID-4F/O), or substitutions on an imidazoline ring nitrogen (IMID-35MO/IN, IMID-26F/2N, IMID-35MO/2N & IMID-4F/2N). An exception to this rule is 4F/IN, which has a substitution at the imidazoline ring nitrogen. IMID-4F/IN produced a small concentration-dependent contraction rather than relaxation and did not displace binding of [^{3}H]-PN200-110, both findings indicating no actions at L-type calcium channels. The reason for this is unclear at this time. There was no evidence in this study that the mono substituted compounds (IMID-1M, IMID-4F, IMID-4ME, IMID-4MO, IMID-35MO & IMID-26F) had any activity at calcium channels.

In conclusion, the results from this study indicate that the relaxation observed in the *in vitro* experiments using isolated segments of artery and the displacement of [^{3}H]-PN200-110 produced by several of the imidazolines in earlier parts of this study may be due to antagonism of L-type calcium channels. However, the antagonism of calcium

channels by several of these compounds is some 100 fold less potent than their K_{ATP} channel antagonism (Chapter 3).

Chapter Five

Characterisation of the Novel Imidazoline Analogues using Radioligand Binding Techniques

5.1 Introduction

Several of the imidazolines characterised in this thesis have been identified as potent K_{ATP} channel antagonists. They have been shown to antagonise levcromakalim in both functional and electrophysiological studies. In addition, the imidazolines were found to have minimal bradycardic actions when assessed in the rat isolated spontaneously beating right atria (Chapter 3). However, as outlined in Chapter 4, a subgroup of the IMID compounds was found to have other actions, in particular, actions at calcium channels. Also, imidazolines and imidazolidines are well known for their actions at α-adrenoceptors (Kobinger & Pichler, 1980). Several studies with alinidine have also identified antimuscarinic actions (Opthof *et al.*, 1986; Ogiwara *et al.*, 1987; Lang & Walland, 1989; Nakane *et al.*, 1991). In our laboratory, studies identified several alinidine analogues that displaced binding of [^{3}H]-QNB, a muscarinic antagonist, to rat cerebral cortex membranes (Challinor-Rogers, 1995). Therefore, the aim of this series of experiments was to assess their activity at a variety of different receptor sites, namely, muscarinic, α_1- and α_2-adrenoceptors, utilising radioligand binding techniques.

As already discussed in Section 1.4.1.1, the opener and blocker sites of the sulphonylurea receptor are negatively allosterically coupled (Bray & Quast, 1992; Quast *et al.*, 1993; Löffler & Quast, 1997). Therefore, it is possible that the IMID compounds may be acting at either site to produce their antagonism of the K_{ATP} channel. To explore this, radioligands which bind to both the opener ([^{3}H]-P1075) and blocker ([^{3}H]-glibenclamide) sites of the sulphonylurea receptor (SUR), were used to explore the possibility that the analogues were interacting at either, one or both of these sites. Rat cerebral cortex membranes were used for the [^{3}H]-glibenclamide binding as in

studies in our laboratory they have been well characterised (Challinor-Rogers *et al.*, 1995). However, the [^{3}H]-P1075 displacement studies were performed using bovine vascular smooth muscle cells following the relatively new methods of Carman-Krzan and coworkers (1997) and Löffler-Walz & Quast (1998). As the studies presented in the preceding Chapters have focussed upon vascular K_{ATP} channels, binding studies using vascular smooth muscle cells was an advantage.

5.2 Materials and Methods

5.2.1 Membrane preparations

5.2.1.1 Cerebral cortex membranes

The ability of the analogues to interact with the sites labelled by the α_2-adrenoceptor antagonist [^{3}H]-rauwolscine, the α_1-adrenoceptor antagonist [^{3}H]-prazosin, the muscarinic receptor antagonist [^{3}H]-QNB and the K_{ATP} channel antagonist [^{3}H]-glibenclamide was investigated using rat cerebral cortex membranes. Cerebral cortex membranes were prepared as previously described in Section 4.2.2.1.1.

5.2.1.2 Bovine smooth muscle cells

The ability of the novel imidazoline compounds to compete for sites labelled by the K_{ATP} channel opener [^{3}H]-P1075 was determined using bovine smooth muscle cells. Bovine aorta smooth muscle cell membranes were prepared by adapting the method of Carman-Krzan and coworkers (1997). Bovine aortae were obtained from the local abattoir and stored in ice-cold storage buffer (composition in mM: NaCl 139, KCl 5, $MgCl_2$ 1.2, HEPES (4-(2-hydroxyethyl)-1-piperazine-ethane-sulphonic acid) 5 and EGTA (ethylene glycol-bis-(2-aminoethylether)-N.N.N',N'-tetra-acetic acid) 1; pH = 7.4). The aortae were then cleared of fat and connective tissue and the smooth muscle dissected from the inner elastic layer. The smooth muscle was then minced in 3 vol/g (wet weight) of the mincing buffer (composition in mM: HEPES 10, EGTA 1, phenylmethylsulphonyl fluoride (PMSF) 0.2, pepstatin A (0.2 μM), leupeptin (10 μM) and soybean trypsin inhibitor (10 μg/ml)) and homogenised. The homogenate was then

sieved through a fine nylon mesh, and centrifuged at 100 x *g* for 10 min at 4 °C. The supernatant was aspirated and further centrifuged at 4.8 x 10^4 x *g* for 15 min at 4 °C. The resulting pellet was then suspended in approximately 20 volumes storage buffer (composition in mM: NaCl 139, KCl 5, $MgCl_2$ 2 and HEPES 20; pH = 7.4), and stored at –80 °C for future use.

5.2.2 Competition studies

5.2.2.1 Using cerebral cortex membranes

General Method

Drug displacement experiments were carried out, in duplicate, by initiating a binding reaction that involved incubating the 500 µl of membrane preparation with tubes already containing 100 µL of the [^{3}H]-ligand ([^{3}H]-prazosin, [^{3}H]-rauwolscine, [^{3}H]-QNB or [^{3}H]-glibenclamide) and 10 µl of either the cold displacing drug (phentolamine, atropine or glibenclamide), or an IMID compound. The incubation mixtures, which had total volume of 1 ml in a phosphate buffer were lightly vortexed and incubated. After the appropriate incubation time, the incubation was terminated by adding 5 ml of ice-cold phosphate buffer. The bound and free ligand was then separated by filtration under vacuum over glass microfibre filters (Whatman GF/B) using a Brandell Harvester. The filters were washed twice with 5 ml of phosphate buffer and counted for ^{3}H in 2.5 ml scintillant (EcoLite, ICN Biomedicals, USA) using a Minaxi Tri-Carb 4000 series β-counter (United Technologies Packard). The disintergrations per minute (dpm) were counted for 5 minutes.

Initially, all displacement experiments were performed using a single high concentration (10 μM) for all the IMID analogues. If a considerable displacement of more than 75 % of total binding was observed, full competition-displacement studies were performed. This involved using a concentration range of 10 nM–100 μM for each of the active IMID compounds.

α-Adrenoceptors

The ability of the IMID compounds to interact with α_1-adrenoceptors was investigated using the α_1-adrenoceptor antagonist, [^{3}H]-prazosin at a final concentration of 0.2 nM. Incubations were for 30 minutes at room temperature. For the α_2-adrenoceptor, the α_2-adrenoceptor antagonist, [^{3}H]-rauwolscine at a final concentration of 0.5 nM was used. Incubations were for 1 hour at room temperature. 500 μl of membrane preparation was used and the non-specific α-adrenoceptor antagonist, phentolamine (10 μM) was used to define non-specific binding for both ligands. The K_D values were calculated in previous hot saturation studies using rat cerebral cortex membranes in our laboratory and were as follows: [^{3}H]-rauwolscine K_D =0.5 nM; [^{3}H]-prazosin K_D =0.15 nM (Challinor-Rogers, 1995).

Muscarinic receptors

The ability of the IMID compounds to interact with muscarinic receptors was assessed using the muscarinic receptor antagonist [^{3}H]-QNB at a final concentration of 0.2 nM. The muscarinic receptor, atropine (10 μM) was used in this series of experiments to define non-specific binding. Incubations using 500 μl of membrane

preparation were carried out for 1 hour at room temperature. As [^{3}H]-QNB is light sensitive incubations were also performed in reduced light and under foil to minimise the exposure to light and therefore, degradation of the ligand.

Sulphonylurea receptors

To investigate the ability of the IMID compounds to interact with the antagonist site of the sulphonylurea receptor the K_{ATP} channel antagonist, [^{3}H]-glibenclamide was used at a final concentration of 0.3 nM. Cold glibenclamide (10 μM) was used to define non-specific binding. Incubations using 200 μl of membrane preparation were carried out for 1 hour at room temperature.

5.2.2.2 Using bovine smooth muscle cells

Sulphonylurea receptors

The ability of the IMID compounds to interact with K_{ATP} channel opener sites on the sulphonylurea labelled by the K_{ATP} channel opener [^{3}H]-P1075 was determined using bovine smooth muscle cells. Drug displacement experiments using the bovine smooth muscle cells were carried out using the method of Löffler-Walz & Quast (1998). The binding reaction was initiated by the addition of 200 μl of the membrane preparation to tubes already containing the binding reagents, 100 μl of [^{3}H]-P1075 (final concentration; 1 nM), and 10 μl of either, levcromakalim (final concentration; 10 μM), glibenclamide (final concentration; 10 μM), or an IMID compound (final concentration; 10 μM). The incubation mixture, which had a total volume of 1 ml including the incubation buffer (composition in mM: NaCl 139, KCl 5, $MgCl_2$ 25, $CaCl_2$ 1.25 and

HEPES 20, creatine phosphate 20, Na_2ATP 3, and creatine phosphokinase (50 U/ml); pH = 7.4) was lightly vortexed and incubated at 37 °C for 30 minutes. The incubation was stopped by adding 5 ml of ice-cold quench solution (Composition in mM: NaCl 154, Tris 50, pH = 7.4). The bound and free ligand was then separated by filtration under vacuum over glass microfibre filters (Whatman GF/B) using a Brandell Harvester. The filters were washed twice with 5 ml of quench solution and counted for ^3H in 2.5 ml scintillant (EcoLite, ICN Biomedicals, USA) using a Minaxi Tri-Carb 4000 series β-counter (United Technologies Packard). The disintergrations per minute (dpm) were counted for 5 minutes.

5.2.3 Analysis of results

In this series of experiments, results were expressed as a % of total binding or % bound. Both the vehicle and drug used to define non-specific binding are also included on the figures for a comparison. For those analogues that significantly displaced binding by more than 75 % of total binding at 10 μM, full competition-displacement studies were performed using a concentration range of 10 nM–100 μM. RADLIG (McPherson, 1995), a computer program, which uses a weighted non-linear curve fitting method involving the Marquardt-Levenberg modifications of the Gauss-Newton technique (Rodbard, 1984) was used to analyse the results and calculate a pK_D ($-\log K_D$) for each analogue (Section 4.2.4.3).

5.2.3.1 Statistics

Results in the text are given as mean ± S.E.M. Statistical methods used were carried out as stated in the text. One way Analysis of Variance (ANOVA) was used to determine if two treatments were significantly different from one another and the Bonferroni *t*-test for all pairwise multiple comparisons was used for post-hoc analysis. Groups were considered significantly different from each other if $P<0.05$, unless otherwise stated. All statistical calculations were performed using SigmaStat (Jandel Scientific, U.S.A.).

5.2.4 Drugs

Radioligands, their specific activity and sources were: [^{3}H]-glibenclamide (specific activity: 47 Ci/mmol; NEN DuPont, U.S.A.); [^{3}H]-P1075 (specific activity: 117 Ci/mmol; Amersham. U.S.A.); [^{3}H]-prazosin (specific activity: 72.2 Ci/mmol; NEN DuPont, U.S.A.); [^{3}H]-QNB (specific activity: 32.9 Ci/mmol; NEN DuPont, U.S.A.); [^{3}H]-rauwolscine (specific activity: 83.0 Ci/mmol; NEN DuPont, U.S.A.).

[^{3}H]-glibenclamide, [^{3}H]-prazosin, [^{3}H]-QNB and [^{3}H]-rauwolscine were made up in phosphate buffer as stock solution of 3, 2, 2, and 5 nM, respectively and all further dilutions were also made in phosphate buffer. [3H]-P1075 was made up in incubation buffer as a stock solution of 10 nM and all further dilutions were also made in incubation buffer.

Drugs used and their sources were: atropine (Sigma Chemical Co., U.S.A); clonidine (Sigma Chemical Co., U.S.A); glibenclamide (Sigma Chemical Co., U.S.A.); IMID compounds (Eva Campi, Department of Chemistry, Monash University; Figure

2.1); levcromakalim (SmithKline Beecham, U.K.); phentolamine (Ciba-Geigy, Australia).

Levcromakalim, glibenclamide, phentolamine and the IMID compounds were made up in 100 % ethanol as stock solutions of 10 mM. Subsequent dilutions were made in distilled water apart from the imidazoline analogues, where the first dilution was made in 40 % EtOH and all further dilutions made in distilled water. Atropine and clonidine were dissolved and diluted in distilled water using an initial stock solution of 10 mM.

5.3 Results

5.3.1 Competition studies

A number of different radioligands were used in this series of experiments to assess the ability of the IMID compounds to displace binding at a variety of receptors in rat cerebral cortex membranes and bovine smooth muscle cells.

5.3.1.1 [^{3}H]-Rauwolscine binding

The ability of the IMID compounds to displace binding of [^{3}H]-rauwolscine to rat cerebral cortex membranes was investigated to characterise their activity at α_2-adrenoceptors. Figure 5.1 illustrates the findings from this study where several of the IMID compounds (10 μM) significantly displaced binding when compared to vehicle control (n=4-16; P<0.05; one way ANOVA with Bonferroni t-test). For the IMID compounds that caused significant displacement the percentage of total binding of [^{3}H]-rauwolscine in the presence of the IMID compounds (most to least potent), was IMID-4MO (41 ± 3 %), IMID-4ME (46 ± 4 %), IMID-1M (47 ± 3 %), IMID-4F/2N (47 ± 4 %), IMID-4F (53 ± 6 %), IMID-35MO/IN (55 ± 4 %), IMID-26F (58 ± 9 %), IMID-4F/IN (61 ± 5 %) and IMID-35MO (71 ± 2 %). The compounds IMID-4F/O (80 ± 6 %) and IMID-35MO/O (82 ± 5 %) did not displace binding of [^{3}H]-rauwolscine since their displacement was not significantly different to that of the vehicle (ethanol, 85 ± 5 %; n=4-16; P>0.05; one way ANOVA). Phentolamine and clonidine were used to define non-specific binding and were found to significantly displace binding to 30 ± 2 % and 28 ± 2 % of total binding, respectively (n=16; P<0.05; one way ANOVA with

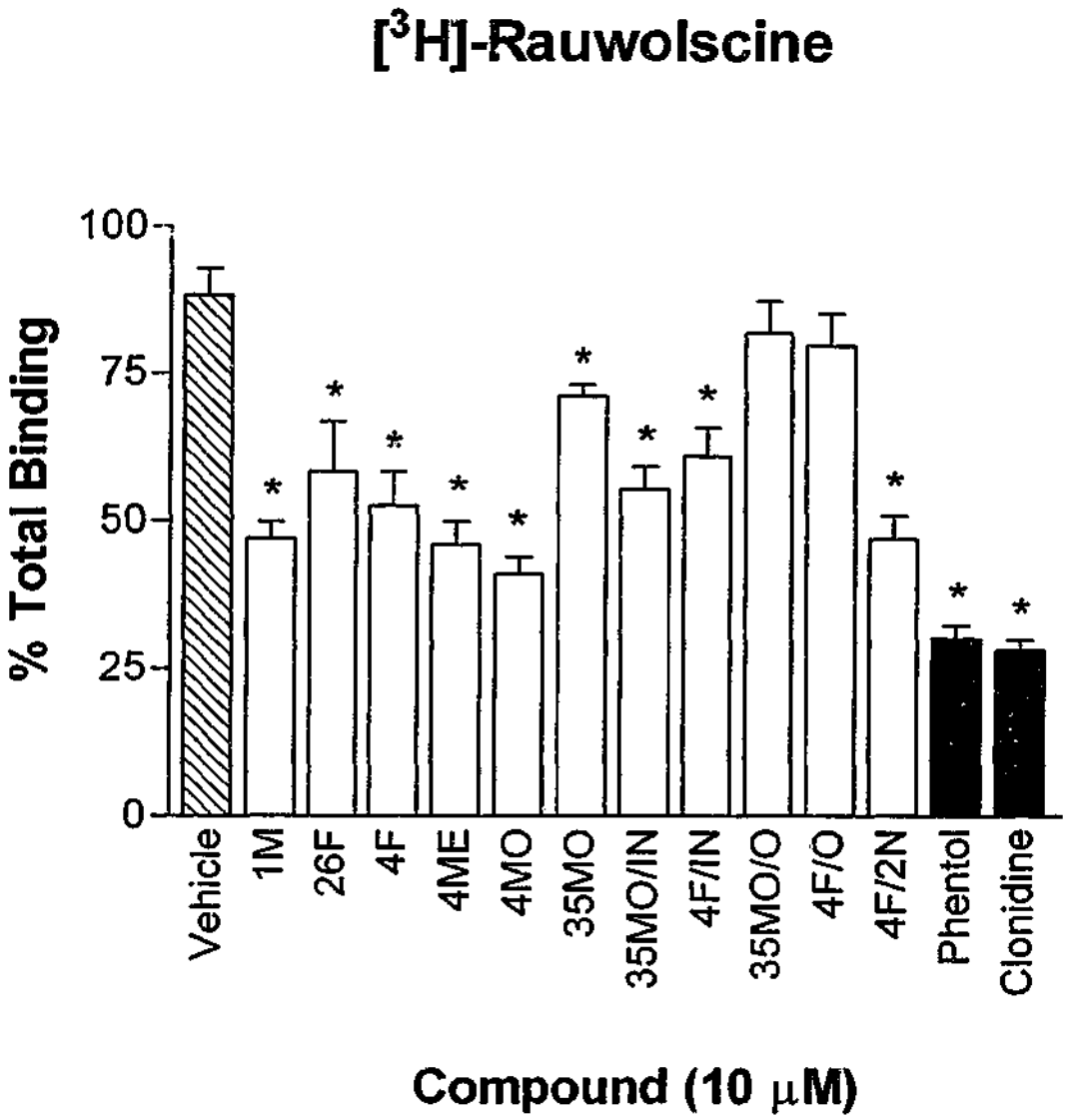

Figure 5.1 Histogram plot illustrating the total binding of [^{3}H]-rauwolscine, in the absence of treatment (vehicle) or in the presence of the IMID compounds, phentolamine (phentol) or clonidine, to rat cerebral cortex membranes. Results are expressed as a % of total binding. Error bars are ± S.E.M. and if not visible are contained within the symbol. * indicates a significant displacement by a treatment when compared to vehicle (n=4-16; P<0.05; one-way ANOVA with Bonferrroni t-test).

Bonferroni *t*-test).

For those compounds that displaced binding, further investigations were carried out. Full concentration-displacement curves were constructed for each IMID compound (10 nM – 100 μM). The pK_D values were calculated using RADLIG for each IMID analogue and are summarised in Table 5.1. Of the IMID compounds (pK_D range 5.65–5.22) that displaced binding none were significantly different from one another (n=4; P>0.05; one way ANOVA). However, all were significantly different from clonidine (7.94 ± 0.1) and phentolamine (7.59 ± 0.1; n=4; P<0.05; one way ANOVA with Bonferroni *t*-test). Figure 5.2 illustrates full concentration-displacement curves for IMID-4F/2N (10 nM–100 μM) and phentolamine (0.1 nM–100 μM). IMID-4F/2N is significantly less potent than phentolamine (n=4; P<0.05; Students *t*-test).

5.3.1.2 [^{3}H]-Prazosin binding

The ability of the IMID compounds to interact with α_1-adrenoceptors was examined by assessing their ability to displace [^{3}H]-prazosin binding to rat cerebral cortex membranes. Figure 5.3 illustrates the findings from this study where several of the IMID compounds (10 μM) significantly displaced binding when compared to vehicle control (n=4-12; P<0.05; one way ANOVA with Bonferroni *t*-test). Those compounds which caused significant displacement in order of most to least displacement, represented as percentage of total binding of [^{3}H]-prazosin, are IMID-4F/2N (31 ± 3 %), IMID-4MO (43 ± 2 %), IMID-4ME (45 ± 4 %), IMID-4F (48 ± 1 %), IMID-26F (57 ± 2 %), IMID-35MO/IN (62 ± 2 %), IMID-IM (64 ± 3 %), IMID-35MO (67 ± 2 %), and IMID-4F/IN (70 ± 4 %). As with [^{3}H]-rauwolscine binding, the

Compound	pK_D	
	[^{3}H]-rauwolscine	[^{3}H]-prazosin
IMID-1M	5.51 ± 0.2	5.35 ± 0.1
IMID-26F	5.49 ± 0.1	5.70 ± 0.3
IMID-4F	5.55 ± 0.2	5.66 ± 0.1
IMID-4ME	5.63 ± 0.1	5.67 ± 0.1
IMID-4MO	5.65 ± 0.2	5.73 ± 0.1
IMID-35MO	5.22 ± 0.3	5.38 ± 0.2
IMID-35MO/IN	5.48 ± 0.1	5.44 ± 0.1
IMID-4F/IN	5.34 ± 0.1	5.34 ± 0.1
IMID-35MO/O	-	-
IMID-4F/O	-	-
IMID-4F/2N	5.50 ± 0.2	5.99 ± 0.2
Phentolamine	7.59 ± 0.1*	7.73 ± 0.3*
Clonidine	7.94 ± 0.1*	✞

- not active
✞ not calculated

Table 5.1 Summary of pK_D values obtained for the IMID compounds for their displacement of [^{3}H]-rauwolscine and [^{3}H]-prazosin binding to rat cerebral cortex membranes. Of the IMID compounds that displaced binding, none were significantly different from each other (n=4-9; P>0.05; one-way ANOVA) although all were significantly different from clonidine and phentolamine (n=4-9; P<0.05; one way ANOVA with Bonferroni t-test).

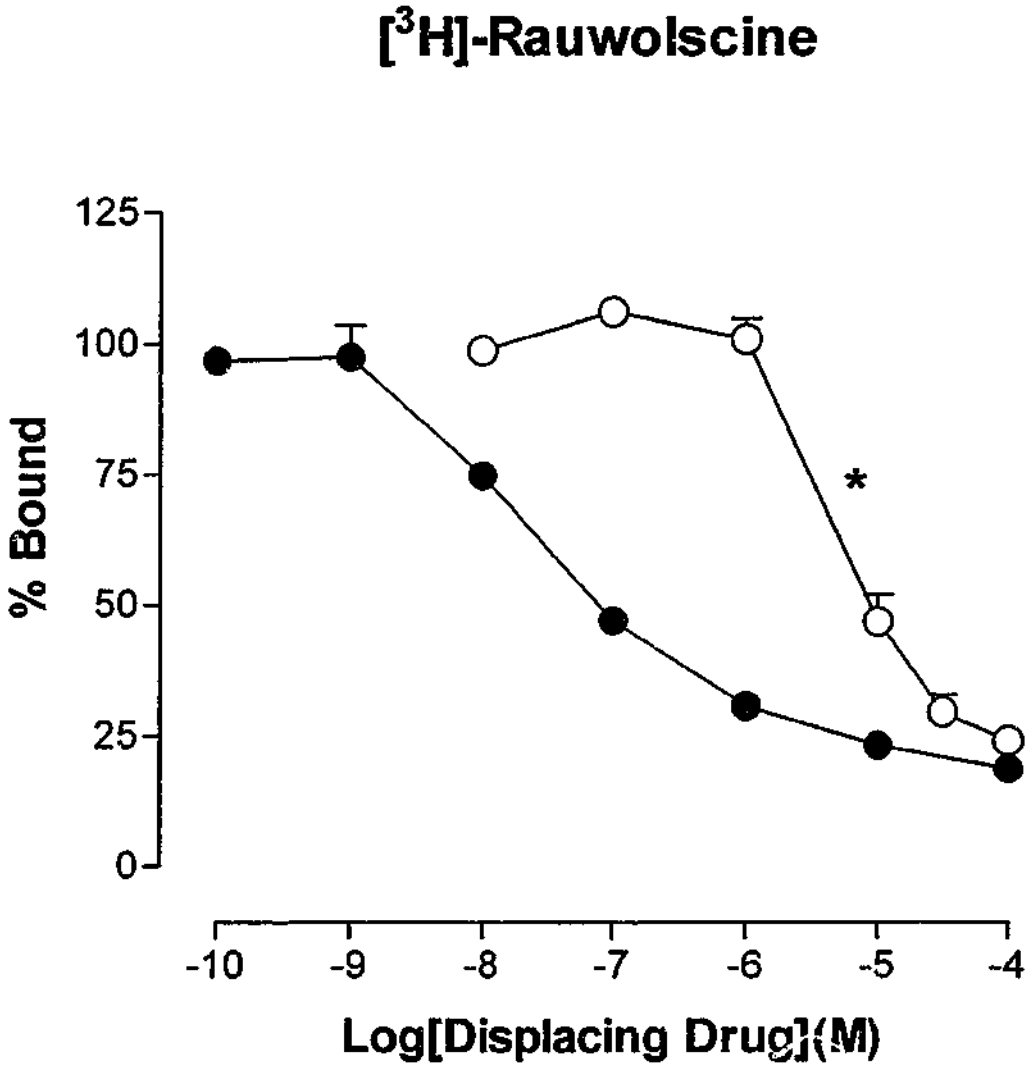

Figure 5.2 Mean displacement curve for [^{3}H]-rauwolscine in the presence of increasing concentrations of phentolamine (●) or IMID-4F/2N (○). Results are expressed as % bound. Error bars are ± S.E.M. and if not visible are contained within the symbol. * indicates a significant difference between treatments (n=4; P<0.05; students t-test).

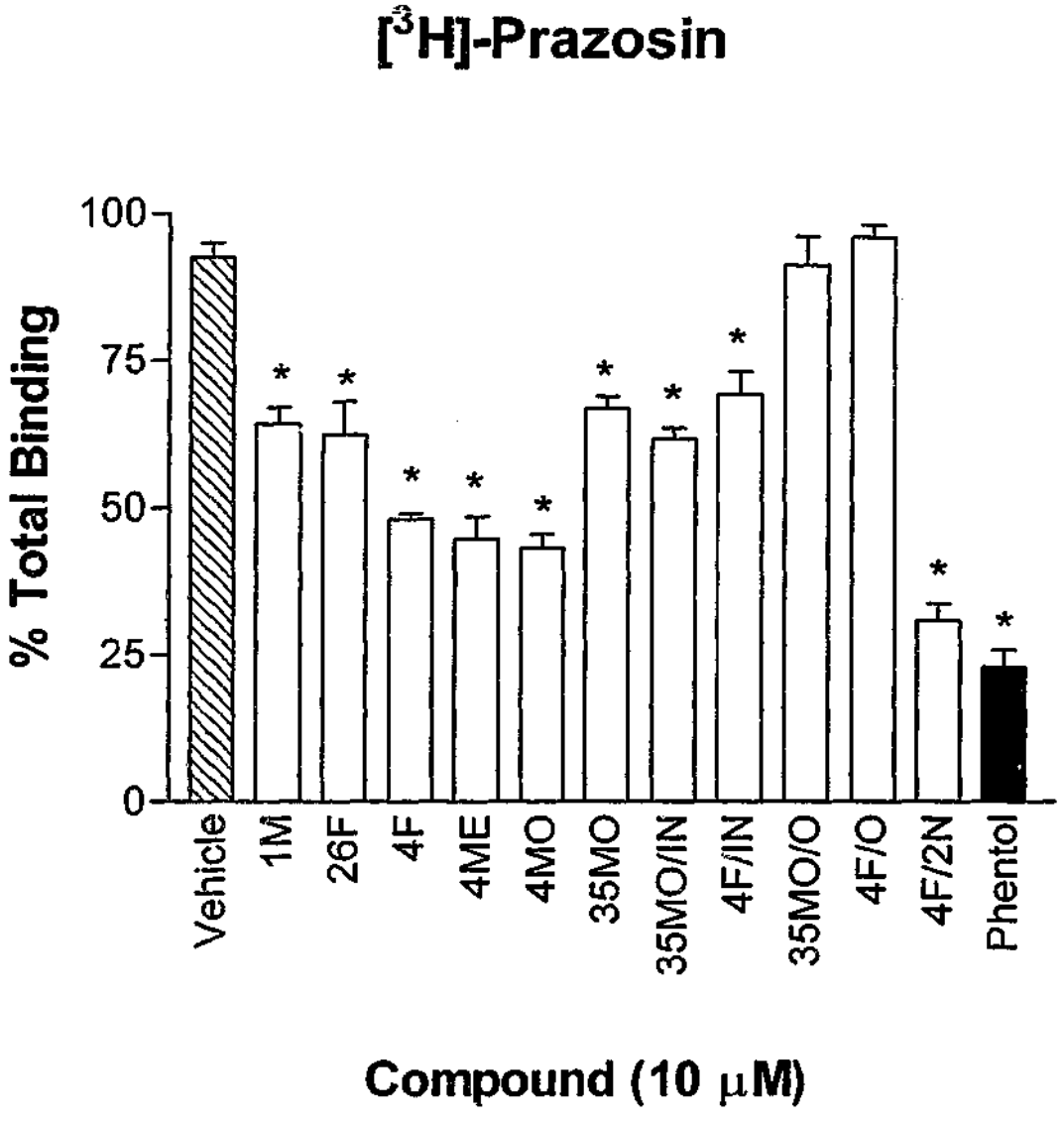

Figure 5.3 Histogram plot illustrating the total binding of [^{3}H]-prazosin, in the absence (vehicle) of treatment or in the presence of the IMID compounds or phentolamine, to rat cerebral cortex membranes. Results are expressed as a % of total binding. Error bars are ± S.E.M. and if not visible are contained within the symbol. * indicates a significant displacement by a treatment when compared to vehicle (n=4-12; P<0.05; one-way ANOVA with Bonferroni t-test).

total binding of [^{3}H]-prazosin in the presence of IMID-35MO/O (91 ± 5 %) and IMID-4F/O (96 ± 2 %) was not significantly different to the vehicle (ethanol, 92 ± 2 %; n=4-12; P>0.05; one way ANOVA). Phentolamine was used to define non-specific binding and significantly displaced [^{3}H]-prazosin binding to 23 ± 3 % of total binding (n=12; P<0.05; Students t-test) when compared to its vehicle.

For those compounds that significantly displaced binding, full concentration-displacement curves were performed for the IMID compounds (10 nM – 100 μM) and phentolamine (0.1 nM – 100 μM). The pK_D values for each compound, calculated using RADLIG, are summarised in Table 5.1. None of the IMID compounds (pK_D range, 5.99 – 5.34) that displaced binding were significantly different from each other (n=4; P>0.05; one way ANOVA), although, they were all significantly different from phentolamine (pK_D 7.73 ± 0.3; n=4-5; P<0.05; one way ANOVA with Bonferroni t-test). Figure 5.4 illustrates the full concentration-displacement curves of [^{3}H]-prazosin in the presence of IMID-4F/2N (10 nM – 100 μM) and phentolamine (0.1 nM – 100 μM). The displacement in the presence of IMID-4F/2N (pK_D 5.99 ± 0.2) was significantly different to phentolamine (pK_D 7.73 ± 0.3; n=4-5; P<0.05; Students t-test).

5.3.1.3 [^{3}H]-QNB binding

To examine the possibility of the IMID compounds having actions at muscarinic receptors the ability of the compounds to displace [^{3}H]-QNB binding to rat cerebral cortex membranes was assessed. A small number of the IMID compounds (10 μM) significantly displaced binding (Figure 5.5; n=4-6; P<0.05; one way ANOVA with Bonferroni t-test). The total binding of those compounds which displaced binding of [^{3}H]-QNB were, IMID-4ME (78 ± 7 %), IMID-4F/2N (81 ± 4 %) and IMID-1M (81 ± 5

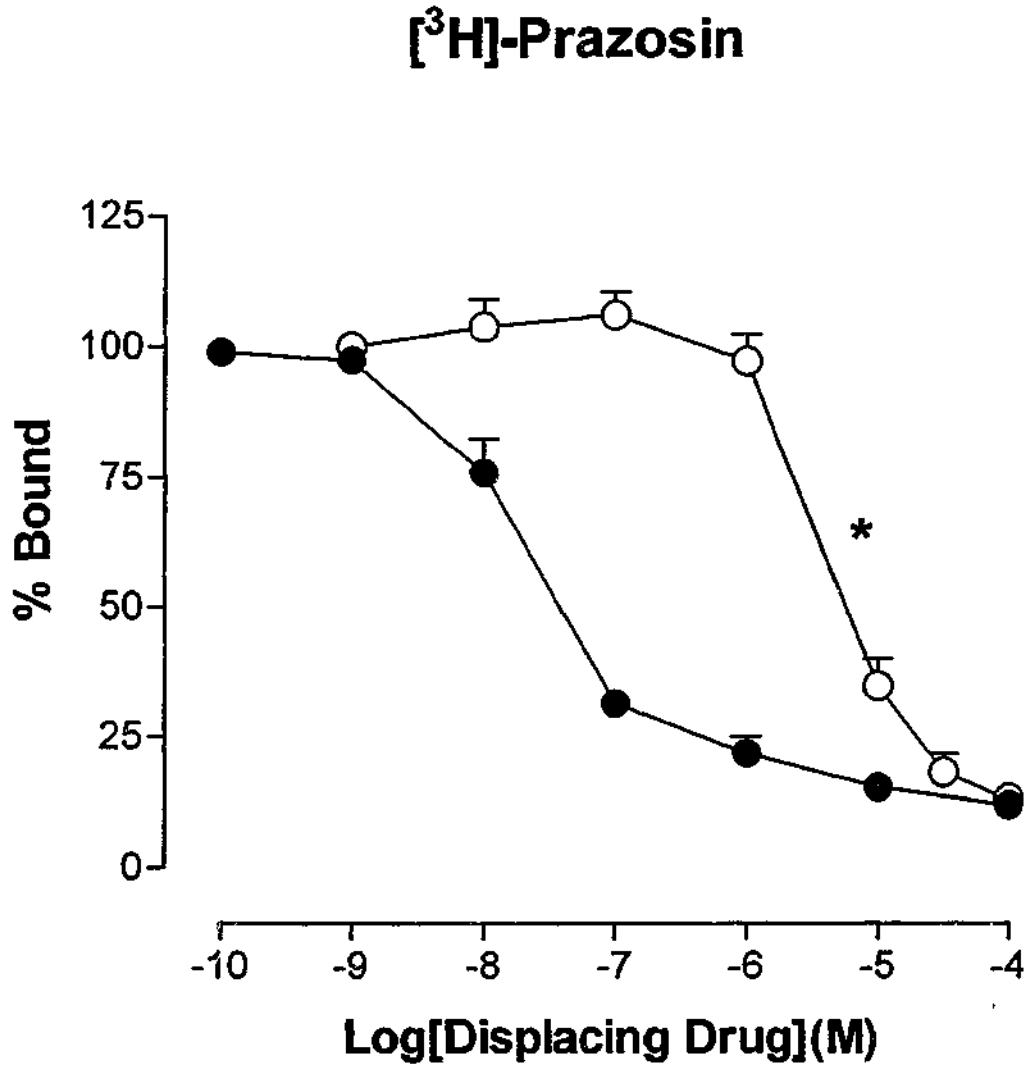

Figure 5.4 Mean displacement curve for [^{3}H]-prazosin in the presence of increasing concentrations of phentolamine (●) or IMID-4F/2N (○). Results are expressed as % bound. Error bars are ± S.E.M. and if not visible are contained within the symbol. * indicates a significant difference between treatments (n=4; P<0.05; students t-test).

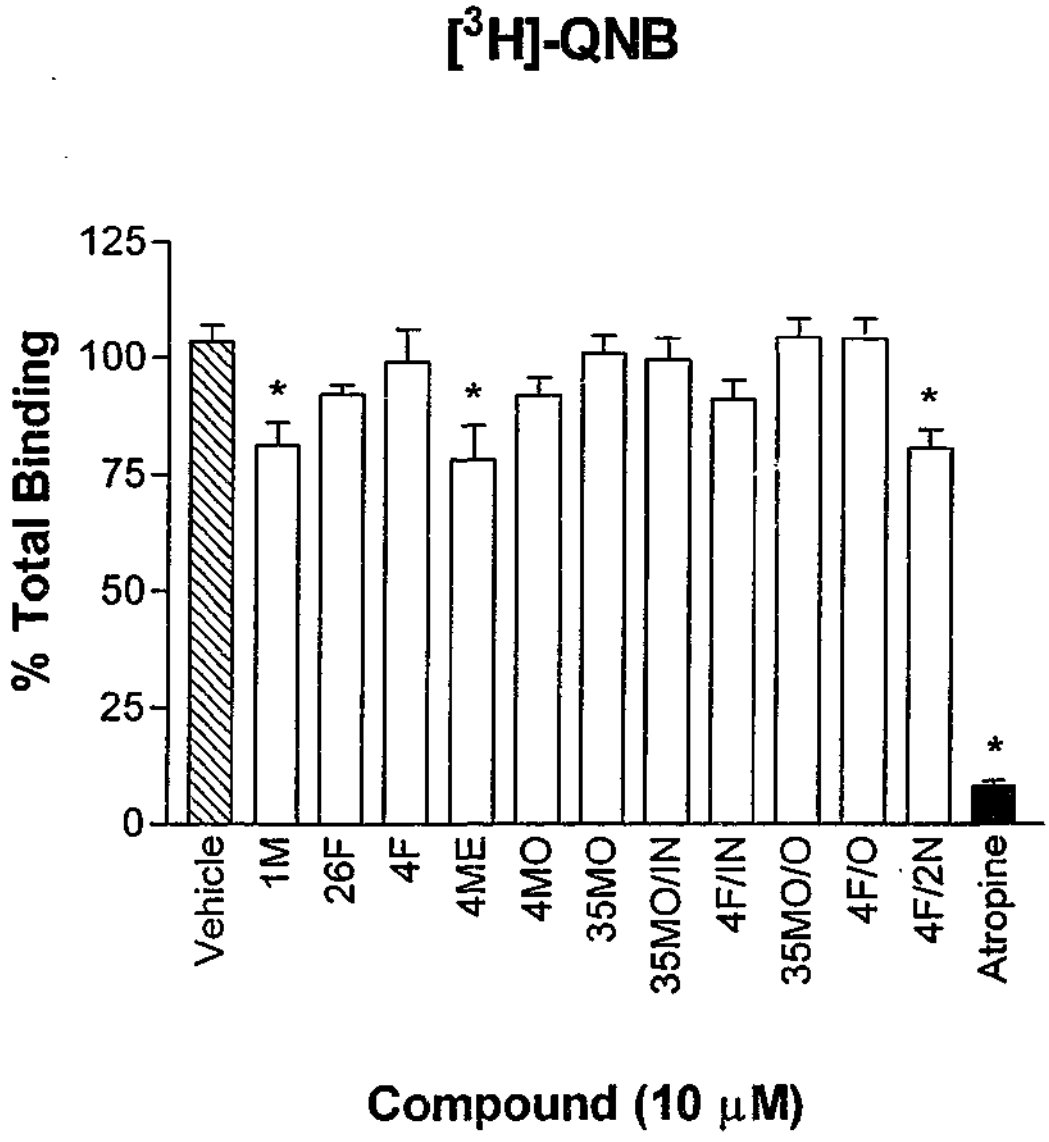

Figure 5.5 Histogram plot illustrating the total binding of [^{3}H]-QNB, in the absence of treatment (vehicle) or in the presence of the IMID compounds or atropine, to rat cerebral cortex membranes. Results are expressed as a % of total binding. Error bars are ± S.E.M. and if not visible are contained within the symbol. * indicates a significant displacement by a treatment when compared to vehicle (n=4-11; P<0.05; one-way ANOVA with Bonferroni t-test).

%). The remaining IMID compounds did not significantly displace binding when compared to their vehicle control (103 ± 4 %; n=4–11; P>0.05; one way ANOVA). As the compounds that did significantly displace binding did not do so to more than 75 % of total binding at the relatively high concentration of 10 μM, full concentration-displacement curves were not performed. Atropine was used to define non-specific binding and significantly displaced [^{3}H]-QNB binding to 8 ± 1 % of total binding (n=11; P<0.05; one way ANOVA with Bonferroni t-test) when compared to its vehicle.

5.3.1.4 [^{3}H]-Glibenclamide binding

In an effort to discover the site of action of the K_{ATP} channel antagonism of the IMID compounds, the ability of the compounds to displace binding of [^{3}H]-glibenclamide to rat cerebral cortex membranes was assessed. Binding of this radioligand is to the antagonist site of the sulphonylurea receptor, which is part of the K_{ATP} channel. None of the IMID compounds (10 μM), levcromakalim (10 μM) or the vehicle (ethanol) significantly displaced binding of [^{3}H]-glibenclamide (Figure 5.6; n=4; P>0.05; one way ANOVA). However, in the presence of unlabelled glibenclamide (10 μM), the drug used to define non-specific binding, [^{3}H]-glibenclamide binding was significantly displaced to 20 ± 3 % of total binding (n=4; P<0.05; one way ANOVA with Bonferroni t-test).

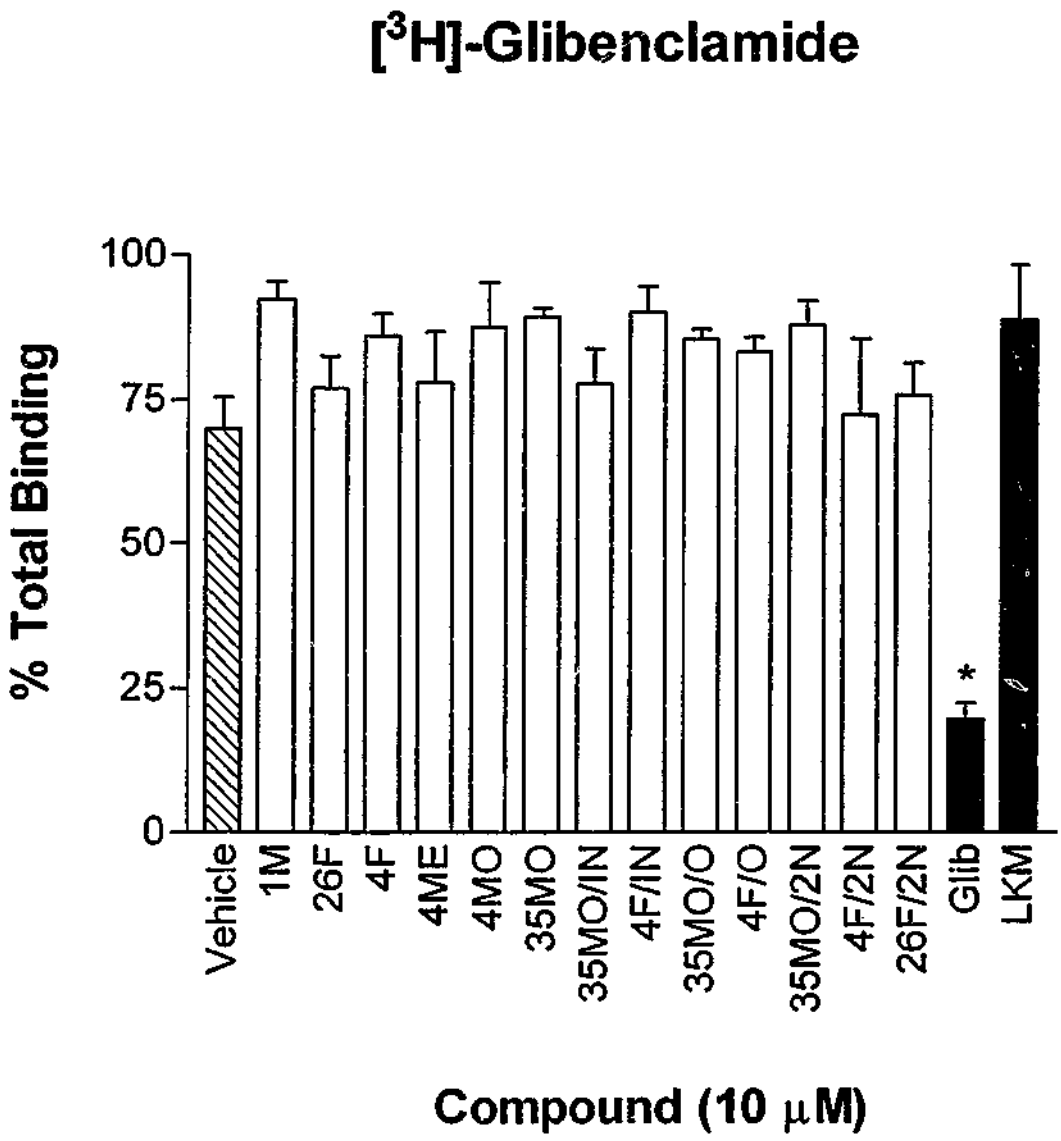

Figure 5.6 Histogram plot illustrating the total binding of [^{3}H]-glibenclamide, in the absence (vehicle) of treatment or in the presence of the IMID compounds, levcromakalim or glibenclamide, to rat cerebral cortex membranes. Results are expressed as a % of total binding. Error bars are ± S.E.M. and if not visible are contained within the symbol. * indicates a significant displacement by a treatment when compared to vehicle (n=4; P<0.05; one-way ANOVA with Bonferroni t-test).

5.3.1.5 [^{3}H]-P1075

These experiments were also performed in an attempt to determine the site of action of the IMID compounds for their K_{ATP} channel antagonism. The ability of the compounds to displace binding of the K_{ATP} channel opener, [^{3}H]-P1075, to bovine smooth muscle cells was evaluated. Two of the IMID compounds significantly displaced binding when compared to vehicle control (Figure 5.7, n=4; P<0.05; one way ANOVA with Bonferroni t-test). They were IMID-4F/2N and IMID-26F/2N, which displaced binding of [^{3}H]-P1075 to 83 ± 6 % and 76 ± 6 % of total binding, respectively. As they both did not displace binding of the radioligand to more than 75 % of total binding, further concentration-displacement studies were not performed. The drugs used to define non-specific binding, levcromakalim (56 ± 3 %) and glibenclamide (64 ± 1 %), both significantly displaced binding of [^{3}H]-P1075 when compared to their vehicle but were not significantly different from one another (n=4; P<0.05; one way ANOVA with Bonferroni t-test).

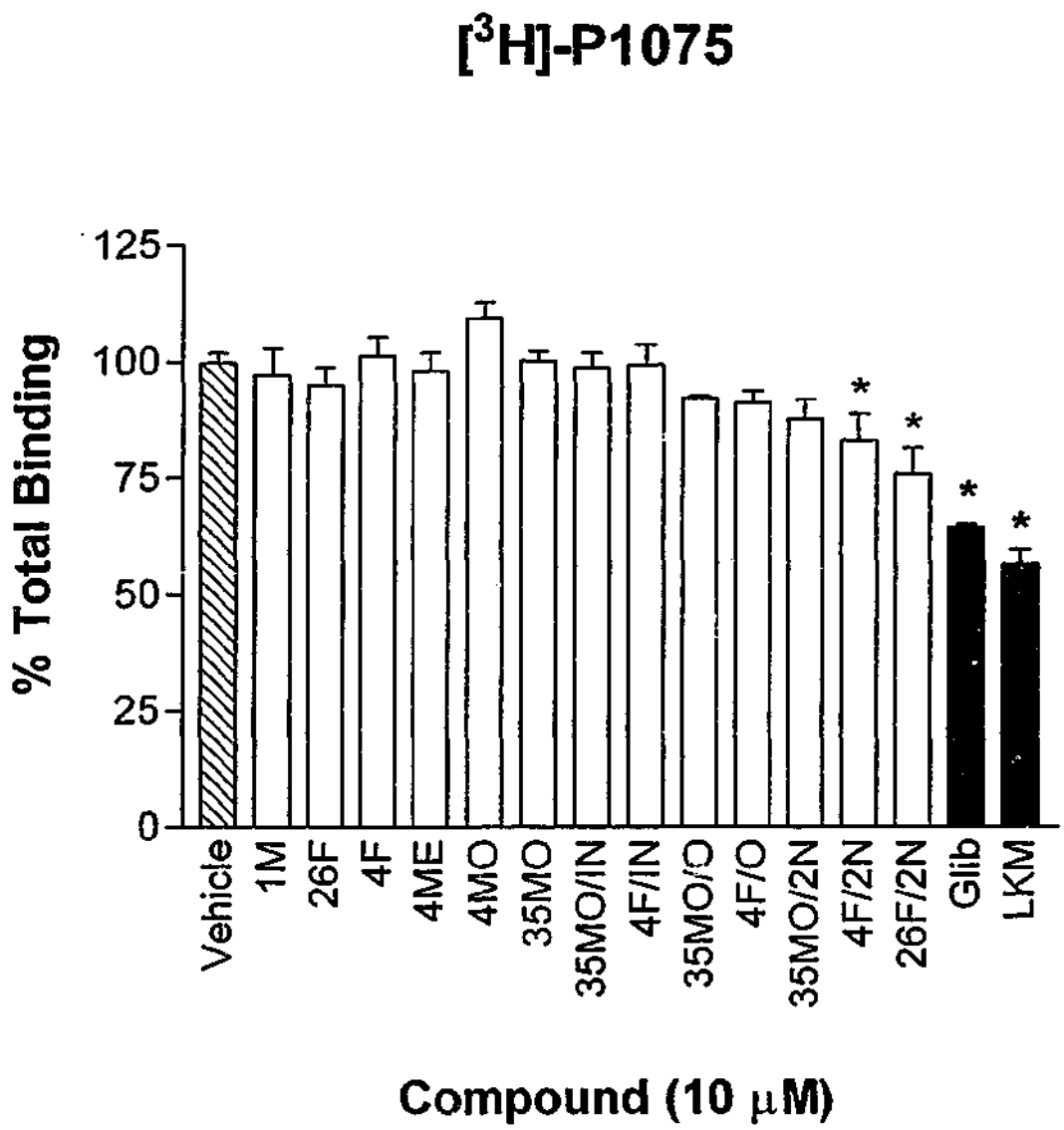

Figure 5.7 Histogram plot illustrating the total binding of [^{3}H]-P1075, in the absence (vehicle) of treatment or in the presence of the IMID compounds, levcromakalim or glibenclamide, to bovine smooth muscle membranes. Results are expressed as a % of total binding. Error bars are ± S.E.M. and if not visible are contained within the symbol. * indicates a significant displacement by a treatment when compared to vehicle (n=4; P<0.05; one-way ANOVA with Bonferroni t-test).

5.4 Discussion

Thus far, together with the ability of the IMID compounds to antagonise K_{ATP} channels, several of the imidazoline analogues have been shown to act at L-type calcium channels and cause bradycardia. However, the concentrations of the IMID compounds required to produce antagonism of calcium channels and to cause bradycardia are much higher (10 μM) than is required to antagonise K_{ATP} channels (0.1 μM). This series of experiments was performed to assess the activity of the IMID compounds at other receptors commonly acted upon by imidazolines, in particular, α_1-, α_2-adrenoceptors and muscarinic receptors. In addition, the possible site of action at K_{ATP} channels was also investigated.

5.4.1 α_1- & α_2-adrenoceptors

Several of the imidazoline analogues possessed activity at both α_1 and α_2-adrenoceptors as evidenced by their ability to displace [^{3}H]-prazosin and [^{3}H]-rauwolscine binding to rat cerebral cortex membranes. Historically, imidazolines and imidazolidines have been well recognised for their actions at α_1- and α_2-adrenoceptors (Kobinger & Pichler, 1980). In fact, clonidine and analogues of clonidine were used significantly in the investigation of α-adrenoceptors and their sub-classification (Docherty & McGrath, 1980; Ruffolo *et al.*, 1980a). This was dependent on the use of analogues with selectivity between the subtypes and selective antagonists such as rauwolscine (α_2) and prasozin (α_1). It is noted however, that a limitation with the use of imidazolines is that selectivity is not guaranteed. For example, the imidazoline, phentolamine is a non-selective α_1- and α_2-adrenoceptor antagonist. Another example

is the imidazoline UK-14304, that was thought to be for many years selective for α_2-adrenoceptors (Cambridge, 1981). However, subsequent studies have shown it to be a partial agonist at α_1-adrenoceptors, possessing both agonist and antagonist properties, albeit at much higher concentrations than that required for its α_2-adrenoceptor agonist effects (Beckeringh *et al.*, 1984).

When applied to the results presented in this Chapter, it is not surprising that the IMID compounds that have α_2-adrenoceptor activity also possess α_1-adrenoceptor activity. None of the pK_D values calculated for the α_1- and α_2-adrenoceptor activity of the IMID compounds that were active are significantly different from each other, in other words they exhibit equal potency at α_1- and α_2-adrenoceptors. However, they are significantly less potent than phentolamine. More importantly, for the IMID compounds that have activity at both adrenoceptors the pK_D values are almost 100 fold greater than the pK_B values for their antagonism of levcromakalim-induced relaxation.

It should also be noted that although the compounds have been shown to have affinity for these receptors they might not possess equal efficacy. In fact, a study by Ruffolo and coworkers (1979) found that although some imidazolines have a high affinity for α_2-adrenoceptors this is not reflected in efficacy, with low levels of efficacy reported for many imidazolines.

Numerous studies assessing structural modifications of imidazoline analogues and their resulting actions at α-adrenoceptors have been conducted. Although these studies aim to find analogues with high affinity and efficacy for one particular subtype we can use them to try and minimise α-adrenoceptor activity in our search for a potent and selective K_{ATP} channel antagonist.

Firstly, a study by Ruffolo and colleagues (1980b) found the α-adrenoceptor activity of tolazoline derivatives was dependent upon the carbon atom between the phenyl and imidazoline rings. Substitutions of more than one carbon atom or deleting it altogether resulted in reduced affinity. In addition, it was found that the α-adrenoceptor selectiveness of clonidine was not affected by substituting the nitrogen bridge for a methylene bridge (Ruffolo *et al.*, 1982). An added finding was that different dimethoxy substitutions of the phenyl ring of tolazoline considerably changed the selectivity for the α-adrenoceptor (Ruffolo & Messick, 1985). For example, 2,5- and 2,3-dimethoxytolazoline are potent and selective α_1-adrenoceptor agonists and α_2-adrenoceptor agonists, respectively. *Para* substitutions of the phenyl ring of clonidine with alkylating groups was found to prolong α-adrenoceptor activity yet, increasing the length of these substitutions decreased affinity for the receptors (Leclerc *et al.*, 1980; Decker *et al.*, 1983).

When substitutions of the imidazoline ring were investigated, methyl and benzyl substitutions, particularly those on the nitrogen atom, resulted in compounds with less α-agonist activity (Miller *et al.*, 1983). Furthermore, once the imidazoline ring was opened there was also reduced affinity for α-adrenoceptors (Hamada *et al.*, 1985). In relation to the work presented in this thesis, it was found that the imidazoline analogues with substitutions at the imidazoline ring, IMID-4F/IN and IMID-35MO/IN, had reduced activity as K_{ATP} channel antagonists (Chapter 3; Table 3.1). Therefore, substitutions of the imidazoline ring may not just affect α-activity but also K_{ATP} channel antagonist activity.

Finally, substitutions of the bridging nitrogen of imidazolidines produced compounds with reduced α_2-adrenoceptor activity (Bechtel *et al.*, 1985). Studies in our

laboratory have also produced comparable results, where alinidine and analogues of alinidine were found to have pK_D values of around 5 (Challinor-Rogers, 1995). As the majority of the compounds assessed in the experiments presented in this Chapter also had substitutions at the bridging nitrogen it is not surprising that the IMID compounds had similar pK_D values for both α-adrenoceptors.

5.4.2 Muscarinic receptors

It has been shown that atropine does not block the well known bradycardic effect of the imidazolidine, alinidine, indicating that this effect is not due to agonist actions at muscarinic receptors (Kobinger *et al.*, 1979). However, in numerous subsequent studies alinidine has been shown to possess some antimuscarinic actions. Opthof and coworkers (1986) found that alinidine decreased the chronotropic effects of ACh and adrenaline. A study by Ogiwara and colleagues (1987) found alinidine had suppressive effects on the chronotropic and inotropic responses of both exogenous choline esters and endogenous ACh released from parasympathetic nerve terminals in the dog heart. In addition, studies in rat atria found an antimuscarinic effect of alinidine, which reversed the descending staircase resulting from the release of ACh (Lang & Walland, 1989). Not only is this true for studies in the heart but also in the vasculature where alinidine was shown to attenuate ACh-induced relaxation in dog coronary arteries (Nakane *et al.*, 1991). Radioligand-binding studies performed in our laboratory under identical conditions to the present studies, assessing instead, analogues of alinidine (TH series; see Section 1.4.2.3.5), also identified several analogues with weak actions at muscarinic receptors (Challinor-Rogers, 1995).

To determine if the imidazoline analogues also interacted with muscarinic receptors, their ability to displace [^{3}H]-QNB binding to rat cerebral cortex membranes was evaluated. A small number of the IMID compounds, IMID-1M, IMID-4ME and IMID-4F/2N significantly displaced binding. However, since they did not displace total binding of [^{3}H]-QNB binding by more than 25 %, additional studies to determine pK_D values were not performed. These results indicate that, at a high concentration (10 μM), these 3 imidazoline analogues have very weak actions at muscarinic receptors. Considering the evidence presented above it is most likely to be antimuscarinic. However, as with the actions of the imidazolines at α-adrenoceptors, the concentrations of the compounds required to produce muscarinic actions is much higher than that required to produce K_{ATP} channel antagonism.

5.4.3 K_{ATP} channels

Additional studies were also carried out in an attempt to discover the site of action of the IMID compounds at K_{ATP} channels. Initially, the ability of the IMID compounds to displace binding to the antagonist site of the SUR was assessed utilising [^{3}H]-glibenclamide binding to rat cerebral cortex membranes. In a range of tissues including rat cerebral cortex membranes, two [^{3}H]-glibenclamide binding sites have been identified, a high affinity site in the nM range and a low affinity site in the μM range (Gopalakrishnan *et al.*, 1991; Zini *et al.*, 1991; Niki & Ashcroft, 1993). In this study, the experimental conditions were optimal to assess binding to the high affinity [^{3}H]-glibenclamide binding site. In binding studies utilising rat isolated aortic rings, the high affinity component of [^{3}H]-glibenclamide binding was found to represent the SUR as both sulphonylureas and K_{ATP} channel openers displaced binding at potencies similar

to those from functional assays (Löffler & Quast, 1997). It also provided further evidence that binding sites for the openers and antagonists (sulphonylureas) are negatively allosterically coupled. As none of the IMID compounds significantly displaced binding they do not appear to antagonise K_{ATP} channels through an interaction with the antagonist site of the SUR.

Subsequently, studies were performed to assess the possibility that the IMID compounds were interacting with the opener site of the SUR. This was achieved by assessing the ability of the IMID compounds to displace binding of [^{3}H]-P1075 to bovine smooth muscle cells. Only two of the IMID compounds significantly inhibited binding of [^{3}H]-P1075 to the SUR of K_{ATP} channels together with levcromakalim and glibenclamide. They were IMID-4F/2N and IMID-26F/2N, the two most potent K_{ATP} channel antagonists identified in the *in vitro* studies using pig isolated coronary arteries. The results from this study do not present clear evidence for a sole mechanism of action of the IMID compounds. If an interaction with the opener site of the SUR was the only mechanism of action it would be expected that more of the IMID compounds would displace binding of [^{3}H]-P1075 at the 10 μM concentration used in this study. This is a concentration approximately 100 fold higher than that required to block K_{ATP} channels in the *in vitro* studies. Instead, it is more likely that IMID-4F/2N and IMID-26F/2N have additional properties at higher concentrations. This may be a physical effect, possibly due to their larger molecule size in comparison to the remaining imidazoline analogues tested. These additional properties may also contribute to their slightly increased potency as K_{ATP} channel antagonists. Therefore, if this is true these studies indicate that that the IMID compounds act predominantly at a different site to levcromakalim and glibenclamide.

Imidazolidines can be positively charged at physiological pH (McPherson & Piekarska, 1994) and it is possible that the IMID compounds may affect K_{ATP} channel opening through an interaction with the channel pore, a mechanism similar to that utilised by the lipophilic quaternary ions. As already discussed in Section 1.4.2.3, quaternary ions, due to their lipophilic nature can pass through cellular membranes and interfere with membrane-bound proteins and therefore have the potential to 'plug' the K_{ATP} channel pore (Gros *et al.*, 1992; Saito *et al.*, 1992). Again, as previously discussed in Section 1.4.2.2.5 a recent study by Proks and Ashcroft (1997) utilising a C-terminally truncated form of $K_{IR}6.2$ in *Xenopus* oocytes found that phentolamine inhibited K_{ATP} currents in a voltage independent manner. This was evidence that the site where phentolamine inhibits the K_{ATP} channel resides on $K_{IR}6.2$. This study was supported by a study in HEK293 cells transfected with cDNA encoding to $K_{IR}6.2\Delta C36$ where identical results were obtained suggesting that it is indeed $K_{IR}6.2$ that phentolamine is inhibiting and not an endogenous protein in *Xenopus* oocytes (Tucker *et al.*, 1997). This is also true for other imidazolines as the antiarrhythmic, cibenzoline, inhibits K_{ATP} channels by binding to $K_{IR}6.2$ (Mukai *et al.*, 1998). Considering this evidence, it is possible that the IMID compounds are also acting in a similar manner, to 'plug' the K_{IR} subunit of the K_{ATP} channel.

5.4.4 Conclusions

In summary, of the imidazoline analogues assessed in this study, several were found have activity at muscarinic, α_1- and α_2-adrenoceptors. However, this study did not provide us with evidence of whether the compounds act as antagonists or agonists of these receptors. The most important finding though, is that they were active over a 100

fold higher concentration range than that for K_{ATP} channel antagonism. Therefore, although these compounds may not be specific they have the potential to be selective as antagonists of the K_{ATP} channel.

In addition, the IMID compounds appear to regulate K_{ATP} channels by a mechanism other than that utilised by levcromakalim and glibenclamide. It is possible and more than likely that they act by interacting directly with the channel pore. It was also found that 2 of the imidazoline analogues had a small affinity for the opener site of the SUR. It is yet to be determined whether this effect is a physical effect due to the size of the molecule or an additional effect that may increase their ability to antagonise K_{ATP} channels.

CHAPTER SIX

IN VIVO CHARACTERISATION OF THE NOVEL IMIDAZOLINE ANALOGUES IN THE ANAESTHETISED RAT

6.1 Introduction

In Chapter 3 it was demonstrated that many of the imidazoline analogues were potent antagonists of K_{ATP} channels, at least in the vasculature. In order to further our studies we have examined their effects on other cardiovascular parameters including blood pressure and heart rate. This will provide important information pertaining to their selectivity and possible clinical relevance.

As discussed previously, K_{ATP} channels are found in many tissues in addition to vascular smooth muscle, such as non-vascular smooth muscle, cardiac and pancreatic tissues. In the β-islet cells of the pancreas, they play a vital role in the regulation of insulin secretion (see Section 1.3.1). Pancreatic β-cell K_{ATP} channels have been shown to be sensitive to a wide variety of agents such as sulphonylureas, K^+ channel openers and, most importantly, imidazolines (see Section 1.4.2.2.2).

Due to their potent antagonist activity at vascular K_{ATP} channels, it was important to determine if these compounds also interacted with pancreatic K_{ATP} channels. Therefore, in this series of experiments, the actions of the IMID compounds at pancreatic K_{ATP} channels were investigated. This action was investigated in two ways. First by assessing the effect of the imidazoline derivatives on blood glucose levels. Secondly, the action of the IMID compounds on plasma insulin levels was also determined.

6.2 Materials and Methods

6.2.1 Anaesthetised rat preparation

Male Sprague-Dawley rats (250–400 g) were fasted overnight and on the day of the experiment were anaesthetised with sodium pentobarbitone (60–100 mg/kg i.p.). A midline incision was made in the cervical region and tracheal, jugular and carotid cannulae inserted (Figure 6.1). A tracheal cannula was inserted in the event that artificial respiration was required. Drugs were administered through the jugular cannula and flushed through with 0.2 ml of 0.9 % saline. The carotid cannula, containing heparinised saline (25 IU/ml/saline) was attached to a pressure transducer for the recording of pulsatile arterial blood pressure and heart rate. These parameters were calculated using an online data acquisition system (CVMS Version 2.0, World Precision Instruments, USA) that also displayed the recordings on a Panasonic printer (Model KX-P3200 Forms Printer). Blood pressure was recorded as mean arterial pressure (MAP), the average of systolic and diastolic blood pressure. Body temperature was monitored via a rectal thermometer and maintained at 37 °C by a heated table and overhead lamp. Anaesthesia was assessed using the paw pinch method and maintained throughout the experiments by the administration of additional anaesthetic (10 mg/kg i.v.) when required. An incision was made in the femoral region and a cannula inserted in the femoral artery to allow blood sampling for the determination of blood glucose and insulin levels.

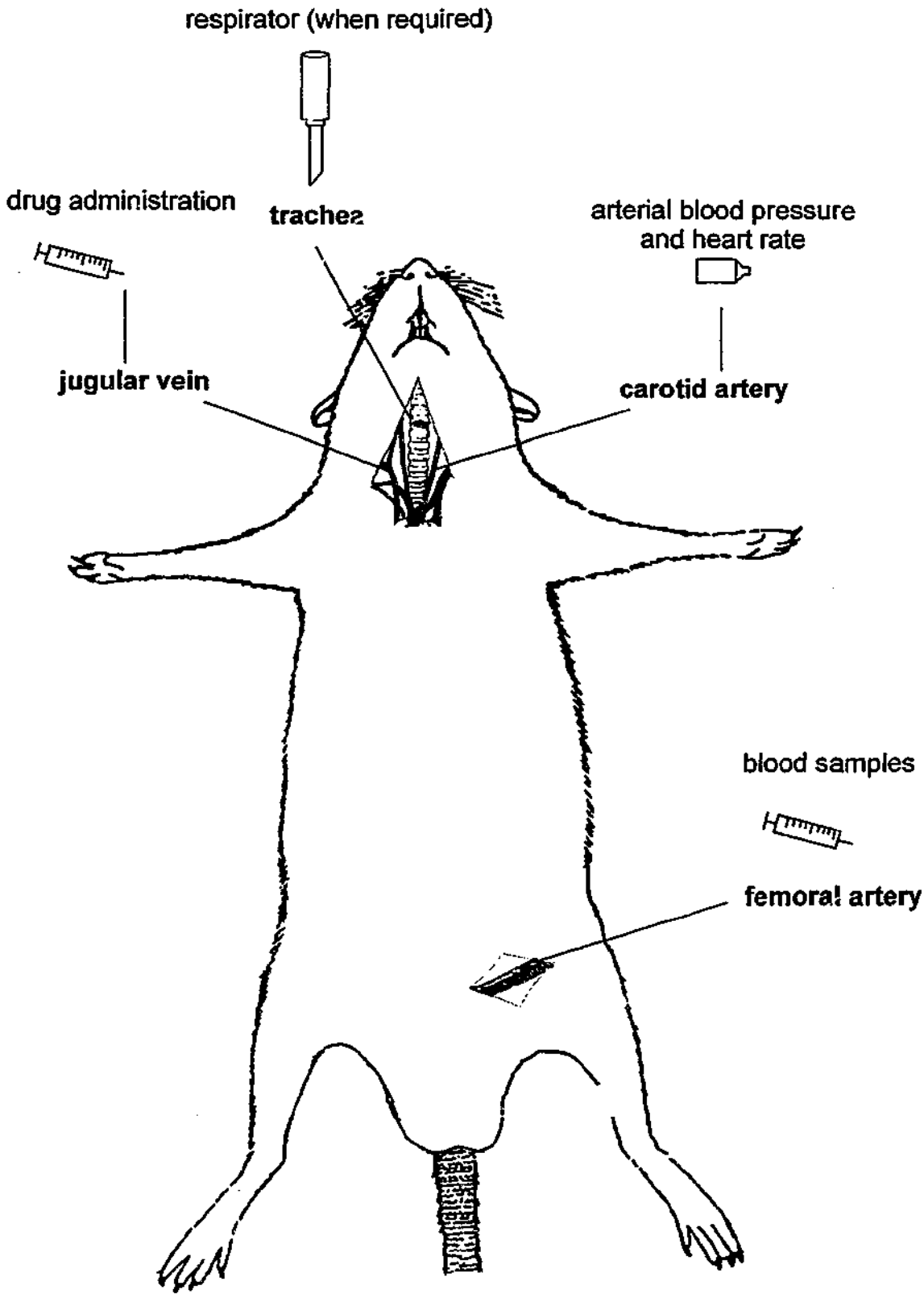

Figure 6.1 Schematic representation of the anaesthetised rat preparation

6.2.1.1 Blood glucose

Blood glucose was determined using the commercially available Ames Glucometer 3 (Bayer, USA). The reagent test pads of the Glucofilm strips were covered with small samples of blood taken from the femoral artery cannula. The test strips specifically measure glucose (1.1-27.7 mmol/L) levels in whole blood. This method is enzyme based, and relies on glucose oxidase catalysing the conversion of glucose to gluconic acid and hydrogen peroxide. The tetramethylbenzidine in the strips is oxidised by the hydrogen peroxide in the presence of glucose peroxidase. This in turn turns the test pad blue, dependent upon the initial amount of glucose. The colour is analysed photometrically to determine the glucose concentration.

6.2.1.2 Insulin Radioimmunoasssay (RIA)

The following assay was performed by Mr Ray Spark from the Department of Biochemistry, Monash University.

Samples of blood (500 µl) were taken from the femoral artery cannula into 1 ml eppendorf tubes containing 5 IU/ml of heparin. Tubes were immediately centrifuged (5,000 rpm for 5 min at 4 °C) using an Eppendorf 5415 C centrifuge and the supernatant (blood plasma; ~ 200 µl) pipetted into an eppendorf tube using disposable glass micropipettes. Samples were then frozen (-80 °C) until required.

Insulin levels were determined using a Sensitive Rat Insulin Radioimmunoassay (RIA) kit (Linco Research Inc., USA). This assay utilises [^{125}I]-Insulin and a rat insulin antiserum to determine the level of rat insulin in plasma by the double antibody/PEG technique (Morgan & Lazarow, 1963). The assay was conducted over 3 days using the

protocol illustrated in Table 6.1. The plasma samples (50 µL) were diluted 1:5 in assay buffer (composition in M: Phosphosaline 0.05, EDTA 0.025, Sodium Azide (0.08 %), RIA grade BSA (0.1 %); pH 7.4).

On the first day, 100 µl aliquots of the standards (known insulin concentrations), quality controls and plasma were incubated with the assay buffer and the Sensitive Rat Insulin antibody (guinea pig anti rat insulin serum in assay buffer) in borosilicate glass tubes (12 x 75 mm). The tubes were vortexed, covered and incubated overnight (20 hours) at 4 °C. On the second day, 100 µl of [^{125}I]-Insulin was added to all tubes, which were again, vortexed, covered and incubated overnight at 4 °C. On the third day, 1 ml of cold (4 °C) precipitating agent (composition: Goat anti guinea pig IgG serum, PEG 3 %, Triton X-100 in 0.05 M Phosphosaline, EDTA 0.025 M and Sodium Azide 0.08 %) was added to all tubes except for the total counts tube. The tubes were vortexed, covered and incubated for 20 minutes at 4 °C, followed by 20 minutes of centrifugation at 3,000 x g at 4 °C. The supernatant was aspirated and all the tubes drained for 60 seconds (except total counts tube). The tubes were counted for ^{125}I using a Packard minaxi 5530 γ-counter (Packard, USA). The disintergrations per minute (dpm) were counted for 1 minute.

The conversion of the counts (dpm) for the plasma samples to insulin levels in ng/ml was performed using the automated data reduction procedures of the γ-counter. This method involved constructing a standard curve using known insulin standards (0.02-1.0 ng/ml) to generate a plot of dpm vs ng/ml. The unknown insulin sample values were extrapolated from this standard curve. Normal fasted rats have insulin levels between 0.5-2 ng/ml and when baseline values were above or below these levels the experiment was not included.

Day 1					Day 2		Day 3		
	Step 1	Step 2-3	Step 4	Step 5	Step 6	Step 7	Step 8	Step 9	Step 10-12
Tube	Assay Buffer	Standard/QC sample	Sensitive Rat Insulin Antibody	Vortex, cover and incubate (20 hrs at 4°C)	[^{125}I]-Insulin	Vortex, cover and incubate (20 hrs at 4°C)	Precipitating agent	Vortex and incubate (20 min at 4°C)	Centrifuge, aspirate and count pellets
1	--	--			100 µl		--		
2	300 µl	--			100 µl		1 ml		
3	200 µl	--	100 µl		100 µl		1 ml		
4	100 µl	100 µl of 0.02 ng/ml	100 µl		100 µl		1 ml		
5	100 µl	100 µl of 0.05 ng/ml	100 µl		100 µl		1 ml		
6	100 µl	100 µl of 0.1 ng/ml	100 µl		100 µl		1 ml		
7	100 µl	100 µl of 0.2 ng/ml	100 µl		100 µl		1 ml		
8	100 µl	100 µl of 0.5 ng/ml	100 µl		100 µl		1 ml		
9	100 µl	100 µl of 1.0 ng/ml	100 µl		100 µl		1 ml		
10	100 µl	100 µl of QC 1	100 µl		100 µl		1 ml		
11	100 µl	100 µl of QC 2	100 µl		100 µl		1 ml		
12,13	100 µl	100 µl of plasma	100 µl		100 µl		1 ml		
14-n	100 µl	100 µl of plasma	100 µl		100 µl		1 ml		

Table 6.1 Protocol for sensitive rat insulin radioimmunoassay (RIA) kit (Linco Research Inc., USA).
QC = quality control

6.2.2 Experimental protocol and Analysis of Results

Initially, *in vivo* experiments were conducted in which cumulative dose-response curves to all the imidazoline analogues were constructed in order to assess their acute effects upon MAP and heart rate. In addition, for some of the most promising derivatives (IMID-4F, IMID-26F, IMID-1M, IMID-4F/2N and IMID-35MO; Chapter 3), the time dependent effects following bolus additions (10 μmol/kg) on MAP, heart rate, blood glucose and insulin levels were assessed over four hours. The time dependent effects of the remaining imidazoline analogues were assessed over one hour.

6.2.2.1 Acute effects of the imidazolines on MAP and heart rate

Blood pressure and heart rate were allowed to stabilise for approximately 15 minutes before cumulative dose-response curves to all the imidazoline derivatives (0.1–10 μmol/kg) were constructed. MAP and heart rate recordings were taken once the response to each dose had reached a plateau. Insulin and blood glucose levels could not be assayed acutely due to the rapidity of the responses and the need for too many blood samples. Increasing volumes of vehicle (20 % EtOH) were administered as a control.

Baseline measurements of MAP and heart rate were recorded prior to administration of the imidazoline analogues and taken as 100 %. All subsequent values are expressed as a % of initial baseline values.

6.2.2.2 Time dependent effects of the imidazolines on MAP, heart rate, blood glucose and insulin

6.2.2.2.1 Four hour study

These experiments were performed to assess the time dependent effects of several of the most potent imidazoline analogues in terms of K_{ATP} channel antagonism, on blood pressure, heart rate, blood glucose and insulin over a four hour period in fasted rats. For comparative purposes, the effects of a bolus dose of glibenclamide (1 μmol/kg) and clonidine (1 μmol/kg) on blood pressure, heart rate, blood glucose and insulin were examined. Glibenclamide was used to compare the effects of the IMID compounds to a known K_{ATP} channel antagonist. Given the imidazoline derivatives were derived from clonidine, it was also used as a comparison. A single dose (10 μmol/kg) of the imidazoline analogues, IMID-4F, IMID-1M, IMID-26F, IMID-4F/2N and IMID-35MO was assessed over a four hour period. The response to the vehicle (20 % EtOH) for the imidazoline analogues over four hours was also examined.

Baseline measurements of MAP, heart rate, blood glucose and insulin were taken 15 and 10 minutes prior to the addition of the drugs and averaged. These baseline values were represented graphically as time 0, as they were taken to represent the parameters immediately prior to drug administration. Measurements of MAP and heart rate were recorded immediately after the addition of the drug (30 seconds) and MAP, heart rate and blood glucose at 15, 30, 45, 60, 90, 180 and 240 minutes. Only limited blood samples could be taken to ensure no adverse effects on haemodynamics. Consequently, insulin measurements were taken 5 and 60 minutes after drug administration.

In some experiments rauwolscine (25 μmol/kg), at a dose previously shown to effectively antagonise α_2-adrenoceptors in anaesthetised rats (DiTullio *et al.*, 1984) and to have no significant effect alone on insulin secretion (Schulz & Hasselblatt, 1988), was used. Rauwolscine was administered 30 minutes prior to the administration of either clonidine or the imidazoline analogues.

The initial baseline recordings of MAP and heart rate were taken as 100 % and all subsequent values expressed as a % of the initial baseline values. Values are represented graphically over time. For measurements of blood glucose and insulin levels, a graph of blood glucose (% of the initial baseline values) or insulin (ng/ml) versus time was generated.

6.2.2.2.2 One hour study

The effects of a bolus administration (10 μmol/kg) of the remaining imidazoline analogues, IMID-4ME, IMID-4MO, IMID-35MO/IN, IMID-4F/IN, IMID-35MO/O, IMID-4F/O, IMID-35MO/2N and IMID-26F/2N, on blood pressure, heart rate, blood glucose and insulin levels were assessed over one hour.

Control measurements of MAP, heart rate, blood glucose and insulin were taken 15 minutes prior to the addition of drugs. Measurements of MAP, heart rate and blood glucose were taken 30 and 60 minutes after the administration of the imidazoline derivatives. Insulin measurements were taken at 5 and 60 minutes after drug administration.

The initial control recordings for MAP, heart rate and blood glucose were taken as 100 % and all subsequent values expressed as % of initial baseline values. Insulin measurements are expressed in ng/ml. All data are presented in tabular form.

6.2.2.3 Statistics

Results in the text are given as mean ± S.E.M. Statistical tests used are stated in the text. In general, all treatments were compared with a two way RM ANOVA with a Bonferroni *t*-test used post ANOVA when a significant difference in the treatments was observed. A one way RM ANOVA with a Bonferroni *t*-test used post ANOVA was performed to indicate a significant difference from the initial 'within animal' control value (0 min). In all instances when a maximum value is cited, significance was determined via a one way RM ANOVA. Groups were considered significantly different from each other if $P<0.05$, unless otherwise stated. All statistical calculations were performed using SigmaStat (Jandel Scientific, USA).

6.2.3 Drugs

Drugs used and their sources were: clonidine (Sigma Chemical Co., U.S.A.); glibenclamide (Sigma Chemical Co., U.S.A.); IMID compounds (Eva Campi, Department of Chemistry, Monash University, Figure 2.1) and rauwolscine (Carl Roth KG, Germany). Clonidine and glibenclamide were dissolved in 100% ethanol as stock solutions of 10 mM and further dilutions were made in saline. The imidazoline analogues were dissolved in 100% ethanol as stock solutions of 50 mM and further dilutions were made in saline. Rauwolscine was dissolved in saline as a stock solution of 10 mM.

The radioligand and its specific activity and source were: [^{125}I]-Insulin (specific activity: 367 μCi/μg; Linco, U.S.A.). The lyophilised powder was hydrated with Label Hydrating Buffer containing Normal Guinea Pig IgG as its carrier.

6.3 Results

6.3.1 Acute effects of the imidazolines on heart rate and MAP

The effect of the IMID compounds on MAP and heart rate was assessed in anaesthetised rats. Cumulative dose-response curves to the IMID compounds (0.1–10 μmol/kg) were constructed. An original trace of the effect of IMID-1M (0.1–10 μmol/kg) on MAP and heart rate is illustrated in Figure 6.2. As the majority of the compounds only had effects at higher doses and no maximums were reached, the potencies of these analogues were assessed by examining the reduction in MAP and heart rate at the highest dose (10 μmol/kg). The control values of MAP and heart rate before the administration of the IMID compounds was 105 ± 3 mmHg (n=56) and 374 ± 7 bpm (n=56), respectively. Increasing concentrations of the vehicle (20 % EtOH) had no significant effect on MAP or heart rate (data not shown).

6.3.1.2 Effects on MAP

Table 6.2 summarises the effects of all the compounds examined on MAP. Figure 6.3a shows graphically the effect of three of these IMID compounds (IMID-35MO/O, IMID-4F and IMID-26F/2N), representing the least to the most potent of the imidazoline analogues upon MAP. A number of the IMID compounds caused significant dose-dependent reductions in MAP (n=4; P<0.05; one way RM ANOVA with Bonferroni t-test). The most potent of these compounds IMID-26F/2N, IMID-35MO/2N, IMID-35MO, IMID-4MO, IMID-26F and IMID-4F, caused significantly greater reductions at 10 μmol/kg than any of the remaining compounds examined

(a)

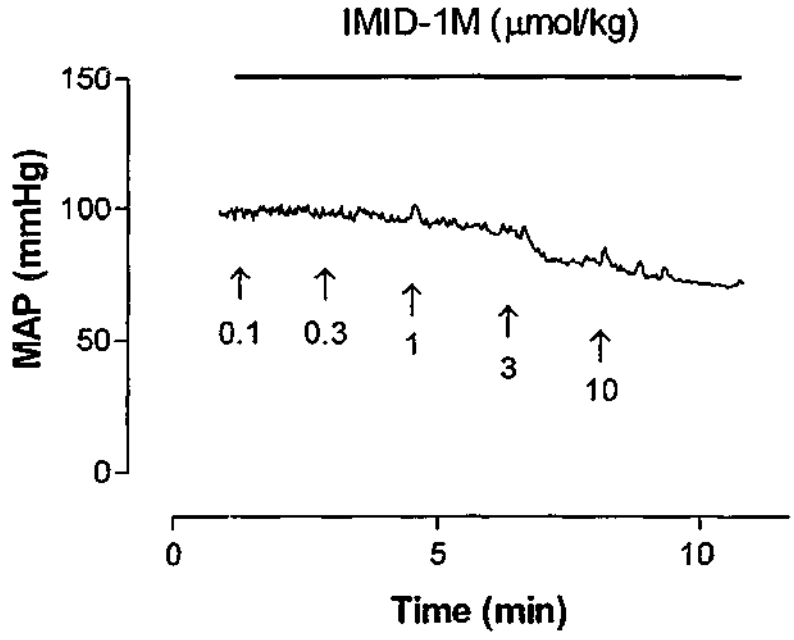

(b)

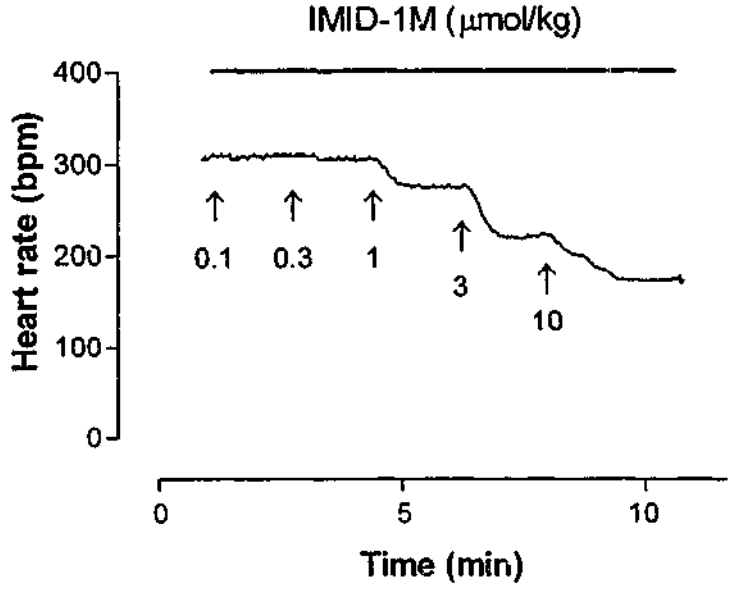

Figure 6.2 An original recording illustrating changes in (a) mean arterial pressure (MAP; mmHg) and (b) heart rate (bpm) in response to IMID-1M (0.1–10 μmol/kg) in the anaesthetised rat.

Compound	MAP (% control)					
	Control	0.1 (μmol/kg)	0.3 (μmol/kg)	1 (μmol/kg)	3 (μmol/kg)	10 (μmol/kg)
IMID-1M	100	101 ± 1	99 ± 1	97 ± 3	92 ± 5	$82 \pm 6^{\#1,2,3,4}$
IMID-26F	100	94 ± 4	93 ± 7	87 ± 6	$81 \pm 6^{\#}$	$72 \pm 5^{\#1,2}$
IMID-4F	100	100 ± 0	99 ± 2	99 ± 2	96 ± 2	$78 \pm 4^{\#1,2}$
IMID-4ME	100	102 ± 1	97 ± 5	103 ± 2	94 ± 4	$86 \pm 6^{1,2,3,4}$
IMID-4MO	100	99 ± 1	98 ± 1	94 ± 3	$86 \pm 5^{\#}$	$64 \pm 7^{\#1,2}$
IMID-35MO	100	102 ± 1	102 ± 2	101 ± 3	$88 \pm 2^{\#}$	$62 \pm 2^{\#1,2}$
IMID-35MO/IN	100	101 ± 0	99 ± 2	95 ± 5	89 ± 5	$85 \pm 6^{\#1,2,3,4}$
IMID-4F/IN	100	100 ± 2	105 ± 2	102 ± 1	100 ± 3	$102 \pm 3^{2,3,4}$
IMID-35MO/O	100	101 ± 3	96 ± 11	101 ± 18	108 ± 16	119 ± 13^{4}
IMID-4F/O	100	99 ± 0	96 ± 2	96 ± 2	99 ± 2	$112 \pm 13^{3,4}$
IMID-35MO/2N	100	95 ± 13	96 ± 15	90 ± 17	$60 \pm 11^{\#}$	$46 \pm 11^{\#1}$
IMID-4F/2N	100	101 ± 1	94 ± 5	98 ± 3	92 ± 6	$73 \pm 10^{\#1,2,3}$
IMID-26F/2N	100	103 ± 1	103 ± 2	98 ± 5	$86 \pm 6^{\#}$	$46 \pm 4^{\#1}$

Table 6.2 Table summarising the effect of the IMID compounds (0.1–10 μmol/kg) on mean arterial pressure (MAP) in the anaesthetised rat. # indicates significant difference from initial within animal control value (n=4; P<0.05; one way RM ANOVA with Bonferroni t-test). Compounds marked with the same number are not significantly different from one another at the highest dose (10 μmol/kg; n=4; P>0.05; one way ANOVA with Bonferroni t-test).

(a)

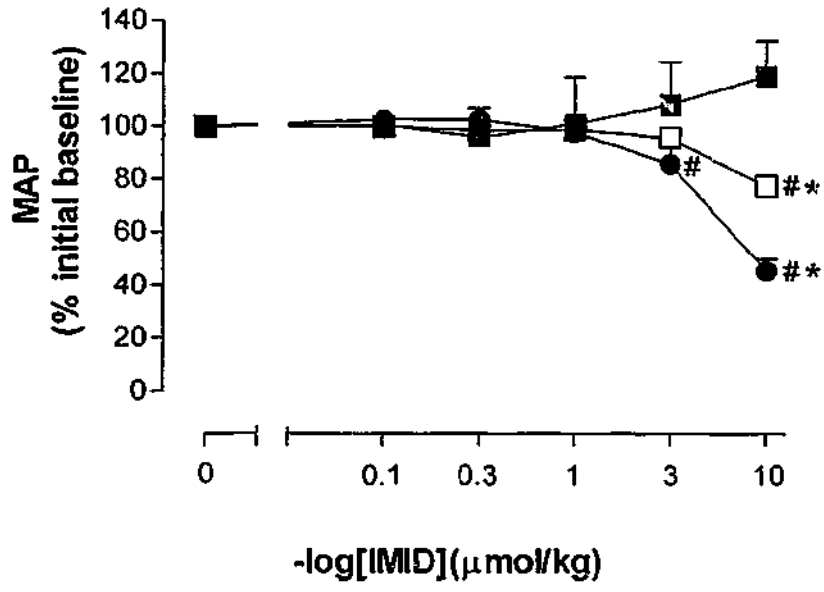

(b)

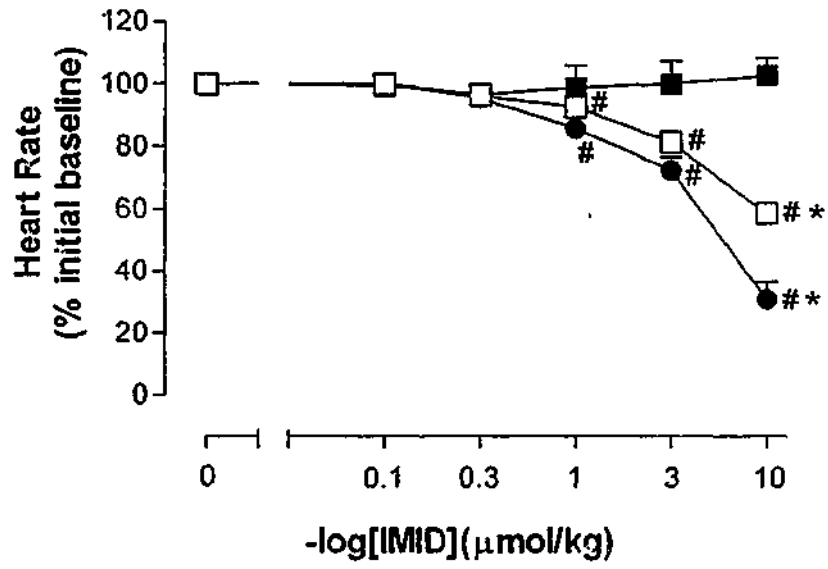

Figure 6.3 Mean dose-response curves illustrating the effect on (a) mean arterial pressure (MAP) and (b) heart rate of the IMID-35MO/O (■), IMID-4F (□), and IMID-26F/2N (●), representing the range of potency of the compounds in the anaesthetised rat. Error bars are ± S.E.M. and if not visible are contained within the symbol. * indicates compound is significantly more potent than other derivatives at the highest dose (10 μmol/kg; n=4; P<0.05; one way ANOVA with Bonferroni t-test). # indicates significant difference from initial within animal baseline value (n=4; P<0.05; one way RM ANOVA with Bonferroni t-test).

(Table 6.2; Figure 6.4a; n=4; P<0.05; one way ANOVA with Bonferroni t-test). By contrast, IMID-4ME (86 ± 6 %), IMID-4F/IN (102 ± 3 %), IMID-4F/O (112 ± 13 %) and IMID-35MO/O (119 ± 13 %) (all at 10 μmol/kg), had no significant effect on MAP (n=4; P>0.05; one way RM ANOVA).

6.3.1.2 Effect on heart rate

The imidazoline analogues were expected to display some bradycardic activity due to their actions on isolated atria (Chapter 3). However, as with the effect of the derivatives on MAP, significant changes in heart rate were only seen at higher doses. Table 6.3 and Figure 6.3b summarise the dose-dependent effects of the IMID compounds on heart rate. Several of the IMID compounds caused a significant dose-dependent reduction in heart rate (Table 6.3; n=4; P<0.05; one way RM ANOVA with Bonferroni t-test). The most potent of these compounds IMID-26F/2N, IMID-4F/2N, IMID-35MO/2N, IMID-1M, IMID-4F, IMID-26F and IMID-35MO caused significantly greater reductions at 10 μmol/kg than the remaining compounds (Figure 6.4b; n=4; P<0.05; one way ANOVA with Bonferroni t-test). The analogues, IMID-4F/O (98 ± 2 %) and IMID-35MO/O (103 ± 6 %) had no significant effect on heart rate (Table 6.3; Figure 6.4b; n=4; P>0.05; one way RM ANOVA).

6.3.2 Time dependent effects of the imidazolines on MAP and heart rate

6.3.2.1 Four hour study

In this series of experiments the effects of a single bolus dose of glibenclamide (1 μmol/kg), clonidine (1 μmol/kg) and five of the imidazoline analogues (IMID-4F,

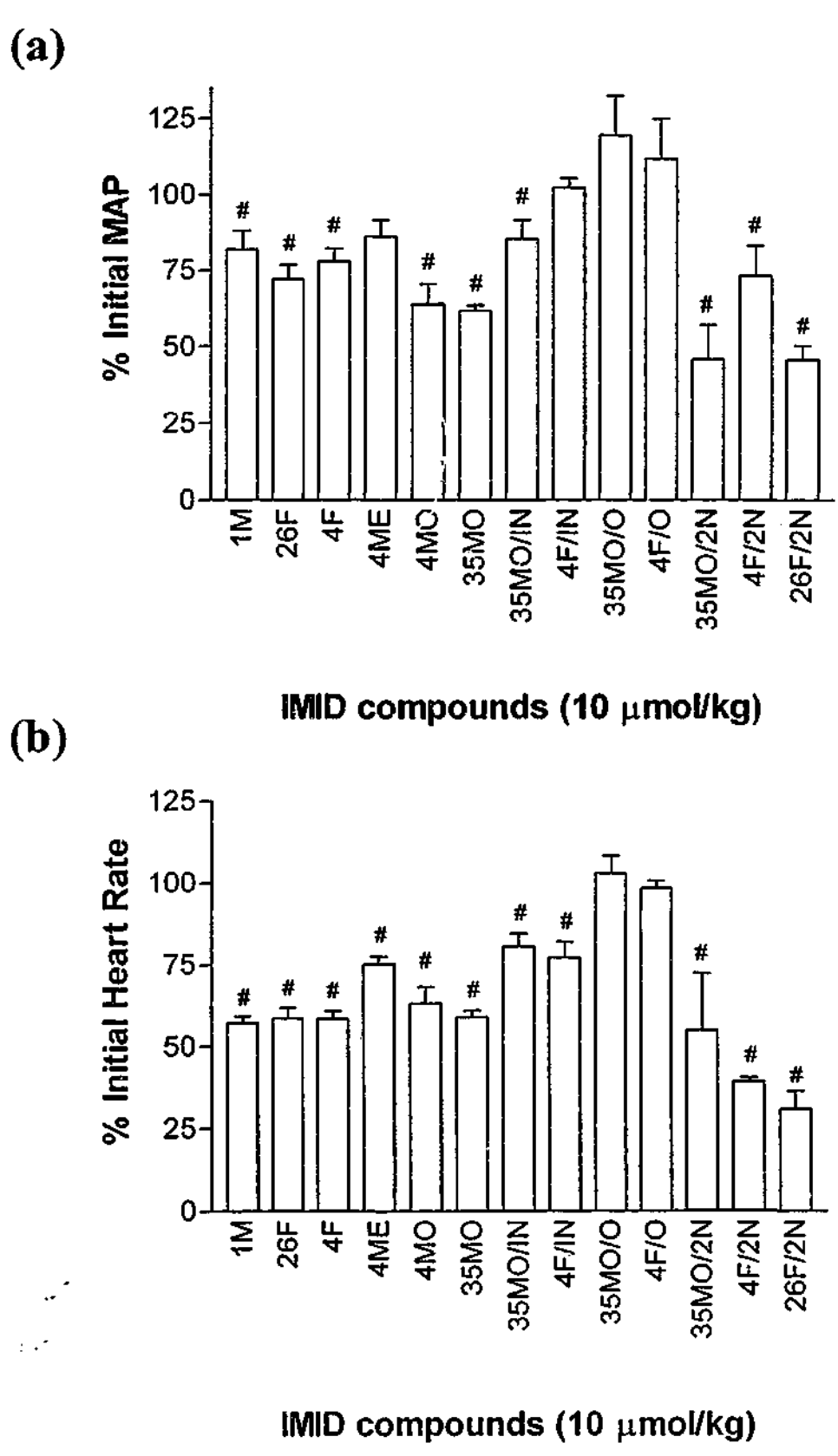

Figure 6.4 Histogram plot illustrating the effect of all the of the IMID compounds (10 μmol/kg) on (a) mean arterial pressure (MAP) and (b) heart rate in the anaesthetised rat. Error bars are ± S.E.M. and if not visible are contained within the symbol. # indicates a significant difference from initial baseline value (n=4; P<0.05; one way RM ANOVA with Bonferroni t-test).

Compound	Heart rate (% control)					
	Control	0.1 (μmol/kg)	0.3 (μmol/kg)	1 (μmol/kg)	3 (μmol/kg)	10 (μmol/kg)
IMID-1M	100	100 ± 0	98 ± 1	91 ± 1$^{\#}$	78 ± 3$^{\#}$	57 ± 2$^{\#1,2}$
IMID-26F	100	95 ± 3	92 ± 4$^{\#}$	85 ± 5$^{\#}$	74 ± 4$^{\#}$	59 ± 3$^{\#1,2}$
IMID-4F	100	100 ± 0	96 ± 0	93 ± 1$^{\#}$	81 ± 1$^{\#}$	59 ± 2$^{\#1,2}$
IMID-4ME	100	104 ± 5	97 ± 2	93 ± 2	88 ± 1$^{\#}$	75 ± 2$^{\#3}$
IMID-4MO	100	99 ± 0	97 ± 0	91 ± 1	81 ± 2$^{\#}$	63 ± 5$^{\#2,3}$
IMID-35MO	100	99 ± 0	97 ± 1	90 ± 1	80 ± 1$^{\#}$	59 ± 2$^{\#1,2}$
IMID-35MO/IN	100	99 ± 0	99 ± 1	97 ± 1	91 ± 3$^{\#}$	81 ± 4$^{\#3}$
IMID-4F/IN	100	99 ± 2	98 ± 2	93 ± 3	89 ± 4$^{\#}$	77 ± 5$^{\#3}$
IMID-35MO/O	100	99 ± 1	97 ± 3	99 ± 7	100 ± 7	103 ± 6^{3}
IMID-4F/O	100	95 ± 2	95 ± 2	95 ± 2	94 ± 2	98 ± 2^{3}
IMID-35MO/2N	100	102 ± 3	103 ± 4	99 ± 9	85 ± 9	55 ± 8$^{\#1,2}$
IMID-4F/2N	100	96 ± 0	83 ± 7$^{\#}$	66 ± 6$^{\#}$	57 ± 2$^{\#}$	39 ± 1$^{\#1}$
IMID-26F/2N	100	100 ± 1	96 ± 2	86 ± 2$^{\#}$	72 ± 4$^{\#}$	31 ± 6$^{\#1}$

Table 6.3 Table summarising the effect of the IMID compounds (0.1–10 μmol/kg) on heart rate in the anaesthetised rat. $^{\#}$ indicates significant difference from initial within animal control value (n=4; P<0.05; one way RM ANOVA with Bonferroni t-test). Compounds marked with the same number are not significantly different from one another at the highest dose (10 μmol/kg; n=4; P>0.05; one way ANOVA with Bonferroni t-test).

IMID-26F, IMID-1M, IMID-4F/2N & IMID-35MO; 10 μmol/kg) on MAP and heart rate were assessed over four hours following administration in the anaesthetised rat. The effect of the α_2-adrenoceptor antagonist, rauwolscine (25 μmol/kg) on responses to clonidine and the five imidazolines was also assessed

The average initial baseline MAP and heart rate before administration of glibenclamide, clonidine or the imidazoline analogues was 109 ± 3 mmHg (n=71) and 380 ± 6 bpm (n=71).

The imidazoline analogues vehicle (20 % EtOH) had no acute or time dependent effect upon MAP or heart rate over four hours (Figure 6.5; n=4-7; P>0.05; one way RM ANOVA). Similarly, glibenclamide (1 μmol/kg) had no significant effect on MAP or heart rate over four hours (Figure 6.5; n=4-8; P>0.05; two way RM ANOVA; one way RM ANOVA).

Clonidine (1 μmol/kg) caused a transient increase in MAP (127 ± 14 % at 0 min) that returned to control values within 15 minutes after administration (Figure 6.6a; n=4-9; P<0.01; one way RM ANOVA). Compared with vehicle, clonidine caused a significant reduction in heart rate (max 75 ± 4 % at 0 min; P<0.01) that was sustained over 4 hours (Figure 6.6b; n=4-8; P<0.05; two way RM ANOVA). Pretreatment with rauwolscine had no significant effect on the heart rate response to clonidine (Figure 6.6b; n=4-8; P>0.05; two way RM ANOVA).

IMID-4F (10 μmol/kg) alone, or in the presence of rauwolscine (25 μmol/kg), had no significant effect on MAP over four hours when compared to vehicle control (Figure 6.7a; n=4-8; P>0.05; two way RM ANOVA; one way RM ANOVA). However, IMID-4F caused an immediate fall in heart rate (max 63 ± 4 % at 0 min) that returned to control values after 60 minutes (Figure 6.7b; n=4-8; P<0.01; one way RM

(a)

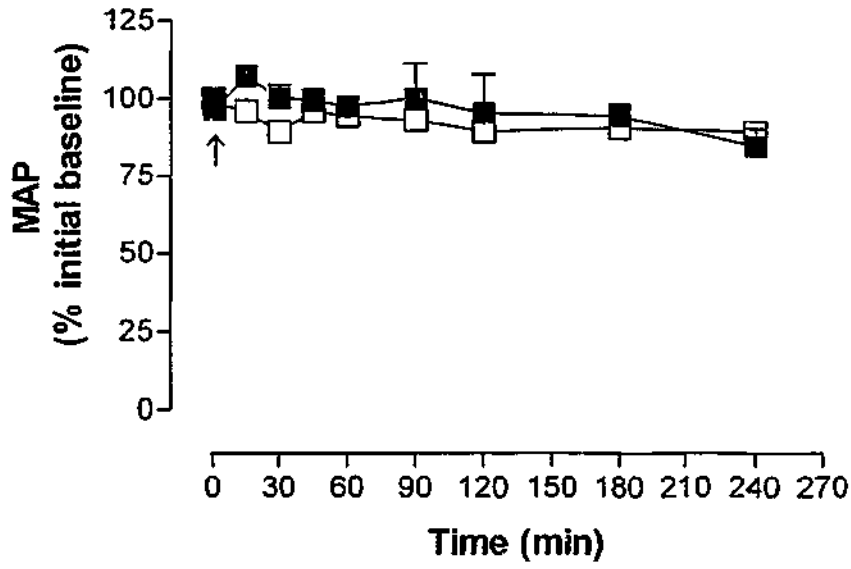

(b)

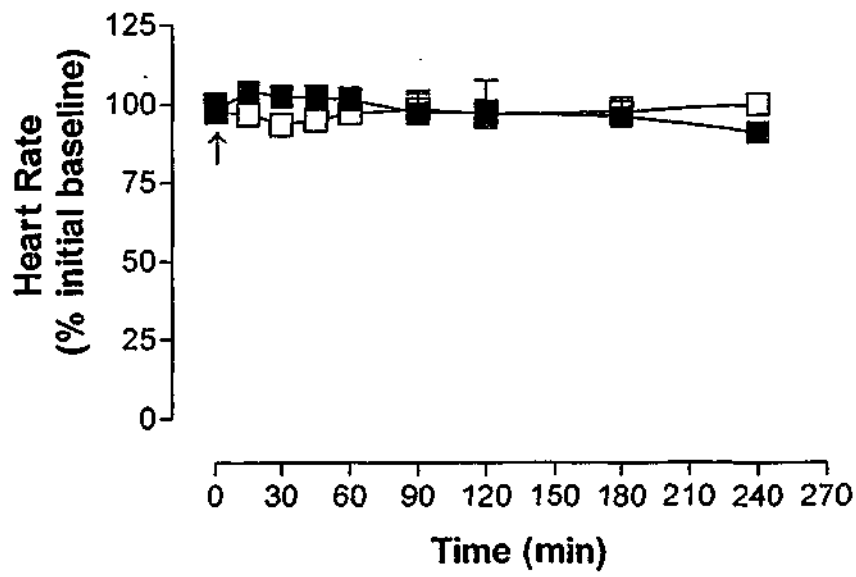

Figure 6.5 Effect of a single dose of glibenclamide (■; 1 μmol/kg) and vehicle (□) on (a) mean arterial pressure (MAP) and (b) heart rate over time in the anaesthetised rat represented as % of baseline value (0 min). ↑ indicates administration of drug. Error bars are ± S.E.M. and if not visible are contained within the symbol (n=4-8; P>0.05; two way RM ANOVA; one way ANOVA).

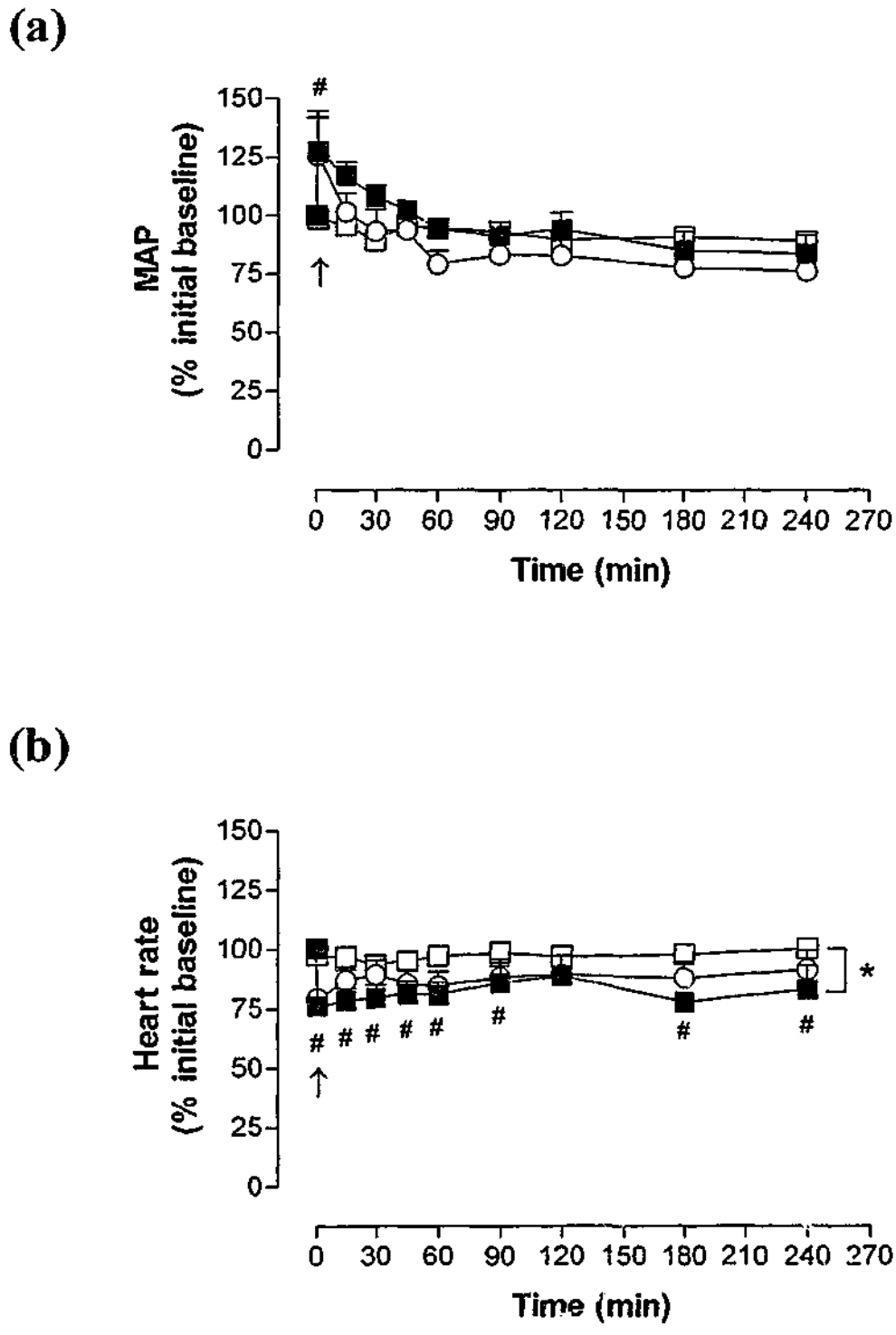

Figure 6.6 Effect of a single dose of clonidine (■; 1 μmol/kg), clonidine in the presence of rauwolscine (○; 25 μmol/kg) and vehicle (□) on (a) mean arterial pressure (MAP) and (b) heart rate over time in the anaesthetised rat represented as % of baseline value (0 min). ↑ indicates administration of drug. Error bars are ± S.E.M. and if not visible are contained within the symbol. * indicates a significant difference from vehicle (n=4-8; P>0.05; two way RM ANOVA). # indicates a significant difference from initial within animal baseline value (n=4-8; P<0.05; one way RM ANOVA).

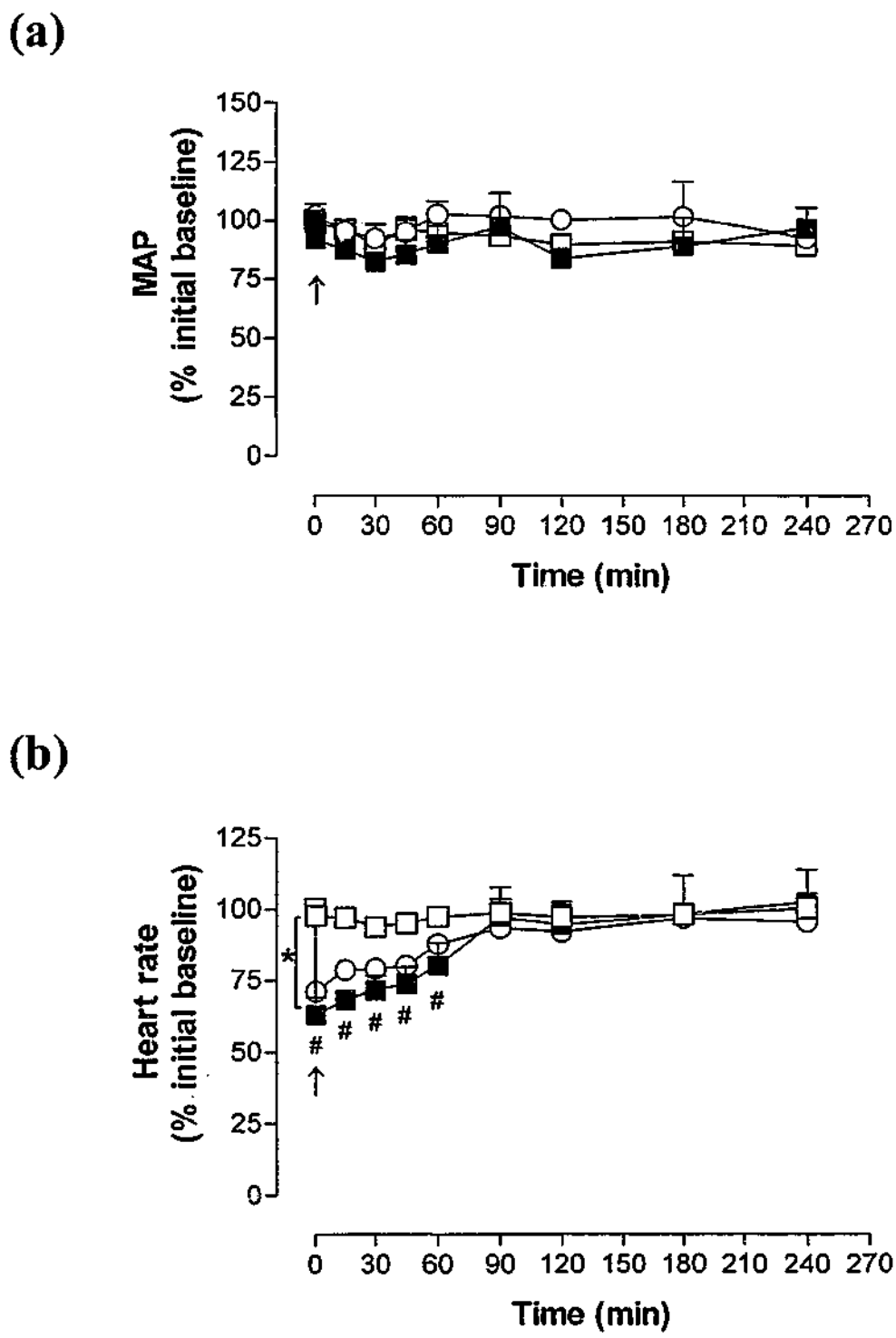

Figure 6.7 Effect of a single dose of IMID-4F (■; 10 μmol/kg), IMID-4F in the presence of rauwolscine (○; 25 μmol/kg) and vehicle (□) on (a) mean arterial pressure (MAP) and (b) heart rate over time in the anaesthetised rat represented as % of baseline value (0 min). ↑ indicates administration of drug. Error bars are ± S.E.M. and if not visible are contained within the symbol. * indicates a significant difference from vehicle (n=4-8; P<0.05; two way RM ANOVA). # indicates a significant difference from initial within animal baseline value (n=4-8; P<0.05; one way RM ANOVA).

ANOVA). Pretreatment with rauwolscine had no significant effect on the heart rate response to IMID-4F (Figure 6.7b; n=4-8; P>0.05; two way RM ANOVA).

Following the administration of IMID-26F (10 μmol/kg), MAP decreased (max 79 ± 5 % at 30 min) and was significantly different from the initial within animal baseline value at 30, 45, 120, 180 and 240 minutes (Figure 6.8a; n=4-8; P<0.01; one way RM ANOVA). Pretreatment with rauwolscine (25 μmol/kg) prevented the fall in MAP mediated by IMID-26F and raised MAP above values recorded in the presence of the vehicle (max 124 ± 10 % at 180 min) over 4 hours (n=4-8; P<0.01; two way RM ANOVA). IMID-26F caused an immediate decrease in heart rate (max 77 ± 5 % at 0 min) which was sustained over four hours (Figure 6.8b; n=4-8; P<0.01; one way RM ANOVA). In the presence of rauwolscine, IMID-26F did not significantly alter the heart rate response when compared to IMID-26F alone (n=4-8; P>0.05; two way RM ANOVA).

A single dose of IMID-1M (10 μmol/kg) caused an immediate reduction in MAP (max 60 ± 1 % at 60 min; P<0.01), which was sustained over the 4 study hour period (Figure 6.9a; n=4-7; P<0.01; two way RM ANOVA; one way RM ANOVA). The administration of rauwolscine (25 μmol/kg), reversed the effects of IMID-1M (n=4-7; P<0.01; two way RM ANOVA) such that MAP responses were no longer significantly different from vehicle control (Figure 6.9a; n=4-7; P>0.05; two way RM ANOVA). IMID-1M caused an immediate, prolonged fall in heart rate (max 50 ± 3 % at 0 min; P<0.01) that was significantly different from vehicle control over four hours (Figure 6.9b; n=4-7; P<0.01; one way ANOVA). The fall in heart rate caused by IMID-1M was partially reversed by pretreatment with rauwolscine (Figure 6.9b; n=4-7; P<0.01; two way RM ANOVA).

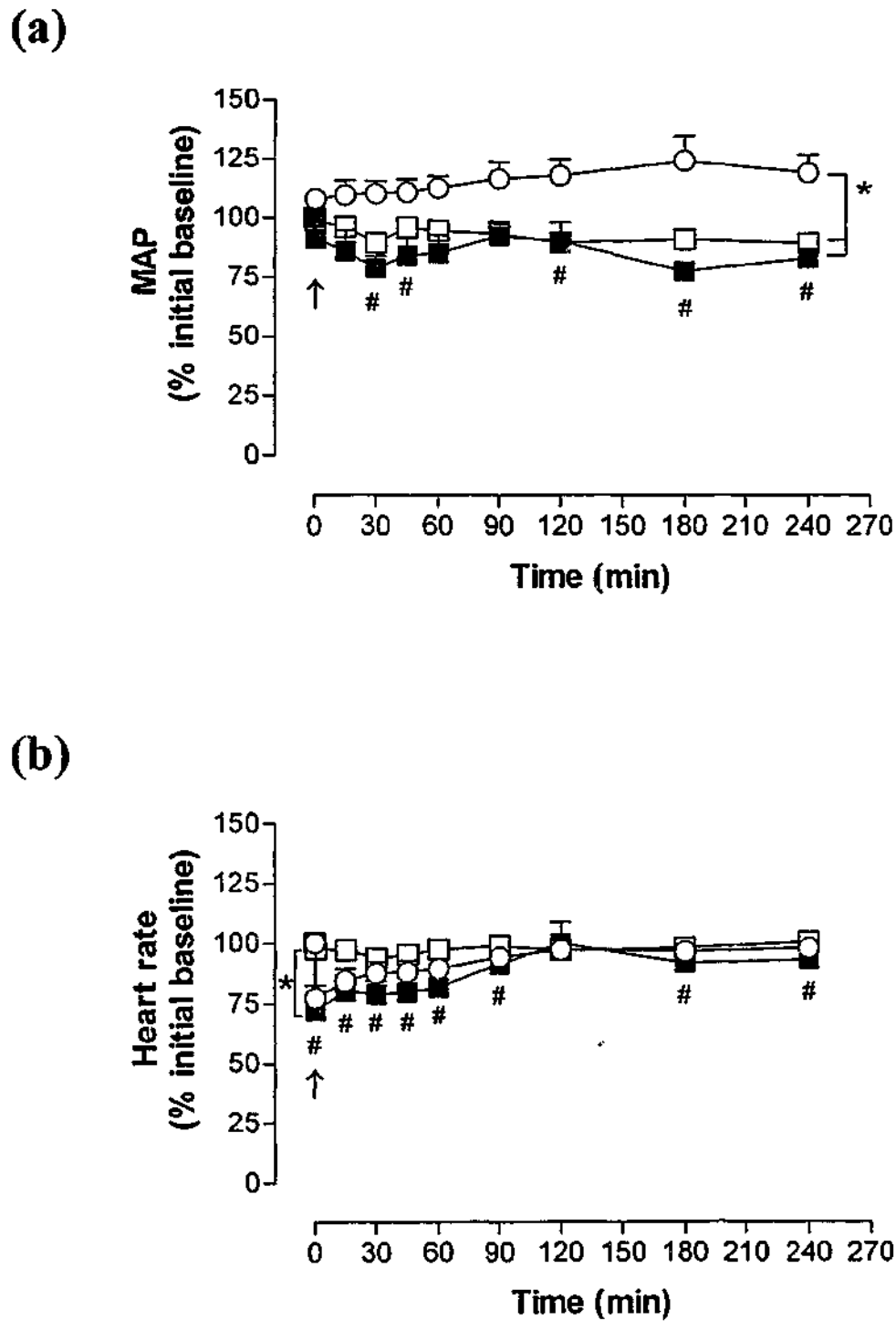

Figure 6.8 Effect of a single dose of IMID-26F (■; 10 μmol/kg), IMID-26F in the presence of rauwolscine (○; 25 μmol/kg) and vehicle (□) on (a) mean arterial pressure (MAP) and (b) heart rate over time in the anaesthetised rat represented as % of baseline value (0 min). ↑ indicates administration of drug (0 min). Error bars are ± S.E.M. and if not visible are contained within the symbol. * indicates a significant difference with treatment (n=4-8; P<0.05; two way RM ANOVA). # indicates a significant difference from initial within animal baseline value (n=4-8; P<0.05; one way RM ANOVA).

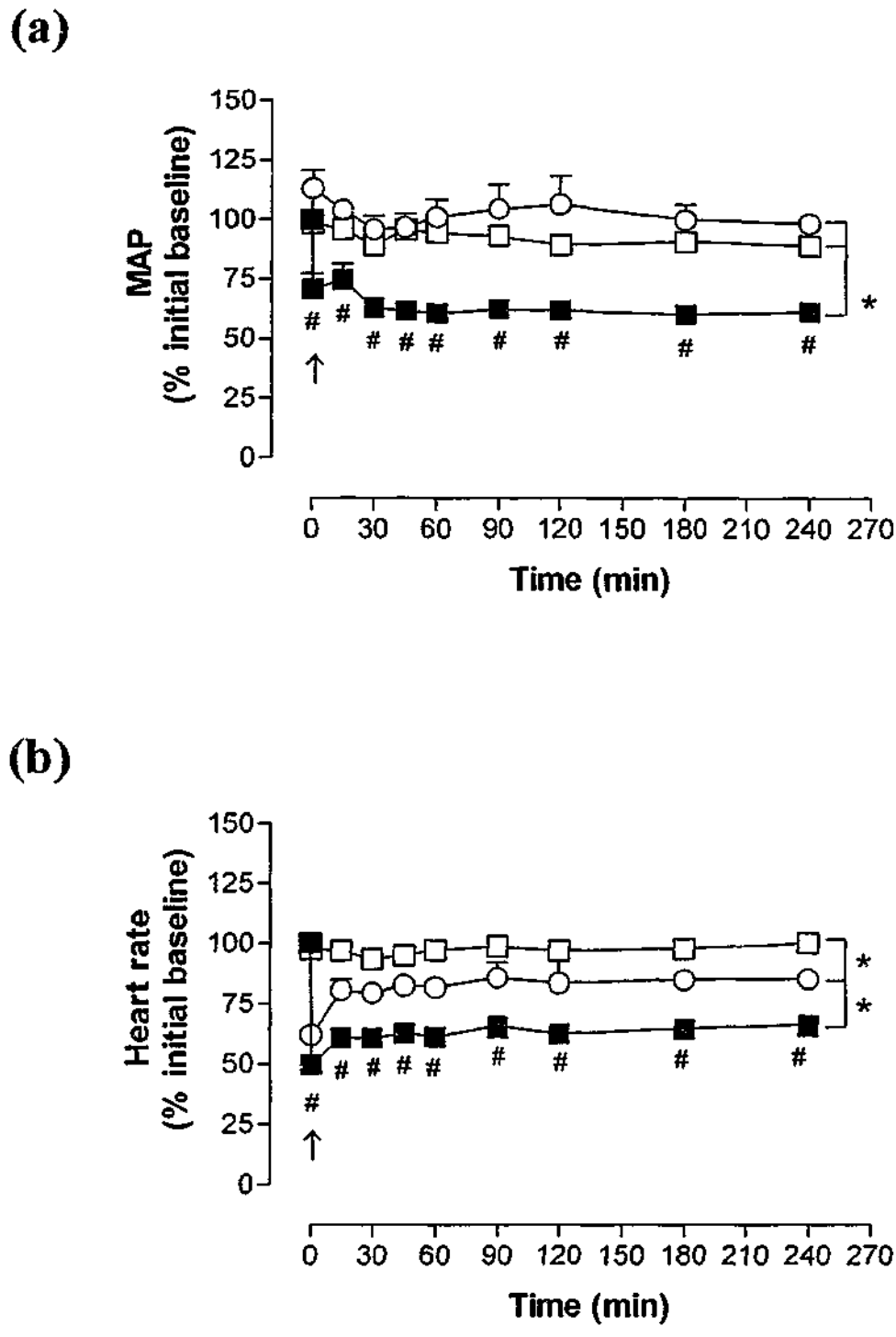

Figure 6.9 Effect of a single dose of IMID-1M (■; 10 μmol/kg), IMID-1M in the presence of rauwolscine (○; 25 μmol/kg) and vehicle (□) on (a) mean arterial pressure and (b) heart rate over time in the anaesthetised rat represented as % of baseline value (0 min). ↑ indicates administration of drug. Error bars are ± S.E.M. and if not visible are contained within the symbol. * indicates a significant difference with treatment (n=4-8; P<0.05; two way RM ANOVA). # indicates a significant difference from initial within animal baseline value (n=4-8; P<0.05; one way RM ANOVA).

IMID-4F/2N (10 μmol/kg), caused significant reductions in MAP (max 85 ± 2 % at 60 min) at 60, 120 and 180 minutes when compared to initial within animal baseline values (Figure 6.10a; n=4-7; P<0.05; one way RM ANOVA). Pretreatment with rauwolscine significantly attenuated this effect (Figure 6.10a; n=4-7; P<0.05; two way RM ANOVA). Both, IMID-4F/2N alone and IMID-4F/2N in the presence of rauwolscine caused a significant drop in heart rate (max IMID-4F/2N alone 51 ± 4 %; plus rauwolscine 50 ± 4 %; P<0.01) that occurred immediately and was sustained over four hours when compared to vehicle (Figure 6.10b; n=4-7; P<0.01; two way RM ANOVA; one way RM ANOVA).

IMID-35MO (10 μmol/kg) caused an immediate reduction in MAP (max 64 ± 5 at 0 min) that was maintained over a period of 4 hours (Figure 6.11a; n=4-8; P<0.01; one way RM ANOVA). In the presence of rauwolscine (25 μmol/kg), the MAP response to IMID-35MO was significantly attenuated and did not differ significantly from vehicle (Figure 6.11a; n=4-8; P>0.05; two way RM ANOVA). Heart rate was significantly decreased by IMID-35MO (max 62 ± 2 % at 0 min) and this decrease was sustained over the four hour study period (Figure 6.11b; n=4-8; P<0.01; one way RM ANOVA). Although pretreatment with rauwolscine appeared to attenuate the response to IMID-35MO at earlier time points (≤ 60 min), MAP responses were not significantly different from IMID-35MO alone (Figure 6.11b; n=4-8; P>0.05; two way RM ANOVA).

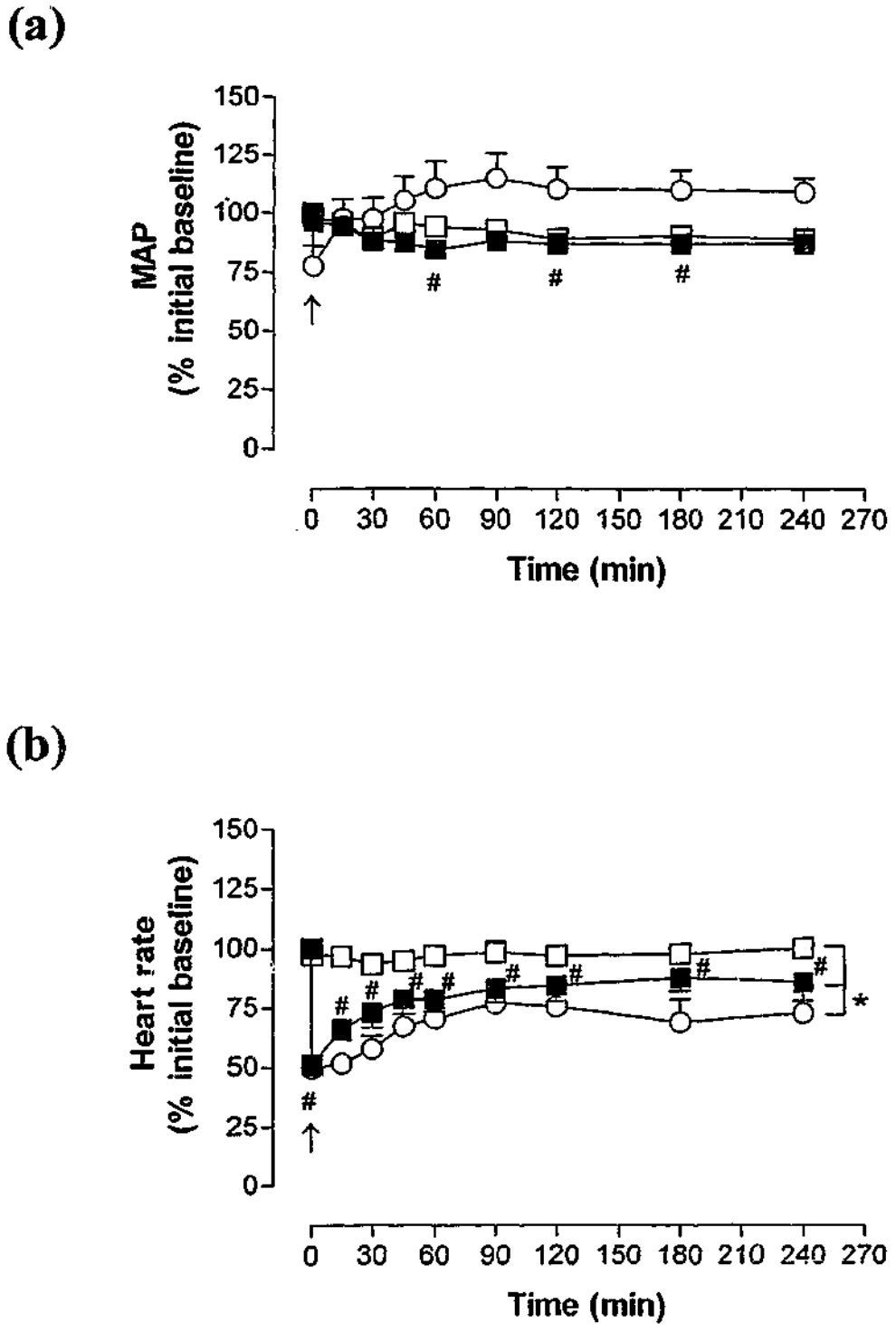

Figure 6.10 Effect of a single dose of IMID-4F/2N (■; 10 μmol/kg), IMID-4F/2N in the presence of rauwolscine (○; 25 μmol/kg) and vehicle (□) on (a) mean arterial pressure (MAP) and (b) heart rate over time in the anaesthetised rat represented as % of baseline value (0 min). ↑ indicates administration of drug. Error bars are ± S.E.M. and if not visible are contained within the symbol. * indicates a significant difference with treatment (n=4; P<0.05; two way RM ANOVA). # indicates a significant difference from initial within animal baseline value (n=4; P<0.05; one way RM ANOVA).

(a)

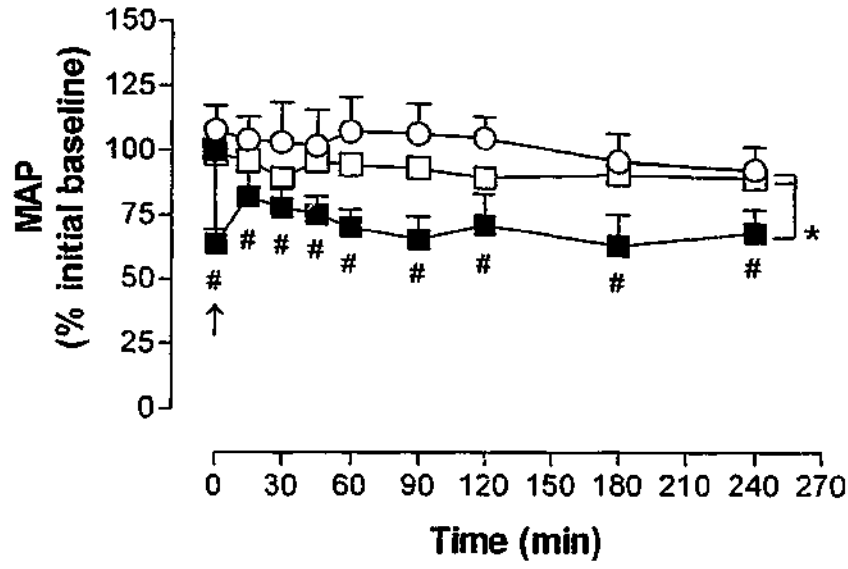

(b)

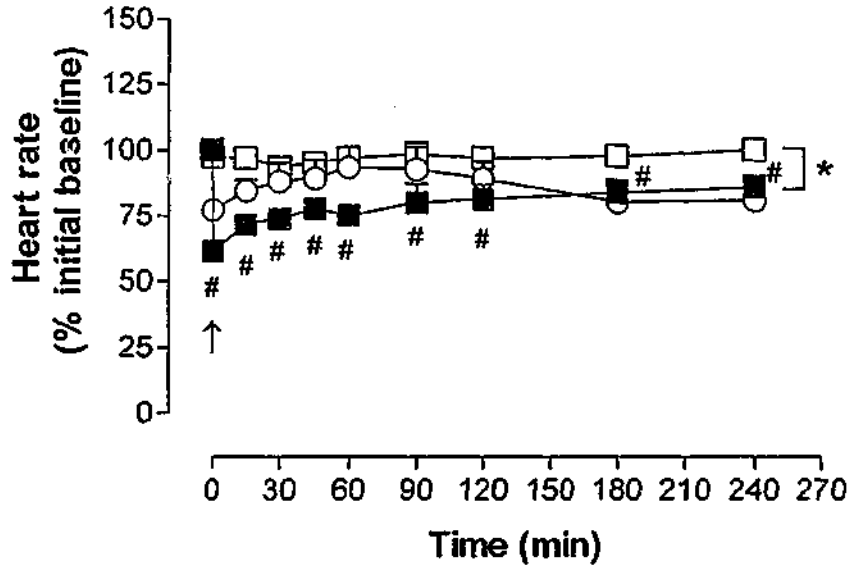

Figure 6.11 Effect of a single dose of IMID-35MO (■; 10 μmol/kg), IMID-35MO in the presence of rauwolscine (○; 25 μmol/kg) and vehicle (□) on (a) mean arterial pressure (MAP) and (b) heart rate over time in the anaesthetised rat represented as % of baseline value (0 min). ↑ indicates administration of drug. Error bars are ± S.E.M. and if not visible are contained within the symbol. * indicates a significant difference with treatment (n=4-8; P<0.05; two way RM ANOVA). # indicates a significant difference from initial within animal baseline value (n=4; P<0.05; one way RM ANOVA).

6.3.2.2 One hour study

In this series of experiments, the effects of the remaining imidazoline analogues, IMID-4ME, IMID-4MO, IMID-35MO/IN, IMID-4F/IN, IMID-35MO/O, IMID-4F/O, IMID-35MO/2N and IMID-26F/2N, on MAP and heart rate were examined in the anaesthetised rat for one hour following their addition at a concentration of 10 μmol/kg.

Table 6.4 summarises the results of this study. IMID-4MO caused a transient decrease in MAP immediately after administration (66 ± 1 %) and reduced MAP again at 60 minutes (77 ± 6 %). A significant fall in MAP in response to IMID-4F/IN (69 ± 3 %) was not observed until 30 minutes after addition. By contrast, both IMID-26F/2N and IMID-35MO/2N caused immediate reductions in MAP (IMID-35MO/2N 46 ± 3 %; IMID-26F/2N 46 ± 5 %) that were resolved after 30 and 60 minutes, respectively. IMID-4ME, IMID-35MO/IN, IMID-35MO/O and IMID-4F/O had no time dependent effects on MAP over one hour of measurement (n=4; P>0.05; one way RM ANOVA).

In addition, several of the IMID compounds significantly reduced heart rate, an effect which was always maximal immediately after administration (Table 6.4; n=4; P<0.01; one way RM ANOVA). The initial decrease in heart rate in response to IMID-4MO (64 ± 6 %) and IMID-4F/IN (76 ± 5 %) was sustained over one hour. Yet, the response to IMID-26F/2N tended towards control values over time. Similarly the transient reductions in heart rate caused by IMID-35MO/2N and IMID-4ME were resolved 30 minutes after administration. IMID-35MO/IN, IMID-35MO/O and IMID-4F/O had no acute or time dependent effects on heart rate over one hour (n=4; P>0.05; one way ANOVA).

Compound	MAP (% control)		
	Post Drug	**30 min**	**60 min**
IMID-4ME	87 ± 7	92 ± 4	96 ± 7
IMID-4MO	66 ± 1#	83 ± 4	77 ± 6#
IMID-35MO/IN	86 ± 8	91 ± 13	95 ± 4
IMID-4F/IN	99 ± 5	69 ± 3#	72 ± 5#
IMID-35MO/O	109 ± 2	95 ± 3	86 ± 5
IMID-4F/O	104 ± 8	105 ± 7	102 ± 10
IMID-35MO/2N	46 ± 3#	76 ± 12#	82 ± 1
IMID-26F/2N	46 ± 5#	86 ± 5	92 ± 5
Compound	**Heart Rate (% control)**		
	Post Drug	**30 min**	**60 min**
IMID-4ME	74 ± 4#	87 ± 3	91 ± 4
IMID-4MO	64 ± 6#	74 ± 3#	75 ± 3#
IMID-35MO/IN	81 ± 5	90 ± 8	93 ± 5
IMID-4F/IN	76 ± 5#	72 ± 4#	73 ± 4#
IMID-35MO/O	98 ± 2	100 ± 3	97 ± 4
IMID-4F/O	93 ± 2	98 ± 2	100 ± 5
IMID-35MO/2N	53 ± 2#	81 ± 12	89 ± 16
IMID-26F/2N	31 ± 6#	80 ± 4#	86 ± 2#

Table 6.4 Table summarising the effects of the imidazoline analogues on mean arterial pressure (MAP) and heart rate in the anaesthetised rat. Measurements of MAP and heart rate were taken prior to administration of the imidazoline analogues and all subsequent values expressed as % change from baseline (100 %). Measurements were taken immediately after drug administration (post drug) and at 30 and 60 minutes. # indicates significant difference from initial within animal baseline value (n=3-4; P<0.01; one way RM ANOVA with Bonferroni t-test).

6.3.3 Time dependent effects of the imidazolines on blood glucose and insulin levels

6.3.3.1 Four hour study

These studies examined the effects of a single dose of glibenclamide (1 μmol/kg), clonidine (1 μmol/kg) and five of the imidazoline analogues (IMID-4F, IMID-26F, IMID-1M, IMID-4F/2N & IMID-1M; 10 μmol/kg) on blood glucose over four hours, and insulin levels over one hour, in the anaesthetised rat. The effects of clonidine and the five imidazolines were also examined in the presence of the α_2-adrenoceptor antagonist, rauwolscine (25 μmol/kg).

The average initial blood glucose level before administration of glibenclamide, clonidine or the imidazoline analogues was 6.9 ± 0.2 mmol/L (n=71).

There was no significant acute or time dependent effect upon blood glucose or insulin levels by the vehicle (20 % EtOH; Figure 6.12) or rauwolscine alone over the measurement period (data not shown; n=4-7; P>0.05; one way RM ANOVA).

Conversely, glibenclamide (1 μmol/kg), caused a significant decrease in blood glucose when compared to vehicle control (Figure 6.12a; n=4-8; P<0.01; two way RM ANOVA). A significant fall in blood glucose was observed 15 minutes after administration of glibenclamide and blood glucose continued to decline for up to 90 minutes (max 52 ± 6 %; n=4-8; P<0.01; one way RM ANOVA). Blood glucose levels then returned towards baseline values such that by 4 hours they were no longer significantly different from control levels. This decrease in blood glucose was reflected by a significant increase in insulin levels (max 3.8 ± 0.4 ng/ml at 5 min; P<0.01) when

(a)

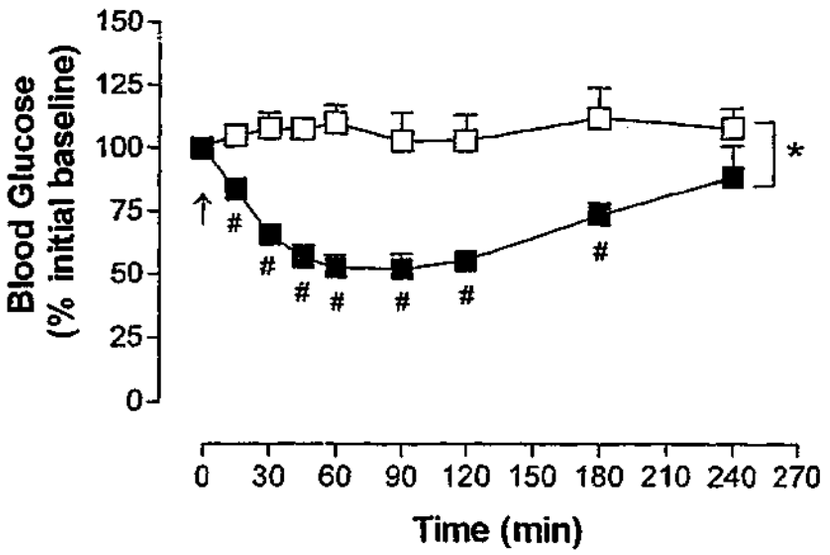

(b)

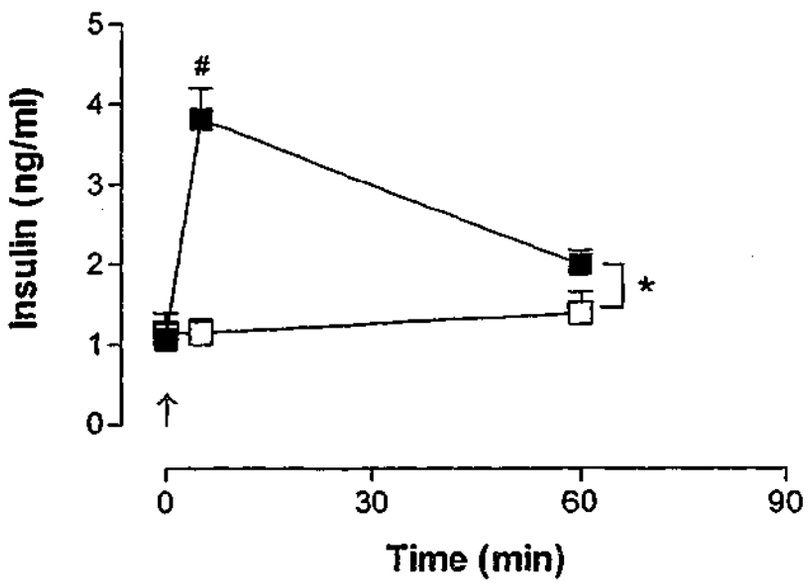

Figure 6.12 Effect of a single dose of glibenclamide (■; 1 μmol/kg) and vehicle (□) on (a) blood glucose represented as % of baseline value (0 min) and (b) insulin (ng/ml) over time in the anaesthetised rat. ↑ indicates administration of drug. Error bars are ± S.E.M. and if not visible are contained within the symbol. * indicates a significant difference from vehicle (n=4-8; P<0.01; two way RM ANOVA). # indicates a significant difference from initial within animal baseline value (n=4-8; P<0.01; one way RM ANOVA).

compared to vehicle control (Figure 6.12b; n=4-8; P<0.01; two way RM ANOVA; one way RM ANOVA).

In contrast to glibenclamide, clonidine (1 μmol/kg) caused a significant increase in blood glucose that began immediately and was sustained over the 4 hour period (max 232 ± 25 % at 90 min; P<0.01; one way RM ANOVA) when compared to vehicle control (Figure 6.13a; n=4-8; P<0.01; two way RM ANOVA). Pretreatment with rauwolscine (25 μmol/kg) significantly inhibited the clonidine-induced blood glucose changes by clonidine (n=4-8; P<0.01; two way RM ANOVA). In addition, the insulin levels in the presence of clonidine were significantly decreased (from 1.15 ± 0.50 to 0.08 ± 0.02 ng/ml at 60 min; P<0.05) when compared to vehicle control (Figure 6.13b; n=4; P<0.05; two way RM ANOVA).

The blood glucose levels after a single dose of IMID-4F (10 μmol/kg) did not differ from vehicle control or the initial within animal baseline value over the 4 hours of measurement (Figure 6.14a; n=4-8; P>0.05; two way RM ANOVA; one way RM ANOVA). However, in the presence of rauwolscine (25 μmol/kg), IMID-4F caused a significant reduction in blood glucose levels (max 66 ± 6 % at 90 min; P<0.01) when compared to both IMID-4F alone and vehicle control (n=4-8; P<0.05; two way RM ANOVA). These results were also reflected by the finding that IMID-4F, in the presence of rauwolscine, caused a prolonged increase in insulin levels (max 5.5 ± 0.7 at 5 min; P<0.01) over one hour that was also significantly different from both IMID-4F alone and vehicle control (n=4; P<0.01; two way RM ANOVA).

There was no acute or time dependent effect on blood glucose by IMID-26F (10 μmol/kg) alone, or IMID-26F in the presence of rauwolscine (25 μmol/kg), when compared to either vehicle control or initial within animal baseline values (Figure 6.15a;

(a)

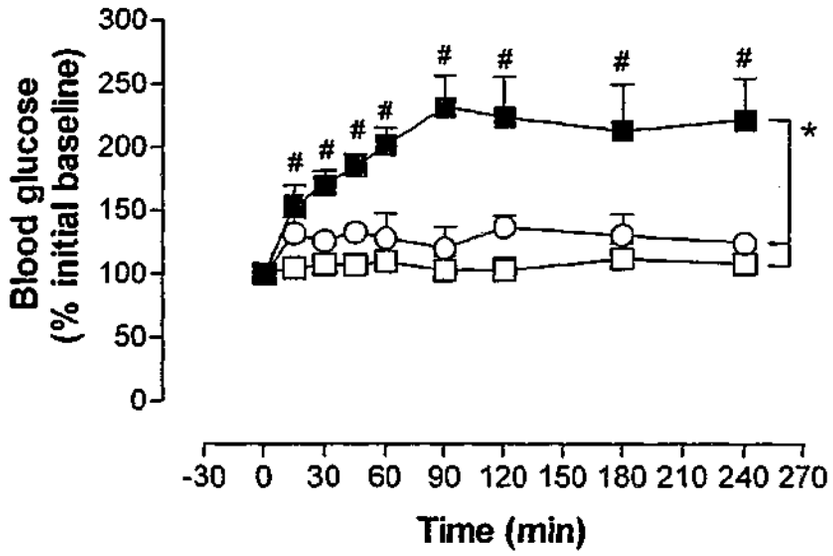

(b)

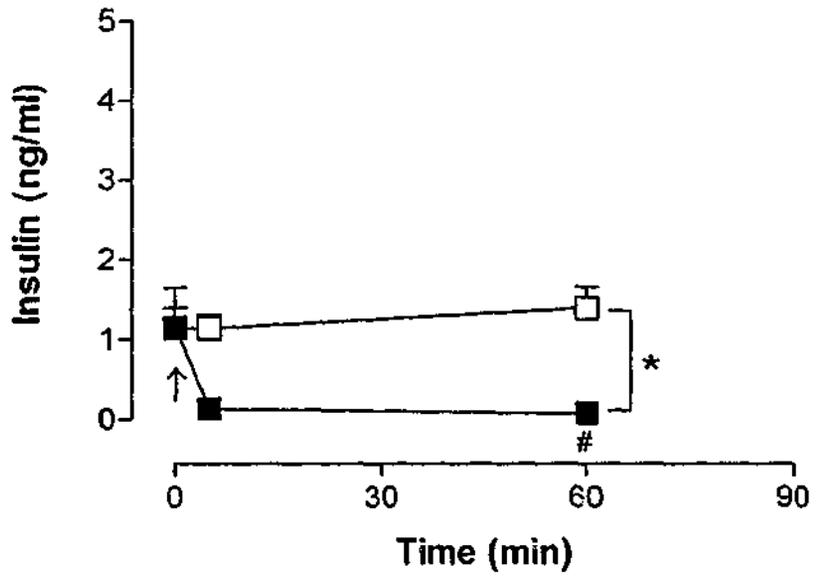

Figure 6.13 Effect of a single dose of clonidine (■; 1 μmol/kg), clonidine in the presence of rauwolscine (○; 25 μmol/kg) and vehicle (□) on (a) blood glucose represented as % of baseline value (0 min) and (b) insulin (ng/ml) over time in the anaesthetised rat. ↑ indicates administration of drug. Error bars are ± S.E.M. and if not visible are contained within the symbol. * indicates a significant difference with treatment (n=4-8; P<0.05; two way RM ANOVA). # indicates a significant difference from initial within animal baseline value (n=4-8; P<0.05; one way RM ANOVA).

(a)

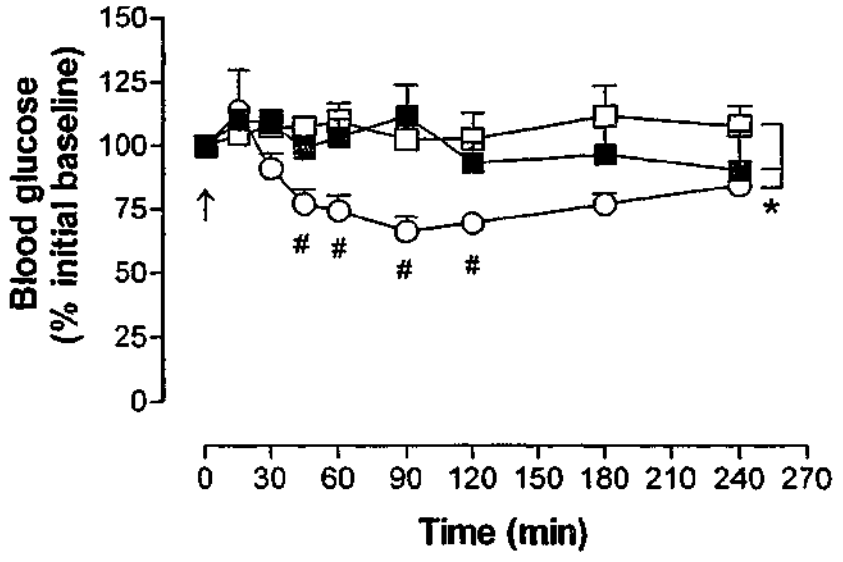

(b)

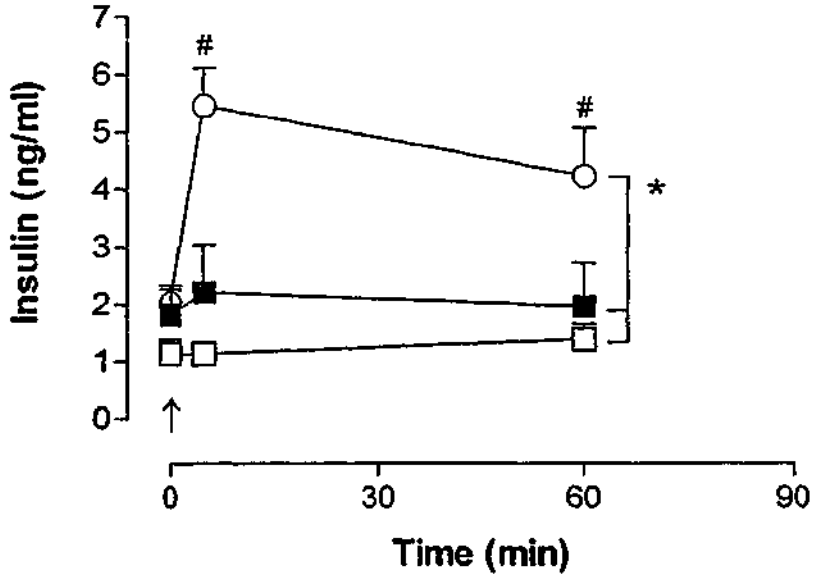

Figure 6.14 Effect of a single dose of IMID-4F (■; 10 μmol/kg), IMID-4F in the presence of rauwolscine (○; 25 μmol/kg) and vehicle (□) on (a) blood glucose represented as % of baseline value (0 min) and (b) insulin (ng/ml) over time in the anaesthetised rat. ↑ indicates administration of drug. Error bars are ± S.E.M. and if not visible are contained within the symbol. * indicates a significant difference with treatment (n=4-8; P<0.05; two way RM ANOVA). # indicates a significant difference from initial within animal baseline value (n=4-8; P<0.05; one way RM ANOVA).

(a)

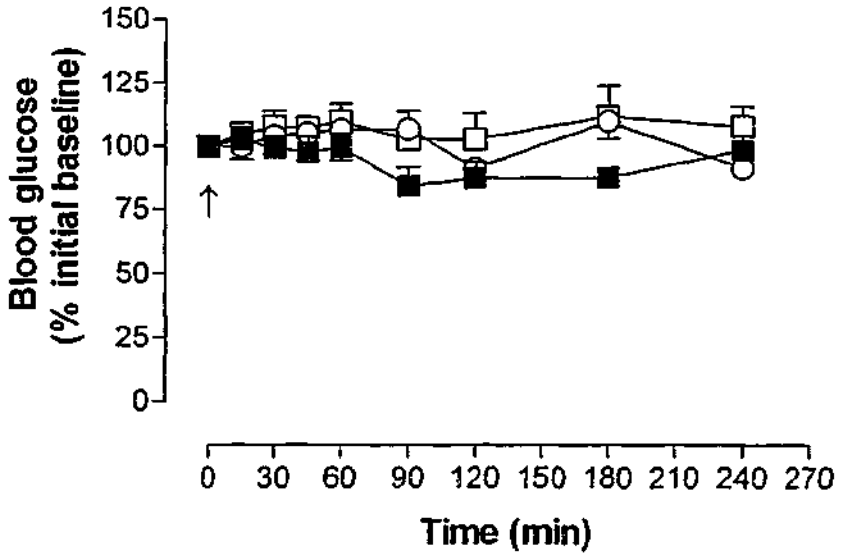

(b)

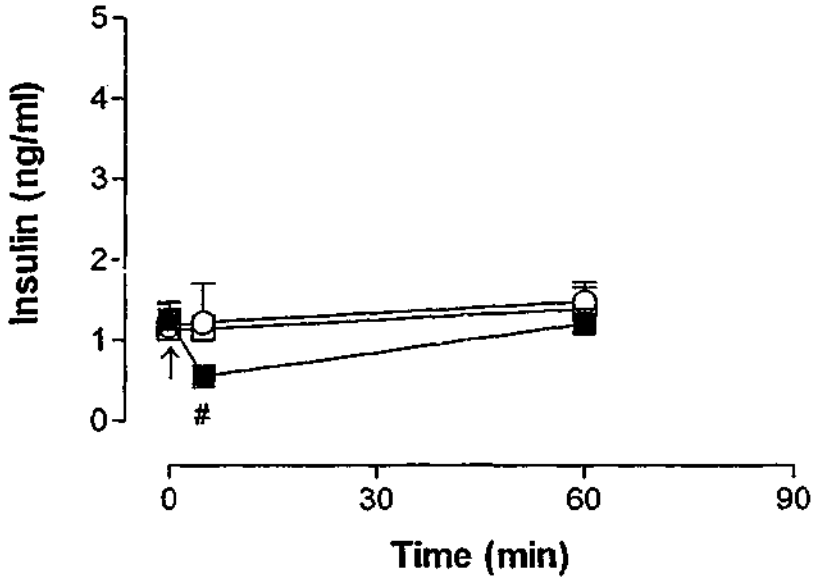

Figure 6.15 Effect of a single dose of IMID-26F (■; 10 μmol/kg), IMID-26F in the presence of rauwolscine (○; 25 μmol/kg) and vehicle (□) on (a) blood glucose represented as % of baseline value (0 min) and (b) insulin (ng/ml) over time in the anaesthetised rat. ↑ indicates administration of drug. Error bars are ± S.E.M. and if not visible are contained within the symbol (n=4-8; P>0.05; two way RM ANOVA). # indicates a significant difference from initial within animal baseline value (n=4-8; P<0.05; one way RM ANOVA).

n=4-8; P>0.05; two way RM ANOVA; one way RM ANOVA). However, IMID-26F alone, caused a transient decrease in insulin levels from a initial value of 1.3 ± 0.2 ng/ml to 0.5 ± 0.1 ng/ml at 5 minutes (Figure 6.15b; n=4; P<0.05; one way RM ANOVA). IMD-26F, in the presence of rauwolscine, did not have a significant effect on insulin levels over 1 hour (Figure 6.15b; n=4; P>0.05; one way RM ANOVA).

IMID-1M (10 μmol/kg) caused a gradual increase in blood glucose (max 175 ± 8 % at 240 min) that was significantly different from its within animal control after 120 minutes (Figure 6.16a; n=4-7; P<0.01; one way RM ANOVA). Accordingly, this increase in blood glucose was reflected by a significant decrease in insulin levels (from 1.1 ± 0.1 to 0.6 ± 0.1 ng/ml at 5 min; Figure 6.16b; n=3; P<0.05; one way RM ANOVA). Pretreatment of animals with rauwolscine (25 μmol/kg) significantly attenuated both the increase in blood glucose and reduction in insulin levels by IMID-1M (Figure 6.16; n=3-7; P<0.05; two way RM ANOVA).

There were no significant acute or time dependent effects on blood glucose or insulin levels by IMID-4F/2N (10 μmol/kg) alone, or in the presence of rauwolscine (25 μmol/kg), over the measurement periods when compared to either vehicle control or the initial within animal control values (Figure 6.17; n=4-8; P>0.05; two way RM ANOVA; one way RM ANOVA).

IMID-35MO (10 μmol/kg), caused an immediate increase in blood glucose (max 158 ± 10 % at 90 min) which was sustained over 120 minutes (Figure 6.18a; n=4-8; P<0.05; one way RM ANOVA). This increase was also reflected by a significant decrease in insulin levels (max 1.0 ± 0.6 ng/ml) at 5 minutes (Figure 6.18b; n=3; P<0.05; one way RM ANOVA). Pretreatment with rauwolscine (25 μmol/kg) significantly attenuated the increase in blood glucose by IMID-35MO (n=3-8; P<0.05;

(a)

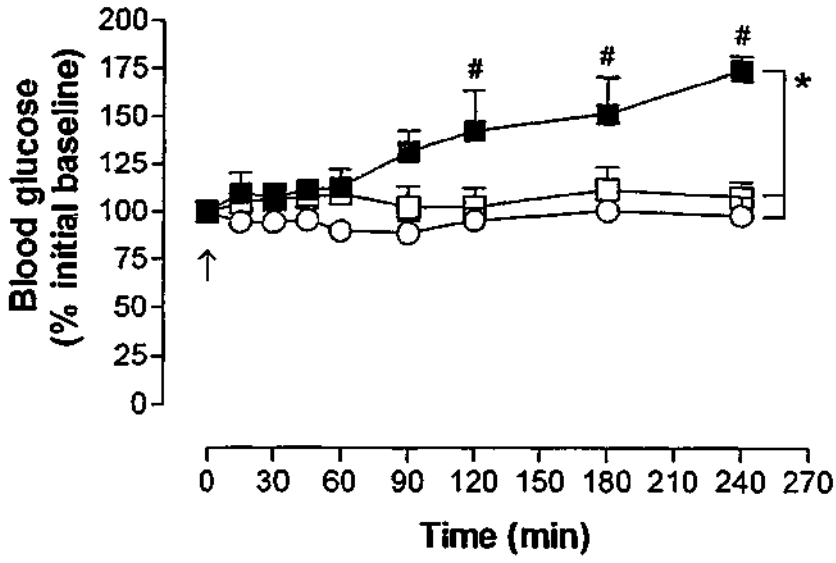

(b)

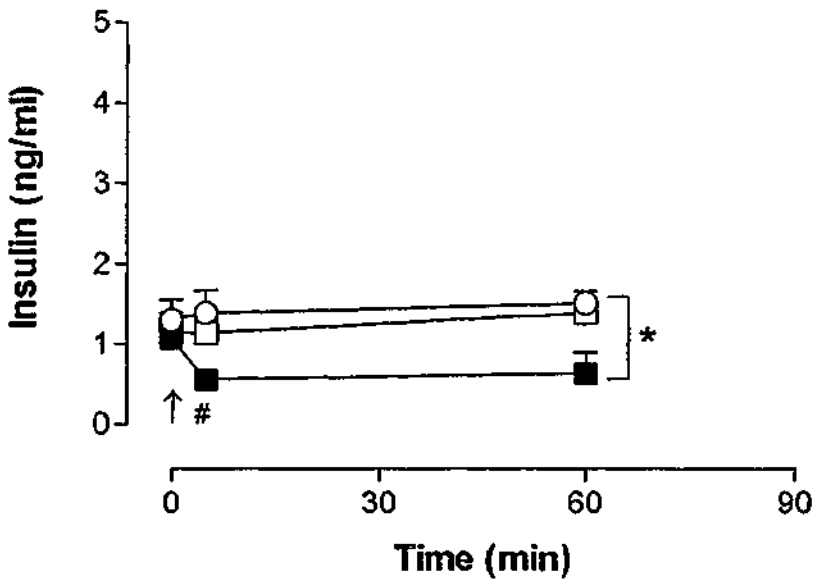

Figure 6.16 Effect of a single dose of IMID-1M (■; 10 μmol/kg), IMID-1M in the presence of rauwolscine (○; 25 μmol/kg) and vehicle (□) on (a) blood glucose represented as % of baseline value (0 min) and (b) insulin (ng/ml) over time in the anaesthetised rat. ↑ indicates administration of drug. Error bars are ± S.E.M. and if not visible are contained within the symbol. * indicates a significant difference with treatment (n=4; P<0.05; two way RM ANOVA). # indicates a significant difference from initial within animal baseline value (n=4; P<0.05; one way RM ANOVA).

(a)

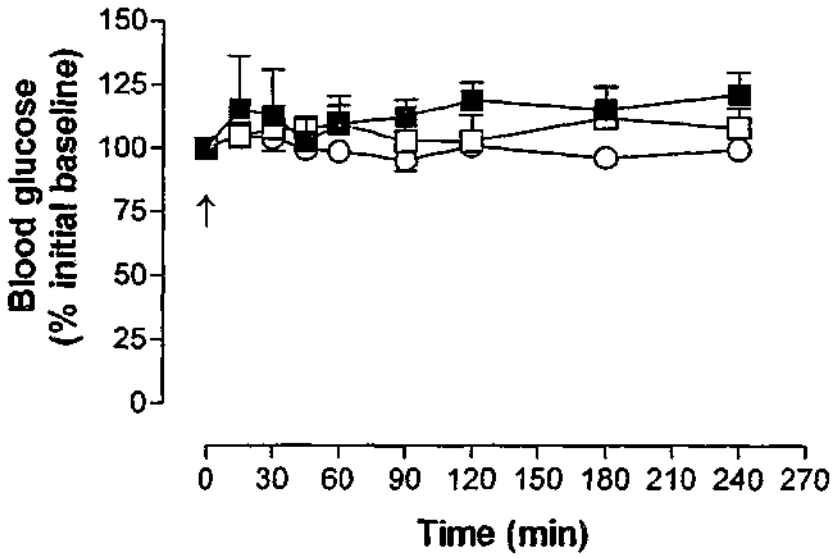

(b)

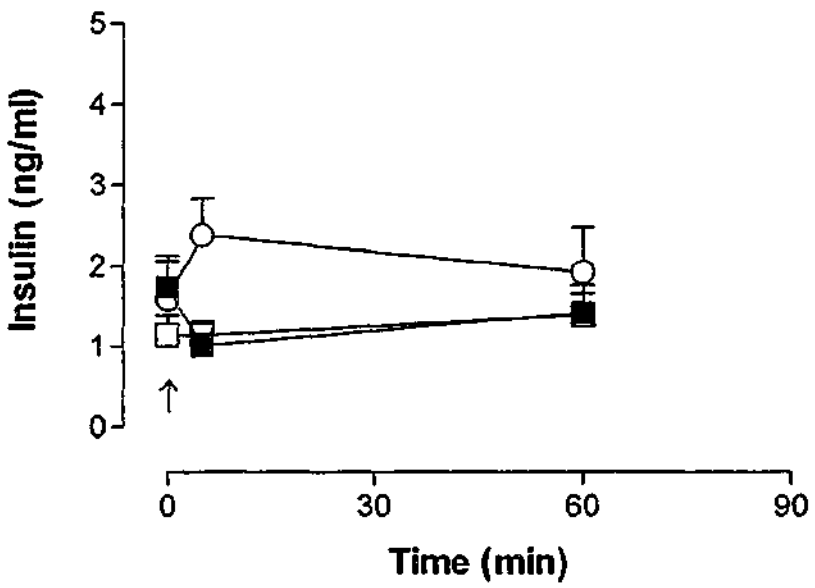

Figure 6.17 Effect of a single dose of IMID-4F/2N (■; 10 μmol/kg), IMID-4F/2N in the presence of rauwolscine (○; 25 μmol/kg) and vehicle (□) on (a) blood glucose represented as % of baseline value (0 min) and (b) insulin (ng/ml) over time in the anaesthetised rat. ↑ indicates administration of drug. Error bars are ± S.E.M. and if not visible are contained within the symbol (n=4; P>0.05; two way RM ANOVA; one way RM ANOVA).

(a)

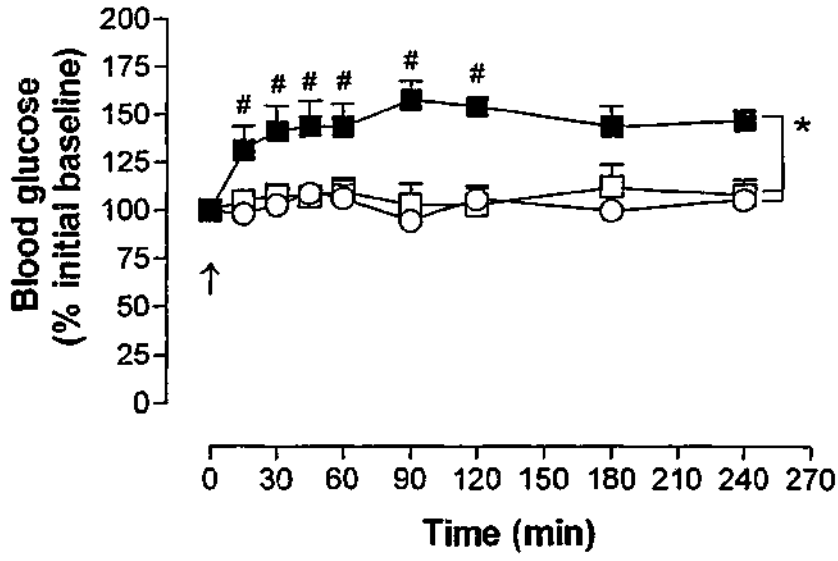

(b)

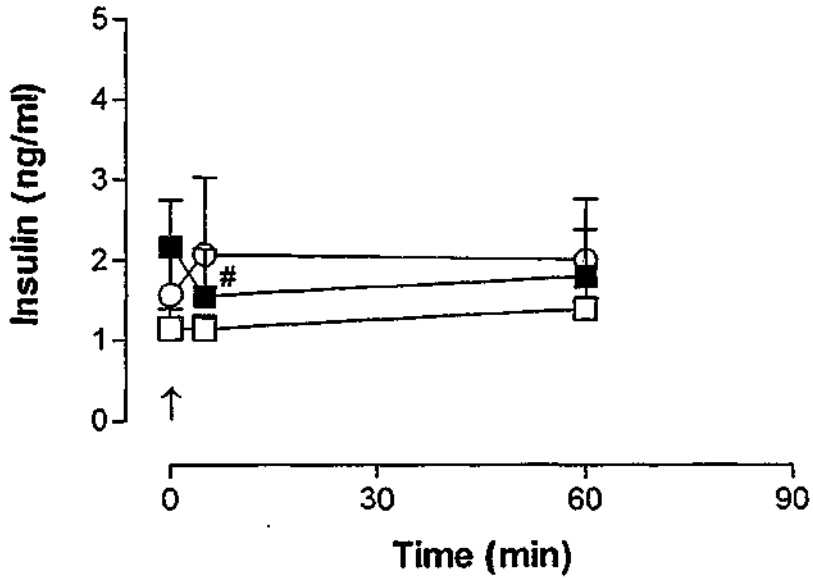

Figure 6.18 Effect of a single dose of IMID-35MO (■; 10 μmol/kg), IMID-35MO in the presence of rauwolscine (○; 25 μmol/kg) and vehicle (□) on (a) blood glucose represented as % of baseline value (0 min) and (b) insulin (ng/ml) over time in the anaesthetised rat. ↑ indicates administration of drug. Error bars are ± S.E.M. and if not visible are contained within the symbol. * indicates a significant difference with treatment (n=4-7; P<0.05; two way RM ANOVA). # indicates a significant difference from initial within animal baseline value (n=4-7; P<0.05; one way RM ANOVA).

two way RM ANOVA). Also, rauwolscine (25 μmol/kg) significantly antagonised the reduction in insulin levels caused by IMID-35MO. (Figure 6.18b; n=4; P>0.05; one way RM ANOVA).

6.3.3.2 One hour study

In this series of experiments the effect of the remaining eight imidazoline analogues (10 μmol/kg) upon insulin and blood glucose were examined for up to one hour post administration. Table 6.5 summarises the results of this study. Administration of IMID-4MO and IMID-4F/IN resulted in a significant prolonged increase in blood glucose at 30 minutes which was sustained for the one hour test period (n=4; P<0.01; one way RM ANOVA). These increases were also reflected by significant decreases in insulin levels after 60 minutes for IMID-4MO (0.6 ± 0.3 ng/ml) and a prolonged decrease after 5 minutes for IMID-4F/IN (max 0.1 ± 0.1 ng/ml at 60 min; n=4; P<0.05; one way RM ANOVA). IMID-4ME, IMID-35MO/IN, IMID-4F/O, IMID-35MO/2N and IMID-26F/2N had no significant effect on blood glucose or insulin levels over one hour (n=4; P>0.05; one way RM ANOVA). IMID-35MO/O caused a transient fall in insulin levels, apparent 5 minutes after administration (n=4; P<0.01; one way RM ANOVA), yet, no significant effect on blood glucose levels.

Compound	Blood glucose (mmol/L)		
	Baseline	**30 min**	**60 min**
IMID-4ME	5.6 ± 0.5	4.9 ± 0.6	4.7 ± 0.3
IMID-4MO	5.7 ± 0.3	7.6 ± 0.6$^{\#}$	7.6 ± 0.2$^{\#}$
IMID-35MO/IN	5.4 ± 0.3	5.2 ± 0.2	6.2 ± 0.9
IMID-4F/IN	5.7 ± 0.4	7.1 ± 0.4$^{\#}$	7.7 ± 0.6$^{\#}$
IMID-35MO/O	6.1 ± 0.4	5.8 ± 0.5	6.4 ± 0.6
IMID-4F/O	6.0 ± 0.4	6.2 ± 1.2	4.4 ± 0.3
IMID-35MO/2N	6.2 ± 0.2	6.2 ± 0.5	6.1 ± 1.1
IMID-26F/2N	6.0 ± 0.3	5.6 ± 0.1	6.0 ± 0.2
Compound	**Insulin (ng/ml)**		
	Baseline	**5 min**	**60 min**
IMID-4ME	0.9 ± 0.1	0.5 ± 0.1	1.0 ± 0.2
IMID-4MO	1.1 ± 0.4	0.6 ± 0.3	0.6 ± 0.1$^{\#}$
IMID-35MO/IN	0.9 ± 0.2	0.6 ± 0.0	1.0 ± 0.1
IMID-4F/IN	0.7 ± 0.1	0.2 ± 0.0$^{\#}$	0.1 ± 0.1$^{\#}$
IMID-35MO/O	1.3 ± 0.2	0.6 ± 0.1$^{\#}$	1.3 ± 0.3
IMID-4F/O	0.6 ± 0.1	0.3 ± 0.0	0.5 ± 0.1
IMID-35MO/2N	1.6 ± 0.4	1.5 ± 0.3	1.4 ± 0.5
IMID-26F/2N	1.6 ± 0.5	1.1 ± 0.6	1.2 ± 0.1

Table 6.5 Table summarising the effects of the imidazoline analogues on blood glucose and insulin levels in the anaesthetised rat. Measurements of blood glucose (mmol/L) and insulin (ng/ml) were taken prior to administration of the imidazoline analogues (-15 min) and 30 and 60 minutes after for blood glucose and 5 and 60 minutes after for insulin levels. $^{\#}$ indicates significant difference from initial within animal baseline values (n=4; P<0.01; one way RM ANOVA with Bonferroni t-test).

6.4 Discussion

In these studies the ability of the IMID compounds to effect MAP and heart rate were characterised in pentobarbitone anaesthetised rats. In addition, as a number of the imidazoline analogues have been shown to be potent antagonists at vascular K_{ATP} channels, their actions at other K_{ATP} channels, namely pancreatic β cell K_{ATP} channels, was also investigated.

6.4.1 Acute and time dependent changes in MAP and heart rate

Many of the clonidine derivatives examined in this study caused dose-dependent reductions in both MAP and heart rate. The most potent of these were IMID-26F, IMID-4F, IMID-4MO, IMID-35MO, IMID-35MO/2N and IMID-26F/2N, which caused reductions in both MAP (46-78 %) and heart rate (31-59 %). Although the analogues IMID-1M and IMID-4F/2N did not have substantial effects upon MAP they were significantly more potent than many of the other IMID compounds in their ability to induce reductions in heart rate (39-57 %).

Furthermore, when the time dependent effects of the IMID compounds (bolus dose of 10 μmol/kg) were assessed over a four hour period, similar initial changes in MAP to those observed acutely were observed. In addition, with the exception of IMID-1M, which reduced MAP further over time, there were no time dependent changes in MAP responses to the analogues. Likewise, changes in heart rate assessed over time were similar to those determined acutely. In addition, apart from IMID-4F, which had no effect on MAP in the four hour study, the reduction in heart rate by the analogues was sustained over the four hours of measurement.

In the shorter studies (one hour), the compounds IMID-4MO, IMID-4F/IN, IMID-35MO/2N and IMID-26F/2N caused significant reductions in MAP at various stages over the one hour of measurement. However, only the MAP reduction induced by IMID-4F/IN was sustained over one hour. The compounds, IMID-4MO, IMID-4F/IN and IMID-26F/2N, caused significant decreases in heart rate that were sustained over the hour measurement period.

Glibenclamide and other sulphonylurea derivatives have been the mainstay of treatment for type II diabetes mellitus over the last 30 years. Appropriately, they have been shown to have no significant effects on MAP or heart rate (Arnala & Uusitupa, 1983; Belloni & Hintze, 1991; Murakami *et al.*, 1992), an attribute that has made sulphonylureas suitable for use in humans. In this study, glibenclamide (1 μmol/kg) also demonstrated no appreciable effects on MAP or heart rate. These findings suggest that the effects of the IMID analogues upon both MAP and heart rate may be due to activity at sites other than K_{ATP} channels.

As previously shown (Chapter 5), many of these compounds have affinity for α-adrenoceptors. All of the imidazoline analogues, excluding the oxygen-substituted derivatives, IMID-35MO/O and IMID-4F/O, significantly displaced binding of [^{3}H]-rauwolscine and [^{3}H]-prazosin to rat cerebral cortex membranes. Secondly, given that the IMID compounds are clonidine analogues, and clonidine has been found to modulate MAP via activity at α_2-adrenoceptors, it is possible their actions may be comparable to clonidine.

It is well established that the response to clonidine on MAP is biphasic, with an initial transient hypertension, followed by a prolonged hypotension being observed (Schmitt *et al.*, 1973). Clonidine was originally thought to induce hypotension via inhibition of sympathetic tone by stimulation of α_2-adrenoceptors in the medulla

(Timmermans *et al.*, 1981). Subsequently, studies by Ernsberger (1987; 1988) found that only imidazolines, and not other adrenergic agonists, caused hypotension. It was later postulated that a novel imidazoline receptor might be involved (Ernsberger *et al.*, 1992a,b). However, this hypothesis was in direct opposition of studies that found clonidine-induced hypotension was peripherally mediated via activation of postjunctional α_{2A}-adrenoceptors in vascular smooth muscle (Pichler & Kobinger, 1978; Docherty & McGrath, 1980; Vayssettes-Courchay *et al.*, 1996). A recent study utilising D79N α_{2A}-adrenoceptor transgenic knockout mice found that α_{2A}-adrenoceptors played a crucial role, since both the hypotensive and bradycardic responses to clonidine were almost abolished in these mice (Zhu *et al.*, 1999), suggesting that an imidazoline receptor was not involved.

In accordance with the literature, in this study, intravenous clonidine (1 μmol/kg) caused an acute increase in MAP. However, in this study, clonidine did not cause the associated hypotension up to four hours after drug administration. A study by Wong (1993) found that high doses of clonidine (3-18 mg/kg) were unable to significantly decrease blood pressure. Therefore, the relatively high dose of clonidine used in the present study may be an explanation for the absence of hypotension.

Clonidine also causes a sustained reduction in heart rate both *in vivo* and *in vitro* (Tsai & Lin, 1987; Aslanian & Renaud, 1989). There have been many explanations for the bradycardia produced by clonidine. One of the first hypotheses was that the systemic administration of clonidine resulted in baroreceptor reflex stimulation or reduced peripheral noradrenaline release (Kobinger & Pichler, 1980). Some studies have reported blockade of clonidine-induced bradycardia by α_2-adrenoceptor antagonists such as rauwolscine (Timmermans *et al.*, 1981) and idazoxan (Aslanian & Renaud, 1989). In addition, vagotomy antagonises the bradycardia induced by

clonidine (Tsai & Lin, 1987). Therefore, the bradycardia may be due to the central actions of clonidine on the sympathetic nervous system resulting in no opposition of vagal tone or, possibly, a direct action on vagal tone.

Pretreatment of animals with the α_2-adrenoceptor antagonist rauwolscine did not affect the initial transient increase in MAP to clonidine in this study. This is in agreement with other studies that found that the pressor effect of clonidine was not influenced by rauwolscine, possibly due to its peripheral mechanism of action (Timmermans *et al.*, 1984). In this study, clonidine also caused bradycardia, which is also consistent with many previous studies. Rauwolscine did not significantly attenuate this response. This is in agreement with studies that found rauwolscine and other α_2-adrenoceptor antagonists, at concentrations that significantly affected the hypotension produced by clonidine, did not affect the bradycardia (Hannah *et al.*, 1983; Timmermans *et al.*, 1984).

Therefore, it is possible that the observed effect of the IMID compounds on cardiovascular parameters may be attributed to activity at α-adrenoceptors. Indeed, all of the reductions in MAP by the imidazoline analogues were significantly attenuated by rauwolscine, indicating that the hypotension was in all probability mediated by α_2-adrenoceptors. The compounds, IMID-35MO/O and IMID-4F/O did not significantly affect MAP or heart in the anaesthetised rat. This was not surprising as *in vitro* studies (Chapter 3) showed that they did not cause bradycardia in rat isolated atria and radioligand binding studies (Chapter 5) showed that they did not exhibit any α_1 or α_2-adrenoceptor activity. IMID-4F was the only compound in the four hour studies that did not affect MAP. This compound also had a lesser effect on heart rate, indicating IMID-4F may have a reduced efficacy at α_2-adrenoceptors, a detail that may be notable

when observing its effects on blood glucose and insulin levels later in this discussion. Otherwise, those that were identified as possessing α-adrenoceptor activity in radioligand binding studies, and were not very potent in reducing MAP, may not have sufficient efficacy to produce a substantial reduction in MAP, or they may act as antagonists rather than agonists.

In contrast to its effects on MAP, rauwolscine did not significantly alter the bradycardia of the majority of the compounds in the four hour study, with the exception of IMID-1M. A study by Timmermans and coworkers (1984) found that the concentration of rauwolscine that attenuated the clonidine-induced hypotension was insufficient in reducing the bradycardia. Therefore, it is possible that the concentration of rauwolscine used in the present study was not high enough to see an effect on heart rate and hence, the effects of the imidazoline analogues on heart rate may still involve α_2-adrenoceptors.

6.4.3 Time dependent changes in blood glucose and insulin levels

It has been proposed that imidazolines may be used as a new oral treatment for Type II diabetes instead of sulphonylureas based on two findings for the imidazoline, efaroxan. One, insulin secretion was increased in the presence of the highest effective dose of glibenclamide (Chan & Morgan, 1990). Two, in the presence of low glucose, efaroxan does not stimulate insulin secretion, reducing the risk of hypoglycaemia, a major life threatening side effect of sulphonylureas (Rustenbeck *et al.*, 1995). In addition, the use of sulphonylureas and their prescribed amounts in the treatment of diabetes is currently under debate due to seemingly increased levels of cardiovascular mortality associated with their use (Leibowitz & Cerasi, 1996; Melander *et al.*, 1998).

The hypoglycaemic effects of sulphonylureas, such as glibenclamide, via their actions at K_{ATP} channels in the pancreatic β cell have been well documented (Sturgess *et al.*, 1985; Trube *et al.*, 1986; Zünkler *et al.*, 1988). In this study, glibenclamide also produced a significant decrease in blood glucose associated with an increase in insulin levels. Conversely, the ability of clonidine to inhibit insulin secretion in a dose-dependent manner, via an action at inhibitory α_2-adrenoceptors, is well documented (Leclercq-Meyer *et al.*, 1980; Nakaki *et al.*, 1980). In this study, clonidine also caused an increase in blood glucose reflected by a decrease in insulin secretion. Together, these results indicated that this assay was able to detect both increases and decreases of blood glucose and insulin levels and provide us with a method of assessing the effects of the novel imidazoline analogues on these parameters. In these experiments a 10 fold higher concentration of the imidazoline analogues, compared to the concentrations of glibenclamide and clonidine, was used to enhance the possibility of observing changes in the parameters.

It has been known for some time that imidazolines such as phentolamine induce the release of insulin via the closure of pancreatic β cell K_{ATP} channels (Plant & Henequin, 1990), resulting from a direct interaction with the channel pore, $K_{IR}6.2$ (Proks & Ashcroft, 1997). The present study focused upon the ability of the IMID compounds to affect blood glucose and insulin secretion as a measure of their activity at pancreatic K_{ATP} channels.

The majority of the imidazolines had either no effect on blood glucose and insulin levels (IMID-4F/2N, IMID-4ME, IMID-35MO/IN, IMID-4F/O, IMID-35MO/2N and IMID-26F/2N) or caused significant increases in blood glucose that were associated with decreased plasma insulin levels (IMID-1M, IMID-35MO, IMID-4F/IN and IMID-4MO). IMID-26F and IMID-35MO/O decreased insulin secretion without

significantly affecting blood glucose. Although both reductions were significant they were possibly not great enough to result in an increase in blood glucose. In the presence of rauwolscine the increases in blood glucose and decrease in insulin levels by IMID-1M and IMID-35MO were no longer significant, indicating that they probably increased blood glucose and decreased insulin secretion via an action at α_2-adrenoceptors. IMID-26F and IMID-4F/2N did not significantly effect blood glucose alone or in the presence of rauwolscine, indicating no appreciable effect at postjunctional α_2-adrenoceptors in the pancreas.

The most interesting finding from this study was that IMID-4F, in the presence of rauwolscine, significantly decreased blood glucose. This decrease in blood glucose was reflected by a significant increase in insulin secretion. This finding suggests that the α_2-adrenoceptor activity of IMID-4F masks the effect of IMID-4F at pancreatic β-cell K_{ATP} channels. This finding is similar to that of phentolamine, which was found to significantly increase glucose-induced insulin release in the presence of rauwolscine (Schulz & Hasselblatt, 1989).

The increase in insulin release by IMID-4F was maintained over the 60 minutes of measurement. Although the dose of IMID-4F (10 μmol/kg) was 10 fold higher than that of glibenclamide (1 μmol/kg), the increase in insulin levels was not only higher than that observed with glibenclamide but was sustained over a longer period. This provides some evidence that imidazolines may be longer acting than sulphonylureas, a desirable action in the treatment of diabetes.

Although it may be assumed that the observed effects of IMID-4F, upon insulin and blood glucose, were due solely to inhibition of pancreatic K_{ATP} channels, the way in which imidazolines regulate insulin secretion appears to be much more complicated

than once thought. Together with their actions at K_{ATP} channels, actions by many imidazolines at sites additional to K_{ATP} channels have been reported. For example, the imidazoline derivative RX871024 has been found to activate PKA and PKC, which sensitises the exocytotic machinery of the pancreatic β cell (Zaitsev *et al.*, 1996). It has also been found to stimulate somatostatin and suppress glucagon release (Efanova *et al.*, 1998a). There is also evidence that RX871024 changes the oxidation/reduction state of the pancreatic β cell, which induces Ca^{2+} mobilisation from intracellular stores, possibly via cytochrome P-450 (Efanova *et al.*, 1998b). In addition, in cells depolarised with 25 mM KCL in the presence of diazoxide (200 μM), conditions that negate the effects of K_{ATP} channels and membrane potential, RX871024 was still able to induce insulin secretion (Zaitsev *et al.*, 1999). Taken together, these findings indicate that either $K_{IR}6.2$ plays a larger role in the regulation of insulin secretion than was first thought or that other binding sites are involved. This binding site may be an imidazoline binding site other then I_1 or I_2 and has been proposed as I_3 (Eglan *et al.*, 1998). Therefore, it is possible that IMID-4F increases insulin secretion in ways that are additional to an affect on pancreatic K_{ATP} channels.

To complicate matters further, a recent finding that not all imidazolines exhibit exactly the same characteristics (Rustenbeck *et al.*, 1999) means that imidazolines can no longer be considered as having homogenous actions. Therefore, IMID-4F may exhibit none, one or all of these additional actions. However, an investigation into the possible actions of IMID-4F on other parameters was beyond the scope of this thesis.

The results of this study indicate that the ability to lower blood glucose did not depend on the vascular K_{ATP} channel activity of the analogues. Compounds of equal potency to IMID-4F, IMID-26F and IMID-4F/2N, did not affect blood glucose alone, either when administered alone or in the presence of rauwolscine. Rather, it seems that

the efficacy of the compounds for α_2-adrenoceptors, or possibly the way in which the compounds access the binding site on $K_{IR}6.2$, which is thought to be intracellular (Proks & Ashcroft, 1997), may regulate their activity. It is also possible that IMID-4F may have actions in addition to an action at pancreatic K_{ATP} channels. Another possibility is that these compounds are more selective for vascular K_{ATP} channels than pancreatic K_{ATP} channels. In the pancreas, imidazolines are thought to act at the channel pore, $K_{IR}6.2$ (Proks & Ashcroft, 1997) while in the vasculature the channel pore is thought to be $K_{IR}6.1$ (Yamada *et al.*, 1997). This raises the possibility that the imidazoline derivatives examined in this thesis are more selective for $K_{IR}6.1$.

6.4.4 Conclusions

In summary, many of the imidazoline analogues assessed in this study caused dose-dependent reductions in MAP and heart rate. Studies which assessed the four hour effects of these compounds also found that many of the effects were prolonged over time. In addition, in studies designed to assess the activity of these compounds as possible hypoglycaemic agents, the majority of the compounds either increased or had no effect on blood glucose. The advantage of a lack of effect of these compounds at pancreatic K_{ATP} channels is that they may be selective for vascular K_{ATP} channels. However one compound, IMID-4F, in the presence of rauwolscine, significantly lowered blood glucose suggesting a possible effect at pancreatic K_{ATP} channels.

In conclusion, these compounds as they are, do not appear to be good alternatives to sulphonylureas in the treatment of diabetes. Therefore, additional studies including diabetic animals and glucose tolerance tests, did not seem warranted. Imidazoline compounds without α-adrenoceptor activity would presumably not

decrease MAP and heart rate or increase blood glucose and decrease insulin levels. For this reason development of imidazoline compounds without α-adrenoceptor activity is highly desirable for use in the treatment of Type II diabetes.

Chapter Seven

General Discussion

The primary aims of this thesis were to design, synthesise and characterise the functional and electrophysiological properties of a novel series of imidazolines and examine their ability to antagonise K_{ATP} channels. Additional aims were to investigate their selectivity and identify their site of action. These aims were examined using *in vitro*, radioligand binding and *in vivo* studies with the purpose of identifying a selective K_{ATP} channel antagonist (see Figure 7.1 for summary).

Several structural modifications of the imidazolidine, clonidine, resulted in the synthesis of 14 novel imidazolines which were studied throughout this thesis. The structural modifications resulted in clonidine analogues with benzyl substitutions on either the central nitrogen of clonidine or an imidazoline nitrogen, benzyl substitutions on both the central and an imidazoline nitrogen or an oxygen substitution in the imidazoline ring. In addition, the benzyl substitutions had varying substituents including fluoro-, methoxy-, or methyl-groups attached.

In this study, IMID-1M, the 'parent' compound, had a benzyl substitution with no substituents attached to the central nitrogen (Figure 2.1). IMID-1M was a potent K_{ATP} channel antagonist. Adding fluoro-groups (IMID-4F & IMID-26F), or two methoxy-groups (IMID-35MO) did not increase or decrease the ability of the compounds to antagonise K_{ATP} channels. However, adding a methyl- (IMID-4ME) or methoxy- (IMID-4MO) substituent decreased the ability of the compounds to antagonise K_{ATP} channels. All of the mono-substituted compounds possessed weak bradycardic actions and none possessed actions at calcium channels.

In radioligand binding studies, all these compounds were found to have weak α_1- and α_2-adrenoceptor activity. In addition, IMID-1M possessed weak muscarinic activity which was unaffected by the addition of a methyl-group (IMID-4ME).

Table 7.1 Table summarising the effect of the imidazoline compounds examined throughout this thesis using *in vitro*, radioligand binding and *in vivo* studies.

✓✓✓ indicates potent activity identified ✓✓ indicates moderate activity identified
✓ indicates weak activity identified ✗ indicates no activity identified
NA indicates that compounds were not assessed for this activity.

K_{ATP} antag.	the ability of the compounds to antagonise vascular K_{ATP} channels in pig isolated coronary arteries
↓ HR	the ability of the compounds to decrease heart rate (HR) in rat isolated spontaneously beating atria
Ca^{2+} channel	the ability of the compounds to cause vasorelaxation of pig isolated coronary arteries
α_1	the ability of the compounds to displace binding of [^{3}H]-prazosin to α_1-adrenoceptors in rat cerebral cortex membranes
α_2	the ability of the compounds to displace binding of [^{3}H]-rauwolscine to α_2-adrenoceptors in rat cerebral cortex membranes
Musc.	the ability of the compounds to displace binding of [^{3}H]-QNB to muscarinic receptors in rat cerebral cortex membranes
Ca^{2+} channel	the ability of the compounds to displace binding of [^{3}H]-PN200-110 to calcium channels in rat cerebral cortex membranes
K_{ATP} opener	the ability of the compounds to displace binding of [^{3}H]-P1075 to the opener site of the SUR in bovine smooth muscle cells
K_{ATP} antag.	the ability of the compounds to displace binding of [^{3}H]-glibenclamide to the antagonist site of the SUR in rat cerebral cortex membranes
↓ MAP	the ability of the compounds to decrease mean arterial pressure (MAP) in the anaesthetised rat
↓ HR	the ability of the compounds to decrease heart rate (HR) in the anaesthetised rat
↑ BG	the ability of the compounds to increase blood glucose (BG) in the anaesthetised rat
↓ Insulin	the ability of the compounds to decrease plasma insulin levels in the anaesthetised rat
↑ Ins. + rauw	the ability of the compounds to increase plasma insulin levels in the presence of rauwolscine in the anaesthetised rat

Compound	*In vitro*			Radioligand Binding						*In vivo*				
	K_{ATP} antag.	↓ HR	Ca^{2+} channel	α_1	α_2	Musc.	Ca^{2+} channel	K_{ATP} opener	K_{ATP} antag.	↓ MAP	↓ HR	↑ BG	↓ Insulin	↑ Ins. + rauw
IMID-1M	✓✓✓	✓	✗	✓	✓	✓	✗	✗	✗	✓	✓✓	✓✓	✓✓	✗
IMID-26F	✓✓✓	✓	✗	✓	✓	✗	✗	✗	✗	✓	✓✓	✗	✓	✗
IMID-4F	✓✓✓	✓	✗	✓	✓	✗	✗	✗	✗	✓	✓✓	✗	✗	✓✓
IMID-4ME	✓✓	✓	✗	✓	✓	✓	✗	✗	✗	✓	✓	✗	✗	NA
IMID-4MO	✓	✓	✗	✓	✓	✗	✗	✗	✗	✓✓	✓✓	✓	✓	NA
IMID-35MO	✓✓✓	✓	✗	✓	✓	✗	✗	✗	✗	✓✓	✓✓	✓✓	✓	✗
IMID-35MO/IN	✓✓	✓	✓	✓	✓	✗	✓	✗	✗	✓	✓	✗	✗	NA
IMID-4F/IN	✓	✓	✗	✓	✓	✗	✗	✗	✗	✗	✓	✓	✓	NA
IMID-35MO/O	✓	✗	✓	✗	✗	✗	✓	✗	✗	✗	✗	✗	✓	NA
IMID-4F/O	✓	✓	✓	✗	✗	✗	✓	✗	✗	✗	✗	✗	✗	NA
IMID-35MO/2N	✓✓✓	✓✓	✓	NA	NA	NA	✓	✗	✗	✓✓	✓✓	✗	✗	NA
IMID-4F/2N	✓✓✓	✓✓	✓	✓	✓	✓	✓	✓	✗	✓	✓✓	✗	✗	✗
IMID-26F/2N	✓✓✓	✓✓	✓	NA	NA	NA	✓	✓	✗	✓✓	✓✓	✗	✗	NA

In contrast, the addition of fluoro- or methoxy-groups abolished the weak activity at muscarinic receptors. None of the mono-substituted compounds had any activity at the L-type calcium channel or the opener or inhibitor sites of the K_{ATP} channel. The latter finding indicated that these compounds were not acting at the SUR and were in all probability acting at the pore of the K_{ATP} channel, the K_{IR} subunit, in a similar fashion to other imidazolines (Proks & Ashcroft, 1997; Mukai *et al.*, 1998).

In vivo characterisation of these compounds revealed they all had similar actions on MAP and heart rate. All of the compounds decreased MAP, with the methoxy-substituted compounds having a more pronounced effect. Similarly, all of the compounds moderately decreased heart rate, although it appears that a methyl-substituent slightly decreases this activity. IMID-1M and the methoxy-derivatives increased blood glucose levels, which was associated with decreased insulin levels. The fluoro- and benzyl- derivatives did not affect blood glucose, however, IMID-26F did cause a decrease in insulin levels while IMID-4F and IMID-4ME did not. It is possible that the decrease in insulin levels was not enough to significantly affect blood glucose. Treatment with rauwolscine to reduce the α_2-adrenoceptor activity of these compounds abolished the increases in blood glucose and decreases in insulin levels to IMID-1M and IMID-35MO. However, treatment with rauwolscine revealed that IMID-4F decreases blood glucose in the presence of α_2-adrenoceptor blockade. This decrease was reflected by an increase in insulin levels. It is possible that these changes in blood glucose and insulin levels are due to IMID-4F possessing actions at pancreatic β cell K_{ATP} channels.

Altering the position of the benzyl-substitution from the central nitrogen of clonidine to one of the imidazoline nitrogens (IMID-35MO/IN and IMID-4F/IN), decreased the potency of these compounds as K_{ATP} channel antagonists. Both possessed

weak bradycardic actions, as did the mono-substituted compounds, but in contrast to those compounds IMID-35MO/IN had weak antagonist actions at calcium channels.

The imidazoline-substituted compounds, IMID-35MO/IN and IMID-4F/IN, had weak α_1- and α_2-adrenoceptor activity and no muscarinic activity, again similar to the mono-substituted compounds. The vasorelaxant activity of IMID-35MO/IN, identified in the *in vitro* studies, was most probably a result of calcium channel blockade as calcium channel activity was detected in radioligand binding studies. No activity at K_{ATP} channel regulation sites on the SUR was observed.

IMID-35MO/IN and IMID-4F/IN had only minor effects on MAP and heart rate when assessed *in vivo*. Both compounds had weak actions on heart rate while only IMID-35MO/IN affected MAP. In contrast, only IMID-4F/IN caused changes in blood glucose and insulin levels. Therefore, changing the substitution from the central nitrogen to the imidazoline nitrogen decreased activity at K_{ATP} channels, conferred calcium channel activity to IMID-35MO/IN and decreased the effects of these compounds on MAP and heart rate *in vivo*.

Substituting an oxygen molecule for a nitrogen in the imidazoline ring of IMID-4F and IMID-35MO produced compounds IMID-4F/O and IMID-35MO/O, respectively. These oxygen-substituted imidazolines were much less potent as K_{ATP} channel antagonists. Substituting an oxygen did not alter the bradycardic activity for IMID-4F/O but did for IMID-35MO/O, which showed no bradycardic activity. However, this substitution gave these derivatives weak calcium channel actions *in vitro* which was confirmed via their displacement of calcium channel binding.

In contrast to all of the other compounds in this study, IMID-35MO/O and IMID-4F/O did not have any actions at α-adrenoceptors in radioligand binding

experiments, indicating that changes in the imidazoline ring may reduce α-adrenoceptor activity.

IMID-35MO/O and IMID-4F/O had little or no effect on any of the parameters examined *in vivo*. The changes in heart rate, blood pressure, blood glucose and insulin levels caused by the mono-substituted and imidazoline ring substituted imidazolines are most likely due to their α_2-activity. As there was no evidence IMID-35MO/O and IMID-4F/O had any α_2-activity, it is not surprising that the oxygen-substituted compounds had no substantial effects upon these parameters. Overall, these compounds are similar in their actions and there was no great difference between the methoxy- or fluoro-substituents.

The final structural modification of these compounds involved substituting benzyl groups with various substituents on both the central and imidazoline nitrogens of clonidine. The compounds synthesised were the bis-substituted compounds, IMID-35MO/2N, IMID-4F/2N and IMID-26/2N. These compounds were the most potent K_{ATP} channel antagonists. However, they also had the greatest non-specific effects. All caused bradycardia but in contrast to all the other compounds, at the highest concentration tested, they caused total abolition of the beating of atria *in vitro*. They also had actions at calcium channels resembling the oxygen-substituted compounds and IMID-35MO/IN, which was also supported by their displacement of calcium channel binding. Together these results indicate that altering the imidazoline ring may confer calcium channel activity to imidazolines.

As the compounds, IMID-35MO/2N and IMID-26F/2N were included late in this study, no radioligand binding for muscarinic receptors, α_1- or α_2-adrenoceptors was performed. However, IMID-4F/2N displaced binding for all these receptors. In addition, the fluoro-substituted bis compounds, IMID-4F/2N and IMID-26F/2N,

displaced binding at the opener site of K_{ATP} channels. It is possible that the size of these compounds produces a physical effect at the SUR.

The results obtained from the *in vivo* studies indicate that these compounds probably have α_2-activity due to their moderate effects of reducing both MAP and heart rate. None of the bis-substituted compounds affected blood glucose or insulin levels. Therefore, although these compounds are slightly more potent as K_{ATP} channel antagonists when compared to the mono-substituted compounds the actions of these compounds on the heart are undesirable.

Conclusions

In this thesis, the examination of novel imidazolines resulted in the identification of several potent K_{ATP} channel antagonists that may ultimately prove useful in the study of vascular K_{ATP} channels due to their apparent vascular selectivity. These compounds appear to inhibit K_{ATP} channels by inhibiting the channel pore, the K_{IR} subunit. In addition, although these compounds possessed actions at other receptor sites, they were approximately 100 fold more potent at K_{ATP} channels, indicating that at the correct concentration they may be selective in their antagonism of K_{ATP} channels.

These studies have shown that small structural modifications of imidazolines can result in substantial changes in activity at various receptors. Imidazolines that are selective for K_{ATP} channels either in the vasculature, heart or the pancreas would be useful in the treatment of conditions such as hypertension, cardiac arrhythmia or diabetes mellitus (Type II). Therefore, further studies assessing additional structural modifications may prove valuable in identifying selective imidazolines with potent actions at K_{ATP} channels.

APPENDICES

A1.1 Receptor antagonism

A fundamental concept of pharmacology is that of antagonism. This involves the effect of one drug (the agonist) being either reduced or completely eliminated in the presence of another (the antagonist) usually by either a block of the receptor or the receptor-effector linkage. An antagonist has no intrinsic activity itself but acts by inhibiting the activity of the agonist. To assess an antagonist, a concentration-response curve to the given agonist is generated in the absence and presence of differing concentrations of the antagonist. A graph is then generated to illustrate the results and it is from this graph that the antagonist can be assessed, firstly by the extent of the shift of the agonist concentration-response curve and secondly by the type of shift.

The extent of the shift given the concentration of antagonist lets us determine the potency, which is very useful in assessing the most effective antagonist at a given receptor. The type of shift seen can help allude to the nature of the antagonism. There are 2 general types of antagonism, competitive and non-competitive, which will now be briefly discussed.

A1.1.1 Competitive antagonism

Characteristics of reversible competitive antagonism involve: (1) surmountability, which is seen by a parallel shift of the concentration-response curve with no reduction in maximal response, (2) the generation of a Schild plot which is close to linear. From the Schild plot a pA_2 is determined as the –log of the concentration of an antagonist that produces a twofold shift to the right in the

concentration-response curve. And, (3) the antagonist can be washed out. A graph illustrating this type of antagonism can be seen in Figure A1.1a.

The principal behind this type of antagonism is that the dissociation rate of the antagonist molecules is high enough, so that with the addition of the agonist, a new equilibrium is quickly determined. Sulphonylureas, such as glibenclamide are a type of K_{ATP} channel antagonist that displays this type of antagonism (Challinor & McPherson, 1993).

A1.1.2 Non-competitive antagonism

In contrast to competitive antagonists, non-competitive antagonists are non-surmountable which is seen, in theory as no rightward shift in the concentration-response curve at the same time as a reduction in the maximal response. However, in practice, this is not always seen, since 'spare receptors' are sometimes present. This allows an increase in antagonist concentration that results in a shift to the right with no decrease in maximum with only higher concentrations resulting in a reduction in maximum. A graph illustrating this type of antagonism can be seen in Figure A1.1b.

The principal behind this type of antagonism is that the antagonists dissociate either very slowly or not at all from the receptors. A non-competitive antagonist is sometimes referred to as an irreversible competitive antagonist. However, the term competitive implies that the agonist and antagonist are competing for the same site which is not always the case, therefore to avoid this confusion they will be termed non-competitive antagonists throughout this thesis. Imidazolines are a type of K_{ATP} channel antagonist that displays this type of antagonism (Challinor & McPherson, 1993).

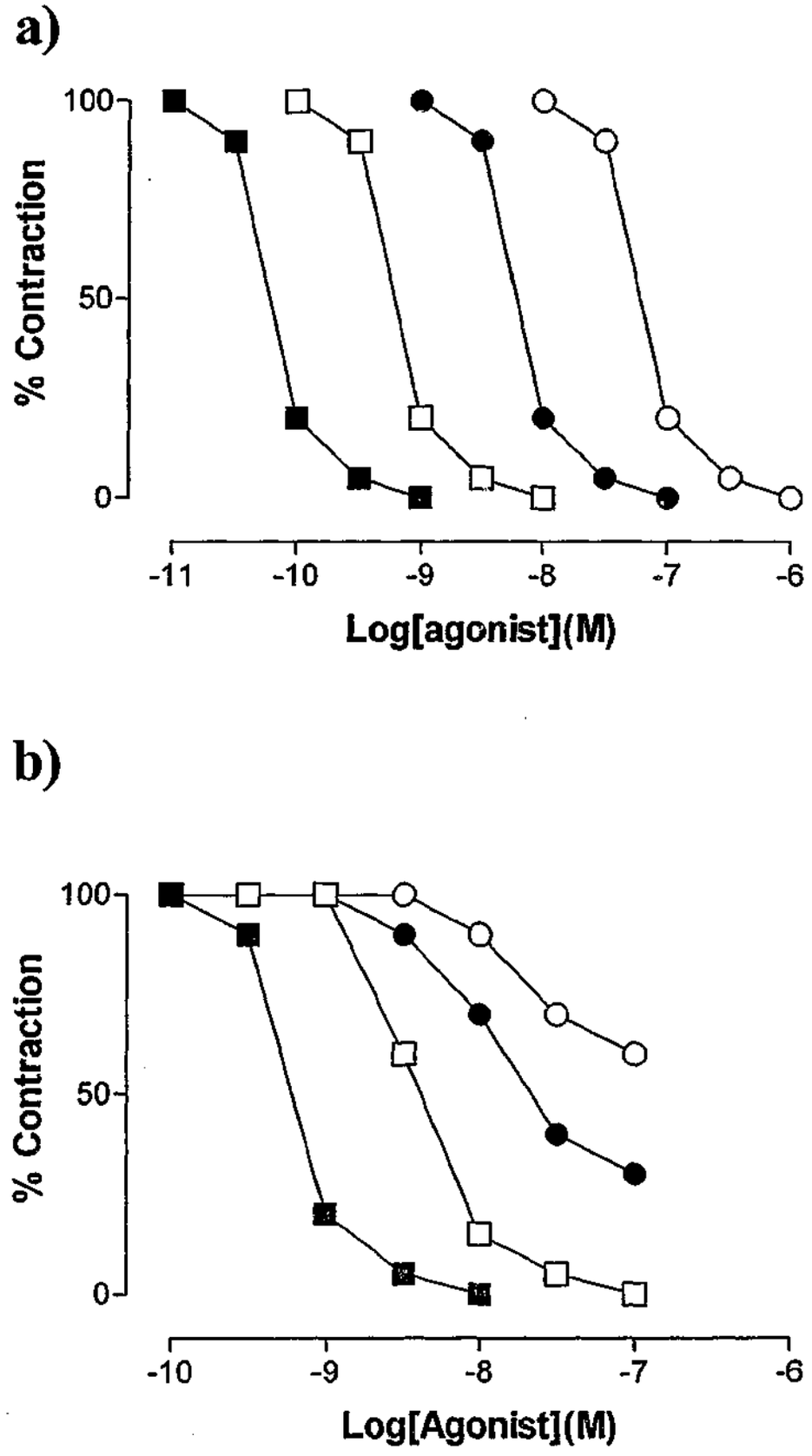

Figure A1.1 Theoretical concentration-response curve obtained in the absence (■) and presence of 1 (□), 10 (●) and 100 (○) μM of a a) competitive antagonist and b) non-competitive antagonist.

REFERENCES

AGUILAR-BRYAN, L., NICHOLS, C., WECHSLER, S., CLEMENT IV, J., BOYD III, A., GONZALEZ, G., HERRERA-SOSA, H., NGUY, K., BRYAN, J. & NELSON, D. (1995). Cloning of the β cell high-affinity sulfonylurea receptor: A regulator of insulin secretion. *Science*, **268**, 423-426.

AGUILAR-BRYAN, L., CLEMENT, J.P., GONZALEZ, G., KUNJILWAR, K., BABENKO, A. & BRYAN, J. (1998). Toward understanding the assembly and structure of K_{ATP} channels. *Physiological Reviews*, **78**, 227-245.

AGUILAR-BRYAN, L. & BRYAN, J. (1999). Molecular biology of adenosine triphosphate-sensitive potassium channels. *Endocrine Reviews*, **20**, 101-135.

ALEKSEEV, A.E., KENNEDY, M.E., NAVARRO, B. & TERZIC, A. (1997). Burst kinetics of co-expressed Kir6.2/SUR1 clones: comparison of recombinant with native ATP-sensitive K^+ channel. *Journal of Membrane Biology*, **159**, 161-168.

ÄMMÄLÄ, C., MOORHOUSE, A., GRIBBLE, F., ASHFIELD, R., PROKS, P., SMITH, P.A., SAKURA, H., COLES, B., ASHCROFT, S.J.H. & ASHCROFT, F.M. (1996a). Promiscuous coupling between the sulphonylurea receptor and inwardly rectifying potassium channels. *Nature*, **379**, 545-548.

ÄMMÄLÄ, C., MOORHOUSE, A. & ASHCROFT, F. (1996b). The sulphonylurea receptor confers diazoxide sensitivity on the inwardly rectifying K^+ channel Kir6.1 expressed in human embryonic kidney cells. *Journal of Physiology*, **494**, 709-714.

ARNALA, L. & UUSITUPA, M. (1983). A double-blind comparison of two glibenclamide preparations, HB 419 and HB 420, in maturity-onset (type 2) diabetic patients. *Annals of Clinical Research*, **15**, 33-35.

ASHCROFT, F.M., HARRISON, D.E. & ASHCROFT, S.J. (1984). Glucose induces closure of single potassium channels in isolated rat pancreatic beta-cells. *Nature*, **312**, 446-448.

ASHCROFT, F.M. & GRIBBLE, F.M. (1998). Correlating structure and function in ATP-sensitive K^+ channels. *Trends in Neuroscience*, **21**, 288-294.

ASHCROFT, F.M. & KAKEI, M. (1989). ATP-sensitive K^+ channels in rat pancreatic β-cells: modulation by ATP and Mg^{2+} ions. *Journal of Physiology*, **416**, 349-367.

ASHCROFT, S. & ASHCROFT, F. (1990). Properties and functions of ATP-sensitive K-channels. *Cell Signalling*, **2**, 197-215.

ASHCROFT, S. & ASHCROFT, F. (1992). The sulphonylurea receptor. *Biochimica et Biophysica Acta*, **1175**, 45-59.

ASHFORD, M.L., STURGESS, N.C., TROUT, N.J., GARDNER, N.J. & HALES, C.N. (1988). Adenosine-5'-triphosphate-sensitive ion channels in neonatal rat cultured central neurones. *Pflügers Archives - European Journal of Physiology*, **412**, 297-304.

ASLANIAN, V. & RENAUD, B. (1989). Changes in serotonin metabolism in the rat raphe magnus and cardiovascular modifications following systemic administration of clonidine and other central alpha 2-agonists: an in vivo voltammetry study. *Neuropharmacology*, **28**, 387-395.

BABENKO, A.P., AGUILAR-BRYAN, L. & BRYAN, J. (1998). A view of SUR/K_{IR}6.x, K_{ATP} channels. *Annual Review of Physiology*, **60**, 667-687.

BABENKO, A.P., GONZALEZ, G., AGUILAR-BRYAN, L. & BRYAN, J. (1999). Sulfonylurea receptors set the maximal open probability, ATP sensitivity and plasma membrane density of K_{ATP} channels. *FEBS Letters*, **445**, 131-136.

BANG, L. & NIELSEN-KUDSK, J. (1992). Smooth muscle relaxation and inhibition of responses to pinacidil and cromakalim induced by phentolamine in guinea-pig isolated trachea. *European Journal of Pharmacology*, **211**, 235-241.

BECHTEL, W.D., MIERAU, J. & TIMMERMANS, P.B.M.W.M. (1985). Inhibition of [^{3}H]clonidine binding to rat brain α-adrenoceptors by imidazolidines: correlation of binding potency and hypotensive activity. *Arzneimittel-Forschung*, **35**, 428-431.

BECKERINGH, J.J., THOOLEN, M.J., DE JONGE, A., WILFFERT, B., TIMMERMANS, P.B. & VAN ZWEITEN, P.A. (1984). The contractions induced in rat and guinea-pig aortic strips by the alpha 2-adrenoceptor selective agonists B-HT 920 and UK 14,304 are mediated by alpha 1-adrenoceptors. *European Journal of Pharmacology*, **104**, 197-203.

BEECH, D., ZHANG, H., NAKAO, K. & BOLTON, T. (1993a). K channel activation by nucleotide diphosphates and its inhibition by glibenclamide in vascular smooth muscle cells. *British Journal of Pharmacology*, **110**, 573-582.

BEECH, D., ZHANG, H., NAKAO, K. & BOLTON, T. (1993b). Single channel and whole-cell K-currents evoked by levcromakalim in smooth muscle cells from the rabbit portal vein. *British Journal of Pharmacology*, **110**, 583-590.

BELLES, B., HESCHELER, J. & TRUBE, G. (1987). Changes of membrane currents in cardiac cells induced by long whole-cell recordings and tolbutamide. *Pflügers Archives - European Journal of Physiology*, **409**, 582-588.

BELLONI, F.L. & HINTZE, T.H. (1991). Glibenclamide attenuates adenosine-induced bradycardia and coronary vasodilatation. *American Journal of Physiology*, **261**, H720-H727.

BERNE, R.M. (1980). The role of adenosine in cardiac blood flow. *Circulation Research*, **47**, 807-813.

BONEV, A.D. & NELSON, M.T. (1996). Vasoconstrictors inhibit ATP-sensitive K^+ channels in arterial smooth muscle through protein kinase C. *Journal of General Physiology*, **108**, 315-323.

BOUCHARD, J.-F., DUMONT, E. & LAMONTAGNE, D. (1994). Evidence that prostaglandins I_2, E_2, and D_2 may activate ATP sensitive potassium channels in the isolated rat heart. *Cardiovascular Research*, **28**, 901-905.

BOUMAN, L.N., DUIVENVOORDEN, J.J., OPTHOF, T. & TREIJTEL, B.W. (1984). Electrophysiological effects of alinidine on nodal and atrial fibres in the guinea-pig heart. *Journal of Pharmacology and Experimental Therapeutics*, **229**, 551-556.

BRAY, K.M. & QUAST, U. (1992). A specific binding site for K^+ channel openers in rat aorta. *Journal of Biological Chemistry*, **267**, 11689-11692.

BROWN, C., CHAN, S., STILLINGS, M., SMITH, S. & MORGAN, N. (1993). Antagonism of the stimulatory effects of efaroxan and glibenclamide in rat pancreatic islets by the imidazoline, RX801080. *British Journal of Pharmacology*, **110**, 1017-1022.

BUCKINGHAM, R.E., HAMILTON, T.C., HOWLETT, D.R., MOOTOO, S. & WILSON, C. (1989). Inhibition by glibenclamide of the vasorelaxant action of cromakalim in the rat. *British Journal of Pharmacology*, **97**, 57-64.

BURR, I.M., MARLISS, E.B., STAUFFACHER, W. & RENOLD, A.E. (1971). Diazoxide effects on biphasic insulin release: 'adrenergic' suppression and enhancement in the perfused rat pancreas. *Journal of Clinical Investigation*, **50**, 1444-1450.

CAMBRIDGE, D. (1981). UK-14304, a potent and selective α_2-adrenoceptor agonist for the characterisation of α-adrenoceptor subtypes. *European Journal of Pharmacology*, **72**, 413-415.

CARMAN-KRZAN, M., KRZAN, M. & SCHUNACK, W. (1997). Pharmacological properties of cardiovascular histamine H_1 receptor binding sites: characterisation with 2-phenylhistamines. *Naunyn-Schmiedeberg's Archives of Pharmacology*, **355**, 431-437.

CASON, B.A., GORDON, H.J., AVERY, E.G.T. & HICKEY, R.F. (1995). The role of ATP sensitive potassium channels in myocardial protection. *Journal of Cardiac Surgery*, **10**, 441-444.

CHALLINOR, J.L. & MCPHERSON, G.A. (1993). Evidence that imidazoli(id)ine- and sulphonylurea-based antagonists of cromakalim act at different sites in the rat thoracic aorta. *Clinical and Experimental Pharmacology and Physiology*, **20**, 467-475.

CHALLINOR-ROGERS, J.L., HAY, T.K.C. & MCPHERSON, G.A. (1994). Comparison of the cromakalim antagonism and bradycardic actions of a series of novel alinidine analogues. *Naunyn-Schmiedeberg's Archives of Pharmacology*, **350**, 158-166.

CHALLINOR-ROGERS, J.L. (1995). Studies with drugs with K_{ATP} channel antagonist actions. PhD, Department of Pharmacology, Monash University, 325.

CHALLINOR-ROGERS, J.L., KONG, D.C.M., ISKANDER, M.N. & MCPHERSON, G.A. (1995). Structure-activity relationship of glibenclamide analogs: A comparison of potency as levcromakalim antagonists in rat aorta vs affinity for [^{3}H]-glibenclamide binding to membranes from rat cerebral cortex. *Journal of Pharmacology and Experimental Therapeutics*, **273**, 778-786.

CHALLINOR-ROGERS, J.L., ROSENFELT, F.L., DU, X. & MCPHERSON, G.A. (1997). Antiischaemic and antiarrythmic activities of some novel alinidine analogs in the rat heart. *Journal of Cardiovascular Pharmacology*, **29**, 499-507.

CHAN, S.L. & MORGAN, N.G. (1990). Stimulation of insulin secretion by efaroxan may involve interaction with potassium channels. *European Journal of Pharmacology*, **176**, 97-101.

CHAN, S.L., DUNNE, M.J., STILLINGS, M.R. & MORGAN, N.G. (1991). The alpha 2-adrenoceptor antagonist efaroxan modulates K^+_{ATP} channels in insulin-secreting cells. *European Journal of Pharmacology*, **204**, 41-48.

CHAN, S.L., BROWN, C.A. & MORGAN, N.G. (1993). Stimulation of insulin secretion by the imidazoline alpha 2-adrenoceptor antagonist efaroxan is mediated by a novel, stereoselective, binding site. *European Journal of Pharmacology*, **230**, 375-378.

CHAN, S.L., BROWN, C.A., SCARPELLO, K.E. & MORGAN, N.G. (1994). The imidazoline site involved in control of insulin secretion: characteristics that distinguish it from I_1- and I_2-sites. *British Journal of Pharmacology*, **112**, 1065-1070.

CHANDY, K. & GUTMAN, G. (1993). Nomenclature for mammalian potassium channel genes. *Trends in Pharmacological Science*, **14**, 434.

CHRISTIE, M. (1995). Molecular diversity and functional diversity of K^+ channels. *Clinical & Experimental Pharmacology & Physiology*, **22**, 944-951.

CHUTKOW, W.A., SIMON, M.C., LE BEAU, M.M. & BURANT, C.F. (1996). Cloning, tissue expression, and chromosomal localization of SUR2, the putative drug-binding subunit of cardiac, skeletal muscle, and vascular K_{ATP} channels. *Diabetes*, **45**, 1439-1445.

CLAPP, L.H. (1995). Regulation of glibenclamide-sensitive K^+ current by nucleotide phosphates in isolated rabbit pulmonary myocytes. *Cardiovascular Research*, **30**, 460-468.

CLAYTON, J., HESS, T., SMITH, M. & GROVER, G. (1992). Coronary reactive hyperaemia and adenosine-induced vasodilation are mediated partially by a glyburide-sensitive mechanism. *Pharmacology*, **44**, 92-100.

CLEMENT, J.P., KUNJILWA, K., GONZALEZ, G., SCHWANSTECHER, M., PANTEN, U., AGUILAR-BRYAN, L. & BRYAN, J. (1997). Association and stoichiometry of K_{ATP} channel subtypes. *Neuron*, **18**, 827-838.

COCKS, T.M., KING, S.J. & ANGUS, J.A. (1990). Glibenclamide is a competitive antagonist of the thromboxane A_2 receptor in dog coronary artery. *British Journal of Pharmacology*, **100**, 375-378.

COOK, D.L. & HALES, C.N. (1984). Intracellular ATP directly blocks K^+ channels in pancreatic β-cells. *Nature*, **311**, 271-273.

CREPEL, V., KRNJEVIC, K. & BEN-ARI, Y. (1993). Sulphonylureas reduce the slowly inactivating D-type outward current in rat hippocampal neurons. *Journal of Physiology*, **466**, 39-54.

CRIDDLE, D.N., GREENWOOD, I.A. & WESTON, A.H. (1994). Levcromakalim-induced modulation of membrane potassium currents, intracellular calcium and mechanical activity in rat mesentric artery. *Naunyn-Schmiedeberg's Archives of Pharmacology*, **349**, 422-430.

DART, C. & STANDEN, N.B. (1993). Adenosine-activated potassium current in smooth muscle cells isolated from the pig coronary artery. *Journal of Physiology*, **471**, 767-786.

DAUT, J., MAIER-RUDOLPH, W., VON BECKERATH, N., MEHRKE, G., GUNTHER, K. & GOEDEL-MEINEN, L. (1990). Hypoxic dilation of coronary arteries is mediated by ATP-sensitive potassium channels. *Science*, **247**, 1341-1344.

DAVIES, N.W., SPRUCE, A.E., STANDEN, N.B. & STANFIELD, P.R. (1989). Multiple blocking mechanisms of ATP-sensitive potassium channels of frog skeletal muscle by tetraethylammonium ions. *Journal of Physiology*, **413**, 31-47.

DAVIES, N.W., STANDEN, N.B. & STANFIELD, P.R. (1991). ATP-dependent potassium channels of muscle cells: their properties, regulation, and possible functions. *Journal of Bioenergetics & Biomembranes*, **23**, 509-535.

DEAN, M. & ALLIKMETS, R. (1995). Evolution of ATP-binding cassette transporter genes. *Current Opinion in Genetic Development*, **5**, 779-785.

DECKER, N., LECLERC, G., QUENNEDEY, M.-C., ROUOT, B. & SCHWARTZ, J. (1983). Study of two alkylating derivatives: the p-isothiocyanato- and the p-methylisothiocyanato-clonidine. *European Journal of Pharmacology*, **93**, 205-211.

DENNIS, P.D. & VAUGHAN WILLIAMS, E.M. (1986). Further studies of alinidine induced bradycardia in the presence of caesium. *Cardiovascular Research*, **20**, 375-378.

DETIMARY, P., JONAS, J.-C. & HENQUIN, J.-C. (1996). Stable and diffusible pools of nucleotides in pancreatic islet cells. *Endocrinology*, **137**, 4671-4676.

DiTullio, N.W., Cieslinski, L., Matthews, W.D. & Storer, B. (1984). Mechanisms involved in the hyperglycemic response induced by clonidine and other alpha-2 adrenoceptor agonists. *Journal of Pharmacology & Experimental Therapeutics*, **228**, 168-73.

Docherty, J.R. & McGrath, J.C. (1980). A comparison of pre- and post-junctional potencies of several α-adrenoceptor agonists in the cardiovascular system and anococcygeus muscle of the rat. Evidence for two types of post-junctional α-adrenoceptors. *Naunyn-Schmiedeberg's Archives of Pharmacology*, **312**, 107.

Doupnik, C., Davidson, N. & Lester, H.A. (1995). The inward rectifier potassium channel family. *Current Opinion in Neurobiology*, **5**, 268-277.

Dunne, M.J. & Petersen, O.H. (1986). Intracellular ADP activates K^+ channels that are inhibited by ATP in an insulin-secreting cell line. *FEBS Letters*, **208**, 59-62.

Dunne, M.J., Ilott, M.C. & Peterson, O.H. (1987). Interactions of diazoxide, tolbutamide and ATP^{4-} on nucleotide-dependent K^+ channels in an insulin-secreting cell line. *Journal of Membrane Biology*, **104**, 271-279.

Dunne, M.J. (1991). Block of ATP-regulated potassium channels by phentolamine and other alpha-adrenoceptor antagonists. *British Journal of Pharmacology*, **103**, 1847-1850.

Dunne, M.J., Harding, E.A., Jaggar, H. & Squires, P.E. (1994). Ion channels and the molecular control of insulin secretion. *Biochemical Society Transactions*, **22**, 6-12.

ECKMAN, D., FRANKOVICH, J. & KEEF, K. (1992). Comparison of the actions of acetylcholine and BRL 38227 in the guinea-pig coronary artery. *British Journal of Pharmacology*, **106**, 9-16.

EDWARDS, G., HENSHAW, M., MILLER, M. & WESTON, A.J. (1991). Comparison of the effects of several potassium-channel openers on rat bladder and rat portal vein in vitro. *British Journal of Pharmacology*, **102**, 679-686.

EDWARDS, G. & WESTON, A. (1995). The role of potassium channels in excitable cells. *Diabetes Research and Clinical Practice*, **28**, S57-S66.

EFANOVA, I.B., ZAITSEV, S.V., EFANOV, A.M., OSTENSON, C.-G., RAAP, A., MEST, H.-J., BERGGREN, P.-O. & EFENDIC, S. (1998a). Effects of imidazoline derivative RX871024 on insulin, glucagon, and somatostatin secretion from isolated perfused rat pancreas. *Biochemical and Biophysical Research Communications*, **252**, 162-165.

EFANOVA, I.B., ZAITSEV, S.V., BROWN, G., BERGGREN, P.-O. & EFANDIC, S. (1998b). RX871024 induces Ca^{2+} mobilisation from Thapsigargin-sensitive stores in mouse pancreatic beta-cells. *Diabetes*, **471**, 211-218.

EGLAN, R.M., HUDSON, A.L., KENDALL, D.A., NUTT, D.J., MORGAN, N.G., WILSON, V.G. & DILLON, M.P. (1998). 'Seeing through a glass darkly': casting light on imidazoline 'I' sites. *Trends in Pharmacological Sciences*, **19**, 381-390.

ELTZE, M. (1989). Glibenclamide is a competitive antagonist of cromakalim, pinacidil and RP 49356 in guinea-pig pulmonary artery. *European Journal of Pharmacology*, **165**, 231-239.

ERNSBERGER, P., MEELEY, P. & REIS, D.J. (1987). Clonidine binds to imidazole binding sites as well as α_2-adrenoceptors in the ventrolateral medulla. *European Journal of Pharmacology*, **134**, 1-13.

ERNSBERGER, P., GIULIANO, R., WILLETT, R.N., GRANATA, A.R. & REIS, D.J. (1988). Hypotensive action of clonidine analogs correlates with binding affinity at imidazole and not α_2-adrenergic receptors in the rostral ventrolateral medulla. *Journal of Hypertension*, **6**, S554-S557.

ERNSBERGER, P., HAXHIU, M.A., DAMON, T.H. & WENDORFF, L.A. (1992a). Imidazoline-I_1 receptors and brainstem autonomic control: membrane binding, autoradiographic and functional studies. *FASEB Journal*, **6**, A1874.

ERNSBERGER, P.R., WESTBROOKS, K.L., CHRISTEN, M.O. & SHAFER, S.G. (1992b). A second generation of centrally acting antihypertensive agents act on putative I_1-imidazoline receptors. *Journal of Cardiovascular Pharmacology*, **20**, S1-S10.

ESCANDE, D., THURINGER, D., LEGUERN, S. & CAVERO, L. (1988). The potassium channel opener cromakalim (BRL 34915) activates ATP-dependent K^+ channels in isolated cardiac myocytes. *Biochemical and Biophysical Research Communications*, **154**, 620-625.

FAN, Z., NAKAYAMA, K. & HIRAOKA, M. (1990). Multiple actions of pinacidil on adenosine triphosphate-sensitive potassium channels in guinea-pig ventricular myocytes. *Journal of Physiology*, **430**, 272-295.

FARACI, F., BREESE, K. & HEISTAD, D. (1994). Cerebral vasodilation during hypercapnia: role of glibenclamide-sensitive potassium channels and nitric oxide. *Stroke*, **25**, 1679-1683.

FINDLAY, I. (1992). Inhibition of ATP-sensitive K^+ channels in cardiac muscle by the sulphonylurea drug glibenclamide. *Journal of Pharmacology and Experimental Therapeutics*, **261**, 540-545.

FOSSET, M., DE WEILLE, J.R., GREEN, R.D., SCHMID-ANTOMARCHI, H. & LAZDUNSKI, M. (1988). Antidiabetic sulphonylureas control action potential properties in heart cells via high affinity receptors that are linked to ATP-dependent K^+ channels. *Journal of Biological Chemistry*, **263**, 7933-7936.

FRENCH, J.F., RIERA, L.C. & SARMIENTO, J.G. (1990). Identification of high and low (GTP-sensitive) affinity [^{3}H]glibenclamide binding sites in cardiac ventricular membranes. *Biochemical and Biophysical Research Communications*, **167**, 1400-1405.

FURUKAWA, K., ITOH, T., KAJIWARA, M., KITAMURA, K., SUZUKI, H., ITO, Y. & KURIYAMA, H. (1981). Vasodilating actions of 2-nicotinamidoethyl nitrate on porcine and guinea-pig coronary arteries. *Journal of Pharmacology and Experimental Therapeutics*, **218**, 248-259.

GAINES, K.L., HAMILTON, S. & BOYD, A.E. (1988). Characterization of the sulfonylurea receptor on beta cell membranes. *Journal of Biological Chemistry*, **263**, 2589-2592.

GARCIA, M.L., HANNER, M., KNAUS, H., KOCH, R., SCHMALHOFER, W., SLAUGHTER, R.S. & KACZOROWSKI, G.J. (1997). Pharmacology of potassium channels. In *Advances in Pharmacology*. pp. 425-471. San Diego: Academic Press.

GARLAND, C.J. & MCPHERSON, G.A. (1992). Evidence that nitric oxide does not mediate the hyperpolarization to acetylcholine in rat small mesenteric artery. *British Journal of Pharmacology*, **105**, 429-435.

GARLID, K., PAUCEK, P., YAROV-YAROVOY, V., MURRAY, H., DARBENZIO, R., D'ALONZO, A., LODGE, N., SMITH, M. & GROVER, G. (1997). Cardioprotective effects of diazoxide and its interaction with mitochondrial ATP-sensitive K^+ channels. *Circulation Research*, **81**, 1072-1082.

GEISEN, K., HITZEL, V., OKOMONOPOULOS, E., PUNTER, J., WEYER, R. & SUMM, H.-D. (1985). Inhibition of ^{3}H-glibenclamide binding to sulphonylurea receptors by oral antidiabetics. *Arzneimittel-Forschung*, **35**, 707-712.

GELBAND, C.H. & MCCULLOUGH, J.R. (1993). Modulation of rabbit aortic Ca^{2+} - activated K^+ channels by pinacidil, cromakalim and glibenclamide. *American Journal of Physiology*, **264**, C1119-C1127.

GHOSH, A., RONNER, P., CHEONG, E., KHALID, P. & MATSCHINSKY, F. (1991). The role of ATP and free ADP in metabolic coupling during fuel-stimulated insulin release from islet β-cells in the isolated rat perfused pancreas. *Journal of Biological Chemistry*, **266**, 22887-22892.

GOGELEIN, H. & GREGER, R. (1987). Properties of single K channels in the basolateral membrane of rabbit proximal straight tubules. *Pflügers Archives - European Journal of Physiology*, **410**, 288-295.

GOPALAKRISHNAN, M., JOHNSON, D.E., JANIS, R.A. & TRIGGLE, D.J. (1991). Characterization of binding of the ATP-sensitive potassium channel ligand [^{3}H]glyburide to neuronal and muscle preparations. *Journal of Pharmacology and Experimental Therapeutics*, **257**, 1162-1171.

GOPALAKRISHNAN, M. & TRIGGLE, D.J. (1992). Regulation of ATP-sensitive K^+ channels by chronic glyburide and pinacidil administration. *Biochemical Pharmacology*, **44**, 1843-1847.

GRIBBLE, F.M., TUCKER, S.J. & ASHCROFT, F.M. (1997a). The essential role of the Walker A motifs of SUR1 in K_{ATP} channel activation by Mg-ADP and diazoxide. *The EMBO Journal*, **16**, 1145-1152.

GRIBBLE, F.M., ASHFIELD, R., AMMALIA, C. & ASHCROFT, F.M. (1997b). Properties of cloned ATP-sensitive K^+ currents expressed in *Xenopus* oocytes. *Journal of Physiology*, **498**, 87-98.

GRISSMER, S. (1997). Potassium channels still hot. *Trends in Pharmacological Sciences*, **18**, 347-350.

GROS, P., TALBOT, F., TANG-WEI, D., BIBI, E. & KABACK, R. (1992). Lipophilic cations: A group of model substrates for the multidrug-resistance transporter. *Biochemistry*, **21**, 1992-1998.

GROSS, G. & AUCHAMPACH, J. (1992). Blockade of ATP-sensitive potassium channels prevents myocardial preconditioning in dogs. *Circulation Research*, **70**, 223-233.

GROVER, G.J., D'ALONZO, A.K., DZWONCZYK, C.S.P. & DARBENZIO, R.B. (1996). Preconditioning is not abolished by the delayed rectifier K^+ blocker dofetilide. *American Journal of Physiology*, **271**, H1207-H1214.

GWILT, M., HENDERSON, C., ORME, J. & ROURKE, J. (1992). Effects of drugs on ventricular fibrillation and ischaemic K^+ loss in a model of ischaemia in perfused guinea-pig hearts in vitro. *European Journal of Pharmacology*, **220**, 231-236.

HAGEMAN, G., NEELY, B., URTHALER, F. & JAMES, T. (1985). Negative chronotropic and parasympatholytic effects of alinidine on canine sinus node and AV junction. *American Journal of Physiology*, **248**, H324-H330.

HAMADA, A., YADEN, E.L., HORNG, J.S., RUFFOLO, R.R., JNR, PATIL, P.N. & MILLER, D.D. (1985). N-substituted imidazolines and ethylenediamines and their action on α- and β-adrenergic receptors. *Journal of Medicinal Chemistry*, **28**, 1269-1273.

HAMILTON, T.C., WEIR, S.W. & WESTON, A.H. (1985). Comparison of the effects of BRL 34915 and verapamil on rat portal vein. *British Journal of Pharmacology*, **86**, 443P.

HAMILTON, T.C., WEIR, S.W. & WESTON, A.H. (1986). Comparison of the effects of BRL 34915 and verapamil on electrical and mechanical activity in rat portal vein. *British Journal of Pharmacology*, **88**, 103-111.

HANET, C., POULEUR, H., HUE, L., CAUCHETEUX, D., GURNE, O., MALDAGUE, P. & ROUSSEAU, M.F. **(1989).** Effects of alinidine on metabolic response to high-demand myocardial ischaemia. *Journal of Cardiovascular Pharmacology*, **13**, 405-411.

HANNAH, J.A.M., HAMILTON, C.A. & REID, J.L. **(1983).** RX781094, a new potent α_2 adrenoceptor antagonist: in vivo and in vitro studies in the rabbit. *Naunyn-Schmiedeberg's Archives of Pharmacology*, **322**, 221-227.

HARDER, D.R. & MADDEN, J.A. **(1984).** Cellular mechanism of force development in cat middle cerebral artery by reduced PCO_2. *Pflügers Archives - European Journal of Physiology*, **403**, 402-404.

HARRON, D.W., BREZINA, M., LILLIE, C. & KOBINGER, W. **(1985).** Antifibrillatory properties of alinidine after coronary artery occlusion in rats. *European Journal of Pharmacology*, **110**, 301-308.

HAY, T.K.C. **(1994).** Synthesis of clonidine analogues for potassium channel blocking activity. Master of Science, Department of Chemistry, Monash University, 86.

HAYASHI, S., HORIE, M., TSUURA, Y., ISHIDA, H., OKADA, Y., SEINO, Y. & SASAYAMA, S. **(1993).** Disopyramide blocks pancreatic ATP-sensitive K^+ channels and enhances insulin release. *American Journal of Physiology*, **265**, C337-C342.

HAYDON, D.A. & HLADKY, S.B. **(1972).** Ion transport across thin lipid membranes: a critical discussion of mechanisms in selected systems. *Quarterly Reviews of Biophysics*, **5**, 187-282.

HEGINBOTHAM, L. & MCKINNON, R. (1992). The aromatic binding site for tetraethylammonium ion on potassium channels. *Neuron*, **8**, 483-491.

HENEQUIN, J.C., CHARLES, S., NENQUIN, M., MATHOT, F. & TAMAGAWA, T. (1982). Diazoxide and D600 inhibition of insulin release. Different mechanisms explain the specificity for different stimulus. *Diabetes*, **31**, 776-783.

HICKS, G.A., HUDSON, A.L. & HENDERSON, G. (1994). Localization of high affinity [^{3}H]glibenclamide binding sites within the substantia nigra zona reticulata of the rat brain. *Neuroscience*, **61**, 285-292.

HONORE, E. & LAZDUNSKI, M. (1991). Hormone-regulated K^+ channels in follicle-enclosed oocytes are activated by vasorelaxing K^+ channel openers and blocked by antidiabetic sulfonylureas. *Proceedings of the National Academy of Sciences*, **88**, 5438-5442.

HORIE, M., ISHIDA-TAKAHASHI, A., AI, T., NISHIMOTO, T., TSUURA, Y., ISHIDA, H., SEINO, Y. & SASAYAMA, S. (1997). Insulin secretion and its modulation by antiarrhythmic and sulfonylurea drugs. *Cardiovasc Res*, **34**, 69-72.

IBBOTSON, T., EDWARDS, G. & WESTON, A.H. (1993). Antagonism of levcromakalim by imidazoline- and guanidine-derivatives in rat portal vein: involvement of the delayed rectifier. *British Journal of Pharmacology*, **110**, 1556-1564.

IMAMURA, Y., TOMOIKE, H., NARISHIGE, T., TAKAHASHI, T., KASUYA, H. & TAKESHITA, A. (1992). Glibenclamide decreases basal coronary blood flow in anaesthetised dogs. *American Journal of Physiology*, **263**, H399-H404.

INAGAKI, N., TSUURA, Y., NAMBA, N., MASUDA, K., GONOI, T., HORIE, M., SEINO, Y., MIZUTA, M. & SEINO, S. (1995a). Cloning and functional characterization of a novel ATP-sensitive potassium channel ubiquitously expressed in rat tissues, including pancreatic islets, pituitary, skeletal muscle, and heart. *Journal of Biological Chemistry*, **270**, 5691-5694.

INAGAKI, N., GONOI, T., CLEMENT IV, J.P., NAMBA, N., INAZAWA, J., GONZALEZ, G., AGUILAR-BRYAN, L., SEINO, S. & BYRAN, J. (1995b). Reconstitution of I_{KATP}: An inward rectifier subunit plus the sulfonylurea receptor. *Science*, **270**, 1166-1170.

INAGAKI, N., GONOI, T., CLEMENT IV, J.P., WANG, C.-Z., AGUILAR-BYRAN, L., BYRAN, J. & SEINO, S. (1996). A family of sulphonylurea receptors determines the pharmacological properties of ATP-sensitive K^+ channels. *Neuron*, **16**, 1011-1017.

INOUE, I., NAGASE, H., KISHI, K. & HIGUTI, T. (1991). ATP-sensitive K^+ channels in the mitochondrial inner membrane. *Nature*, **352**, 244-247.

INOUE, Y., EMOTO, M., INOUE, H., KAKU, K. & KANEKO, T. (1995). Characterization of the binding sites for [^{3}H] glibenclamide in rat liver membranes. *European Journal of Pharmacology*, **284**, 77-82.

ISHIDA-TAKAHASHI, A., HORIE, M., TSUURA, Y., ISHIDA, H., AI, T. & SASAYAMA, S. (1996). Block of ATP-sensitive K^+ channels and insulinotrophic action by the antiarrhythmic agent, cibenzoline. *British Journal of Pharmacology*, **117**, 1749-1755.

ISHIZAKA, H. & KUO, L. (1996). Acidosis-induced coronary arteriolar dilation is mediated by ATP-sensitive potassium channels in vascular smooth muscle. *Circulation Research*, **78**, 50-57.

ISHIZAKA, H., GUDI, S.R., FRANGOS, J.A. & KUO, L. (1999). Coronary arteriolar dilation to acidosis: role of ATP-sensitive potassium channels and pertussis toxin-sensitive G proteins. *Circulation*, **99**, 558-563.

ISOMOTO, S., KONDO, C., YAMADA, M., MATSUMOTO, S., HIGASHIGUCHI, O., HORIO, Y., MATSUZAWA, Y. & KURACHI, Y. (1996). A novel sulfonylurea receptor forms with BIR (Kir6.2) a smooth muscle type ATP-sensitive K^+ channel. *Journal of Biological Chemistry*, **271**, 24321-24324.

ITOH, T., FURAKAWA, K., KAJIWARA, M., KITAMURA, L., SUZUKI, Y., ITO, Y. & KURIOYAMA, H. (1981). Effects of 2-nicotinamidoethyl nitrate on smooth muscle cells and on adrenergic transmission in the guinea-pig and porcine mesenteric arteries. *Journal of Pharmacology and Experimental Therapeutics*, **218**, 260-270.

IWAMOTO, T., MIURA, T., URABE, K., ITOYA, M., SHIMAMOTO, K. & IIMURA, O. (1993). Effect of nicorandil on post-ischaemic contractile dysfunction in the heart: roles of its ATP-sensitive K^+ channel opening property and nitrate property. *Clinical & Experimental Pharmacology & Physiology*, **20**, 595-602.

JAN, L. & JAN, Y. (1994). Potassium channels and their evolving gates. *Nature*, **371**, 119-22.

JAN, L. & JAN, Y. (1997). Cloned potassium channels from eukaryotes and prokaryotes. *Annual Review of Neuroscience*, **20**, 91-123.

JENKINSON, D. (1991). How we describe competitive antagonists: three questions of usage. *Trends in Pharmacological Sciences*, **12**, 53-54.

JING, L., JAGADEESH, J.M., DE LOS ANGELES, J., MILLER, D.D. & PATIL, P.N. (1999). Depolarization of membrane potential and the smooth muscle contraction by isothiocyanatobenzyl imidazoline in guinea-pig stomach circular muscle. *Naunyn-Schmiedeberg's Archives of Pharmacology*, **360**, 337-343.

JONAS, J.C., PLANT, T.D. & HENQUIN, J.C. (1992). Imidazoline antagonists of alpha 2-adrenoceptors increase insulin release in vitro by inhibiting ATP-sensitive K^+ channels in pancreatic beta-cells. *British Journal of Pharmacology*, **107**, 8-14.

KAMIGAKI, M., ICHIHARA, K. & ABIKO, Y. (1994). Enhancement of ischaemic myocardial metabolic derangement by glibenclamide. *Japanese Journal of Pharmacology*, **65**, 121-129.

KAUBISCH, N., HAMMER, R., WOLHEIM, C., RENOLD, A.E. & OFFORD, R.E. (1982). Specific receptors for sulphonylureas in brain and in β-cell tumor of the rat. *Biochemical Pharmacology*, **31**, 1171-1174.

KAWADA, M., SATOH, K. & TAIRA, N. (1984). Selectivity of alinidine, a bradycardic agent, for SA nodal automaticity versus other cardiac activities in isolated, blood-perfused dog-heart preparations. *Archives Internationales de Pharmacolynamie et de Therapie*, **272**, 88-102.

KEMP, B.K. & MCPHERSON, G.A. (1998). Interspecies differences in thromboxane A_2 receptors are distinguished by glibenclamide. *European Journal of Pharmacology*, **354**, 173-178.

KILPATRICK, E. & COCKS, T. (1994). Evidence for differential roles of nitric oxide (NO) and hyperpolarization in endothelium-dependent relaxation of pig isolated coronary artery. *British Journal of Pharmacology*, **112**, 557-565.

KINDMARK, H., KOHLER, M., GERWINS, P., LARSSON, O., KHAN, A., WAHL, M.A. & BERGGREN, P.-O. (1994). The imidazoline derivative calmidazolium inhibits voltage-gated Ca^{2+}-channels and insulin release but has no effect on the phospholipase C system in insulin producing RINm5F-cells. *Bioscience Reports*, **14**, 145-158.

KLIEBER, H.-G. & DAUT, J. (1994). A glibenclamide sensitive potassium conductance in terminal arterioles isolated from guinea pig heart. *Cardiovascular Research*, **28**, 823-830.

KLODOS, I. & PLESNER, L. (1992). The influence of membrane charge on kinetic properties of Na, K-ATPase. *Acta Physiologica Scandinavia*, **146**, 235-239.

KOBINGER, W., LILLIE, C. & PICHLER, L. (1979). N-allyl-derivative of clonidine, a substance with specific bradycardic action at a cardiac site. *Naunyn-Schmiedeberg's Archives of Pharmacology*, **306**, 255-262.

KOBINGER, W. & PICHLER, L. (1980). Relation between central sympathoinhibitory and peripheral pre- and postsynaptic alpha-adrenoceptors as evaluated by different clonidine-like substances in rats. *Naunyn-Schmiedeberg's Archives of Pharmacology*, **315**, 21-27.

KONTOS, H.A. & WEI, E.P. (1996). Arginine analogues inhibit responses mediated by ATP-sensitive potassium channels. *American Journal of Physiology*, **271**, H1498-H1506.

KSOLL, E., PARSONS, A., MACKERT, J., SCHILLING, L. & WAHL, M. (1991). Analysis of cromakalim-, pinacidil-, and nicorandil-induced relaxation of the 5-hydroxytryptamine precontracted rat isolated basilar artery. *Naunyn-Schmiedeberg's Archives of Pharmacology*, **343**, 377-383.

LANCOMBE, C., VIALLARD, V. & PARIS, H. (1993). Identification of α_2-adrenoceptors and of non-adrenergic idazoxan binding sites in pancreatic islets from young and adult hamsters. *International Journal of Biochemistry*, **25**, 1077.

LANG, U. & WALLAND, A. (1989). Alinidine reverses the descending staircase of isolated rat atria by an antimuscarinic action. *Naunyn-Schmiedeberg's Archives of Pharmacology*, **339**, 456-463.

LARRSON, O., ÄMMÄLÄ, C., BOKVIST, K., FREDHOLM, B. & RORSMAN, P. (1993). Stimulation of the K_{ATP} channel by ADP and diazoxide requires nucleotide hydrolysis in mouse pancreatic β-cells. *Journal of Physiology*, **463**, 349-365.

LECLERC, G., ROUOT, B., SCHWARTZ, J., VELLY, J. & WERMUTH, C.G. (1980). Studies on some para-substituted clonidine derivatives that exhibit an a-adrenoceptor stimulant activity. *British Journal of Pharmacology*, **71**, 5-9.

LECLERCQ-MEYER, V., HERCHUELZ, A., VALVERDE, I., COUTURIER, E., MARCHAND, J. & MALAISSE, W.J. (1980). Mode of action of clonidine upon islet function: dissociated effects upon the time course and magnitude of insulin release. *Diabetes*, **29**, 193-200.

LEE, K., GROH, W.J., BLAIR, T.A., MAYLIE, J.G. & ADELMAN, J.P. (1995). Imidazoline compounds inhibit K_{ATP} channels in guinea pig ventricular myocytes. *European Journal of Pharmacology*, **285**, 309-312.

LEI, L., VAGHY, P.L., SLAVICA, M., DE LOS ANGELES, J., SMITH, B., MILLER, D.D. & FELLER, D.R. (1998). Activation of L-type calcium channel by tolazine derivatives: role of isothiocyanate moiety. *Journal of Cardiovascular Pharmacology*, **31**, 721-733.

LEIBOWITZ, G. & CERASI, E. (1996). Sulphonylurea treatment of NIDDM patients with cardiovascular disease: a mixed blessing? *Diabetologia*, **39**, 503-514.

LIGHT, P.E., SABIR, A.A., ALLEN, B.G., WALSH, M.P. & FRENCH, R.J. (1996). Protein kinase C-induced changes in the stoichiometry of ATP binding activate cardiac ATP-sensitive K^+ channels. A possible mechanistic link to ischemic preconditioning. *Circulation Research*, **79**, 399-406.

LIGHT, P.E. (1999). Cardiac K_{ATP} channels and ischemic preconditioning: current perspectives. *Canadian Journal of Cardiology*, **15**, 1123-1130.

LILLIE, C. & KOBINGER, W. (1983a). Actions of alinidine and AQ-A 39 on rate and contractility of guinea-pig atria during β-adrenoceptor stimulation. *Journal of Cardiovascular Pharmacology*, **5**, 1048-1051.

LILLIE, C. & KOBINGER, W. (1983b). Comparison of the bradycardic effects of alinidine (St 567), AQ-A 39 and verapamil on guinea-pig sinoatrial node superfused with different Ca^{2+} and NaCl solutions. *European Journal of Pharmacology*, **87**, 25-33.

LIU, Y., GAO, W.D., O'ROURKE, B. & MARBAN, E. (1996). Synergistic modulation of ATP-sensitive K^+ currents by protein kinase C and adenosine. Implications for ischemic preconditioning. *Circulation Research*, **78**, 443-454.

LIU, Y., SATO, T., SEHARASEYON, J., SZEWCZYK, A., O'ROURKE, B. & MARBAN, E. (1999). Mitochondrial ATP-dependent potassium channels. Viable candidate effectors of ischemic preconditioning. *Annals of the New York Academy of Sciences*, **874**, 27-37.

LÖFFLER, C. & QUAST, U. (1997). Pharmacological characterization of the sulphonylurea receptor in rat isolated aorta. *British Journal of Pharmacology*, **120**, 476-480.

LÖFFLER -WALZ, C. & QUAST, U. (1998). Binding of K_{ATP} channel modulators in rat cardiac membranes. *British Journal of Pharmacology*, **123**, 1395-1402.

LONGMORE, J., BRAY, K.M. & WESTON, A.H. (1991). The contribution of Rb-permeable potassium channels to the relaxant and membrane hyperpolarising actions of cromakalim, RP49356 and diazoxide in bovine tracheal smooth muscle. *British Journal of Pharmacology*, **102**, 979-985.

LUPO, B. & BATAILLE, D. (1987). A binding site for [^{3}H] glipizide in the rat cerebral cortex. *European Journal of Pharmacology*, **140**, 157-169.

MARSHALL, J.M., THOMAS, T. & TURNER, L. (1993). A link between adenosine, ATP-sensitive K^+ channels, potassium and muscle vasodilatation in the rat in systemic hypoxia. *Journal of Physiology*, **472**, 1-9.

MARTZ, A., JO, I. & JUNG, C. (1989). Sulphonylurea binding to adipocyte membranes and potentiation of insulin-stimulated hexose transport. *Journal of Biological Chemistry*, **264**, 13672-13678.

MCMURRAY, J. (1988). *Organic Chemistry*: Brooks/Cole Publishing Company.

MCPHERSON, G.A. (1985). Analysis of radioligand binding experiments: A collection of computer programs for the IBM PC. *Journal of Pharmacological Methods*, **14**, 213-238.

MCPHERSON, G.A. & ANGUS, J.A. (1989). Phentolamine and structurally related compounds selectively antagonise the vascular actions of the K^+ channel opener, cromakalim. *British Journal of Pharmacology*, **97**, 941-949.

MCPHERSON, G.A. & ANGUS, J.A. (1990). Characterisation of responses to cromakalim and pinacidil in smooth and cardiac muscle by use of selective antagonists. *British Journal of Pharmacology*, **100**, 201-206.

MCPHERSON, G.A. & ANGUS, J.A. (1991). Evidence that acetylcholine-mediated hyperpolarization of the rat small mesenteric artery does not involve the K^+ channel opened by cromakalim. *British Journal of Pharmacology*, **103**, 1184-1190.

McPherson, G. (1992a). Optimal conditions assessing vascular reactivity in small resistance arteries in the small vessel myograph. *Clinical and Experimental Pharmacology and Physiology*, **19**, 815-825.

McPherson, G.A. (1992b). Assessing vascular reactivity of arteries in the small vessel myograph. *Clinical and Experimental Pharmacology and Physiology*, **19**, 815-825.

McPherson, G.A. & Stork, A.P. (1992). The resistance of some rat cerebral arteries to the vasorelaxant effect of cromakalim and other K^+ channel openers. *British Journal of Pharmacology*, **105**, 51-58.

McPherson, G.A. & Piekarska, A.E. (1994). Antagonism by lipophilic quaternary ions of the K^+ channel opener, levcromakalim, in vascular smooth muscle. *British Journal of Pharmacology*, **112**, 1223-1229.

McPherson, G.A. (1995). *RADLIG: Version 4 of KINETIC, EBDA, LIGAND, LOWRY for IBM PC.* Cambridge, UK: BIOSOFT.

McPherson, G.A., Choi, R.T., Kong, D.C.M. & Iskander, M.N. (1997). The thromboxane A_2 and K_{ATP} channel antagonist effects of a series of sulphonylurea derivatives in the pig coronary artery. *European Journal of Pharmacology*, **324**, 193-200.

McPherson, G.A., Bell, K.L., Favaloro, J.L., Kubo, M. & Standen, N.B. (1999). Functional and electrophysiological effects of a novel imidazoline-based K_{ATP} channel blocker, IMID-4F. *British Journal of Pharmacology*, **128**, 1636-1642.

MELANDER, A., DONNELLY, R. & RYDBERG, T. (1998). Is there a concentration-effect relationship for sulphonylureas. *Clinical Pharmacokinetics*, **34**, 181-88.

MERKEL, L.A., LAPPE, R.W., RIVERA, L.M., COX, B.F. & PERRONE, M.H. (1992). Demonstration of vasorelaxant activity with an A_1-selective adenosine agonist in porcine coronary artery: Involvement of potassium channels. *Journal of Pharmacology and Experimental Therapeutics*, **260**, 437-443.

MICHEL, M. & INSEL, P. (1989). Are there multiple imidazoline binding sites? *Trends in Pharmacological Sciences*, **10**, 342-345.

MICHEL, M.C. & ERNSBERGER, P. (1992). Keeping an eye on the I site: imidazoline-preferring receptors. *Trends in Pharmacological Sciences*, **13**, 369-370.

MILLAR, J.S. & VAUGHAN WILLIAMS, E.M. (1981a). Pacemaker selectivity: influence on rabbit atria of ionic environment and of alinidine, a possible anion antagonist. *Cardiovascular Research*, **15**, 335-350.

MILLAR, J.S. & VAUGHAN WILLIAMS, E.M. (1981b). Anion antagonism- a fifth class of antiarrhythmic action? *Lancet*, **1**, 1291-1293.

MILLAR, J.S. & VAUGHAN WILLIAMS, E.M. (1983). Pharmacological mapping of regional effects in the rabbit heart of some new antiarrhythmic drugs. *British Journal of Pharmacology*, **78**, 701-709.

MILLER, D.D., HAMADA, A., CRAIG, E.C., CHRISTOPH, G.G., GALLUCCI, J.C., RICE, P.J., BANNING, J.W. & PATIL, P.N. (1983). Optically active catecholimidazolines: a study of steric interactions at alpha-adrenoceptors. *Annals of the New York Academy of Sciences*, **763**, 591-605.

MISLER, S., FALKE, L.C., GILLIS, K. & MCDANIEL, M.L. (1986). A metabolite-regulated potassium channel in rat pancreatic β-cells. *Proceedings of the National Academy of Science of the United States of America*, **83**, 7119-7123.

MIYOSHI, Y. & NAKAYA, Y. (1991). Angiotensin II blocks ATP-sensitive K^+ channels in porcine coronary artery smooth muscle cells. *Biochemical and Biophysical Research Communications*, **181**, 700-706.

MIYOSHI, Y., NAKAYA, Y., WAKATSUKI, T., NAKAYA, S., FUJINO, K., SAITO, K. & INOUE, I. (1992). Endothelin blocks ATP-sensitive K^+ channels and depolarises smooth muscle cells of porcine coronary artery. *Circulation Research*, **70**, 612-616.

MORGAN, C.R. & LAZAROW, A. (1963). Immunoassay of insulin: Two antibody system. Plasma insulin levels of normal, subdiabetic and diabetic rats. *Diabetes*, **12**, 115-126.

MOSER, C., HEHL, S. & NEUMCKE, B. (1995). Inhibition of ATP-sensitive K^+ channels of mouse skeletal muscle by disopyramide. *European Journal of Pharmacology*, **284**, 35-41.

MUKAI, E., ISHIDA, H., HORIE, M., NOMA, A., SEINO, Y. & TAKANO, M. (1998). The antiarrhythmic agent cibenzoline inhibits K_{ATP} channels by binding to Kir6.2. *Biochemical and Biophysical Research Communications*, **251**, 477-481.

MULVANY, M.J. & HALPERN, W. (1977). Contractile properties of small arterial resistance vessels in spontaneously hypertensive and normotensive rat. *Circulation Research*, **41**, 19-26.

MURAKAMI, M., FURUKAWA, Y., KARASAWA, Y., REN, L.M., TAKAYAMA, S. & CHIBA, S. (1992). Inhibition by glibenclamide of negative chronotropic and inotropic responses to pinacidil, acetylcholine, and adenosine in the isolated dog heart. *Journal of Cardiovascular Pharmacology*, **19**, 618-624.

MURRAY, M., BOYLE, J. & SMALL, R. (1989). Cromakalim-induced relaxation of guinea-pig isolated trachealis: antagonism by glibenclamide and by phentolamine. *British Journal of Pharmacology*, **98**, 865-874.

NAGAO, T., ILLIANO, S. & VANHOUTTE, P.M. (1992). Heterogenous distribution of endothelium-dependent relaxations resistant to N^G-nitro-L-arginine in rats. *American Journal of Physiology*, **263**, H1090-H1094.

NAKAKI, T., NAKADATE, T. & KATO, R. (1980). Alpha 2-adrenoceptors modulating insulin release from isolated pancreatic islets. *Naunyn-Schmiedeberg's Archives of Pharmacology*, **313**, 151-153.

NAKANE, T., FURUKAWA, Y. & CHIBA, S. (1991). Anti-muscarinic effect of alinidine on acetylcholine-induced vasodilation in isolated and perfused dog coronary arteries. *Tohoku Journal of Experimental Medicine*, **165**, 105-113.

NAKHOSTINE, N. & LAMONTAGNE, D. (1993). Adenosine contributes to hypoxia-induced vasodilation through ATP-sensitive K^+ channel activation. *American Journal of Physiology*, **265**, H1289-H1293.

NAKHOSTINE, N. & LAMONTAGNE, D. (1994). Contribution of prostaglandins in hypoxia-induced vasodilatation in isolated rabbit hearts. Relation to adenosine and K_{ATP} channels. *Pflügers Archives - European Journal of Physiology*, **4281**, 526-532.

NELSON, D., AGUILAR-BRYAN, L. & BRYAN, J. (1992). Specificity of photolabelling of β-cell membrane proteins with an ^{125}I-labelled glyburide analog. *Journal of Biological Chemistry*, **267**, 14928-14933.

NICHOLS, C.G. & LEDERER, W.J. (1991). Adenosine triphosphate-sensitive potassium channels in the cardiovascular system. *American Journal of Physiology*, **261**, H1675-H1686.

NIKI, I., KELLY, R., ASHCROFT, S. & ASHCROFT, F. (1989). ATP-sensitive K-channels in HIT T15 β-cells studies by patch-clamp methods, ^{86}Rb efflux and glibenclamide binding. *Pflügers Archives - European Journal of Physiology*, **415**, 47-55.

NIKI, I. & ASHCROFT, S.J.H. (1993). Characterization and solubilization of the sulphonylurea receptor in rat brain. *Neuropharmacology*, **32**, 951-957.

NOACK, T., EDWARDS, G., DIETMER, P. & WESTON, A.H. (1992). Potassium channel modulation in rat portal vein by ATP depletion: a comparison with the effects of levcromakalim (BRL 38227). *British Journal of Pharmacology*, **107**, 945-955.

NOMA, A. (1983). ATP-regulated K^+ channels in cardiac muscle. *Nature*, **305**, 147-148.

NOTSU, T., TANAKA, I., TAKANO, M. & NOMA, A. (1992). Blockade of ATP-sensitive K^+ channels by 5-hydroxydecanoate in guinea-pig ventricular myocytes. *Journal of Pharmacology and Experimental Therapeutics*, **260**, 702-708.

OGIWARA, Y., FURUKAWA, Y., TAKEDA, M. & CHIBA, S. (1987). Blocking effects of alinidine on negative chronotropic and inotropic responses to vagal stimulation and injected acetylcholine and carbachol in dogs. *Journal of Pharmacology and Experimental Therapeutics*, **243**, 1113-1120.

OHRNBERGER, C., KHAN, S.A. & MEISHERI, K.D. (1993). Synergistic effects of glyburide and U-37883A two structurally different vascular ATP-sensitive potassium channel antagonists. *Journal of Pharmacology and Experimental Therapeutics*, **267**, 25-30.

OKUMURA, K., ICHIHARA, K. & NAGASKA, M. (1992). Effects of imidazoline-related compounds on the mechanical response to nicorandil in the rat portal vein. *European Journal of Pharmacology*, **215**, 253-257.

OKUYAMA, Y., YAMADA, M., KONDO, C., SATOH, E., ISOMOTO, S., SHINDO, T., HORIO, Y., KITAKAZE, M., HORI, M. & KURACHI, Y. (1998). The effects of nucleotides and potassium channel openers on the SUR2A/K_{IR}6.2 complex K^+ channel expressed in mammalian cell line, HEK293T cells. *Pflügers Archives - European Journal of Physiology*, **435**, 495-603.

OLMOS, G., KULKARNI, R.N., HAQUE, M. & MACDERMOT, J. (1994). Imidazolines stimulate release of insulin from RIN-5AH cells independently from imidazoline I_1 and I_2 receptors. *European Journal of Pharmacology*, **262**, 41-48.

OLSON, L.K., SCHROEDER, W., ROBERTSON, R.P., GOLDBERG, N.D. & WALSETH, T.F. (1996). Suppression of adenylate kinase catalyzed phosphotransfer precedes and is associated with glucose-induced insulin secretion in intact HIT-T15 cells. *Journal of Biological Chemistry*, **271**, 16544-16552.

OPTHOF, T., DUIVENVOORDEN, J.J., VANGINNEKEN, A.C.G., JONGSMA, H.J. & BOUMAN, L.N. (1986). Electrophysiological effects of alindine (ST 567) on sinoatrial node fibres in the rabbit heart. *Cardiovascular Research*, **20**, 727-739.

PAN, J., HAMM, J., ROTHMAN, D. & SHULMAN, R. (1988). Intracellular pH in human skeletal muscle by ^{1}H NMR. *Proceedings of the National Academy of Science of the United States of America*, 85, 7836.

PANTEN, U., BURGFELD, J., GOERKE, F., RENNICKE, M., SCHWANSTECHER, M., WALLASCH, A., ZÜNKLER, B.J. & LENZEN, S. (1989). Control of insulin secretion by sulfonylureas, meglitinide and diazoxide in relation to their binding to the sulfonylurea receptor in pancreatic islets. *Biochemical Pharmacology*, **38**, 1217-1229.

PARENT, L., CARDINAL, J. & SAUVE, R. (1988). Single-channel analysis of a K channel at basolateral membrane of rabbit proximal convoluted tubule. *Biochemical Pharmacology*, 38, 1217-1229.

PATON, W.D.M. & RANG, H.P. (1965). The uptake of atropine and related drugs by the intestinal smooth muscle of the guinea-pig in relation to acetylcholine receptors. *Proceedings of the Royal Society of London B Biological Sciences*, **163**, 1.

PAUCEK, P., MIRONOVA, G., MAHDI, F., BEAVIS, A.D., WOLDEGIORGIS, G. & GARLID, K. (1992). Reconstitution and partial purification of the glibenclamide-sensitive ATP-dependent K^+ channel from rat liver and beef heart mitochondria. *Journal of Biological Chemistry*, **267**, 26062-26069.

PENNY, W.J. (1984). The deleterious effects of myocardial catecholamines on cellular electrophysiology and arrhythmias during ischaemia and reperfusion. *European Heart Journal*, **5**, 960-973.

PENNY, W., CULLING, W., LEWIS, M. & SHERIDAN, D. (1985). Antiarrhythmic and electrophysiological effects of alpha adrenoceptor blockade during myocardial ischemia and reperfusion in isolated guinea-pig heart. *Journal of Molecular Cellular Cardiology*, **17**, 399-409.

PICHLER, L. & KOBINGER, W. (1978). Presynaptic activity at peripheral adrenergic sites and blood pressure effect of a adrenoceptor stimulating drugs. *European Journal of Pharmacology*, **52**, 287-295.

PIEKARSKA, A.E. & MCPHERSON, G.A. (1997). Structure-activity relationship of quarternary ion antagonism of levcromakalin-induced relaxation of the pig coronary artery. *European Journal of Pharmacology*, **322**, 37-44.

PLANE, F. & GARLAND, C.J. (1993). Differential effects of acetylcholine, nitric oxide and levcromakalim on smooth muscle membrane potential and tone in the rabbit basilar artery. *British Journal of Pharmacology*, **110**, 651-656.

PLANT, T. & HENQUIN, J. (1990). Phentolamine and yohimbine inhibit ATP-sensitive K^+ channels in mouse pancreatic β-cells. *British Journal of Pharmacology*, **101**, 115-120.

PONGS, O. (1992). Molecular biology of voltage-dependent potassium channels. *Physiological Reviews*, **72**, S69-S88.

PROKS, P. & ASHCROFT, F.M. (1997). Phentolamine block of K_{ATP} channels is mediated by Kir6.2. *Proceedings of the National Academy of Science United States of America*, **94**, 11716-11720.

QUAST, U. (1987). Effect of the K^+ efflux stimulating vasodilator BRL 34915 on $^{86}Rb^+$ efflux and spontaneous activity in guinea-pig portal vein. *British Journal of Pharmacology*, **91**, 569-578.

QUAST, U. & COOK, N.S. (1988). Potent inhibitors of the effect of K^+ channel opener BRL 34915 in vascular smooth muscle. *British Journal of Pharmacology*, **930**, 240P.

QUAST, U. & COOK, N.S. (1989). In vitro and in vivo comparison of two K^+ channel openers, diazoxide and cromakalim, and their inhibition by glibenclamide. *Journal of Pharmacology & Experimental Therapeutics*, **250**, 261-271.

QUAST, U. & WEBSTER, C. (1989). Sulphonylureas and tetraethylammonium ions as inhibitors of cromakalim-stimulated 86Rb efflux. *Naunyn-Schmiedeberg's Archives of Pharmacology*, **339**, R64.

QUAST, U. (1993). Do the K^+ channel openers relax smooth muscle by opening K^+ channels? *Trends in Pharmacological Sciences*, **14**, 332-337.

QUAST, U., BRAY, K.M., ANDRES, H., MANLEY, P.W., BAUMLIN, Y. & DOSOGNE, J. (1993). Binding of the K^+ channel opener [^{3}H]P1075 in rat isolated aorta: Relationship to functional effects of openers and blockers. *Molecular Pharmacology*, **43**, 474-481.

QUAYLE, J.M. & STANDEN, N.B. (1994). K_{ATP} channels in vascular smooth muscle. *Cardiovascular Research*, **28**, 797-804.

QUAYLE, J.M., BONEV, A.D., BRAYDEN, J.U.E. & NELSON, M.T. (1995). Pharmacology of ATP-sensitive K^+ currents in smooth muscle cells from rabbit mesenteric artery. *American Journal of Physiology*, **269**, C1112-C1118.

QUAYLE, J.M., NELSON, M.T. & STANDEN, N.B. (1997). ATP-sensitive and inwardly rectifying potassium channels in smooth muscle. *Physiological Reviews*, **77**, 1165-1221.

RANDALL, M. & MCCULLOCH, A. (1995). The involvement of ATP-sensitive potassium channels in β-adrenoceptor-mediated vasorelaxation in the rat isolated mesenteric arterial bed. *British Journal of Pharmacology*, **115**, 607-612.

REICHHALTER, R., LILLIE, C. & KOBINGER, W. (1988). Effects of alinidine on survival and infarct size in rats with coronary artery occlusion. *European Journal of Pharmacology*, **157**, 75-81.

REMAURY, A. & PARIS, H. (1992). The insulin-secreting cell line, RINm5F, expresses an alpha-2D adrenoceptor and nonadrenergic idazoxan-binding sites. *Journal of Pharmacology and Experimental Therapeutics*, **260**, 417-426.

RESHEF, A., SPERLING, O. & ZOREF-SHANI, E. (1998). Opening of ATP-sensitive potassium channels by cromakalim confers tolerance against chemical ischaemia in rat neuronal cultures. *Neuroscience Letters*, **250**, 111-114.

RODBARD, D. (1984). Lessons from the computerizations of radioimmunoassays: An introduction to basic principles of modelling. In *Computers in Endocrinology*. ed. Rodbard, D. & Forte, G. New York: Raven Press.

RORSMAN, P. & TRUBE, G. (1985). Evidence that glucose-induced depolarization in the pancreatic β-cell involves the closure of an ATP dependent K^+ channel. *Acta Physiologica Scandinavia*, **124**, 147.

ROUOT, B., LECLERC, G. & WERMUTH, C.G. (1976). Clonidine and related analogues. Quantitative correlation. *Journal of Medicinal Chemistry*, **19**, 1049-1054.

RUFFOLO, R.R.J., ROSING, E.Y. & WADDELL, J.E. (1979). Receptor interactions of imidazolines. I. Affinity and efficacy of alpha adrenergic receptors in rat aorta. *Journal of Pharmacology and Experimental Therapeutics*, **209**, 429-436.

RUFFOLO, R.R., JR., YADEN, E.L. & WADDELL, J.E. (1980a). Receptor interactions of imidazolines. V. Clonidine differentiates postsynaptic alpha adrenergic receptor subtypes in tissues from the rat. *Journal of Pharmacology and Experimental Therapeutics*, **213**, 557-561.

RUFFOLO, R.R., JR., YADEN, E.L., WADDELL, J.E. & DILLARD, R.D. (1980b). Receptor interactrions of imidazolines. VI. Significance of carbon bridge separating phenyl and imidazoline rings of tolazoline-like alpha adrenergic imidazolines. *Journal of Pharmacology and Experimental Therapeutics*, **214**, 535-540.

RUFFOLO, R.R., JR., YADEN, E.L., WADDELL, J.E. & WARD, J.S. (1982). Receptor interactions of imidazolines. XI. Alpha-adrenergic and antihypertensive effects of clonidine and its methylene-bridged analog, St 1913. *Pharmacology*, **25**, 187-201.

RUFFOLO, R.R., JR. & MESSICK, K. (1985). Evaluation of the alpha-1 and alpha-2 adrenoceptor-mediated effects of a series of dimethoxy-substituted tolazoline derivatives in the cardiovascular system of the pithed rat. *Journal of Pharmacology and Experimental Therapeutics*, **232**, 94-99.

RUSTENBECK, I., KOWALEWSKI, R., HERRMANN, C. & HASSELBLATT, A. (1995). Insulinotropic imidazoline compounds act by binding to an intracellular site. *Diabetologia*, **38**, A95.

RUSTENBECK, I., LEUPOLT, L., KOWALEWSKI, R. & HASSELBLATT, A. (1999). Heterogeneous characteristics of imidazoline-induced insulin secretion. *Naunyn-Schmiedeberg's Archives of Pharmacology*, **359**, 235-242.

SAITO, S., MURAKAMI, Y., MIYAUCHI, S. & KAMO, N. (1992). Measurement of plasma membrane potential in isolated rat hepatocytes using the lipophilic cation, tetraphenylphosphonium: correction of probe intracellular binding and mitochondrial accumulation. *Biochemical and Biophysical Research Communications*, **1111**, 221-230.

SAKURA, H., ÄMMÄLÄ, C., SMITH, P.A., GRIBBLE, F.M. & ASHCROFT, F.M. (1995). Cloning and functional expression of the cDNA encoding a novel ATP-sensitive potassium channel subunit expressed in pancreatic β-cells, brain, heart and skeletal muscle. *FEBS Letters*, **377**, 338-344.

SAKUTA, H. & OKAMOTO, K. (1994). Inhibition by imidazoline and imidazolidine derivatives of glibenclamide-sensitive K^+ currents in *Xenopus* oocytes. *European Journal of Pharmacology*, **259**, 223-231.

SALKOFF, L., BAKER, K., BUTLER, A., COVARRUBIAS, M., PAK, M. & WEI, A. (1992). An essential 'set' of K^+ channels conserved in flies, mice and humans. *Trends in Neuroscience*, **15**, 161-166.

SAMAHA, F.F., HEINEMAN, F.W., INCE, C., FLEMING, J. & BALABAN, R.S. (1992). ATP-sensitive potassium channel is essential to maintain basal coronary vascular tone in vivo. *American Journal of Physiology*, **262**, C1220-C1227.

SATO, T., O'ROURKE, B. & MARBAN, E. (1998). Modulation of mitochondrial ATP-dependent K^+ channels by protein kinase C. *Circulation Research*, **83**, 110-114.

SATOH, H. & HASHIMOTO, K. (1986). Electrophysiogical study of alinidine in voltage clamped rabbit sinoatrial node cells. *European Journal of Pharmacology*, **121**, 211-219.

SCHMID-ANTOMARCHI, H., DE WEILLE, J., FOSSET, M. & LAZDUNSKI, M. (1987). The receptor for antidiabetic sulphonylureas controls the activity of the ATP-modulated K^+ channel in insulin-secreting cells. *Journal of Biological Chemistry*, **262**, 15840-15844.

SCHMIDT, H.H.H.W., LOHMANN, S.M. & WALTER, U. (1993). The nitric oxide and cGMP signal transduction system: regulation and mechanism of action. *Biochimica et Biophysica Acta*, **1178**, 153-178.

SCHMITT, H., SCHMITT, H. & FENARD, S. (1973). Action of α-adrenergic blocking drugs on the sympathetic centers and their interactions with the central sympatho-inhibitory effect of clonidine. *Arzneimittel-Forschung*, **23**, 40-43.

SCHULZ, A. & HASSELBLATT, A. (1988). Phentolamine, a deceptive tool to investigate sympathetic nervous control of insulin release. *Naunyn-Schmiedeberg's Archives of Pharmacology*, **337**, 637-643.

SCHULZ, A. & HASSELBLATT, A. (1989). An insulin-releasing property of imidazoline derivatives is not limited to compounds that block alpha-adrenoceptors. *Naunyn-Schmiedeberg's Archives of Pharmacology*, **340**, 321-327.

SCHULZ, R., ROSE, J. & HEUSCH, G. (1994). Involvement of activation of ATP-dependent potassium channels in ischemic preconditioning in swine. *American Journal of Physiology*, **267**, H1341-H1352.

SCHWANSTECHER, M., BRANDT, C., BEHRENDS, S., SCHAUPP, U. & PANTEN, U. (1992). Effect of MgATP on pinacidil-induced displacement of glibenclamide from the sulphonylurea receptor in a pancreatic β-cell line and rat cerebral cortex. *British Journal of Pharmacology*, **106**, 295-301.

SCHWANSTECHER, M., SIEVERDING, C., DORSCHNER, H., GROSS, I., AGUILAR-BRYAN, L., SCHWANSTECHER, C. & BRYAN, J. (1998). Potassium channel openers require ATP to bind to and act through sulfonylurea receptors. *The EMBO Journal*, **17**, 5529-5535.

SCHWENKE, W.B., SOBOLL, S., SEITZ, H.J. & SIES, H. (1981). Mitochondrial and cytosolic ATP/ADP ratios in rat liver in vivo. *Biochemical Journal*, **200**, 405-408.

SEINO, S. (1999). ATP-sensitive potassium channels: a model of heteromultimeric potassium channel/receptor assemblies. *Annual Review of Physiology*, **61**, 337-362.

SEUTIN, V., SHEN, K.-Z., NORTH, R.A. & JOHNSON, S.W. (1996). Sulphonylurea-sensitive potassium current evoked by sodium-loading in rat midbrain dopamine neurones. *Neuroscience*, **71**, 709-719.

SHEN, W.K., TUNG, R.T., MACHULDA, M.M. & KURACHI, Y. (1991). Essential role of nucleotide diphosphates in nicorandil-mediated activation of cardiac ATP-sensitive K^+ channel. *Circulation Research*, **69**, 1152-1158.

SHERIDAN, D.J., PENOSKE, P.A., SOBEL, B.E. & CORR, P.B. (1980). Alpha adrenergic contributions to dysrhythmia during myocardial ischemia and reperfusion in cats. *Journal of Clinical Investigation*, **65**, 161-171.

SHYNG, S.L. & NICHOLS, C.G. (1998). Membrane phospholipid control of nucleotide sensitivity of K_{ATP} channels. *Science*, **282**, 1138-1141.

SIEGL, P., WENGER, H. & SWEET, C. (1984). Comparison of cardiovascular responses to the bradycardic drugs, alinidine, AQ-A 39, and mixidine, in the anaesthetised dog. *Journal of Cardiovascular Pharmacology*, **6**, 565-574.

SILBERBERG, S.D. & VAN BREEMAN, C. (1992). A potassium current activated by lemakalim and metabolic inhibition in rabbit mesentric artery. *Pflügers Archives - European Journal of Physiology*, **420**, 118-120.

SLAVICA, M., LEI, L., PATIL, P.N., KEREZY, A., FELLER, D.R. & MILLER, D.D. (1994). Synthesis and biological activities of a new set of irreversibly acting 2-(4'-isothiocyanatobenzyl)imidazoline analogs in rat thoracic aorta. *Journal of Medicinal Chemistry*, **37**, 1874-1881.

SLESINGER, P.A., PATIL, N., LIAO, Y.J., JAN, Y.N., JAN, L.Y. & COX, D.R. (1996). Functional effects of the mouse weaver mutation of G protein-gated inwardly rectifying K^+ channels. *Neuron*, **16**, 321-331.

SPRUCE, A.E., STANDEN, N.B. & STANFIELD, P.R. (1985). Voltage-dependent ATP-sensitive potassium channels of skeletal muscle membrane. *Nature*, **316**, 736-738.

SPRUCE, A.E., STANDEN, N.B. & STANFIELD, P.R. (1986). Rubidium permeability of ATP-dependent potassium channels of frog skeletal muscle. *Journal of Physiology*, **378**, 105P.

STÄHLE, H. & POOK, K.-H. (1971). Synthesen in der 2-amino-imidazolin-reihe. *Liebigs Annals Chemistry*, **751**, 159-175.

STANFIELD, P.R., DAVIES, N.W., SHELTON, P.A., SUTCLIFFE, M.F., KHAN, I.A., BRAMMAR, W.J. & CONLEY, E.C. (1994). A single aspartate residue is involved in both intrinsic gating and blockage by Mg^{2+} of the inward rectifier, IRK1. *Journal of Physiology*, **478**, 1-6.

STRELLER, I. & WALLAND, A. (1990). Antiischemic effects of alinidine in paced isolated rat hearts. *Basic Research in Cardiology*, **85**, 71-77.

STURGESS, N., ASHFORD, M., COOK, D. & HALES, C. (1985). The sulphonylurea receptor may be an ATP-sensitive potassium channel. *Lancet*, **8453**, 474-475.

STURGESS, N., KOZLOWSKI, R., CARRINGTON, C., HALES, C. & ASHFORD, M. (1988). Effects of sulphonylureas and diazoxide on insulin secretion and nucleotide-sensitive channels in an insulin-secreting cell line. *British Journal of Pharmacology*, **95**, 83-94.

TAKANO, M. & NOMA, A. (1993). The ATP-sensitive K^+ channel. *Progress in Neurobiology*, **41**, 21-30.

TERZIC, A., JAHANGER, A. & KURACHI, Y. (1995). Cardiac ATP-sensitive K^+ channels: regulation by intracellular nucleotides and K^+ channel-opening drugs. *American Journal of Physiology*, **269**, C525-545.

THANDOROYEN, F.T., WORTHINGTON, M.G., HIGGINSON, L.M. & OPIE, L.H. (1983). The effect of alpha- and beta-adrenoceptor antagonists on reperfusion ventricular fibrillation and metabolic status in the isolated perfused rat heart. *Journal of the American College of Cardiology*, 4, 1056-1066.

THURINGER, D. & ESCANDE, D. (1989). Apparent competition between ATP and the potassium channel opener RP 49356 on ATP-sensitive K^+ channel of cardiac myocytes. *Molecular Pharmacology*, **36**, 897-902.

TIMMERMANS, P.B., SCHOOP, A.M.C., KWA, H.Y. & VAN ZWEITEN, P.A. (1981). Characterisation of α adrenoceptors participating in the central hypotensive and sedative effects of clonidine using yohimbine, rauwolscine and corynanthine. *European Journal of Pharmacology*, **70**, 7-15.

TIMMERMANS, P., QIAN, J., RUFFOLO, R.J. & VAN ZWIETEN, P. (1984). A study of the selectivity and potency of rauwolscine, RX 781094 and RS 21361 as antagonists of alpha-1 and alpha-2 adrenoceptors. *Journal of Pharmacology & Experimental Therapeutics*, **228**, 739-748.

TRITTHART, H.A., WINDISCH, H. & HEUBERGER, S. (1981). The effects of the bradycardia-producing compound alinidine on action potentials and tension development in cardiac fibres. *Naunyn-Schmiedeberg's Archives of Pharmacology*, **316**, 172-177.

TRUBE, G., RORSMAN, P. & OHNO-SHOSAKU, T. (1986). Opposite effects of tolbutimide and diazoxide on the ATP-dependent K^+ channel in mouse pancreatic β-cells. *Pflügers Archives - European Journal of Physiology*, **407**, 493-499.

TSAI, M.L. & LIN, M.T. (1987). Participation of a bulbospinal serotonergic pathway in the rat brain in clonidine-induced hypotension and bradycardia. *Pharmacology*, **35**, 279-285.

TUCKER, S.J., GRIBBLE, F.M., ZHAO, C., TRAPP, S. & ASHCROFT, F.M. (1997). Truncation of Kir6.2 produces ATP-sensitive K^+ channels in the absence of the sulphonylurea receptor. *Nature*, **387**, 179-183.

TUSNADY, G., BAKOS, E., VARADI, A. & SARKADI, B. (1997). Membrane topology distinguishes a subfamily of the ATP-binding cassette (ABC) transporters. *FEBS Letters*, **402**, 1-3.

TWEEDIE, K., BOACHIE-ANSAH, G., KANE, K. & HENDERSON, C. (1992). Phentolamine attenuates hypoxia-induced abbreviation of the cardiac action potential. *British Journal of Pharmacology*, **107**, 269P.

UEDA, K., INAGAKI, N. & SEINO, S. (1997). MgADP antagonism to Mg^{2+}-independent ATP binding of the sulfonylurea receptor SUR1. *Journal of Biological Chemistry*, **272**, 22983-22986.

VAYSSETTES-COURCHAY, C., BOUYSSET, F., CORDI, A.A., LAUBIE, M. & VERBEUREN, T.J. (1996). A comparative study of the reversal by different α_2-adrenoceptor antagonists of the central sympatho-inhibitory effect of clonidine. *British Journal of Pharmacology,* **117**, 587-593.

VON BECKERATH, N., CYRYS, S., DISCHNER, A. & DAUT, J. (1991). Hypoxic vasodilatation in isolated, perfused guinea-pig heart: an analysis of the underlying mechanisms. *Journal of Physiology*, **442**, 297-319.

WAKATSUKI, T., NAKAYA, Y. & INOUE, I. (1992). Vasopressin modulates K^+-channel activities of cultured smooth muscle cells from porcine coronary artery. *American Journal of Physiology*, **263**, H491-H496.

WARLTIER, D.C., AUCHAMPACH, J.A. & GROSS, G.J. (1993). Relationship of severity of myocardial stunning to ATP dependent potassium channel modulation. *Journal of Cardiac Surgery*, **8**, 279-283.

WATSON, S. & GIRDLESTONE, D. (1999). K^+ channels. *Trends in Pharmacological Sciences*, **Receptor and ion channel nomenclaure supplement**, 95-100.

WEIK, R. & NEMUCKE, B. (1990). Effects of potassium channel openers on single potassium channels in mouse skeletal muscle. *Naunyn-Schmiedeberg's Archives of Pharmacology*, **342**, 258-263.

WIBLE, B.A., TAGLIALATELA, M., FICKER, E. & BROWN, A.M. (1994). Gating of inwardly rectifying K^+ channels localised to a single negatively charged residue. *Nature*, **371**, 246-249.

WILDE, A.A.M., VELDKAMP, M.W., VAN GINNEKEN, A.C.G. & OPTHOF, T. (1994). Phentolamine blocks ATP sensitive potassium channels in cardiac ventricular cells. *Cardiovascular Research*, **28**, 847-850.

WILFFERT, B., TIMMERMANS, P.B. & VAN ZWEITEN, P.A. (1982). Extrasynaptic location of alpha-2 and noninnervated beta-2 adrenoceptors in the vascular system of the pithed normotensive rat. *Journal of Pharmacology and Experimental Therapeutics*, **221**, 762-768.

WINQUIST, R.J., HEANEY, L.A. & WALLACE, A.A. (1989). Glyburide blocks the relaxation response to BRL 34915 (cromakalim), minoxidil sulfate and diazoxide in vascular smooth muscle. *Journal of Pharmacology and Experimental Therapeutics*, **248**, 149-156.

WONG, K.K. (1993). Cardiovascular effects of low and high doses of clonidine in rats. *Artery*, **20**, 180-188.

WRAY, S. (1988). Smooth muscle intracellular pH: measurement, regulation, and function. *American Journal of Physiology*, **254**, C213-C225.

YAMADA, M., ISOMOTO, S., MATSUMOTO, S., KONDO, C., SHINDO, T., HORIO, Y. & KURACHI, Y. (1997). Sulphonylurea receptor 2B and $K_{IR}6.1$ form a sulphonylurea-sensitive but ATP insensitive K^+ channel. *Journal of Physiology*, **499**, 715-720.

YAO, Z. & GROSS, G. (1994). The ATP-dependent potassium channel: an endogenous cardioprotective mechanism. *Journal of Cardiovascular Pharmacology*, **24**, S25-S34.

ZAITSEV, S.V., EFANOV, A.M., EFANOVA, I.B., LARSSON, O., OSTENSON, C.-G., GOLD, G., BERGGREN, P.-O. & EFENDIC, S. (1996). Imidazoline compounds stimulate insulin release by inhibition of K_{ATP} channels and interaction with the exocytotic machinery. *Diabetes*, **45**, 1610-1618.

ZAITSEV, S.V., EFANOV, A.M., RAAP, A., EFANOVA, I.B., SCHLOOS, J., STECKEL-HAMANN, B., LARSSON, O., OSTENSON, C.G., BERGGREN, P.O., MEST, H.J. & EFENDIC, S. (1999). Different modes of action of the imidazoline compound RX871024 in pancreatic beta-cells. Blocking of K^+ channels, mobilization of Ca^{2+} from endoplasmic reticulum, and interaction with exocytotic machinery. *Annals of the New York Academy of Sciences*, **881**, 241-252.

ZHANG, H.L. & BOLTON, T.B. (1995). Activation by intracellular GDP, metabolic inhibition and pinacidil of a glibenclamide-sensitive K-channel in smooth muscle cells of rat mesenteric artery. *British Journal of Pharmacology*, **114**, 662-672.

ZHANG, H.L. & BOLTON, T.B. (1996). Two types of ATP-sensitive potassium channels in rat portal vein smooth muscle cells. *British Journal of Pharmacology*, **118**, 105-114.

ZHANG, H.L., BOLTON, T.B., PIEKARSKA, A.E. & MCPHERSON, G.A. (1998). The electrophysiological effects of tetraphenylphosphonium on vascular smooth muscle. *European Journal of Pharmacology*, **347**, 119-123.

ZHU, Q.-M., LESNICK, J.D., JASPER, J.R., MACLENNAN, S.J., DILLON, M.P., EGLAN, R.M. & BLUE, J., D.R. (1999). Cardiovascular effects of rilmenidine, mononidine and clonidine in conscious wild-type and D79N α_{2A}-adrenoceptor transgenic mice. *British Journal of Pharmacology*, **126**, 1522-1530.

ZINI, S., BEN-ARI, Y. & ASHFORD, M.L.J. (1991). Characterisation of sulfonylurea receptors and the action of potassium channel openers on cholinergic neurotransmission in guinea pig isolated small intestine. *Journal of Pharmacology and Experimental Therapeutics*, **259**, 566-573.

ZÜNKLER, B.J., LINS, S., OHNO-SHOSAKU, T., TRUBE, G. & PANTEN, U. (1988). Cytosolic ADP enhances the sensitivity to tolbutamide of ATP-dependent K^+ channels from pancreatic β-cells. *FEBS Letters*, **239**, 241-244.

ERRATA

Page xiii (Abbreviations) insert:

5HT	5-Hydroxytryptamine
EDHF	Endothelium-derived hyperpolarizing factor
TPP	Tetraphenylphosphonium
NO	Nitric Oxide
cGMP	Cyclic Guanosine Monophosphate

Page 6, Figure 1.1 legend: insert CNG = cyclic nucleotide-gated channels

Page 24, Paragraph 3, Line 1: "the role K_{ATP}" should read "the role of K_{ATP}"

Page 36, Table 1.3: "TPP" should read "Tetraphenyl phosphonium"

Page 45, Paragraph 2, Line 14: "site in concentration-dependent" should read "site in a concentration-dependent"

Page 51, Paragraph 3, Line10: "posses" should read "possess"

Page 65, Scheme 2.2: "bis-subsituted" should read "bis-substituted"

Page 85, Line 9: After "and cut into 4 mm long segments." insert "The lumen of all rings was gently rubbed with a wooden rod to remove the endothelium."

Page 92, Paragraph 2, Line 18: "concentrations of the either" should read "concentrations of either"

Page 95, Paragraph 2, Line 8: After "50% of the KPSS contraction" insert "(18.8 ± 0.5 g; n=75)."

Page 101, Figure 3.7: "concentrations used were 0.1 (□), 0.3 (●), 3 (○), 10 (▼) and 30 (▽) μM" should read "concentrations used were 0.3 (□), 1 (●), 3 (○), 10 (▼) and 30 (▽) μM"

Page 104, Table 3.1: IMID-4F, "3 μM" should read "1 μM"

Page 113, Line 5: insert "more than" before "224, 295, 269"

Page 121, Paragraph 2, Line 6: insert "greater than or equal to" before "224, 295, 269".

Page 149, para 2: "The haem group present..." should read "the haem group within soluble guanylate cyclase binds to nitric oxide and the enzyme is activated"

Page 181, Paragraph 2, Line 18: "indicate that that the" should read "indicate that the"

Page 186, Paragraph 1, Line 12: "the average of systolic and diastolic blood pressure" should read " diastolic pressure plus a third of systolic minus diastolic pressure"

Page 209, Paragraph 2, Line 9: MAP should read heart rate

Page 216, Paragraph 1, Line 2: remove "one way RM ANOVA"

Page 220, Paragraph 4, Line 4: "(1.0 ± 0.6 ng/ml)" should read "(1.5 ± 0.6 ng/ml)"

Page 229, Paragraph 3, Line 6: "heart in" should read "heart rate in"